



**HAL**  
open science

## The Scientific Objectives of the SPIRAL2 project

D. Ackermann, L. Adoui, G. de Angelis, G. Auger, T. Aumann, F. Azaiez, E. Balanzat, G. Baldacchino, M.F. Barthe, E. Bauge, et al.

► **To cite this version:**

D. Ackermann, L. Adoui, G. de Angelis, G. Auger, T. Aumann, et al.. The Scientific Objectives of the SPIRAL2 project. [Research Report] GANIL. 2006, pp.1-182. in2p3-00101412

**HAL Id: in2p3-00101412**

**<https://hal.in2p3.fr/in2p3-00101412>**

Submitted on 27 Sep 2006

**HAL** is a multi-disciplinary open access archive for the deposit and dissemination of scientific research documents, whether they are published or not. The documents may come from teaching and research institutions in France or abroad, or from public or private research centers.

L'archive ouverte pluridisciplinaire **HAL**, est destinée au dépôt et à la diffusion de documents scientifiques de niveau recherche, publiés ou non, émanant des établissements d'enseignement et de recherche français ou étrangers, des laboratoires publics ou privés.



# The Scientific Objectives of the SPIRAL 2 Project

Published by GANIL  
Grand Accélérateur National d'Ions Lourds  
BP 55027 – 14076 Caen cedex 5 - France

June 2006



# CONTENTS

1. Introduction: understanding the nature of matter	5
2. Structure of exotic nuclei: the challenges	9
2.1. Masses and drip lines	
2.2. Weakly bound halo, borromean and cluster system	
2.3. Magic numbers and deformations: shell structure far from stability	
2.4. Creation of new elements: superheavy nuclei	
2.5. Symmetries	
2.6. Collective excitation in unstable and weakly bound nuclei	
2.7. What forces are responsible for the binding of nuclei?	
3. Dynamics and thermodynamics of charge asymmetric nuclear matter	83
3.1. Thermodynamical aspects	
3.2. Large amplitude motion	
3.3. Reaction mechanisms at Fermi energies	
4. Elements and their origin	97
4.1. Introduction	
4.2. Classical novae and X-ray bursts	
4.3. The s-process nucleosynthesis	
4.4. The r-process nucleosynthesis	
5. Fundamental interactions: searching for physics beyond the Standard Model	111
5.1. Nuclear structure for examining the Standard Model: the properties of super-allowed $\beta$ -decay	
5.2. Kinematics of $\beta$ -decay: correlation parameters and the quest for new physics	
5.3. First-forbidden $\beta$ -decay	
5.4. Atomic parity non-conservation	
6. Neutrons for science at SPIRAL2	128
6.1. Introduction	

6.2. Neutron time-of-flight measurements	
6.3. Quasi mono-energetic neutrons	
6.4. Astrophysics with neutrons at SPIRAL2	
6.5. Material irradiation studies	
<b>7. Interdisciplinary Research: Perspectives offered by SPIRAL2</b>	<b>144</b>
7.1. Fast ion – slow ion collisions	
7.2. Probing nuclear properties with atomic measurements on ion beams	
7.3. The nuclear radioactive probe for solid state physics	
7.4. A high intensity low-energy positron beam for material science	
7.5. Radiation Damage and radiation chemistry	
7.6. Radiobiology	
7.7. Production of radioactive isotopes for biology, medical imaging and nuclear medicine	
<b>8. The SPIRAL 2 facility</b>	<b>165</b>
8.1. Introduction	
8.2. The genesis of the SPIRAL 2 project	
8.3. The facility	
8.4. Beams of stable isotopes from LINAG	
8.5. Radioactive beams	
8.6. The performances of the CIME cyclotron	
8.7. Mass purification	
8.8. Comparison with other facilities	
8.9. Accessible regions of the chart of nuclei	
8.10. High-intensity neutron beams	
8.11. Operation of the GANIL/SPIRAL/SPIRAL 2 facility	
<b>9. List of contributors</b>	<b>182</b>

# ***1. INTRODUCTION: UNDERSTANDING THE NATURE OF MATTER***

The atomic nucleus contains more than 99.9% of the mass of the atom. It is made of nucleons: protons, each with a positive charge, and neutrons with no charge. The nucleons are held within nuclei by the strong interaction. The number of protons ( $Z$ ) determines the charge of the nucleus, which then fixes the number of negatively charged electrons orbiting around the nucleus in a neutral atom. This also determines the atomic number, and consequently the chemical element to which the atom belongs. The number of neutrons ( $N$ ) plus the number of protons in a nucleus determines its mass number ( $A$ ). The nucleons themselves are each composed of three quarks interacting via the exchange of gluons, the vectors of the strong interaction. It is these forces which confine the quarks. The creation of nuclear species and their observed abundances today reflect the diverse phases of the evolution of the Universe. They remain as evidence of its long history. While the lighter elements were produced in the first minutes after the Big Bang, the heavier elements were – and still are – synthesised in the cores of stars. It is not just nucleosynthesis but all energetic cosmic phenomena that bring nuclear forces into play. The understanding of our world, its origin and its evolution is thus intimately related to progress in our knowledge of nuclear physics.

Modern nuclear physics has four, clearly defined frontiers, namely:

- **Hadron physics.** It is concerned with the attempts to understand the most primitive nucleus, the nucleon, in terms of the interactions between the constituent quarks and to answer such questions as how the nucleon mass is composed of quark masses and how the nucleon spin is determined by the spins of its components.

- **The phase diagram of nuclear matter.** The properties of nuclear matter can be summarised in a phase diagram just like any other form of matter. The main goal here is to find how the nature of nuclear matter changes as we vary the temperature and baryon density. In particular the phase change to a quark-gluon plasma is thought to be typical of the period following the Big Bang. To understand nuclear matter and its evolution in the Universe, one needs to determine whether the phase change is a first- or second-order transition, to seek a critical point and to study the nuclear equation-of state.

- **The structure of nuclei.** The nucleons appear robust enough to retain their integrity in the presence of other nucleons. The quark substructure of nucleons does not seem to play a direct role in the dynamics of nuclei at low and intermediate energy. In this energy regime nuclei can be regarded as aggregates of interacting nucleons. To understand their structure it is vital to produce, identify and study exotic nuclei. This is the vital pre-requisite for understanding how nuclear properties vary with the ratio of neutrons to protons. This information is essential for determining the nuclear equation-of-state and provides the underpinning for theoretical models of nuclear structure.

- **The application of our knowledge and understanding of nuclear properties.** Amongst the many applications of nuclear science one of the most prominent is nuclear astrophysics. Put simply it tries to answer the question: how do nuclei and particles participate in the evolution of the Universe? The goal here is not only to understand the processes in which the chemical elements were and are being created but to use that knowledge to understand the dynamics of explosive astrophysical events.

It is the last two of these frontiers which will be the principal domain of SPIRAL2, although it will help to shed some light on the first two.

The most basic question in nuclear physics relates to the structure of quarks and gluons in nucleons, and the possible alteration of this structure when the nucleons are “bound” in a nucleus. In order to reveal the internal structure of the nucleons in the nucleus it is necessary to use the finest probes, such as electrons of very high energy. However, the forces between nucleons within nuclei result from the interactions between the constituent quarks and gluons. Therefore, understanding the forces between nucleons provides indirect tests of their internal structure. In this way, the research made possible by the SPIRAL2 facility will contribute to uncover the quark structure of subatomic particles.

The link between interacting nucleons and the underlying structure of quarks and gluons remains an open question. The modifications induced by the nuclear medium, the existence of charges and currents, the motion of nucleons at speeds close to that of light, the effects of the laws of quantum mechanics – the Pauli Exclusion Principle and Heisenberg’s Uncertainty Principle – make the problem even more complex. The current situation is that, even though the reactions between free nucleons have been studied in detail, our knowledge of the forces that bind the nucleons in the nucleus is far from being satisfactory. In particular, nucleons appear to interact not only in pairs, but three-body forces also seem to make an essential contribution to nuclear binding. This phenomenon is quite unique in physics. Thus studies of nuclear structure and reactions relate to the interactions between nucleons in nuclei. SPIRAL2 will allow us to access information that will shed light on these fundamental questions.

Studies of reactions with SPIRAL2 will allow us to explore the isospin degree-of-freedom. A deeper understanding of the behaviour of neutrons and protons in a charge asymmetric nuclear medium is essential to test and extend our present knowledge of the nuclear interaction. The structure of the nucleon-nucleon effective force, the nucleon effective mass and the competition between mean-field and two-body collisional effects certainly all depend on the charge asymmetry of the systems considered. Hence it is clear that the isospin degree-of-freedom opens a stimulating new field of exploration, allowing us to obtain an insight into new nuclear properties. In this way one can investigate the properties of the nuclear equation-of-state (EOS) and the associated phase diagram, to learn about the static properties of asymmetric matter and access the thermodynamics of exotic nuclei.

To understand the properties of the nucleus it is not sufficient just to establish the interaction between its components; it is also necessary to determine the arrangement of the nucleons, and to identify the phenomena at the root of the observed structures and of their binding.

A major part of the recent progress in studying the nucleus and the interactions between its components is linked to the synthesis of new nuclei, developments of experimental methods for investigating them as well as improvements in theoretically modelling the nucleus. Because of their very unusual proton-to-neutron ratio, these “exotic” nuclei allow one to perform unprecedented studies of the phenomena underlying the binding of nuclei. SPIRAL2 will give access to a whole range of experiments on exotic nuclei, which have been impossible up to now. In particular it will provide intense beams of neutron-rich, exotic nuclei whose properties are little explored at present.

In our studies of nuclear structure there are many unanswered questions:

- What are the limits to nuclear existence? Very little is known in particular on where the neutron drip-line lies or what the upper limit is for the number of protons in a nucleus.

- What new forms of nuclear matter will be found in nuclei far from stability?
- Will new forms of collective motion be observed far from stability?
- What is the ordering of quantum levels in nuclei far from stability? Put another way: what happens to the well known shell structure seen in stable nuclei as we move away from stability?
  - What will be the forms of nuclear matter at the extremes of stability? It is already known that some neutron-rich, light nuclei have a halo of neutrons. Do they develop into neutron skins in heavier nuclei?
  - Do the dynamical symmetries seen in near-stable nuclei appear in exotic nuclei as well?

SPIRAL2 will produce high quality beams of exotic nuclei which will allow us to address these and many other questions that are common to much of modern science. One can summarise one such question very simply:

*Why and how is it that complex systems are composed of a few elementary ingredients?*

It is true of nucleons, nuclei, atoms, DNA, and superconductors for example. Typically atomic nuclei have radii of the order of femtometres because they are bound by the short range of the nuclear interaction. However they share much in common with nano-structures such as atomic clusters, quantum dots etc. This raises a second general question:

*Why is it that complex, many-body systems display surprising regularities and simple excitation patterns?*

Atomic nuclei exhibit a broad variety of phenomena at low energy. As indicated above many of these phenomena are of a universal character and appear in other physical systems. The importance of their study exceeds the strict framework of nuclear physics. Shells and magic numbers, pairing and superfluidity, symmetries and their spontaneous breaking, resonances, collective motion, penetration of barriers by composite systems, level densities and the thermodynamics of small systems, entropy and phase transitions are some of the many general phenomena in physics for which the atomic nucleus provides an excellent laboratory.

The processes of nucleosynthesis in stars and other astrophysical sites imply the formation of many radioactive nuclei. Owing to their short lifetimes, the majority of these nuclei are no longer present on Earth today. To be studied, short-lived exotic nuclei must be synthesised in the laboratory. SPIRAL2 will produce exotic nuclei in abundance and will thus open up many new fields to investigation including the detailed study of many of the reactions important to astrophysical processes.

Matter in the Universe exists in forms very different from those found on Earth. Atomic nuclei are immersed in fluxes of photons, protons, neutrons, neutrinos etc., undergo collisions and are heated and compressed to form neutron stars (or their precursors) which represent assemblies of nucleons compressed to densities close to those of the atomic nuclei, but containing the equivalent of all the matter enclosed in the Sun. Understanding these phenomena demands new studies in nuclear physics, particularly studies of nuclei that one does not find naturally on Earth, for example, those which are very neutron-rich. SPIRAL2 will allow such studies of astrophysical relevance to be made.

The beams of exotic nuclei and neutrons from SPIRAL2 will allow us to attack problems in many other areas of science and technology. New nuclear data are needed for the nuclear power systems of the future: IV<sup>th</sup> Generation reactor systems, radioactive waste management and fusion all demand that the interactions between fast neutrons and matter is fully understood. If partitioning and transmutation are to be pursued then one also needs a lot of

information on neutron-rich, exotic nuclei. SPIRAL2 will be one of the World's most potent fast neutron sources for the foreseeable future and will provide an important platform for materials studies even after other sources such as IFMIF come into operation. The beams from SPIRAL2 will also be important in studies of atomic physics, condensed matter and biology. The GANIL laboratory has a long and successful history, with the CIRIL laboratory, of applied nuclear science. SPIRAL2 will both widen and deepen these interdisciplinary activities in the future.

The chapters which follow this general introduction deal with the detailed questions to be addressed by experiments with the beams from SPIRAL2. In chapter 2 the many unanswered questions related to the structure of exotic nuclei are posed and the role of SPIRAL2 in answering them outlined. Chapter 3 deals with the dynamics and thermodynamics of asymmetric nuclear systems. Chapter 4 is concerned with questions of nuclear astrophysics which are intimately related to the properties of exotic nuclei. Chapter 5 indicates how the atomic nucleus can act as a laboratory for tests of the Standard model of Particle Physics and Chapter 6 shows how the production of intense fluxes of neutrons at SPIRAL2 make it an excellent tool to address both questions related to damage in materials of importance in nuclear installations and to the s- and r-processes of nucleosynthesis. In chapter 7 we turn to the application, of the radioactive beams from SPIRAL2 and the radionuclides produced by it, to study condensed matter and radiobiology. Finally in the eighth and last chapter the reader can find an account of the historical development of the SPIRAL2 facility and this is followed by an outline of the machine design and a summary of the capabilities of the facility.

## 2. *STRUCTURE OF EXOTIC NUCLEI: THE CHALLENGES*

One finds in Nature a great variety of atomic nuclei: all the elements which constitute the Universe, from the lightest, hydrogen, containing only one proton, to uranium, the heaviest of the natural elements, containing 92 protons. Our knowledge of this sub-atomic world is far from complete. It has been gleaned mainly from studies of the nuclear systems one finds in the Earth's crust, the remnants of the nuclei forged in stars several billion years ago, prior to the formation of the Solar system. These nuclei are sufficiently stable to have survived until our time.

In the simplest picture of atomic nuclei we know that they consist of protons and neutrons, which, in turn, are composed of quarks and gluons. The forces between quarks no doubt dictate the interactions between nucleons but otherwise their presence in nuclei is hidden. It is these forces, for which we have no adequate theory at distances corresponding to nucleon sizes, that dictate which combinations of neutrons and protons are stable, i.e. their nuclear binding energy is such that radioactive transmutations are not possible. For a given mass number ( $A$ ), the proportion of neutrons and protons that corresponds to the most stable configuration is determined by the combined action of the various phenomena that govern nuclear binding. In this way the line of stability is located on the Chart of the Nuclides, on which each bound nucleus is plotted as a function of  $N$  and  $Z$ .

However, Nature in the processes of nucleosynthesis, and more recently Man using particle accelerators, can produce unstable nuclei. It is the exploration of the properties of such nuclei which constitutes the field of exotic nuclei; nuclei which do not occur on Earth.

Not far from stability these nuclei generally convert into stable nuclei by  $\beta$ -decay of neutrons into protons or vice versa. It is the Weak interaction which is responsible for this transmutation, which explains the very long times required for  $\beta$ -decay processes, spanning from a few milliseconds to millions of years.

For very heavy nuclei, the path towards stability can be different. Indeed some can gain more stability by emitting a light nucleus, usually  ${}^4\text{He}$ , i.e.  $\alpha$ -particle radioactivity. They can also spontaneously fission into two nuclei of comparable masses. In cases where these emissions require tunnelling through a potential (energy) barrier, the half-lives of the radioactive nuclei are of the same order-of-magnitude as for  $\beta$ -decay.

Far away from stability the limits of nuclear existence are reached, where one or more nucleons are no longer bound. An unbound nuclear system disintegrates quasi-instantaneously (in a time interval of the order of  $10^{-21}$  s). The locus of points on the Chart of the Nuclides joining nuclei that are unbound to proton(neutron) emission in the ground state is called the proton(neutron) drip line. These drip lines form the "edges" of the nuclear chart. About 280 stable or very long-lived nuclear species are found on Earth but, according to current estimates, from 5000 to 7000 bound nuclei should exist in the Universe. Only 2000 have been synthesised and observed to date, but very little information is available about these unstable nuclei. Their lifetimes, masses or sizes are often unknown, their modes of radioactive decay have seldom been identified and information on their excited levels is very limited or non-existent.

Today our aim is to explore the whole nuclear chart in order to improve our understanding of nuclear binding. There are several important goals:

- To identify the effective forces which provide nuclear binding.
- To single out the phenomena responsible for bulk nuclear properties.
- To develop and test theoretical approaches that will be able to describe these phenomena.

One way of probing a nucleus with the aim of characterising its properties is to make it undergo nuclear reactions. In the case of the stable nuclei, one usually makes a target containing the nuclei of interest and bombards it with a beam of suitable particles. Exotic nuclei, however, are unstable and rare and thus cannot be formed into a target. Hence for a long time studying reactions on these nuclei seemed to be impossible. All this was transformed with the possibility of producing beams of exotic nuclei. Instead of bombarding the nucleus of interest with stable probe particles, the nuclei being studied are directed onto a target containing the probe particles. Radioactive Ion Beams (RIBs) thus open up a vast field of research with inestimable potential not just for answering the questions we have now but for new discoveries as well.

## 2.1 NUCLEAR MASSES AND THE DRIP LINES

The mass represents a basic characteristic of the nuclear system. The difference between the mass of a nucleus and the sum of the masses of its constituent free nucleons, i.e. the binding energy, reflects the forces of cohesion and provides direct information about the complex mechanisms that are responsible for the nuclear binding. Perhaps the most fundamental question in low-energy nuclear physics is: which combinations of protons and neutrons can form a nucleus that is bound in its ground state? Fewer than 300 stable nuclei occur in Nature, where by stable we mean that they have survived long enough (more than  $10^9$  y) since their formation in the Universe to be found on Earth. All other nuclei convert to these nuclei by radioactive decay with lifetimes ranging from seconds or even less to million of years. The stable nuclei thus define the “valley of stability”. By adding either protons or neutrons, radioactive nuclei away from stability are formed, finally reaching the drip lines where the forces between nucleons are not strong enough to bind them together.

The stability with respect to nuclear binding is determined by the separation energy, i.e. the energy required to separate a single nucleon from the nucleus. The drip line is reached when either the proton or the neutron separation energy, which is positive for nuclei that are bound in their ground state, becomes negative. Equivalently, the drip line is defined by the locus of the values of the proton number  $Z$  and the neutron number  $N$  for which the last nucleon is no longer bound and the nucleus undergoes radioactive decay with the emission of a nucleon. When masses of neighbouring nuclei are compared, the two-particle separation energies are a smooth function of particle number. The same holds for one-particle separation energies provided one corrects for the odd-even staggering that results from pairing correlations.

The proton drip line lies not too far from the valley of stability. As a result we have some experimental information on the one-proton drip line for elements up to  $Z=91$ . In contrast, for neutron-rich nuclei the drip line is very far from stability and much more difficult to reach. Except for the lightest nuclei, the position of the neutron drip line can only be estimated from nuclear models. However, depending on the model used, the predicted position of the drip lines may vary dramatically, especially on the neutron-rich side. Thus measuring the nuclear mass, a simple, clearly defined observable, is important since it allows us a) to locate the drip

lines experimentally thus providing an excellent means of testing our nuclear models and b) to recognise where the shell structure occurs far from stability.

The structure of nuclei far from stability and close to the particle drip lines is very rich. In neutron-rich nuclei, in particular, exotic phenomena include the weak binding of the outermost neutrons, pronounced effects of the coupling between bound states and the particle continuum, regions of nuclei with very diffuse neutron densities and the formation of neutron skin and halo structures. The modification of the effective nuclear potential produces a suppression of shell effects, the disappearance of spherical magic numbers, and the onset of deformation and shape coexistence. Isovector quadrupole deformations could develop at the neutron drip-lines, and experimental evidence for the occurrence of low-energy “pygmy” excitations has been reported. Very neutron-rich nuclei also offer the opportunity to study pairing phenomena in systems with strong density variations.

Extremely proton-rich nuclei are important for nuclear structure studies, in astrophysical applications, and for probing fundamental interactions or symmetries. They are characterized by exotic ground-state decay modes such as direct emission of charged particles and  $\beta$ -decays with large Q-values. The phenomenon of proton emission from the ground state has been extensively investigated in medium-heavy and heavy, spherical and deformed nuclei, providing information on the single particle states in these nuclei. More recently direct two-proton decay from  $^{45}\text{Fe}$  and  $^{54}\text{Zn}$  has been observed.

Studies of a particular species of exotic nucleus usually begin with establishing its existence. This can mean identifying it by N and Z and placing a lower limit on its lifetime or by measuring its radioactive decay and hence the half-life, i.e the average time needed for half of the considered nuclei to disintegrate. These steps often precede the measurement of its mass. The probability of  $\beta$ -decay to states in the daughter nucleus provides information on the degree of overlap between the neutron and proton states in the parent and daughter nucleus. When the radioactive decay populates excited states of the daughter nucleus, observation of the radiation associated with their de-excitation yields invaluable spectroscopic information on the energies and characteristics of low-lying excited states. This spectrum of states enables one to characterise the structure of the daughter nucleus, concerning, e.g., its rigidity, its deformation or the arrangement of its particles. This information is supplemented by studies using reactions, which make it possible to reach states not populated in radioactive decay.

The production cross-sections for reactions induced by radioactive ions can only be estimated at present. In the case of fusion-evaporation or deep-inelastic reactions the general trend is that, for a given evaporation or transfer channel, the cross-section decreases with increasing distance of the composite system from  $\beta$  stability, making the synthesis of exotic nuclei increasingly difficult. Nevertheless, one can optimistically assume that the loss in intensity compared to reactions induced by beams of stable isotopes is compensated by the combined gain with respect to production cross-section for the isotope of interest, purity of its production compared to that of contaminants and improvements in the techniques for detecting exotic nuclei and their decay radiation.

***Identification, mass measurements and radioactivity studies of exotic nuclei at SPIRAL2***

*At SPIRAL2, ground-state properties of exotic nuclei can be studied either in the low-energy experimental hall (LIRAT) or after postacceleration in the high-energy area. The latter method is chosen if the nuclear state of interest is too short-lived to be released from the target/ion source system including, in particular, unbound nuclei, or is produced there in*

*too low quantity due to the low release efficiency for (short-lived) nuclei of certain elements. Accelerated beams of radioactive nuclei delivered by CIME at specific energies of the order of 3 to 20 MeV/nucleon can be used to induce reactions for producing and investigating nuclei that are even further away from stability (and thus more short-lived) than the isotopes delivered by the target/ion source system. In this case the nuclei are studied after recoiling from a thin target, mass analysis and capture on a suitable foil or tape. Experiments in the high-energy area will use multinucleon-transfer and fusion-evaporation reactions, yielding neutron-rich and neutron-deficient isotopes, respectively (Coulomb excitation is not considered in connection with the topic 'masses and drip lines'). A particularly attractive feature of these 'production paths' compared to fragmentation reactions is that the former predominantly populate high-spin states.*

*Examples of CIME beams that are relevant for inducing, e.g., fusion-evaporation or multinucleon-transfer are  ${}^6\text{He}$ ,  ${}^{60}\text{Zn}$ ,  ${}^{62}\text{Zn}$ ,  ${}^{80}\text{Zn}$ ,  ${}^{74}\text{Kr}$ ,  ${}^{90}\text{Kr}$  and  ${}^{140}\text{Xe}$ , their intensities ranging from  $10^6$  to  $10^{11}$  atoms/s. The latter values are, of course, orders-of-magnitude below the intensities of stable-isotope beams, which have reached levels of  $10^{11}$  to  $10^{13}$  atoms/s in recent experiments on such reactions at similar beam energies. Taking the case of the  $(21^+)$  isomer of  ${}^{94}\text{Ag}$ , a ratio of  $0.8 \times 10^{-12}$  between secondary and primary beam intensity can be assumed for a production cross-section of 70 nb. This recent experiment on direct and  $\beta$ -delayed charged-particle decay has reached a sensitivity that corresponds to production cross-sections well below the nb level and beam intensities of atoms/h for the radioactive isotope of interest.*

to production cross-section for the isotope of interest, purity of its production compared to that of contaminants and improvements in the techniques for detecting exotic nuclei and their decay radiation. While the spectroscopic aspects of using these as well as Coulomb excitation and single-nucleon transfer reactions will be described elsewhere in this text, the focus here is on determining masses and decay properties of ground states and long-lived isomeric states. The relevant decay modes are the direct emission of nucleons and clusters as well as  $\beta$ -decay, including  $\beta$ -delayed emission of  $\gamma$ -rays, nucleons and clusters. In addition to mass, lifetime and decay modes, a nuclear state has additional properties like spin, parity and nuclear moments. The measurement of these properties is important for testing nuclear model predictions.

### **2.1.1 The quest for new nuclides**

Of the 5000 to 7000 nuclei predicted to be bound in their ground state, about 2000 have been observed to date. The identification of new, or more correctly previously unobserved, nuclei often opens novel fields of investigation, leading to discoveries such as nuclei with neutron and proton halos, the disappearance of “shells”, “molecular” structures in nuclei, new types of pairing and new regions of deformation. Thus, one of the prime objectives of SPIRAL2 will be to produce new nuclei with the aim of giving access to new areas of the nuclear chart and, in particular, to approach the drip lines. The current nuclear models do not agree on the position of these limits to the existence of nuclei and thus the observation (or non-observation) of a nucleus in the vicinity of the drip line places a strong constraint on nuclear theory.

In addition to the bound nuclides, some unbound systems survive for a sufficiently long time that their properties can be determined. Such nuclides represent resonances located beyond the drip line. Very often these resonances correspond to systems which, from the point of view of classical mechanics, would be stable because the release of any of their

component nucleons would require a temporary addition of energy to surmount the potential (energy) barrier. It is quantum mechanics, permitting the passage of particles through such potential barriers, which makes these systems particle-unstable. These nuclides at the edges of nuclear existence highlight various phenomena related to the binding of nucleons in the nucleus.

Nuclei can also be found in excited states with lifetimes much longer than the states around them in excitation energy, called “isomers”, which allow one to investigate variations of some characteristics such as shape or speed of rotation in comparison to those of the ground state of the nucleus under consideration. Because their internal structure is very different from the states below them their decay is inhibited. As a result it is possible to make such states in nuclei very far from stability, where the ground state is unbound to particle emission, and hence study them. One disintegration mode that we anticipate must occur that has not yet been observed is neutron radioactivity from an isomeric state. In this case the state would be unbound energetically but would face a potential barrier because the neutrons are in high orbital angular momentum states and face a potential barrier because of that. Under these circumstances the state may decay by neutron emission by quantum-mechanical tunnelling through the barrier. This hitherto unobserved phenomenon of direct one-neutron or two-neutron radioactivity has to be distinguished from corresponding  $\beta$ -delayed decay modes that are a common feature of very neutron-rich isotopes. In these cases the beta decay populates a state above the energy threshold for neutron decay which occurs promptly.

***Discovery of new nuclides at SPIRAL2: long-lived isomers and nuclei beyond the drip lines***

*SPIRAL2 will allow one to synthesise new nuclei and thus extend the limits of our knowledge. So far, the production of exotic nuclei was mainly achieved by using MeV/nucleon to GeV/nucleon beams of stable nuclides, the use of beams of radioactive isotopes for inducing nuclear reactions being in its infancy. The intense beams of stable nuclides from SPIRAL2 will make it possible to exceed the present limits, both on the neutron-rich and proton-rich slope of the valley of stability. In general, the identification of a new nucleus indicates that it has 'survived' the separation process, thus yielding a lower limit for its half-life. Further information on its decay mode(s) is often obtained already in the identification measurement.*

*The broad, hence short-lived, resonances forming the ground state or low-lying excited states of unbound nuclei can be reached by direct reactions induced by, e.g.,  ${}^6\text{He}$  beams. For example, the 'superheavy' isotopes of hydrogen and helium,  ${}^5\text{H}$  and  ${}^7\text{He}$ , which represent a research topic of considerable current controversy, can be produced in the reactions  ${}^9\text{Be}({}^6\text{He}, {}^5\text{H}){}^8\text{Li}$  and  ${}^9\text{Be}({}^6\text{He}, {}^7\text{He})\alpha$ . In the latter case, the experimental trigger on two  $\alpha$  particles promises excellent experimental sensitivity.*

*The first possibility for 'hunting new nuclides' will be given by using low-energy beams at LIRAT. Here a tape collector equipped with a  $\beta$ - $\gamma$  detector array will be used. The alternative experimental facility for searching for new nuclei will make use of fusion evaporation or deep-inelastic reactions induced on stable-nuclide targets by radioactive-ion beams accelerated by CIME. In this case, a magnetic spectrometer, combined with time-of-flight techniques and a detector array for charged particles, neutrons and  $\gamma$ -rays are appropriate. The latter array will be placed either around the target or at the focal plane of the spectrometer, where implantation and decay-tagging methods will be used.*

## 2.1.2 Nuclear masses

There are many reasons for measuring the masses both of nuclei in their ground or isomeric states, and of short-lived, unbound resonances. The development of nuclear structure models crucially depends on masses as experimental input. Such data are particularly valuable

if obtained for long chains of isotopes or isotones and extend (far) beyond the well-known shell-closures for stable nuclei. Mass measurements are also important as input in nuclear astrophysics, and in studies of fundamental symmetries and interactions.

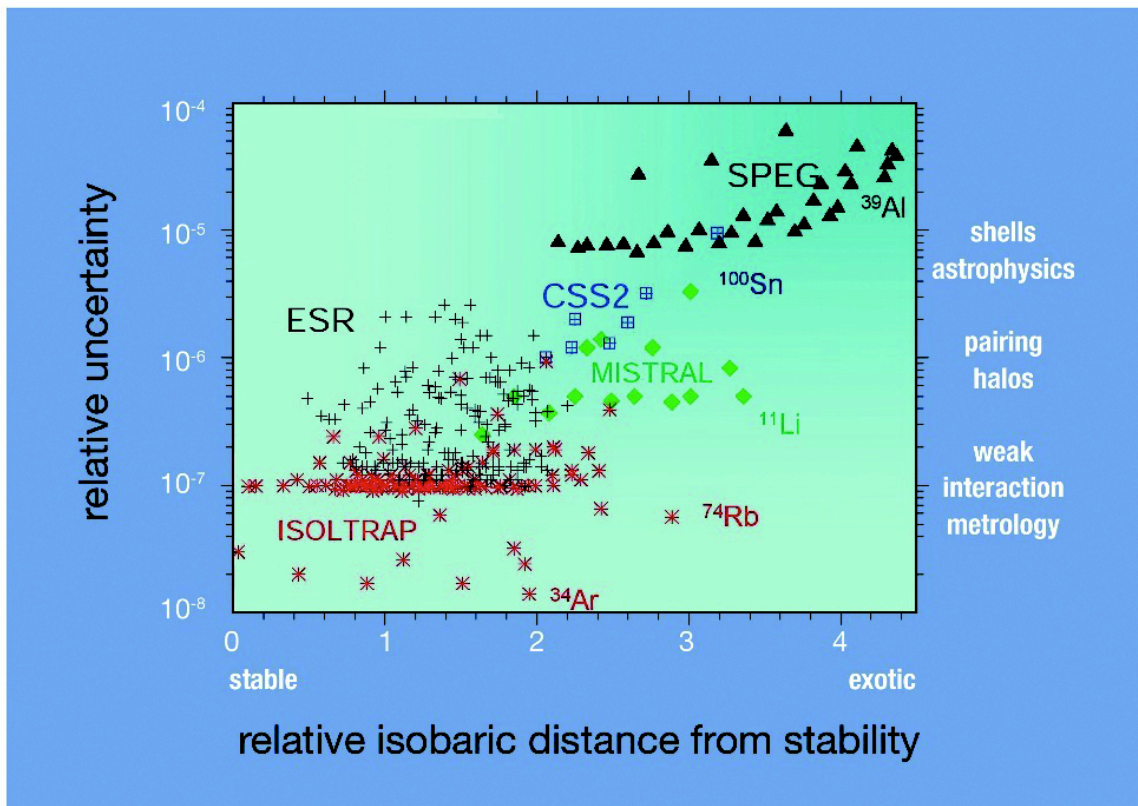


**Figure 2.1.1:** Relative uncertainty of mass data plotted as a function of weighted isobaric distance from stability. The experimental data, taken from papers published since 1994, were obtained by the various (direct) techniques of mass spectrometry. They involve the lengthened time-of-flight basis of a cyclotron (CSS2) at GANIL, the Experimental Storage Ring (ESR) at GSI, the ion trap at ISOLDE/CERN (ISOLTRAP), the radio-frequency transmission spectrometer (MISTRAL) at ISOLDE/CERN and the high-resolution spectrometer (SPEG) at GANIL. On the right-hand side of the figure, the physics topics are indicated that are associated with the required uncertainty.

Attempts to develop theoretical models that can accurately estimate nuclear masses go back to the 1935 semi-empirical mass formula of von Weizsäcker. Improvements of this early liquid-drop mass formula have led to the development of macroscopic-microscopic models, in which microscopic corrections to the liquid drop part are introduced in a phenomenological way. In this framework the macroscopic and microscopic features are treated independently, with both parts being related to the experimental masses exclusively by a parameter fit. Later developments incorporated empirical properties of infinite and semi-infinite nuclear matter, and the finite-range character of nuclear forces. Until recently nuclear masses were calculated using various versions of the empirical liquid-drop model, the most sophisticated being the finite-range droplet model (FRDM). Although the FRDM formula is very successful in fitting experimental masses beyond nitrogen with a root mean square (rms) deviation of 0.66 MeV, it suffers from major shortcomings. Among them are the incoherent link between the macroscopic part and the microscopic correction, the instability of the mass predictions to different parameter sets, and the instability of the shell correction. These make the mass predictions unreliable for ground and excited states of nuclei far away from the

experimentally known region. However, generally speaking, the better the microscopic foundations of a mass formula, the better one would expect its predictive power to be.

An interesting recent development is the first macroscopic-microscopic mass formula which separates, on the one hand, saturation and single-particle properties and, on the other hand, a residual interaction that permits the method to be pushed beyond pure mean-field by admitting a general configuration mixing. As far as microscopic models are concerned, the framework of self-consistent mean-field models is particularly suited for large-scale calculations of nuclear masses. This approach to nuclear structure represents an approximate implementation of Kohn-Sham density functional theory, and it enables a description of the nuclear many-body problem in terms of a universal energy density functional.

In fact, one of the major goals of modern nuclear structure is to build a universal energy density functional, in the sense that the same functional is used to describe all properties for all nuclei with the same set of parameters. The first step in this direction has been achieved with the construction of self-consistent Skyrme Hartree-Fock (HF) and Skyrme Hartree-Fock-Bogoliubov (HFB) mass formulae, which have been shown to compete with the most accurate droplet-like formula in terms of reproducing the experimental masses with the same level of accuracy.

These new mass predictions consider modified parametrisations of the effective interaction (in particular the nucleon effective mass and nuclear-matter symmetry energy), as well as the role of the density dependence of the pairing force and the restoration of broken symmetries. In addition, although the effective interactions have been adjusted only to masses, they also give excellent results in the prediction of absolute charge radii and charge isotope shifts. Figure 2.1.2 compares FRDM and HFB-9 masses for all nuclei with  $8 \leq Z \leq 110$ , lying between the proton and neutron drip lines. Large deviations, caused in particular by different shell and deformation effects are found. When compared to droplet-like models, the HFB mass formulas show a weaker (though not totally vanishing) closure of neutron shells near the neutron drip line.

Despite the better quality of the Skyrme-HFB mass formulae, a number of improvements in the description of the interaction, particularly the pairing force, symmetry-breaking effects and many-body correlations, are crucially needed. These include, for example, the highly localized  $T=0$  neutron-proton pairing correlations that are of importance for  $N \approx Z$  nuclei, or the interplay between the Coulomb and strong interactions which could be at the origin of the Nolen-Schiffer anomaly, i.e. the systematic reduction of the estimated differences between binding energies of mirror nuclei with respect to experiment. Additional correlations, related to the restoration of broken symmetries and to fluctuations in collective degrees-of-freedom around a static mean field state also need to be taken into account with improved techniques.

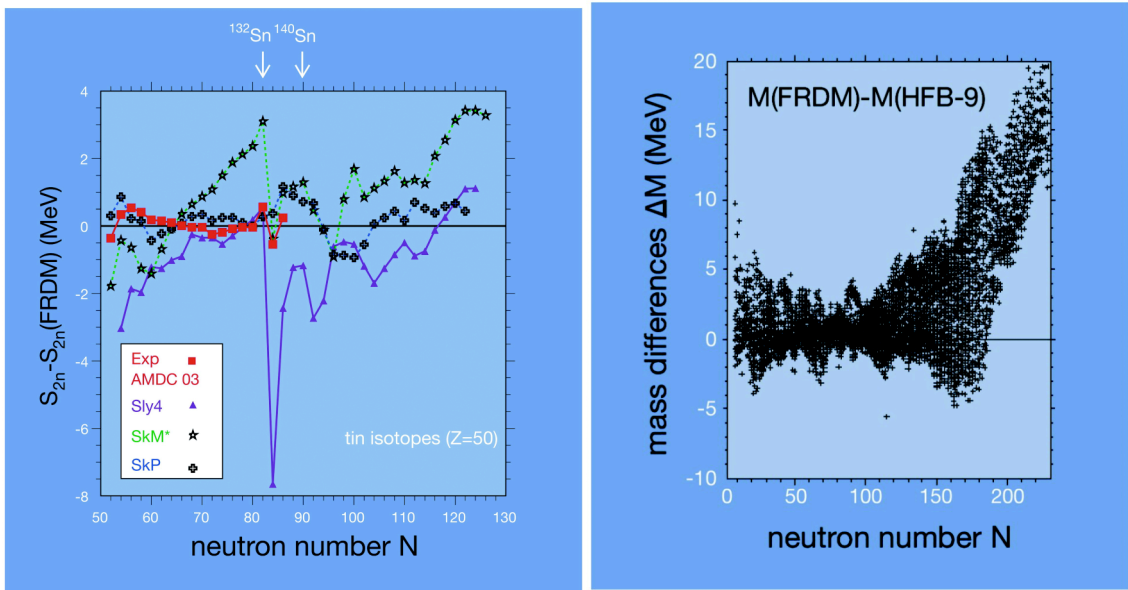


**Figure 2.1.2:** Left: Differences between two-neutron separation energies ( $S_{2n}$ ) calculated with the finite-range droplet model (FRDM) and measured values for the tin isotopes. Also shown are the differences between FRDM and the predictions from the HFB model assuming various parametrisations of nucleon-nucleon effective interactions (Sly4, SkM\*, SkP). Right: Predictions of nuclear masses: Differences  $\Delta M$  between the results of (FRDM) and the Hartree-Fock-Bogoliubov calculations (HFB-9), plotted as a function of the neutron number  $N$ .

The Generator Coordinate Method (GCM) of projected mean-field states enables a description of ground state correlations on the same footing as collective excitations. Such a scheme has recently been introduced and applied to a study of the quadrupole correlation energy of about 600 even-even nuclei. While the correlation energy on the average does not depend much on the mass and isospin of the system calculated, it shows fluctuations that are clearly related to shell structure and locally modify the mass surface. This is particularly evident around doubly-magic nuclei. In taking it further it will also be important to include additional correlation modes such as dynamical pairing correlations, or octupole vibrations, to find a way to describe odd nuclei effectively in the same framework.

In order to constrain better the properties of the effective interaction that determine the masses far from stability we need more information, from excited states for instance. At the same time it is clearly essential to establish a link to ab-initio methods. For instance, an effective pairing interaction for mean-field calculations has recently been derived from the bare nucleon-nucleon force. Initial applications to finite nuclei are promising, but more work in this direction is clearly needed. Future shell model calculations (e.g. the quantum Monte-Carlo approach) will certainly provide further insight into the nuclear properties of exotic nuclei (e.g. shell model calculations have recently revealed the importance of the spin-isospin dependent part of the nucleon-nucleon interaction in the prediction of the  $N=8, 20$  magicity for neutron-rich nuclei) and guide mean-field models in the quest for a universal effective interaction.

Nuclear masses are usually measured either “indirectly” using a reaction or radioactive decay and energy conservation or “indirectly through frequency or time-of-flight

measurements. While the former methods involve a knowledge of the details of the relevant reaction or decay, the latter involve the calibration of the corresponding frequency or time-of-flight scale.

The masses of very exotic nuclei, that are important for the understanding of nuclear structure and of astrophysical nucleosynthesis-processes, have to be measured with an accuracy ranging from  $10^{-7}$  to  $10^{-5}$ . Of particular interest are neutron-rich isotopes with mass numbers between 80 and 160 as the shell structure is predicted to be modified with the weakening of the well-known magic numbers ( $Z=28$ ;  $N$ ,  $Z=50$ ;  $N=82$ ) and the possible appearance of new shell gaps.

### ***Measuring nuclear masses at SPIRAL2***

*With SPIRAL2, direct mass measurements will be performed in the low-energy area either by making the radioactive ions of interest oscillate in electromagnetic traps or by time-of-flight through a second cyclotron or through a suitable spectrometer. Alternatively, they can be accelerated in the cyclotron CIME, using it as a time-of-flight spectrometer. This acceleration is only possible if the forces of containment (magnetic fields) and the frequency of acceleration (high-frequency oscillating electric fields) are matched exactly to the inertia of the nucleus. The power of direct time-of-flight mass spectrometry, based on the measurement of the phase of the accelerated ions for different radio-frequencies, has been demonstrated at GANIL by using the cyclotron CSS2 to measure the mass of  $^{100}\text{Sn}$ .*

*The strategy of the mass measurement will be to determine a few selected masses with high accuracy and to use these data for calibration of experimental devices such as time-of-flight spectrometers that are able to measure the masses of several nuclides in one experiment. Their mass will be deduced by simultaneously measuring their momentum (with a magnetic spectrometer) and their speed (by time-of-flight over a fixed distance). The mass of nuclei produced by bombarding a target with radioactive-ion beams accelerated by CIME, will be measured in the same way. In the chain of tin isotopes, for example,  $^{134}\text{Sn}$  is the heaviest nucleus with known mass. By using  $^{238}\text{U}(^{140}\text{Xe}, 2p)$  multinucleon-transfer reactions and applying a two-proton trigger,  $^{138}\text{Sn}$  will be reached. The determination of the mass of this nucleus is important since it corresponds to an extension of the chain of tin isotopes by 6 neutrons beyond the  $N=82$  shell closure.*

The mass or binding energy of a particle-unbound resonance can be obtained by a complete kinematical study of direct reactions. The unknown mass as well as the Q-value of, e.g., (d,p) transfer reaction can be obtained with good resolution using the new concept of an active target. Two other examples of such single-nucleon transfer reactions have already been mentioned above, namely the reactions  $^9\text{Be}(^6\text{He}, ^5\text{H})^8\text{Li}$  and  $^7\text{He}^9\text{Be}(^6\text{He}, ^7\text{He})\alpha\alpha$ , leading to 'superheavy' isotopes of hydrogen and helium.

## **2.1.3 Radioactivity of neutron-rich nuclides**

### **Theoretical aspects of the neutron drip line and open quantum systems**

Studies of short-lived nuclei far from  $\beta$ -stability offer a unique test of those aspects of the many-body problem that depend on the isospin degree-of-freedom. The challenge to microscopic theory is to predict and provide reliable calculations of the properties of these exotic systems. For medium-mass and heavy nuclei, the objective is a universal energy density functional, that will enable a description of finite nuclei (static properties, collective states, large-amplitude collective motion), as well as extended asymmetric nucleonic matter

(e.g. as found in neutron stars). When extrapolating from ordinary stable nuclei to extended nuclear matter found in very neutron-rich nuclei, a number of effects have to be taken into account. The diffuseness of the neutron surface implies that the gradient terms in the density functional are as important in defining the energy relations, as those depending on the local density. When approaching the one-nucleon drip line, pairing correlations become as important as mean-field effects. Pairing correlations modify the asymptotic properties of single-nucleon densities and, therefore, the dependence of weakly-bound systems on the detailed features of effective nuclear interactions is much stronger than in ordinary stable nuclei. Such a microscopic calculation necessitates a simultaneous description of particle-hole, pairing, and continuum effects - a challenge that could only be addressed very recently by mean-field methods.

In addition to the intrinsic nuclear structure interest, many properties of nuclei far from the valley of  $\beta$ -stability are crucial for a deeper understanding of the nuclear processes governing stellar nucleosynthesis. From a theoretical point of view, the principal goal is to achieve a consistent picture of structure and reaction aspects of weakly bound and unbound nuclei, which requires an accurate description of both the many-body correlations and the continuum of positive-energy states and decay channels. A coherent description of the relation between scattering states, resonances and bound states in the many-body wave function necessitates a close interplay between methods of nuclear structure and reaction theory. This mutual cross-fertilisation presents an opportunity to open a new era in the theory of loosely bound systems.

### Measurement of decay properties of neutron-rich isotopes

The properties of neutron-rich isotopes, in particular the doubly closed shell nuclei  $^{48}\text{Ca}$  ( $Z=20$ ,  $N=28$ ),  $^{78}\text{Ni}$  ( $Z=28$ ,  $N=50$ ),  $^{132}\text{Sn}$  ( $Z=50$ ,  $N=82$ ) and their nearest neighbours are of considerable nuclear-structure and astrophysical interest, some of them being candidates for waiting points in the astrophysical r-process. In this context, the study of the features of radioactive decay plays a crucial role. Most of the recent progress in decay experiments has been achieved by using fragmentation, fission or multinucleon-transfer reactions. In the last of these, stable isotopes such as  $^{48}\text{Ca}$  or  $^{64}\text{Ni}$  have been used as projectiles and  $^{238}\text{U}$  as the target. For example, a challenging test of shell-model predictions beyond the double shell-closure at  $^{48}\text{Ca}$  has been achieved by identifying excited states of  $^{54}\text{Ti}$  ( $Z=22$ ). This work was based on combining a study of the  $\beta$ -decay of  $^{54}\text{Sc}$ , created in fragmentation reactions, with a measurement of the population of high-spin states in  $^{64}\text{Ni} + ^{238}\text{U}$  multinucleon-transfer reactions. Further investigations of the latter type of reaction may help to clarify the optimum kinematical conditions (projectile energy, target thickness, angle of ejectile emission) for this promising method of synthesis.

The spectroscopic information on  $^{78}\text{Ni}$  is rather poor to date since it is restricted to the half-life. This quantity was measured following its production in the fragmentation of relativistic beams of stable isotopes. An experiment based on  $^{238}\text{U}$  fission yielded a lower limit while a value of about 0.1 s was recently found following  $^{86}\text{Kr}$  fragmentation. The decay properties of  $^{132}\text{Sn}$  and its nearest neighbours are fairly well known. The heaviest silver-to-indium isotopes with known properties below  $^{132}\text{Sn}$  are  $^{130}\text{Ag}$  ( $Z=47$ ),  $^{133}\text{Cd}$  ( $Z=48$ ) and  $^{135}\text{In}$  ( $Z=49$ ). One of the future tasks for experimenters will be to gain information on the nearest neighbours of  $^{78}\text{Ni}$ , to go beyond the neutron shell closures at  $N=50$  and  $N=82$ , and to search for neutron-radioactive isomers. The latter phenomenon, which has not been observed to date, has been predicted to occur, e.g., in  $^{63}\text{Ti}$  ( $Z=22$ ) as a  $\{p(1f_{7/2}^2)_{6+n}(1g_{9/2})\}_{21/2^+}$  configuration with a half-life of 4 s, and in  $^{67}\text{Fe}$  ( $Z=26$ ) as a  $\{p(1f_{7/2}^2)_{6+n}(1g_{9/2})\}_{19/2^+}$  configuration with a

half-life of 50  $\mu$ s. Concerning the two-neutron radioactivity, in particular for nuclear states whose decay by one-neutron emission is energetically forbidden, it probably needs much greater progress in experimental approaches towards and beyond the one-neutron and two-neutron drip lines, before a firm basis will be reached for planning a search for two-neutron radioactivity.

### ***Search for direct neutron radioactivity of isomers at SPIRAL2***

*CIME beams of neutron-rich isotopes, e.g.,  $^{80}\text{Zn}$ ,  $^{90}\text{Kr}$  and  $^{140}\text{Xe}$ , and  $^{238}\text{U}$  targets will be used to perform in-beam and decay spectroscopy of neutron-rich isotopes and to search for the hitherto unobserved phenomenon of neutron radioactivity. The attempts will focus on very neutron-rich nuclei near the double shell closures at  $^{48}\text{Ca}$ ,  $^{78}\text{N}$  and  $^{132}\text{Sn}$ .*

*It is admittedly somewhat speculative to assume that the neutron-unbound isomers in  $^{63}\text{Ti}$  and  $^{67}\text{Fe}$  exist and will be produced in useful quantity by means of  $^{80}\text{Zn}$  or  $^{90}\text{Kr}$  induced multinucleon-transfer reactions on  $^{238}\text{U}$  targets. The transfer channels correspond to the stripping of 8 protons and 9 neutrons off the projectile in the former and 10 protons and 13 neutrons in the latter case. However, the main yield flow of such reactions is governed by N/Z equilibration between projectile and target. This ratio is approximately the same for reaction partners and residues, hence an appreciable production cross-section can be expected. The search for neutron radioactivity will be performed by using a magnetic spectrometer such as VAMOS and ancillary detectors for neutrons, charged-particle and  $\gamma$ -rays. These detectors will be placed both at the target position and at the focal plane of the spectrometer. In the former case, the high multiplicity of the emitted protons and neutrons will be used as a trigger yielding high sensitivity.*

### ***In-beam and decay spectroscopy of neutron-rich isotopes***

*Concerning decay measurements on  $^{78}\text{Ni}$ ,  $^{132}\text{Sn}$  and neighbouring nuclei, one of the tasks is to try to synthesise, for example,  $^{130}\text{Ag}$ ,  $^{133}\text{Cd}$  and  $^{135}\text{In}$ , the most neutron-rich isotopes identified so far for these three elements. The decay of some of the comparatively long-lived nuclei among them can already be studied in the low-energy area, making use of a tape collector and a  $\beta$ - $\gamma$ -neutron detector array. However, the more neutron-rich isotopes will be investigated by in-beam and decay spectroscopy in the high-energy area, making use of similar reaction and detection techniques as described in connection with the search for neutron radioactivity. Examples of relevant multinucleon-transfer reactions are, e.g.  $^{238}\text{U}(^{90}\text{Kr}, 8p4n)^{78}\text{Ni}$  and  $^{238}\text{U}(^{140}\text{Xe}, 7p2n)^{130}\text{Ag}$ , which probably represent weaker channels than those mentioned above. Two separate measurements with the  $\beta$ - $\gamma$ -neutron detector array will be performed, namely one with high-resolution  $\gamma$ -ray detectors and another one with a total absorption  $\gamma$ -ray spectrometer. This double strategy is required in order to avoid the problem of missing  $\gamma$  intensity in high-resolution measurements of  $\beta$ -delayed  $\gamma$  radiation.*

## **2.1.4 Radioactivity of proton-rich nuclides**

### **The proton drip line and proton radioactivity**

Experimentally, the proton drip line has been fully mapped up to  $Z=30$  and, in a fragmentary way, for odd- $Z$  nuclei up to  $Z=91$ . The whole spectrum of theoretical models has been employed in mapping the proton drip line. These include the finite-range droplet model, the semi-empirical shell-model mass formula, and the framework of non-relativistic and relativistic self-consistent Hartree-Fock and Hartree-Fock-Bogoliubov models (see figure 2.1.3). In general, a very good agreement has been found between the proton drip lines predicted by these models, and the experimental results for odd- $Z$  elements.

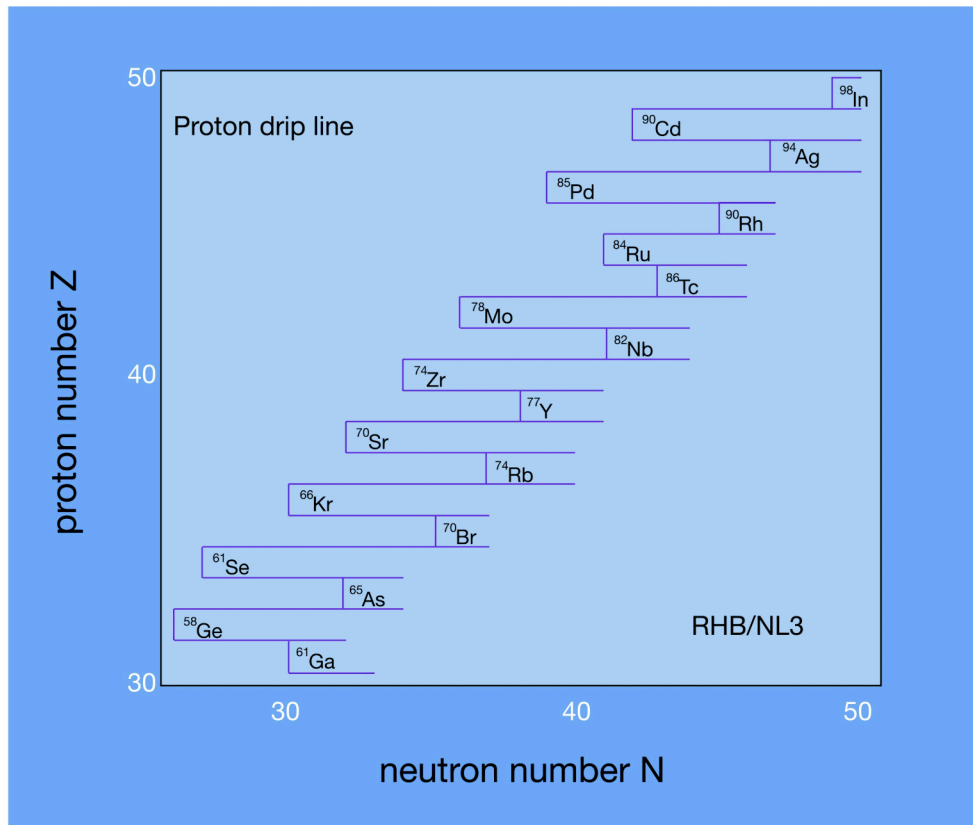


**Figure 2.1.3:** Section of the chart of nuclides in the region below  $^{100}\text{Sn}$ , showing the results of a relativistic Hartree-Bogoliubov calculation for the proton drip line of elements from gallium ( $Z=31$ ) to indium ( $Z=49$ ). For each element the figure indicates the lightest isotopes of each element, whose ground state is predicted to be bound against one-proton emission. Experimental information is not available at all for even- $Z$  nuclei near the proton drip line and is very scarce for odd- $Z$  nuclei beyond the drip line, such as  $^{69}\text{Br}$ ,  $^{76}\text{Y}$  or  $^{73}\text{Rb}$ . All the marked odd- $Z$  nuclei, i.e.  $^{61}\text{Ga}$  to  $^{74}\text{Rb}$ ,  $^{77}\text{Y}$  and  $^{82}\text{Nb}$  to  $^{98}\text{In}$ , have been reached in experiment. However, the knowledge of their decay data properties is rather limited and in general far from meeting the requirements of nuclear structure theory, astrophysical applications, or studies of fundamental symmetries.

Model predictions of the location of the proton drip line are important for the synthesis of new elements, nuclear structure studies, astrophysical applications, or for probing fundamental interactions or symmetries. All the recently discovered isotopes of the superheavy elements, in particular, belong to very neutron-deficient systems. The properties of neutron-deficient nuclei are also relevant to our understanding of nucleosynthesis by the rapid proton (rp) capture process.

Decay by direct proton emission provides the opportunity to study the structure of unbound systems even beyond the drip line. The phenomenon of ground-state proton radioactivity is determined by a delicate interplay between the nuclear attraction and the Coulomb and centrifugal terms of the effective potential. Although the highest-lying protons occupy states with positive energy, they still experience the Coulomb and centrifugal barriers. Ground state proton emission is thus dictated by quantum-mechanical tunnelling. The emitted proton is characterized by a discrete value of the energy and a resonance width or its inverse, the half-life. While proton unbound nuclear ground states below  $Z=50$  exist only as broad, short-lived resonances, because of the relatively high potential energy barriers the protons

face, such states in medium-heavy and heavy nuclei are narrow and long-lived, which facilitates their observation.

At the drip-line, proton emission competes with  $\beta^+$ -decay, whereas for heavy nuclei fission and  $\alpha$ -decay also have to be taken into account. For most elements one has to go beyond the drip line by several isotopes, before proton emission becomes the dominant decay mode. Proton radioactivity in odd- $Z$  nuclei has been investigated in the two spherical regions from  $51 \leq Z \leq 55$  and  $69 \leq Z \leq 83$ , as well as in a series of strongly deformed nuclei in the light rare-earth region. Proton-radioactive ground states have been observed in almost all odd- $Z$  nuclei between tin ( $Z=50$ ) and bismuth ( $Z=83$ ). Proton emitters with even- $Z$  are much more difficult to find, because in nuclei with an even number of protons the residual pairing interaction produces extra binding, which makes them more stable with respect to the neighbouring odd- $Z$  nuclei. A theoretical description of spherical proton emitters is relatively simple, but accurate models for proton decay rates from deformed nuclei have been developed only very recently. Even the most realistic calculations, however, are not based on a fully microscopic and self-consistent description of proton unstable nuclei. It is still not possible, for instance, to predict within the same theoretical framework which nuclei are likely to be proton emitters, and to calculate the respective decay rates.

The half-life for proton emission depends mainly on the spectroscopic factor and the penetrability. The spectroscopic factor describes the overlap of the wave functions of parent and daughter states, and thus carries information on their structure. Concerning the penetrability, the Coulomb barrier is lower than in the case of  $\alpha$ -decay, since it depends linearly on the charge of the emitted particle, whereas the centrifugal barrier is higher, since it depends inversely on the mass, and this implies a greater dependence on the orbital angular momentum.

A particularly interesting proton transition is that from an odd-even nucleus to the ground state of its even-even daughter. For nuclei in which either neutrons or protons are close to a magic number, the spectroscopic factor is just the probability that the single particle level of the last unpaired proton is found empty in the daughter nucleus. The emitted proton has the angular momentum of the odd-proton state, i.e. the angular momentum of the single particle level closest to the Fermi surface. Since the half-life depends strongly on the angular momentum, in this case it is possible to determine the position of the Fermi surface and the properties of the mean field far away from stability. In the region of light rare-earth nuclei most proton emitters have pronounced quadrupole deformations. The calculation of the penetrability is much more complicated in this case, because the barrier is two- or three-dimensional (if one takes into account the possibility of a non-axial deformation). This very difficult problem has been solved only recently, either by obtaining solutions for resonances in a deformed potential, or by integrating the coupled-channel Schrödinger equation. For these nuclei the angular momentum of the ground state of the odd- $Z$  parent nucleus can be different from the angular momentum of the single-particle level occupied by the unpaired proton. The spectroscopic factor depends not only on the occupation probability, but also on the amplitude of the component of the Nilsson wave function with angular momentum equal to that of the ground state. Therefore, in addition to the position of the Fermi surface, it is possible to obtain detailed information on components of the wave function that can be quite small and not detectable by other means.

Another important case is proton emission from odd-odd nuclei. The daughter nucleus has an odd number of nucleons, and its angular momentum is determined by the Nilsson level

occupied by the odd neutron. Different combinations of the angular momenta of the odd neutron and the emitted proton are possible. The odd neutron, therefore, behaves as an “influential spectator” and, without actively participating in the decay, affects the corresponding half-life.

Below  $Z=50$ , proton decay from the ground state has not been observed experimentally, but some excited proton-emitting states have been identified with long half-lives in  $^{53}\text{Co}$  and  $^{94}\text{Ag}$  and in nuclei near the doubly magic  $^{56}\text{Ni}$ . In the last of these cases, the decaying states are highly deformed whereas the final states are almost spherical. The pronounced difference between the wave functions of the parent and daughter nuclei strongly hinders the decay. Such a process cannot be described within a simple single-particle framework and, therefore, presents a serious challenge for the modelling of proton emission.

Of particular interest are even- $Z$  nuclei that lie beyond the two-proton drip line but cannot, because of the presence of pairing correlations, decay by emitting one proton. In these cases, sequential emission of two protons is forbidden, because the intermediate nucleus is energetically not accessible. The two protons, therefore, have to be emitted simultaneously. Despite much effort, the present experimental situation concerning this “true three-body decay” is still somewhat confusing. This may improve once angular correlation data become available, e.g., for the recently discovered cases of two-proton radioactivity in  $^{45}\text{Fe}$  and  $^{54}\text{Zn}$ . The theoretical description of this decay necessitates a consistent treatment of configuration mixing, the anti-symmetrization of the many-body wave function in the parent nucleus and the daughter subsystems, and the three-body asymptotics of the final state. These ingredients have recently been included in the microscopic description of di-proton radioactivity in the framework of the continuum shell-model. This allows the study of the relation between the many-body correlations in the parent nucleus, as given by the effective NN interaction, and the asymptotic spatial/energy correlations of the decay products. In this way, one may be able to extract information on the pairing field and its radial dependence from the experimental data on correlations in the true three-body decay.

## Measurement of decay properties of proton-rich nuclides

Experiments on direct proton and two-proton radioactivity have identified emission from ground states as well as isomers. In the case of the latter this includes low-lying, short-lived states of moderate spin and high-spin isomers, identified by the detection of  $\gamma$ -rays and charged-particles. In both cases, fusion-evaporation reactions were used to produce the species of interest.

High-lying spin-gap isomers occur in nuclei below the double shell closures at  $^{56}\text{Ni}$  ( $Z=N=26$ ) and  $^{100}\text{Sn}$  ( $Z=N=50$ ) due to the strong interaction between proton and neutron holes in identical orbits. Such spin-gap isomers present the chance to determine nuclear structure properties of highly unstable, neutron-deficient isotopes in three ways. Firstly, the internal, electromagnetic de-excitation of the isomers can be measured. In this way, individual (single-particle) states and their  $B(E2)$  and  $B(E4)$  rates can be measured. Examples of such studies are the determination of  $B(E4)$  values for the  $12^+$  isomers in  $^{52}\text{Fe}$  (46 s) and  $^{98}\text{Cd}$  (0.23  $\mu\text{s}$ ). A particular challenge is to study the de-excitation of the  $6^+$  isomer that is expected to occur in  $^{100}\text{Sn}$ , and thus to identify for the first time, excited states in this doubly closed-shell nucleus far from the  $\beta$ -stability line. Secondly,  $\beta$ -delayed  $\gamma$ -ray and charged particle emission allows one to deduce information on the properties of excited states of the – still neutron-deficient – daughter nuclei for these disintegration modes. Thirdly, if the isomer is unbound against, e.g., proton, two-proton or  $\alpha$  emission, the possibilities to study these direct (spontaneous) decay modes opens up.

While the proton-radioactive isomer  $^{53\text{m}}\text{Co}$  ( $Z=27$ ) has been known for some time, additional cases of proton emission from short-lived, but well defined excited states were found in nuclei near the doubly magic  $^{56}\text{Ni}$ . Moreover, direct proton and two-proton decay of the truly exotic ( $21^+$ ) isomer in  $^{94}\text{Ag}$  (see figure 2.1.4) was identified recently in the  $^{58}\text{Ni}(^{40}\text{Ca},\text{p}3\text{n})$  fusion-evaporation reaction.

By investigating direct and  $\beta$ -delayed charged-particle decay, with a coincidence condition being set on the (multiple)  $\gamma$ -ray emission, sensitivities have been reached that correspond to production cross-sections well below the nb level and beam intensities of atoms/h for the radioactive isotope of interest. Even though only an upper limit has been determined so far for the internal E4 de-excitation of the ( $21^+$ ) isomer, its decay represents an unusually rich source of nuclear structure information on the parent state as well as high-spin states in the five daughter nuclei  $^{92}\text{Ru}$ ,  $^{92}\text{Rh}$ ,  $^{93}\text{Rh}$ ,  $^{93}\text{Pd}$  and  $^{94}\text{Pd}$ . The remarkable experimental feat in this measurement is that the four decay modes involving proton emission were identified by setting very selective coincidence conditions on the high-multiplicity  $\gamma$ -ray cascade that de-excites the high-spin state(s) in one of the four daughter nuclides.

Further candidates for long-lived proton-unbound isomers are probably  $^{95\text{m}}\text{Ag}$  ( $37/2^+$ ) and  $^{98\text{m}}\text{Cd}$  ( $12^+$ ), which were recently identified by  $\gamma$ -ray spectroscopy, or have been predicted to occur in  $^{96}\text{Cd}$  ( $16^+$ ),  $^{97}\text{Cd}$  ( $25/2^+$ ) and  $^{100}\text{Sn}$  ( $6^+$ ). While the search for proton radioactivity of the first two of these isomers will presumably be the subject of experiments with stable-isotope beams, radioactive-beam induced reactions may be needed to reach the last of them.

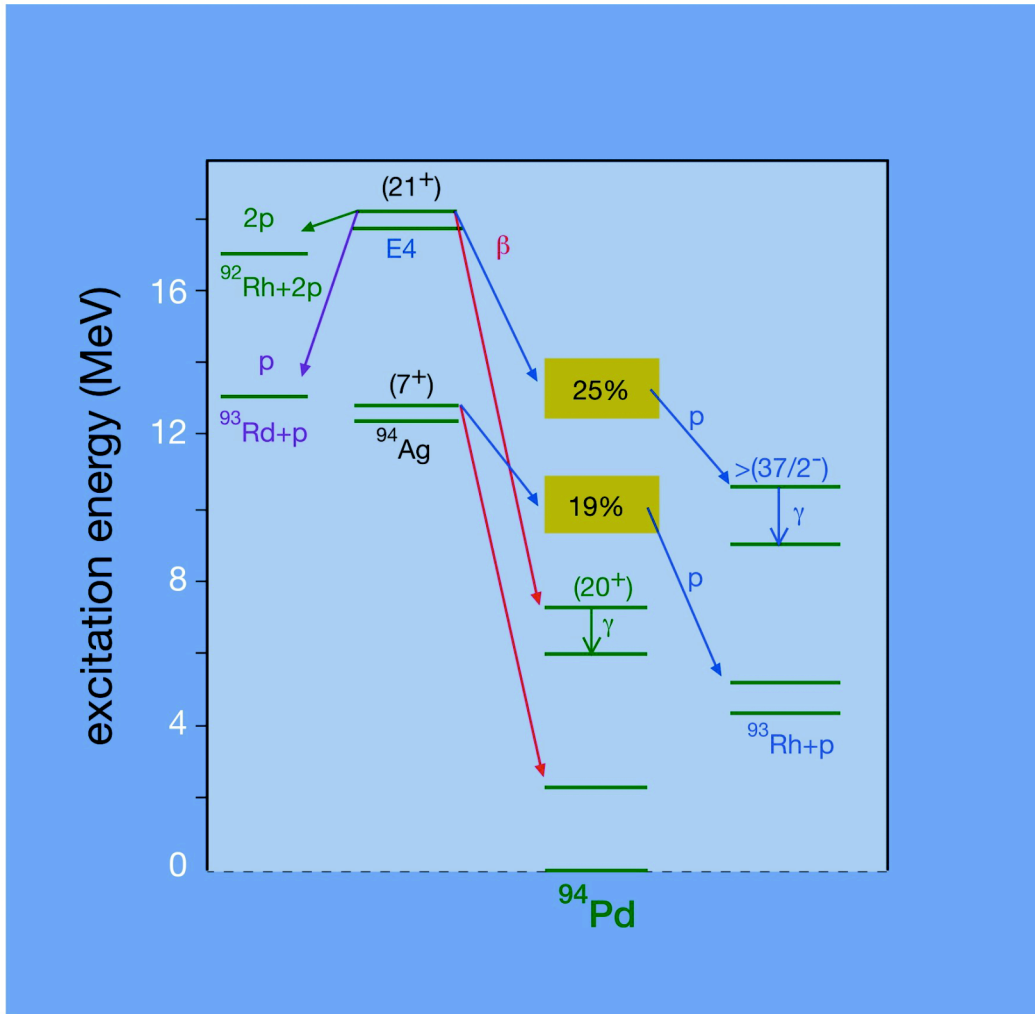


**Figure 2.1.4:** Decay properties of the  $(7^+)$  and  $(21^+)$  isomers in  $^{94}\text{Ag}$ . The half-lives of the isomers are 0.39(4) and 0.51(2) s, respectively. The  $(21^+)$  isomer is unique in the entire Segré chart in terms of the combined features of high spin, high excitation energy of 6.7 MeV, long half-life and five-fold disintegration modes, i.e.  $\beta$ -delayed  $\gamma$ -ray, proton and two-proton emission as well as direct proton and two-proton radioactivity (The  $\beta$ -delayed two-proton decay mode is not shown in the figure).

Another interesting feature of heavy  $N \approx Z$  nuclei is the occurrence of an island of  $\alpha$  emission beyond  $^{100}\text{Sn}$ . Almost forty years ago it was suggested that the reduced width for  $\alpha$ -decay in this region of nuclei should be anomalously large due to an enhanced probability of forming the  $\alpha$  particle from nucleons in identical (shell-model) orbits. Recent experiments have found only weak evidence for this so-called, super-allowed  $\alpha$ -decay of  $^{106}\text{Te}$ ,  $^{110}\text{Xe}$  and  $^{114}\text{Ba}$ , produced in  $^{58}\text{Ni} + ^{58}\text{Ni}$  fusion-evaporation reactions. The experimental sensitivity is comparable to that given above for the  $(21^+)$  isomer of  $^{94}\text{Ag}$ . However, the prime candidates for super-allowed  $\alpha$ -decay are the  $N=Z$  nuclei  $^{104}\text{Te}$ ,  $^{108}\text{Xe}$  and  $^{112}\text{Ba}$ . These nuclei have not been observed so far, due to the low production cross-sections in suitable fragmentation or fusion-evaporation reactions induced by stable-isotope beams, and due to the short half-lives of these  $\alpha$  emitters, which are anticipated to be in the  $\mu\text{s}$  range.

On this island of  $\alpha$  emission beyond  $^{100}\text{Sn}$ , the spontaneous emission of  $^{12}\text{C}$  or other heavy clusters is also expected to occur. This heavy-ion radioactivity is mainly related to the cusp of

the mass-energy surface originating from the double shell closure, corresponding to the situation beyond  $^{208}\text{Pb}$  where numerous such decays have been observed. Identifying heavy-ion radioactivity of trans-tin isotopes would enable one to test more stringently the model predictions. The models differ in their underlying assumptions but all yield reasonably good agreement with the trans-lead data. However, the search for  $^{12}\text{C}$  radioactivity of  $^{114}\text{Ba}$  ( $Z=56$ ), has yielded only an upper limit of  $3.4 \times 10^{-5}$  for a  $^{12}\text{C}$  decay branch. Thus it is indeed a challenge to search for  $^{12}\text{C}$  radioactivity for  $^{112}\text{Ba}$  or other proton-rich nuclei above the double shell closure of  $^{100}\text{Sn}$ .

Last but not least, the  $\beta$ -decay of  $^{100}\text{Sn}$  is a challenging experimental target, as it is expected to populate essentially one and only one  $1^+$  state in  $^{100}\text{In}$ . This ‘Super Gamow-Teller transition’ has not been identified so far, even though experiments with  $^{50}\text{Cr}(^{58}\text{Ni},\alpha 4n)$  fusion-evaporation reactions have reached a sensitivity level of the order of a nb for the production cross-section and atoms/h for the  $^{100}\text{Sn}$  beam-intensity.

***Decay spectroscopy of proton-unbound states at SPIRAL2***

*It is a challenge to search for new cases of direct proton and two-proton decay, including long-lived spin-gap isomers beyond the two already identified in  $^{53}\text{Co}$  and  $^{94}\text{Ag}$ . Such isomers are expected to occur, e.g. in  $^{96}\text{Cd}$ ,  $^{97}\text{C}$  and  $^{100}\text{Sn}$ . Instead of the stable-isotope projectiles ( $^{40}\text{Ca}$ ) used in the  $^{94m}\text{Ag}$  measurement so far,  $^{60}\text{Zn}$  or  $^{74}\text{Kr}$  beams from CIME will be used. They will allow one to study the  $^{40}\text{Ca}(^{60}\text{Zn},\alpha)^{96}\text{Cd}$ ,  $^{40}\text{Ca}(^{60}\text{Zn},2pn)^{97}\text{Cd}$  and  $^{42}\text{Ca}(^{60}\text{Zn},2n)^{100}\text{Sn}$  and  $^{40}\text{Ca}(^{74}\text{Kr},3\alpha 2n)^{100}\text{Sn}$  fusion-evaporation reactions. The experiments will be performed at a magnetic spectrometer and include neutron, charged-particle and  $\gamma$ -ray detection at the target position as well as charged-particle and  $\gamma$ -ray detection at the focal plane.*

***Study of the ‘Super’ Gamow-Teller resonance in the  $\beta$ -decay of  $^{100}\text{Sn}$  at SPIRAL2***

*The  $\beta$ -decay of  $^{100}\text{Sn}$  will be investigated at SPIRAL2 by using either the low-energy (60 keV) beam or radioactive-ion beam induced fusion-evaporation reactions, e.g.  $^{40}\text{Ca}(^{62}\text{Zn},2n)$  or  $^{40}\text{Ca}(^{74}\text{Kr},3\alpha 2n)$ . The latter suggestion is based on the tentative assumption that the sensitivity achieved in radioactive-ion beam induced reactions is beyond that reached by studies involving the stable-isotope induced reaction  $^{58}\text{Ni}(^{50}\text{Cr},\alpha 4n)$ . Both the low-energy and the high-energy experiments involve magnetic separation as well as high-resolution and total-absorption  $\gamma$ -ray spectroscopy. The latter technique is necessary if we are to avoid the problem of missing  $\gamma$  intensity in high-resolution measurements.*

### ***Search for super-allowed $\beta$ -decay and for $^{12}\text{C}$ radioactivity beyond $^{100}\text{Sn}$ at SPIRAL2***

*By using radioactive ion beams from SPIRAL2 in the search for super-allowed  $\alpha$ -decay, the nuclei  $^{108}\text{Xe}$  and  $^{112}\text{Ba}$  will be produced through  $^{40}\text{Ca}(^{74}\text{Kr},\alpha 2n)$  and  $^{40}\text{Ca}(^{74}\text{Kr},2n)$  reactions, respectively. The intensity of the  $^{112}\text{Ba}$  beam produced in this way will, of course, be less than the amount obtained for  $^{114}\text{Ba}$ . This is due to the enhancement of the prompt emission of protons and  $\alpha$  particles versus that of neutrons for the case of  $^{112}\text{Ba}$  compared with  $^{114}\text{Ba}$ . The intensities of  $^{104}\text{Te}$ ,  $^{108}\text{Xe}$  and  $^{112}\text{Ba}$  beams are probably of the order of atoms/d which, however, may still allow one to determine the reduced  $\alpha$  width of these isotopes by measuring their half-life,  $\alpha$ -decay energy and branching ratio for  $\alpha$ -decay. The experimental method to reach this goal involves the measurement of correlated recoil-decay events at a spectrometer. The experiment will also allow one to investigate neighbouring nuclei such as  $^{106}\text{Te}$ ,  $^{108}\text{Xe}$  and  $^{114}\text{Ba}$ , which have been studied without yielding firm evidence for super-allowed  $\alpha$ -decay so far. All these studies will yield  $\alpha$ -decay energies which, by linking them to (daughter) nuclei of known mass, allow one to determine masses of highly unstable  $N=Z$  nuclei.*

*The  $^{40}\text{Ca}(^{74}\text{Kr},2n)$  reaction will also be used to search for the  $^{12}\text{C}$  radioactivity of  $^{112}\text{Ba}$  by using a magnetic spectrometer and the recoil-decay correlation method. The latter has to be developed to meet the challenge of unambiguously detecting a small number of  $^{12}\text{C}$  events of low-energy (21 MeV) in the presence of the dominant  $\alpha$ -decay rate. It will have to be investigated whether a time-projection chamber, which will allow the three-dimensional reconstruction of the tracks of all the decay products, will enable one to identify  $^{12}\text{C}$  emission against the strong background of  $\alpha$  and  $\beta$  particles.*

## **2.2 WEAKLY BOUND HALO, BORROMEAN AND CLUSTER SYSTEMS**

### **2.2.1 Borromean and Other Three-body Nuclei**

Weakly bound systems provide a sensitive test of the nuclear force, and the neighbourhood of the drip-lines provides a unique proving ground for the development of our understanding of this interaction which is of fundamental importance. Figure 2.2.1 shows how the three-body system changes as we make the transition across the drip-line. On the bound side of the drip-line lies a variety of rather intriguing substructures. Amongst them the Borromean nuclei possess the property that none of the two-particle subsystems are bound, and it requires three-body correlations to bind the system. An example of such a nucleus would be  $^6\text{He}$  ( $^4\text{He}+n+n$ ). Equally, it is possible to have 3-body systems in which only two of the constituents are bound, for example  $^6\text{Li}$  ( $^4\text{He}+n+p$ ) where the  $n$  and  $p$  are bound but the  $^4\text{He}+n$  and  $^4\text{He}+p$  subsystems are not. The comparison between these nuclei and Borromean systems allows a detailed understanding of the 3-body correlations to be realised. Not only is it essential to study the properties of the bound 3-body states, but the resonance in the unbound 2-body constituents and those in the unbound 3-body systems. Such measurements journey across the drip-line, necessitating measurements of the properties of nuclei which lead only a fleeting existence of  $<10^{-15}$  seconds.

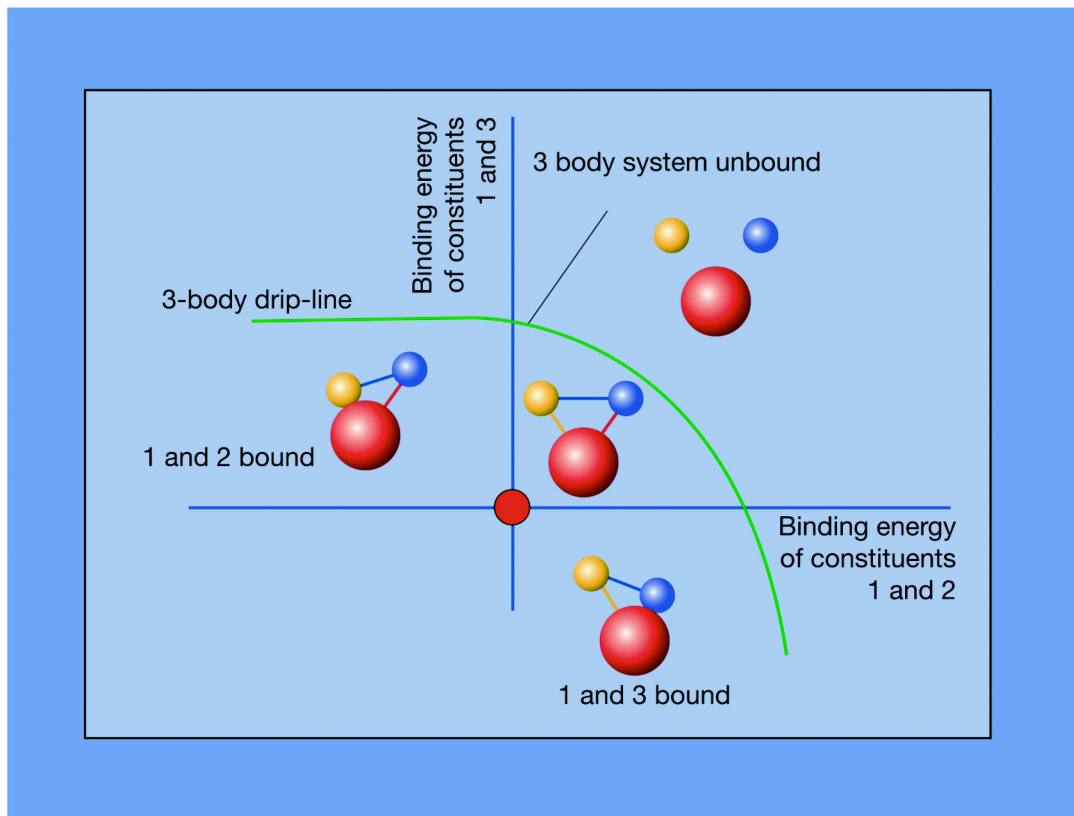


**Figure 2.2.1:** Properties of three body-systems close to the drip-line.

Such a structure has already been observed in a certain number of cases:  ${}^6\text{He}$ ,  ${}^9\text{Be}$ ,  ${}^{14}\text{Be}$ ,  ${}^{11}\text{Li}$ ,  ${}^{17}\text{B}$  and  ${}^{19}\text{B}$ . There is no other physical system in Nature that has such a structure: the atomic nucleus is thus a unique laboratory in the world of physics. The best-known nuclei with halos of neutrons are  ${}^{11}\text{Be}$  (halo of 1 neutron) and  ${}^6\text{He}$ ,  ${}^{11}\text{Li}$ , and  ${}^{14}\text{Be}$  (Borromean). Their existence was indicated in the nineteen-eighties by measurements of abnormally high total reaction cross-sections. Using optical-model Glauber analyses based on spherical densities, it was found that the nuclei with halos are between 20% and 30% larger than the well-established  $A^{1/3}$  rule for stable nuclei. The distance between the halo and the core is distinctly larger than the range of the nuclear force, which is 2 to 3 fm. The valence nucleons thus have a very high probability of being very far from the core, which implies that they have a high probability of tunnelling through the potential barrier (nuclear and centrifugal), and to penetrate into the classically forbidden regions. Furthermore, there are significant pairing effects between the neutrons of a Borromean system, even when both nucleons are in classically forbidden space.

With regard to the nuclei with proton halos, the Coulomb barrier constitutes an additional obstacle for diffusion of the protons via the tunnelling effect. Their existence is thus much more improbable than in the case of neutrons. However, three possible cases of nuclei with proton halos are today under discussion ( ${}^8\text{B}$ ,  ${}^{17}\text{F}$  and  ${}^{17}\text{Ne}$ ) and these need to be confirmed by a variety of measurements (reaction cross-sections,  $S_{1p}$  and  $S_{2p}$  binding energies, magnetic and electric moments).

***SPIRAL2: beams of halo nuclei***

*The light radioactive nuclei such as  ${}^6\text{He}$ ,  ${}^8\text{He}$ ,  ${}^8\text{Li}$ ,  ${}^9\text{Li}$ ,  ${}^{11}\text{Be}$ ,  ${}^{15}\text{C}$ ,  ${}^{16}\text{N}$ ,  ${}^{17}\text{N}$ ,  ${}^{18}\text{N}$ ,  ${}^{23}\text{Ne}$ ,  ${}^{25}\text{Ne}$ ,  ${}^{25}\text{Na}$  and  ${}^{26}\text{Na}$  will be produced at SPIRAL2 with high intensities. For example, up to  $10^{12}$ – $10^{13}$  atoms/s in the cases of  ${}^6\text{He}$  or  ${}^{15}\text{O}$ . By comparing the cross-sections for “pickup” of one and two neutrons, one can extract information on neutron-neutron correlations for the halos. Similarly, the “stripping” reactions permit spectroscopy of the nuclei up to, and even beyond, the drip line. Further, such high intensity beams will allow much more precise measurements of the fusion process for such loosely bound systems at or below the Coulomb barrier.*

### **2.2.2 Reactions with weakly bound nuclei**

Important parameters in formulating an understanding of the nature of the correlations responsible for the binding of these nuclei are measurements of the mass, spin and parity, moments and matter distributions. For heavy nuclei laser spectroscopy may be used to measure mean-square charge radii to gain an insight into the charge distribution, however the mass shift in lighter systems inhibits such studies. Measurements of nuclear and Coulomb elastic and inelastic scattering provide some information on the charge and matter radii. It has been observed that the very weak binding which characterises such systems, gives rise to extended density distributions and halo-like characteristics, where the weakly bound particles have a significant fraction (50%) of their wave-function beyond the core. These effects happen mainly when the valence particles are neutrons in low angular momentum orbits (s- and p-states). The attenuated centrifugal barrier then permits the tunnelling of the wave-function far into the classically forbidden region. These extended distributions have an impact on the refractive and diffractive behaviour of the scattering process. A second approach which has been developed with some success to study the wave-functions of such weakly bound valence nucleons is that of sub-barrier transfer. Here the collision energy is adjusted so that the effect of the Coulomb repulsion of the target on the projectile varies with the distance of closest approach. The exponential nature of the valence particle wave-function ensures that the transfer-process is dominated by the impact parameters close to zero orbital angular momentum, i.e. the direct-line of approach. This variation in collision energy permits a mapping of the tail of the neutron wave-function. Such studies require intense beams in order that the precision of the measurements is sufficient.

It might be anticipated that an extended distribution of neutrons would lead to enhanced fusion probabilities below the Coulomb barrier, where the neutron tail which extends well beyond the charged core provides a conduit by which the nuclear densities of the target and projectile may overlap at longer range than for the core nucleons. Thus, the enhanced fusion of  ${}^6\text{He}$ , for example, compared to the core  ${}^4\text{He}$ , might be predicted. However, recent measurements indicate that there is no significant enhancement in fusion, rather that transfer-like processes dominate. Such studies, where the reactions of the composite many-body system is held at a controlled distance from the nuclear force of the target under the target’s repulsive Coulomb field may, with intense beams, provide new insights into the nature of the halo.

As mentioned above, the most recent results show that the halo of  ${}^6\text{He}$  does not enhance the fusion probability, confirming the prominent role of neutron transfers in  ${}^6\text{He}$ -induced fusion reactions. Hence, there is evidence for a real new effect with radioactive ion beams, and with the stable nucleus  ${}^6\text{Li}$ , namely the occurrence of non-conventional transfer/stripping processes with large cross-sections most probably originating from the small binding energy of the projectile. One therefore needs to investigate a rather new process in the dynamics of the interaction at the Coulomb barrier with such loosely bound halo nuclei. The understanding of the reaction dynamics involving couplings to the break-up channels requires the explicit

measurement of precise elastic scattering data as well as yields leading to the break-up and transfer (incomplete fusion) channels. A more complete knowledge of fusion cross-sections is essential if neutron-rich beams such as  ${}^6,8\text{He}$  are to be used in secondary reactions to produce neutron rich nuclei in any quantity.

The complexity of such reactions, whereby many processes compete on an equal footing, necessitates kinematically and spectroscopically complete measurements, i.e. experiments in which all processes from elastic scattering to fusion are measured simultaneously, providing a technical challenge in the design of broad range detection systems.

### ***SPIRAL2: reactions of halo nuclei***

*The theoretical expectations call for more sophisticated and complete experiments with the higher-intensity beams available at SPIRAL2, in conjunction with large-coverage  $\gamma$ -ray detectors for fusion, with high-resolution magnetic spectrometers to measure the beam-like fragments combined with neutron detector arrays. Such a facility will enable a better understanding of the details of halo reaction dynamics in the vicinity of the Coulomb barrier. Precise exclusive experiments are needed to determine in detail the angular correlations of the light charged particles and of the individual neutrons.*

The above approaches would provide an insight into the averaged densities of the valence particles, whereas the details of the correlations of the valence particles in 3-body systems are of equal, if not greater, significance. These correlations contribute significantly to the binding of the system and thus their determination is of pre-eminent importance. Such correlations are hard to extract unambiguously, but two-neutron transfer reactions in which the two valence nucleons are removed in a single step has been used in the past to provide an insight into the spatial correlations, though these require a detailed and careful understanding of the competing two-step process, which may only be arrived at with intense beams. An alternate approach employs the fact that the wave-functions of two valence neutrons are entangled via the underlying quantum statistics, the Pauli exclusion principle. A measurement of correlations in the relative momentum of the two neutrons may be used to extract the space-time extent of the volume occupied by the valence neutrons, analogous to the Hanbury-Brown-Twiss effect for measuring the sizes of stars. Once again it is important to understand the contribution to this process from the decays of the 3-body system via the short-lived resonances in the 2-body partitions.

Halos in 2-body systems hold a fascination just as strong as those of their more complex 3-body counterparts. Again, studies of fusion and sub-barrier transfer with intense beams offer possible new insights into the nature and reactions of such systems.

SPIRAL2 will produce intense beams of light nuclei with halo-like characteristics, which will provide the prospect of answering many of the above questions. For example, the 2-body halo nuclei  ${}^{11}\text{Be}$  and  ${}^{15}\text{C}$ , in addition to nuclei such as  ${}^{25}\text{Ne}$  and  ${}^{18}\text{N}$ , which may have halo-like excited states, and the 3-body systems  ${}^6,8\text{He}$  will all be available as beams.

### **2.2.3 Nuclear clusters and molecules close to the limits of stability**

The usual structure of the ground-states of many of the weakly bound nuclei in the vicinity of the drip-line provides the basis for the formation of equally complex structures in other nuclei. For example, the coalescence of  ${}^6\text{He}$  and  ${}^4\text{He}$  to form  ${}^{10}\text{Be}$ , produces a system in which the two halo nucleons in  ${}^6\text{He}$  are exchanged between the  ${}^4\text{He}$  core of the  ${}^6\text{He}$  nucleus

and the remaining  ${}^4\text{He}$ , in a manner which is extremely similar to the exchange of electrons in covalently bound atomic molecules. Such nuclear systems where the valence, and often halo, nucleons are shared between cores, one of which is an  $\alpha$ -particle, may be explored in resonant elastic scattering measurements, where, for example, the radioactive ion beam is decelerated through a helium gas and resonances in the intermediate system are scanned as the projectile slows. Systems of particular interest would be those which have weakly bound neutrons and those which have comparatively inert clusters as cores, e.g.  ${}^6,8\text{He}$ ,  ${}^{15,16}\text{C}$ ,  ${}^{11}\text{Be}$  and  ${}^{23,25}\text{Ne}$ . Some models [e.g. Antisymmetrized Molecular Dynamics] suggest that many nuclei close to the drip-line will possess a structure which has a large component which may be described as relatively inert cluster cores embedded within a sea of valence neutrons, for example  ${}^{19}\text{B}$  is believed to possess this structure (see figure 2.2.2). The study of the process by which the cloud of valence nucleons is exchanged between the cluster cores, described above, should provide an insight into the possible structures at the drip-line also.

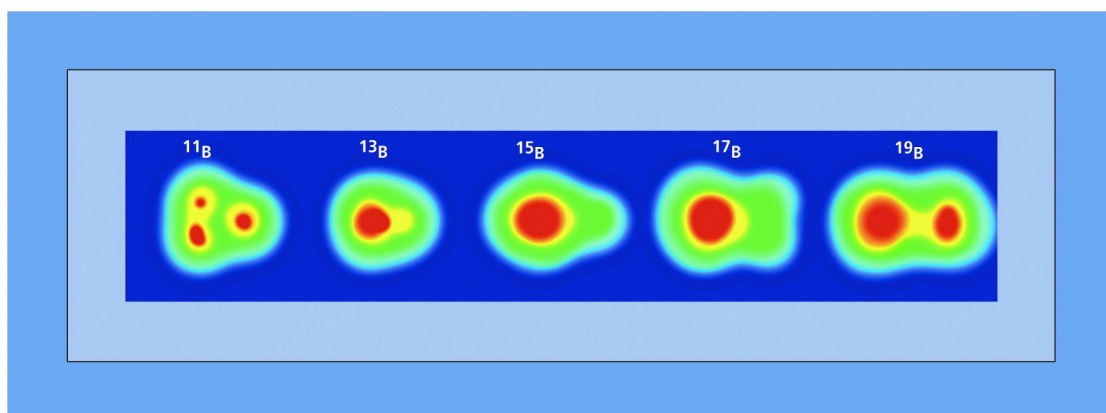


**Figure 2.2.2:** Antisymmetrized molecular dynamics calculation of the ground states of light nuclei showing a strongly clustered system.

### ***SPIRAL2: capture measurements for cluster studies***

*Resonant  $\alpha$ -particle capture measurements, whereby the incident beam of radioactive,  $\beta$ -unstable, nuclei traverses a  ${}^4\text{He}$  gas, scanning out resonances in the composite system provides a very sensitive tool for the probing of cluster states. Such measurements provide very detailed information regarding the spin, parity and partial widths of exotic cluster states.*

*Such measurements require beams with intensities in excess of  $10^6$  particles per second. This limit will be surpassed by SPIRAL2 for a very broad spectrum of light nuclei, allowing unprecedented access to exotic cluster states.*

### **2.2.4 Halo-characteristics in heavy nuclei**

The appearance of the halo coincides with two important characteristics; the weak binding of the valence neutrons and the occupancy of low angular momentum orbits (for which the centrifugal barrier is suppressed). It is the characteristic lowering of the 2s orbit from the sd-shell, so that it competes spectroscopically with the p-orbits in the 1p-shell, which is largely responsible for the appearance of halo-structures in, for example, the ground state of  ${}^{11}\text{Be}$ . The reappearance of zero angular momentum orbits does not occur again until close to the completion of the magic number 82. Relativistic Hartree-Bogoliubov theory predicts that

beyond the nucleus  $^{122}\text{Zr}$  ( $N=82$ ,  $Z=50$ ) giant halo structures involving up to 6 neutrons will emerge. Given the distance from stability and the refractory nature of this element the beams from SPIRAL2 will not enable us to reach to these extremes. However, studies of the evolution of the  $3s_{1/2}$  level with neutron and proton number will provide an insight into the possibility of such structures and, moreover, provide a firmer basis from which the calculations may be extrapolated. Transfer reactions, especially sub-barrier, may provide a hint of possible development of halo characteristics for neutrons in the  $3s_{1/2}$  level for less exotic systems.

### 2.2.5 Neutron skins in Neutron-rich nuclei

While many neutron-deficient nuclei can be produced in nuclear reactions using stable-isotope beam-target combinations, the region of neutron-rich nuclei is largely “terra incognita”. Therefore, exotic nuclei on the neutron-rich side of stability will attract most attention in nuclear physics in the future. The neutron drip line lies much farther away from the valley of stability than the proton drip line, since the repulsive electric force does not act on neutrons. With advanced radioactive ion beam facilities the neutron drip line will at least be reached for elements up to  $Z=25$ . The study of nuclei with large neutron excess does not, however, focus solely on the location of the drip line but is rather motivated by the unusual nuclear structure features that are expected, and in addition, by astrophysical requirements for nuclear data in this uncharted region.

In stable nuclei, the strong proton-neutron attraction keeps the volumes occupied by the two species of nucleons almost identical; proton and neutron matter radii differ only marginally and their chemical potentials differ mainly because of Coulomb effects. This is no longer the case in nuclei with large neutron excess. The chemical potentials of protons and neutrons shift away from each other and the surface region is predominantly occupied by neutrons. Thus nuclei with neutron skins are predicted for example in the area of Xe. These nuclei are characterized not only by a very great spatial extension but also by a weaker binding energy of the last few neutrons and by a high density of nucleons at the interior of the nucleus. Whereas the densities of protons and neutrons in  $^{100}\text{Sn}$  (located at the very limit of the neutron-deficient side of the nuclear chart) are expected to be very similar, they differ by more than a factor of 2 in  $^{100}\text{Zn}$ , a nucleus very rich in neutrons. From the point of view of their structure, this is due to the fact that in one case ( $^{100}\text{Sn}$ ,  $N=Z$ ), the orbitals occupied by the protons and the neutrons are very similar, whereas in the other case they are very different. Thus for  $^{100}\text{Zn}$ , the so-called “Fermi energies” of the neutrons and protons are also very different.

Elastic and inelastic proton scattering can be used as a valuable tool to probe details of the nuclear densities such as neutron skins to which the proton probe is especially sensitive. As evidenced in figure 2.2.3 for  $^{100}\text{Zn}$ , small details of the neutron density distributions translate into sizeable differences in the elastic and inelastic scattering cross sections. For the centre-of-mass angles of about 60 degrees, a measurement of the elastic cross-sections with a 5 mb/sr precision would be sufficient to discriminate between the two calculations. For inelastic cross section, a precision of less than 1 mb/sr is needed. Inelastic proton scattering also provides insight into the collectivity of the target nucleus.

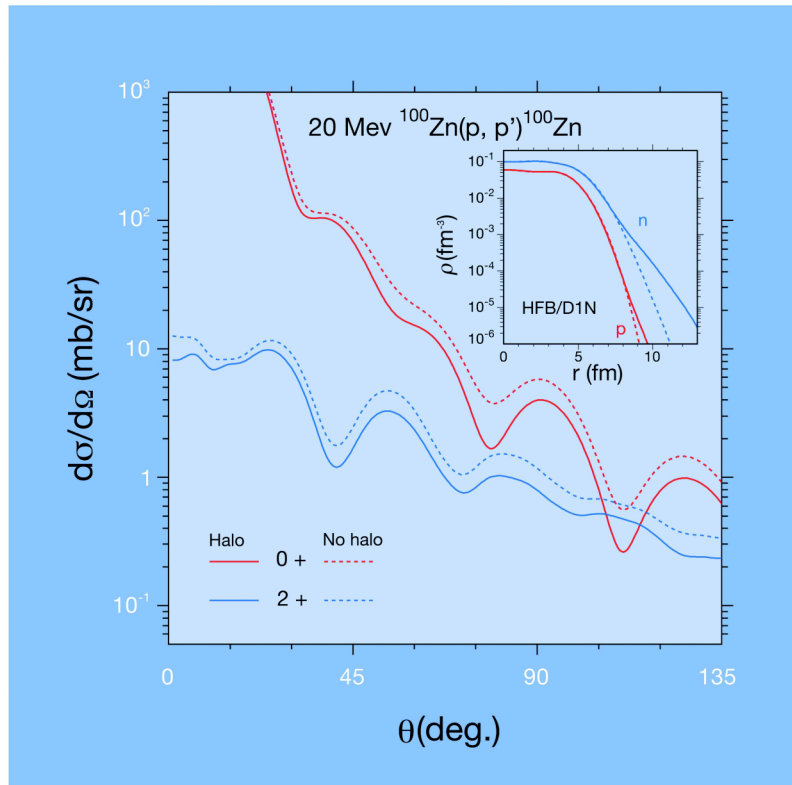


**Figure 2.2.3 :** Elastic and inelastic proton scattering on  $^{100}\text{Zn}$ . A small variation in the neutron densities (the neutron densities produced with large ("halo") or small ("no halo") oscillator basis differ only significantly for radii where the density is 1/100th of the saturation density) induces large differences in the scattering cross sections. This calculation has been performed with the semi-microscopic JLM approach with radial densities from HFB calculations using the D1N Gogny interaction.

Although predictions differ considerably they suggest a neutron skin thickness of up to about 1 fm for nuclei within reach of experiments. When the neutron skin thickness for tin isotopes is calculated in different approaches, two groups of calculated results appear, and the difference can be traced to different asymmetry parameters in the underlying nuclear equation of state. A skin thickness of the size predicted would mean that the strongly neutron-enriched outer zone comprises up to half of the entire nuclear volume. Within this surface zone, the composition of the nuclear medium approaches that of pure neutron matter with an average density significantly below the saturation density in stable nuclei. Evidently, this provides an ideal site for probing both the isospin and density dependence of the effective in-medium interactions. The evolution of neutron skins with increasing neutron excess is expected to be a global trend. The first experimental evidence for such a systematic trend was recently observed for sodium isotopes.

### ***Searching for nuclei with neutron skins and the study of their properties***

*Nuclei with a neutron skin are predicted in the area of the neutron-rich nuclei between Sn and Xe. SPIRAL2 will produce these elements in abundance. Transfer reactions of the type  $A(d,p)B$  with energies close to the Coulomb barrier could be used to measure the radii of the orbitals occupied by the valence neutrons. These experiments are done in inverse kinematics, since the nucleus of interest is radioactive, on a target containing the particle which is used*

*as probe. The light recoil nucleus is detected in a charged-particle detector while the heavy ejectile is detected in coincidence in a spectrometer. These experiments need beam intensities of the order of  $10^5$ – $10^6$  atoms/s.*

*The rotation of neutron-rich nuclei, for example the exotic Xe nuclei, can be observed and the impact of the skin of neutrons on the rotation of the core studied in detail by observation of the states of high angular momenta in these nuclei. This can be done by deep inelastic reactions with the aid of a granular  $\gamma$ -ray detector in coincidence with a recoil-spectrometer for identification of the reaction path and correction for the Doppler effect.*

## **2.3 MAGIC NUMBERS AND DEFORMATIONS: SHELL STRUCTURE FAR FROM STABILITY**

The atomic nucleus is a many-fermion system of strongly interacting particles and its constituents are, in principle, strongly correlated. In the spirit of the Landau-Migdal theory, it can be described very well as a system of almost independent quasiparticles that move in a common potential. Such a description assumes that nuclear forces saturate at a specific density of particles and that the quasiparticles correspond to elementary modes of excitation that carry quantum numbers of nucleons. The motion of quasiparticles in a common potential leads immediately to the single-particle shell structure of the nucleus. Characteristic shell gaps that appear in the single-particle spectrum induce particular properties of nuclei that have the numbers of neutrons or protons equal to the so-called "magic numbers".

The magic numbers, that are well established for nuclides in the vicinity of the valley of stability, are 2, 8, 20, 28, 50, 82 and 126. For these particle numbers, the single-particle shells are filled, i.e., these shells are closed and the corresponding nuclei are called the magic nuclei. They have increased particle stability, spherical form, and require a larger energy to be excited, these properties being consistently confirmed by experiment. The magic numbers are corner-stones for the modelling of nuclear structure and the understanding of nuclear properties: they were benchmarks for Maria Goeppert-Mayer and Jensen, Axel and Suess to establish the basis of the nuclear shell model. It is anticipated, however, that far away from the valley of stability the shell structure is modified. This is directly related to the lower surface densities in nuclei far from stability.

Many other quantum systems also exhibit shell structure; for example, well-known atomic magic numbers lead to an increased stability and the characteristic chemical neutrality of noble gases; metal clusters of atoms show a well established shell structure for electrons moving in the common potential well, created by the positive ions of the cluster. Shell structures are also present in quantum dots and wires.

For atoms, the well-known gradual changes of the shell structure with increasing atomic number, as compared to that of the hydrogen atom, are predominantly related to relativistic corrections for electrons moving in the inner shells. Spectacular changes of such a kind are expected in superheavy nuclei where the changing shell structure may disturb the order in which elements are placed in the Mendeleev table. A fascinating subject of nuclear research concerns neutron-rich nuclei far from stability for which very significant changes of the shell structure are predicted.

### 2.3.1 Shell effects in many-body systems and the theoretical concept of single-particle levels

The shell-structure of nuclei pertains to their single-particle features, i.e., relates to a certain approximation or simplification of their true many-body nature. For example, the single-particle levels are purely theoretical constructs that need to be carefully defined within a given description, and then have to be related to certain observables, e.g., one-particle separation energies. Experiment always deals with the whole many-body system, although special experimental techniques can focus on its one-body properties. Therefore, it is a very delicate issue to infer the shell-structure (one-body theoretical picture) from experiments performed on many-body systems, and the appearance or disappearance of the magic numbers should always be carefully evaluated in view of the possible many-body effects and correlations. In a nutshell, the positions of single-particle levels defined in a given theoretical description are always only indirectly related to specific nuclear observables.

A simple way to understand the effect of correlations is provided by nuclear pairing, where even systems of particles exhibit increased binding compared to the odd ones. Therefore, removal of a nucleon from an even nucleus, which in principle should give us information on the underlying single-particle state and its binding energy, is perturbed by pairing correlations. Such effects may become quite dramatic in weakly bound nuclei where the single-particle and pairing binding energies become comparable.

In weakly bound systems, the Fermi level is very close to the positive-energy phase space of unbound states. Thus, when moving toward the drip lines, the residual correlations built upon the simplest mean field picture mix the bound and scattering levels in the nucleus. This leads to a system in which there is no clear separation between the discrete and continuous parts of the spectrum anymore, and where the excited states are open channels. This can even be observed for a ground state beyond the drip line, as is the case for the proton emitters and the hypothetical neutron emitters.

These weakly bound states or resonances cannot be described in the formalism appropriate for closed quantum systems. This has recently stimulated a renewed interest in nuclear models in which the bound and scattering states are treated on the same footing and which are able to describe all data in a consistent manner. Developments of the models, including the coupling to the continuum, are in progress in the self-consistent mean field model in the HFB approach, and also in the shell model framework.

The importance of the particle continuum was already discussed in the early days of the multi-configurational shell model. However, the generalisation of the shell model concept to open quantum systems has only been introduced recently e.g. in the framework of the Gamow Shell-Model or the Shell Model Embedded in the Continuum. These models include the coupling between discrete states, resonant states and the complex non-resonant continuum of scattering states. This coupling to the decay channels breaks the symmetry of the Hamiltonian and modifies the effective nucleon-nucleon interaction, an effect recently studied in the *sd*-shell nuclei. In general terms, the effective nucleon-nucleon interaction in weakly bound systems explicitly depends on the location of various emission thresholds and on the structure of the poles of the scattering matrix that dominate the corresponding decays. The continuum coupling increases smoothly when approaching the emission threshold and exhibits a strong dependence on the structure of the many-body wave functions. The novel feature, absent in

the standard shell model, is the strong influence of the poles of the scattering matrix on the weakly bound and unbound states which, for low- $l$  orbits ( $l=0,1$ ) may (i) induce a non-perturbative rearrangement of the many-body wave functions with a significant ( $l=0,1$ ) single-particle content, (ii) modify the spin-orbit spacings and therefore change the magicity for certain neutron/proton numbers and (iii) induce singular variations of the spectroscopic amplitudes near the particle emission threshold.

### 2.3.2 Shell structure and particle separation energies

The mass or binding energy is the simplest and often most readily available piece of information about a given nucleus. When masses of several neighbouring nuclei are compared with one another, the shell effects and magic numbers are readily observed. Indeed, for most nuclei the two-neutron separation energies are smooth functions of particle numbers, apart from conspicuous discontinuities appearing along the magic neutron numbers (see figure 2.3.1). The same observation holds for the two-proton separation energies, which reveal the proton magic numbers. The one-particle separation energies exhibit the same behaviour after the odd-even staggering due to the pairing correlations is eliminated. Therefore, changes in the magnitudes or positions of these discontinuities, which may appear in exotic nuclei, would indicate modifications of the shell structure.

*In first approximation, the magnitude of the discontinuity in the two-particle separation-energy surface can be interpreted as being twice the size of the magic shell gap. A quantitative analysis of changes of shell gaps in exotic nuclei requires, however, a more careful approach. Indeed, even in stable nuclei such discontinuities vary in magnitude for various reasons, the most important being the variations of quadrupole collectivity in semi-magic nuclei. Correspondingly, the shell gaps inferred from the discontinuities in the mass surface appear to be at their largest in doubly magic nuclei. Therefore, changes observed in exotic nuclei have to be interpreted as a*

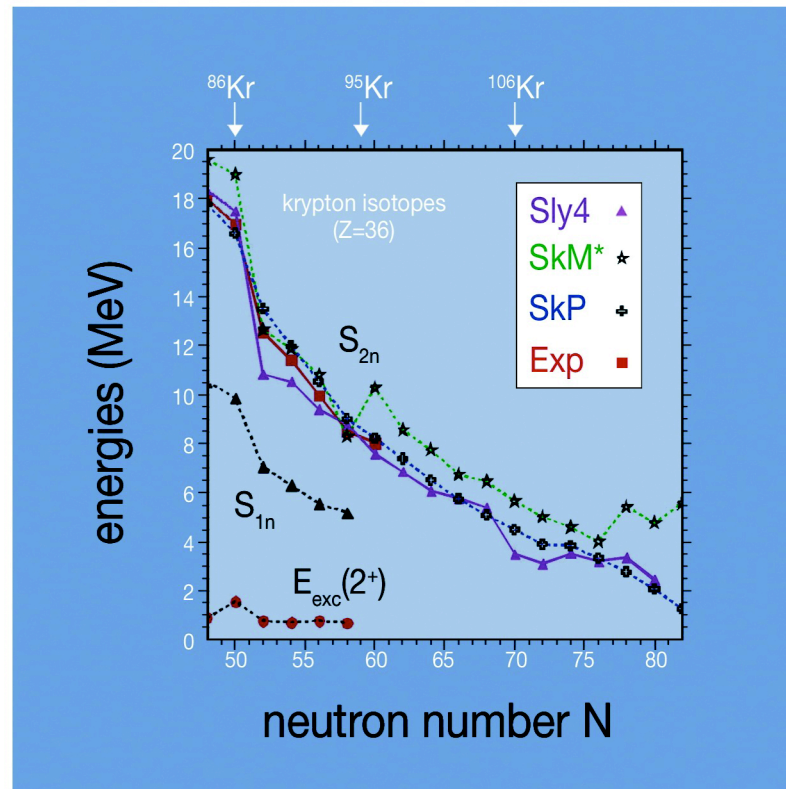


**Figure 2.3.1:** Calculated and experimental two-neutron separation energies, as a function of the neutron number  $N$ , for the even isotopes of krypton ( $Z=36$ ). The calculations have been performed within the HFB model, assuming three different nucleon-nucleon effective interactions (Sly4, SkM\*, SkP). For comparison, the experimental one neutron separation energy ( $S_{1n}$ ) and excitation energy of the first  $2^+$  state ( $E_{exc}(2^+)$ ) are shown. The trend of the  $2^+$  curve, compared to the expected  $S_{2n}$  values, shows that the excited states in the low-lying energy spectrum of the krypton isotopes close to the drip-line, are likely to be mostly unbound states. Depending on the effective interaction, the location of the drip-line may vary by a few units in neutron number.

function of distance from shell closures. For example, one expects that these discontinuities will increase (decrease) in magnitude when approaching (moving away from) a doubly magic system. Discontinuities in the mass surface may indicate a variation in the size of the shell gap as well as other changes of physical properties, e.g., a sudden onset of deformation or competition between co-existing shapes. Altogether, information gained by measuring nuclear masses will be invaluable in terms of teaching us about the new features of the shell structure in exotic nuclei only if accompanied by a proper theoretical analysis.

The magic numbers and other shell structures are also visible when nuclear charge radii are plotted as a function of neutron and proton numbers. Such a dependence most often exhibits kinks or edges when magic particle numbers are crossed (see figure 2.3.2). Also this observable can be used to draw quantitative conclusions only after taking into account other physical effects that may influence nuclear radii, e.g., occupations of orbitals that may have varying spatial sizes.

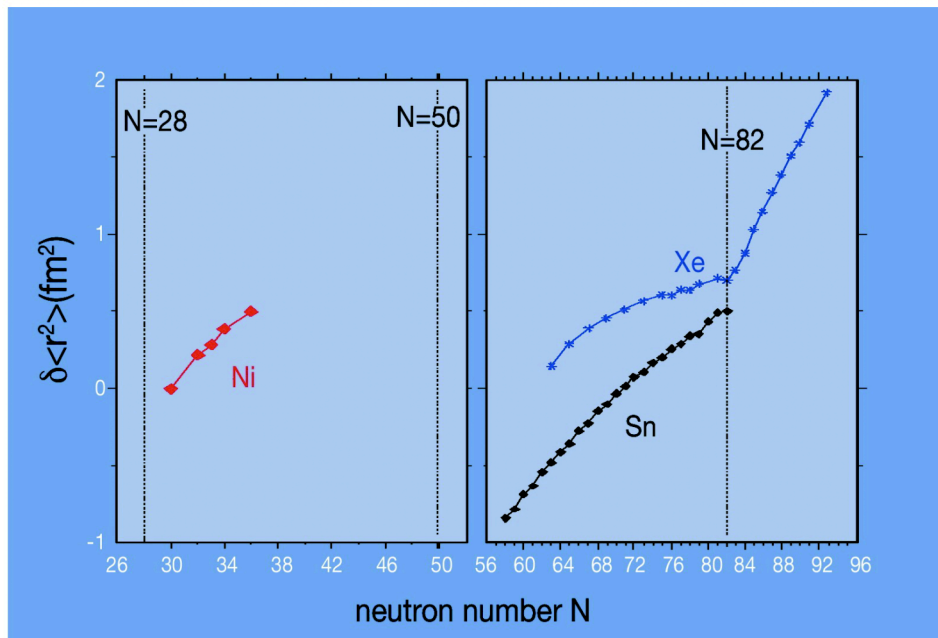


**Figure 2.3.2:** Radius measurements using laser spectroscopy for nickel, tin and xenon isotopes. The dotted lines indicate the position of the well-known magic numbers. The sharp kink observed in the xenon chain is a clear signature of the crossing of the  $N=82$  shell gap

***Shell structure far from stability measured at SPIRAL2***

*One- and two-neutron separation energies ( $S_{1n}$ ,  $S_{2n}$ ), as deduced from mass measurements at SPIRAL2, will be the very first piece of information on shell effects very far off stability. Measurements of radii using laser-spectroscopy methods are also extremely sensitive to shell effects. By tuning the laser frequency, this technique allows selective ionisation of the nuclei of interest and yields not only the charge radius, but also the nuclear moments via their hyperfine structure. The minimum secondary beam intensity required is of the order of  $10^6$  atoms/s. The mass separation is obtained directly from time-of-flight measurements using the laser pulse and the ion detection. One of the best example of such an experiment can be found at the  $N=82$  magic shell gap for xenon isotopes. With the accuracy of this laser-spectroscopy technique, a pronounced kink has been observed in the radius variation at the crossing of the magic shell showing strong shell effects in the valley of stability. With the yield expected from SPIRAL2, radii measurements across the doubly magic  $^{78}\text{Ni}$  and  $^{132}\text{Sn}$  gaps will be feasible at LIRAT.*

### ***Measurements of spectroscopic factors of neutron-rich nuclei***

*Single-neutron transfer reactions such as  $(d,p)$  in inverse kinematics at  $\sim 4$  MeV/nucleon, which have already been mentioned in connection with studies of unbound nuclei, are also a valuable tool for determining spectroscopic factors. Pioneering experiments of this kind with radioactive ion beams have recently been initiated for the reactions  $d(^{82}\text{Ga},p)^{83}\text{Ga}$  and  $^9\text{Be}(^{134}\text{Te}, ^8\text{Be})^{135}\text{Te}$ . The studies were based on proton detection in the former and  $\gamma$ -ray detection in the latter case, the  $^{82}\text{Ga}$  and  $^{134}\text{Te}$  beam intensity amounting to  $10^4$  and  $2 \times 10^6$  atoms/s, respectively. The higher beam intensities delivered by SPIRAL2 will allow one to considerably improve the data on spectroscopic factors.*

### **2.3.3 Collectivity in low-lying excited states**

The evolution of shell structure in neutron-rich nuclei is intimately related to the nature of the spin and isospin dependence of the in-medium, nucleon-nucleon interaction. Exotic phenomena such as neutron haloes and neutron skins could develop in very neutron-rich nuclei and shell effects could thereby emerge, inducing different shapes for the proton and neutron fluids. For instance, figure 2.3.3 shows a prediction of nuclear deformation  $\beta$  for all even-even nuclei from drip-line to drip-line obtained from HFB calculations with the D1S Gogny force. In contrast with stable and near stable nuclei, where a strong proton-neutron interaction is a key ingredient in inducing deformation of the whole nucleus, decoupling between the valence neutrons and the proton core could occur in very neutron-rich nuclei. Decoupling or strong polarisation effects in nuclei could be sought by measuring the evolution of the reduced rate for electric quadrupole transitions,  $B(E2)$ , along singly-magic isotopic chains. The  $B(E2)$  value is an electromagnetic quantity, sensitive to the proton contribution to the excitation.

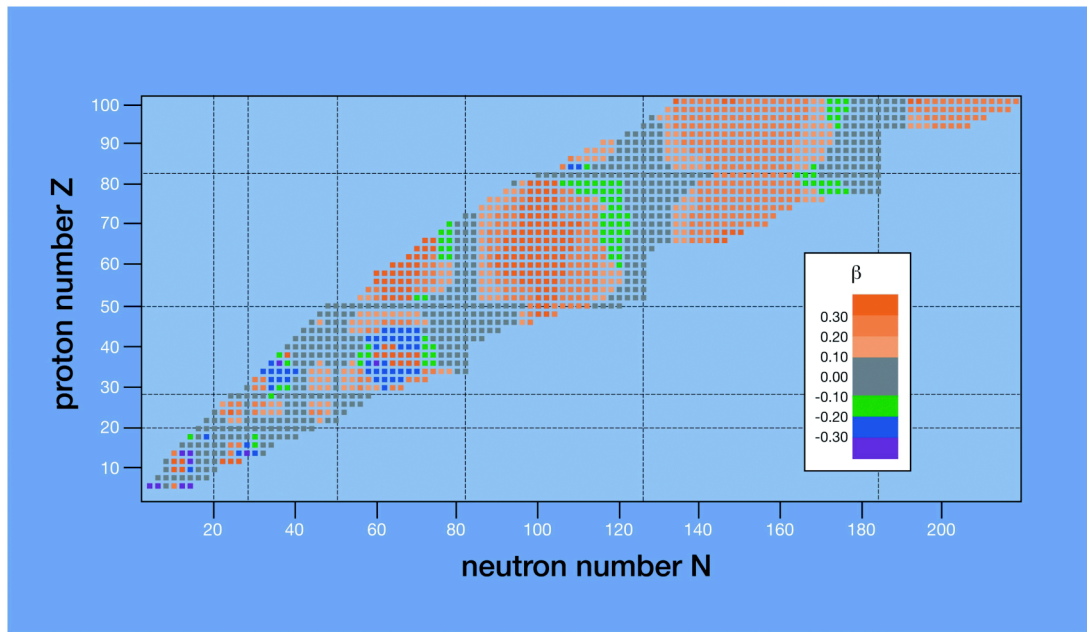


**Figure 2.3.3:** Quadrupole deformation of all even-even nuclei from drip-line to drip-line from HFB calculations with the Gogny D1S force.

Thus a very elegant way to identify shell effects experimentally is to measure the nuclear collectivity. In particular, Coulomb excitation combined with the measurement of the de-excitation  $\gamma$ -rays, gives access to the energy of the first  $2^+$  excited state and the associated  $B(E2)$  transition rate in even-even nuclei. When such data are systematically analysed as a function of proton and neutron numbers, the magic gaps are signalled by peaks in the  $2^+$  energies associated with corresponding dips in the  $B(E2)$  values. Deviations from the corresponding trends observed in stable nuclei may be used as indications of changes in the shell structure of nuclei. Again, the quantitative analysis must involve careful consideration of possible shape coexistence effects and/or effects associated with the proton-neutron composition of low-lying collective vibrational states, keeping in mind that only the proton component is responsible for the electromagnetic de-excitation.

These Coulomb excitation experiments have to be combined with studies of the inelastic scattering of nuclei on protons. Indeed, inelastic proton scattering at low energy is more sensitive to neutrons than to protons. Therefore the combination of these two measurements will disentangle the proton and neutron contributions, and lead to an assessment of the independent or mutual contributions of the neutrons and protons to the nuclear excitation.

### ***Coulomb excitation and inelastic scattering measurements***

*A knowledge of the excitation energies and transition strengths of low-lying collective states can be obtained from Coulomb excitation studies. The projectile is excited by a high-Z target, and the decay  $\gamma$ -rays are detected. Such experiments can be performed with very low beam intensities (down to 1000 atoms/s) and require a highly efficient granular  $\gamma$ -ray detector such as EXOGAM or, even better, AGATA. CIME energies are well adapted to such reactions. As pure an incident beam as possible is very important. Long isotopic chains that could be investigated are  $^{72}\text{Kr}$  to  $^{94}\text{Kr}$ , the chain  $^{112}\text{Xe}$  to  $^{145}\text{Xe}$ , and  $^{125}\text{Sn}$  to  $^{134}\text{Sn}$ .*

*The combination of the VAMOS spectrometer and state-of-the-art light charged-particle and  $\gamma$ -ray arrays such as MUST2, TIARA and AGATA will permit one to carry out*

*experiments with the aim of determining the contributions of protons and neutrons to nuclear excitation. These kinds of experiment can be carried out with beam intensities as low as a few hundred atoms per second and will allow us to extend the systematics for zirconium isotopes beyond the  $N=70$  and for the nickel isotopes beyond the  $N=50$  shell closure.*

### 2.3.4 Spins and nuclear moments

It is important to understand how the nucleus builds its spin from its constituent nucleons and from their organisation. Indeed, while orbiting in the nucleus, protons and neutrons can add their angular momentum to their intrinsic spin. The parity is also a characteristic of the nuclear wave function arising from its structure. Past measurements of exotic nuclei have already proven that the spins and parities observed do not correspond to expectations based on extrapolation from known nuclei. This failure suggests that there is a major rearrangement of the internal structure of the nuclei when one moves away from stability.

The single-particle magnetic moment for a valence nucleon around a doubly magic core is uniquely defined by the quantum numbers  $l$  and  $j$  of the occupied single particle orbit. These moments can be calculated using the free proton and neutron moments. However, in a nucleus, all the other nucleons influence the single-particle magnetic moment. Therefore, one uses an effective moment, expressed by the  $g$  factor. Corrections to the free moments include the influence of meson exchange currents as well as core polarization effects that can either add up or cancel. It is thus very important to measure the magnetic moments of states in nuclei one particle removed from doubly magic nuclei.

Nuclear magnetic moments are sensitive to the orbits occupied by the valence particles (or holes) and can thus be used to test the configuration purity. The quadrupole moment probes the deformation and collective behaviour of nuclei both at low and high excitation energy. Generally speaking, the magnetic moments are sensitive to 1p-1h excitations across a magic shell gap whereas quadrupole moments are sensitive to quadrupole, particle-core coupling interactions (2p-2h excitations). Both quantities can be directly compared with theoretical predictions, thus providing an excellent tool to test their validity. This plays an important role in understanding the basic ingredients needed to explain the changes in the nuclear shell structure of nuclei far from stability.

#### ***Spins, parities and moments observable with SPIRAL2***

*Doubly-magic nuclei, their nearest neighbours and the islands of inversion can be studied via their electromagnetic moments. Nuclear spins and moments can be measured for nuclei produced with an intensity of more than  $10^3$  atoms/s and with a purity  $\geq 70\%$ .*

*Spin-orientation is a crucial issue in the study of nuclear moments. However, radioactive ion beams released from target-ion sources are obviously not spin-oriented and only isotopes with a sufficiently long lifetime (to survive the collection, re-ionization and mass selection process, typically of the order of milliseconds and depending on each particular target-ion source combination) are accessible. Using a collinear laser set-up or in-source laser spectroscopy one can measure the moments and spins of very exotic low-energy radioactive nuclei to a few percent precision. For higher precision nuclear moment measurements on these radioactive ion beams, using e.g.  $\beta$ -Nuclear Magnetic Resonance methods, it is important that methods of polarising these radioactive ion beams are developed.*

*Many of the measurements on radioactive nuclei will be carried out directly around the (secondary) target station, without a preceding selection procedure ('in-beam' experiments). This is required for example if one is interested in studying the properties of extremely short-*

*lived excited states. In this case the radioactive nuclei are produced and stopped in (or immediately after) the target and the radiation emitted at the target position is detected. Using the spin-orientation obtained during the reaction process (fusion-evaporation, transfer with radioactive ion beams, Coulomb excitation), nuclear moments of very short-lived states can be studied (down to the time-of-flight in the recoil mass separator, typically 200 ns, or even as short as 1 ns provided the experiment is performed in-beam). It is obvious that in-beam studies of very exotic nuclei require advanced detection methods in order to detect the small number of decays of interest in the intense background of radiation coming from all the radioactive species produced. The use of powerful detectors for  $\alpha$ -,  $\beta$ - and  $\gamma$ -rays will thus be essential.*

*Depending on the production method, the decay process, the lifetime and the spin range different techniques have to be applied including Nuclear Magnetic Resonance, Level Mixing Resonance, Level Mixing Spectroscopy, Time Differential Perturbed Angular Distributions, Transient Field and Laser Spectroscopy methods, etc.*

## 2.3.5 Single-particle levels far from stability

### Single-particle properties within the mean-field picture

With increasing proton/neutron excess one expects modifications of the nuclear mean-field potentials, which in turn modify the position of the single-particle levels. The simplest effect of this kind is related to the nuclear volume and radius; indeed, when the number of nucleons increases, the corresponding radii of the proton and neutron distributions gets larger, hence the nuclear potentials are modified. Similarly, changes in the diffuseness of the particle distributions influence the diffuseness of nuclear mean-field potentials. Since the neutron-proton interaction is strong, the neutron potential depends not only on the neutron but also on the proton number. Overall one observes a gradual migration of single-particle levels, which may even cross within one major shell.

This effect is very nicely illustrated in the case of neutron-rich copper isotopes located one particle away from the singly-magic  $^{68}\text{Ni}$ . Due to the coupling between the valence proton and the additional pairs of neutrons filling the  $1g_{9/2}$  orbital, the excitation energy of the  $1f_{5/2}$  proton orbital decreases from 1.214 MeV to 0.166 MeV when moving from  $^{69}\text{Cu}$  to  $^{73}\text{Cu}$ . This so-called "monopole migration" phenomenon may induce an inversion of the  $1f_{5/2}$  and  $2p_{3/2}$  proton orbitals in  $^{77}\text{Cu}$  or  $^{79}\text{Cu}$  (see figure 2.3.4). Such a migration may have major consequences for the size of the magic gaps, and therefore on the modification of the known magic numbers for nuclei far from stability.

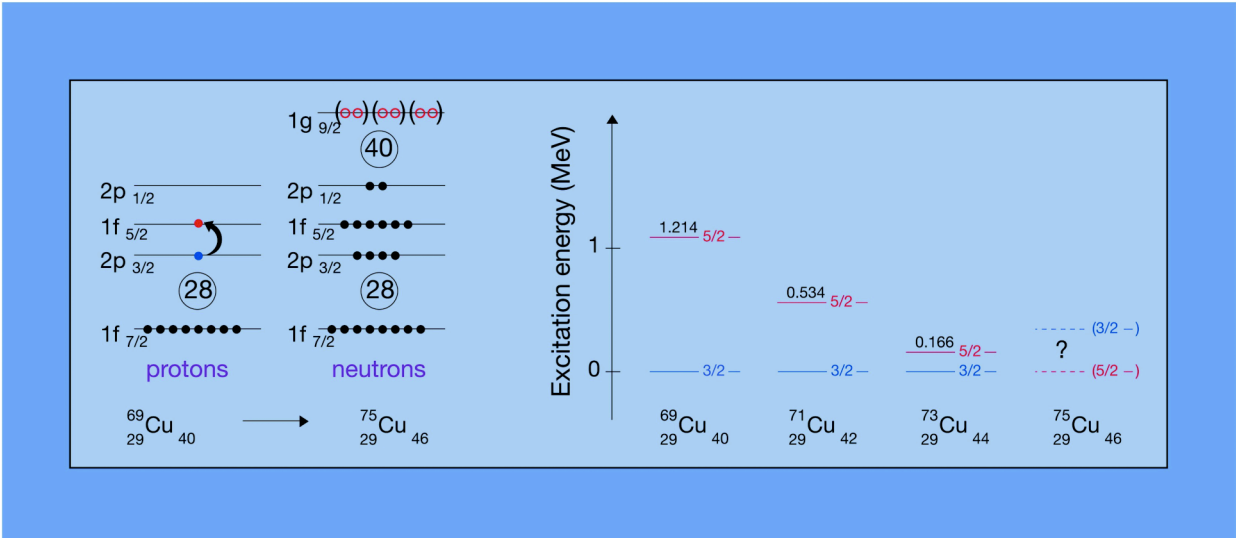


**Figure 2.3.4:** Part of the single-particle structure of the odd-A copper isotopes from  $^{69}\text{Cu}$  to  $^{75}\text{Cu}$ . As the  $n1g_{9/2}$  neutron orbital is being filled, the excitation energy of the  $1f_{5/2}$  proton orbital drastically decreases due to the residual p-n interaction.

When leaving the valley of  $\beta$ -stability, changes in the spin-orbit strength may occur, since the spin-orbit effects strongly depend on the gradients of the particle distributions. Thus an increase in the surface diffuseness may lead to a decrease in the spin-orbit potentials. However, this may have different consequences for the spin-orbit splitting of levels, because it depends crucially on the surface localization of the high-spin orbitals relative to the spin-orbit potential. This would mean that orbitals of the same parities (i.e. resulting from a shell with the same principal quantum N) would tend to group together. As illustrated in figure 2.3.5, new magic numbers such as N=40 or 70 could then appear. Similar effects are expected for lighter neutron-rich nuclei around N=20 and 28

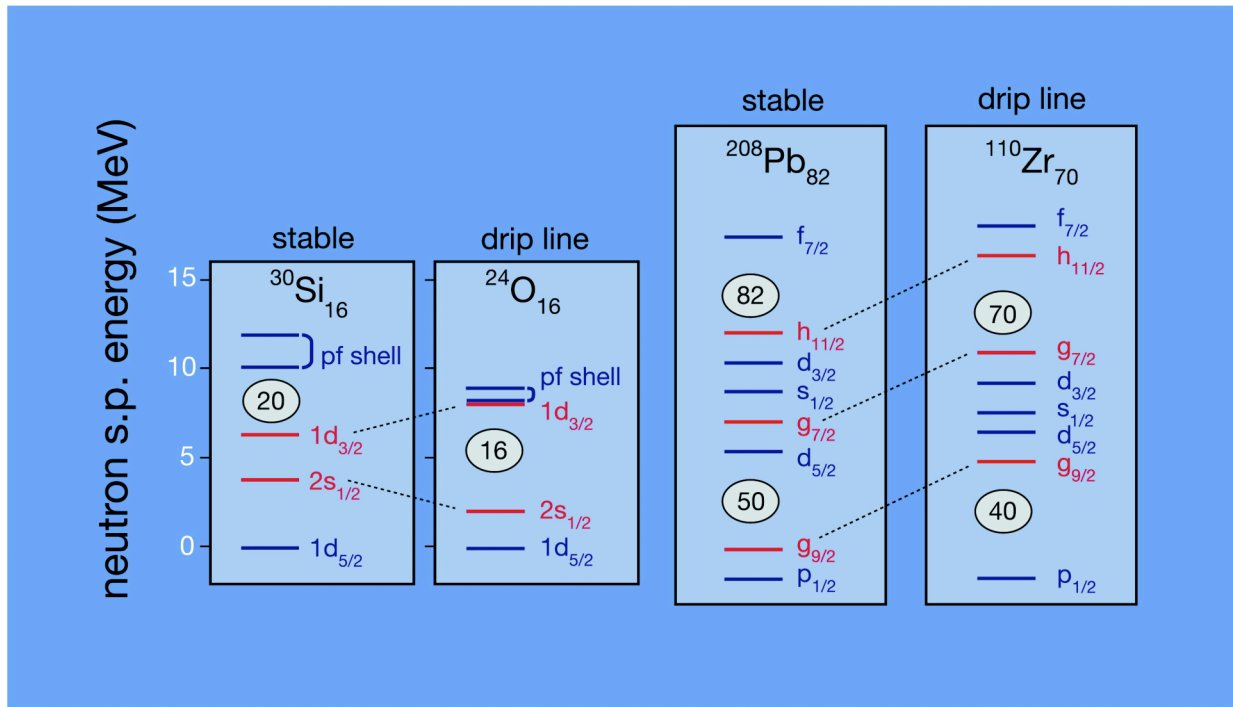


**Figure 2.3.5:** Left: experimental studies show that the magic number  $N=20$  established in the valley of stability is modified and that the new relevant shell gap at the oxygen drip-line corresponds to  $N=16$ . Right: the same phenomenon is expected for heavier neutron-rich nuclei, with the numbers  $N=40, 70$  becoming the new relevant shell gaps far away from stability.

At the time of writing the migration of single-particle levels is the subject of intensive investigation. Around  $^{132}\text{Sn}$ , for example, some energy levels are known in  $^{133}\text{Sn}$ ,  $^{131}\text{Sn}$ ,  $^{133}\text{Sb}$  and  $^{131}\text{In}$ , which make it possible to determine the separation in energy between the  $g_{7/2}$  and  $g_{9/2}$  proton orbits, or the  $h_{9/2}$  and  $h_{11/2}$  neutron orbits. How these orbits vary with energy, when moving towards the neutron drip line, can be used to deduce the spin-orbit coupling and hence test the theories that predict a fairly shallow potential well and a very diffuse nuclear surface far from stability. In the comparison, however, the many-body effects discussed below should be taken into account. In particular one should take account of the coupling of the single particle states to vibrations, which changes the effective mass of the nucleon near the Fermi energy.

### Single-particle properties and many-body effects

Apart from the migration of pure single-particle levels, which results from modifications of the mean fields when the number of nucleons varies, there are many other physical phenomena that may influence the single-particle shell structure of nuclei. The most spectacular are those related to deformation effects, whereby open-shell nuclei exhibit single-particle levels characteristic of nucleons moving in a deformed mean field. This can be understood as a strong coupling, mostly of a quadrupole character, between the individual particles and the core formed by all the other nucleons.

Such phenomena are often interpreted as level-level interactions, which result in specific shifts of single-particle states and allow for consistent interpretations of experimental data. For example, the proton-neutron attraction exerted by a high- $j$  intruder level can be considered to be at the origin of a sudden onset of deformation along some isotopic chains. This is often called the Federman-Pittel effect. Similar interactions are thought to be the reason for shifts in the single-particle levels in light nuclei, and are potentially able to change magic numbers. For example, in neutron-rich oxygen isotopes, the shell closure occurs at  $N=16$  instead of  $N=20$ , as observed for nuclei close to stability (see figure 2.3.5). This modification breaks the magicity of  $^{28}\text{O}$ , which even appears to be unbound. In general, single-particle levels used in the many-body shell-model calculations have to be gradually adjusted as a function of particle numbers due to the monopole interactions. Such changes may have their origin in the three-body nuclear forces, and are essential to describe the correct saturation properties of nuclei. Single-particle levels in weakly-bound systems may also be significantly influenced by the coupling to the particle continuum.

The ideas based on level-level interactions and shifts, although essential to interpret experimental data, do not address properly the questions of what really are the "bare" or "non-interacting" single-particle states. Indeed, improved theories should be developed, which are able to derive both the single-particle energies and interactions from bare forces within a consistent approach. Such ambiguities illustrate once again that the many-body description of a nucleus as a whole should be used to validate the simple single-particle picture.

### **Intruder states**

In a deformed mean field, the energies of high- $j$  orbitals depend very strongly on the deformation, and such single-particle orbitals may fairly easily cross the spherical gap of a magic nucleus. Therefore, by exciting particles across the magic gap, and into these deformation-driving states, one obtains deformed intruder configurations that are observed in various regions of the nuclear chart. The intruder configurations are very interesting from the point of view of measuring the sizes of magic gaps. However, they can provide useful information about the single-particle structure only after careful analysis of the many-body aspects of the problem. Indeed, the energies of such intruder configurations depend not only on the "initial" positions of high- $j$  orbitals at spherical shapes, but also on the strength of the quadrupole-quadrupole component of the nuclear interaction as well as its monopole components (e.g. pairing) that act towards restoring the spherical symmetry. Moreover, these many-body configurations can easily mix with the ground-state magic configurations thus perturbing the magicity of certain nuclei. Altogether, the study of intruder states requires a comprehensive approach which can potentially provide invaluable information on nuclei near magicity.

The evolution of nuclear properties measured along extended isotopic chains, will be particularly important in improving theoretical descriptions. Transfer reactions give direct access to the energies of individual particles and the corresponding excited levels in the nucleus. The identification and the localization of these individual levels, as well as the determination of spectroscopic factors, make it possible to test the shell model far from stability. These measurements are complementary to decay experiments.

### ***$\beta$ -decay studies around magic nuclei at SPIRAL2: probing the single-particle state interaction***

*As shown in the case of the even copper isotopes with more than 40 neutrons, the residual interaction between the valence proton in the  $2p_{3/2}$  orbital and the valence neutron in the  $1g_{9/2}$  orbital is the dominant contribution to a low-lying quadruplet of states with spins ranging from 3 to 6. The mean energy of the multiplet and the relative energy differences between the states are related, respectively, to the monopole and to the quadrupole part of the residual interaction. The measurements of these quantities in even nickel isotopes from  $^{68}\text{Ni}$  to  $^{80}\text{Ni}$  will be performed in  $\beta$ -decay experiments at SPIRAL2 and will lead to a better understanding of the proton-neutron interaction inside the atomic nucleus.*

### ***Spectroscopic studies with direct reactions***

*Transfer reactions provide direct access to the single-particle shell structure of nuclei. SPIRAL2 will allow us to perform one and two-nucleon transfer reactions in the vicinity of the doubly magic nuclei  $^{78}\text{Ni}$ ,  $^{132}\text{Sn}$  and  $^{110}\text{Zr}$ . Such experiments are performed in inverse kinematics where the beam of interest impinges on a target containing the light probe ( $p$ ,  $d$ , and  $t$ ). The light recoil nucleus is identified in a position-sensitive particle detector such as MUST or TIARA in coincidence with the heavy ejectile detected in a spectrometer like VAMOS. The differential cross-sections are reconstructed from the complete measurement of the reaction kinematics. In particular, the small centre-of-mass angles in the direct reactions are obtained from the unambiguous identification of the reaction products and from the precise measurement of the light recoil at energies below 5 MeV. This technique requires low-energy threshold devices allowing energy vs time-of-flight correlations and has been developed successfully already in the context of radioactive ion beams. Experiments which have already been initiated with SPIRAL are the  $^{6,8}\text{He}(p,p')$  reaction, the spectroscopy of beams of exotic nuclei with no bound excited states or the spectroscopy of exotic beams and unbound isotopes via one-nucleon transfer reactions.*

*The measurement of  $\gamma$ -rays and charged-particles in coincidence with the ejectile in a spectrometer is essential if we are to identify the reaction unambiguously and extract the low-lying bound states from the continuum. The required minimum beam intensity is approximately  $10^4$  atoms/s and it should be pure ( $\geq 90\%$ ). The energy of the beams delivered by CIME (e.g. 4.9 MeV/nucleon for  $^{132}\text{Sn}$  in the most probable charge state) is sufficient for ( $d, p$ ) and ( $d, t$ ) transfer reactions with a small angular momentum window. By increasing the charge state of the isotopes extracted from the charge-breeder, it is possible to double the beam energy but this reduces the intensity by an order-of-magnitude.*

*This technique will be required to explore the shell structure of very neutron-rich nuclei and measure their unbound excited states. Indeed, as we move towards the drip line, the neutron-rich nuclei are more weakly-bound, and have few or no bound excited states, like the known even-even drip-line nuclei ( $^8\text{He}$  to  $^{24}\text{O}$ ) which have no bound excited state. For instance the ( $d,p$ ) reaction with a  $^{134}\text{Sn}$  beam will allow the study of the low-lying unbound states of  $^{135}\text{Sn}$  lying above the neutron threshold.*

### **2.3.6 Shapes of exotic nuclei; exotic shapes of nuclei**

Nuclei with a large excess of neutrons may be deformed in novel ways and hence may adopt unusual shapes. This can be due primarily to a large skin composed of neutrons, weakly

coupled to the proton-neutron core compared with the situation in stable nuclei which have comparable proton and neutron distributions (see figure 2.3.6).

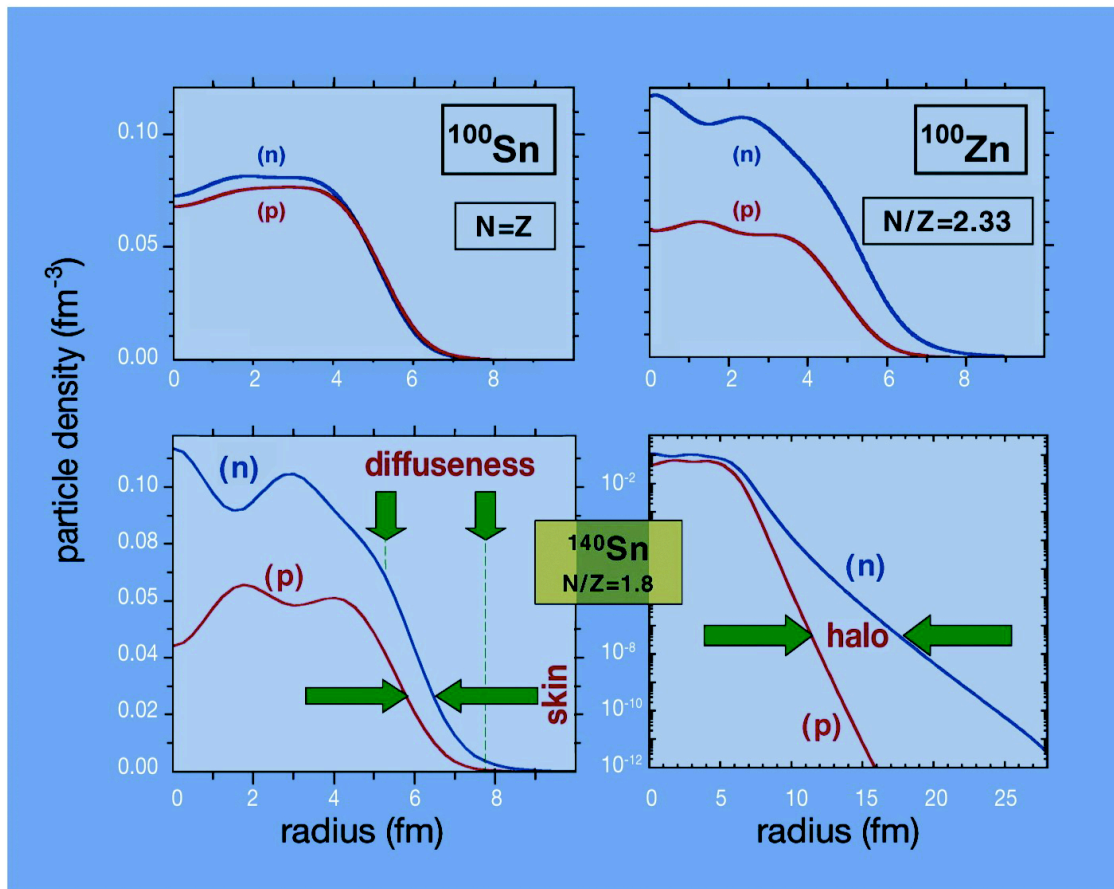


**Figure 2.3.6:** top panels: neutron and proton densities calculated for  $A=100$  nuclei, namely the proton-rich  $N=Z$  nucleus  $^{100}\text{Sn}$  and the neutron-rich nucleus  $^{100}\text{Zn}$ . The neutron density of the latter extends much further out compared to the former. This is even more visible in the bottom panels which show the density on a linear (left) and logarithmic (right) scale for  $^{140}\text{Sn}$ . These densities have been calculated in the self-consistent Hartree-Fock-Bogoliubov approach.

The neutron-skins can deform, or assume a different shape, more easily than the core, leading to a conspicuous enhancement of the isovector components in nuclear deformations. Correspondingly, one may observe unusual shape coexistence phenomena, whereby the isovector shapes will co-exist with the isoscalar ones. Such effects are abundantly predicted for small-amplitude vibrational states. However, the same arguments also apply for all kinds of low-lying collective excitations, which should probably be described by novel types of collective model that take the isospin degrees-of-freedom explicitly into account. One can also expect that exotic shapes, e.g. tetrahedral or octahedral, occur in nuclei far from stability.

#### Shape co-existence in drip-line nuclei

The shape of a given nucleus can vary in a very dramatic way, particularly when an intruder orbital from a higher oscillator shell mixes with orbitals of normal parity. An example is provided by the neutron-deficient mercury nuclei, which have a very deformed, prolate ground state (i.e. shaped like a rugby ball) whereas the heavier isotopes are associated with a weak oblate deformation (like a pumpkin). The phenomenon of shape co-existence

occurs when several nuclear states having different intrinsic properties are very close in energy.

There are some quite dramatic examples of the shape co-existence phenomenon, such as the superdeformed states, the deformed states located at low energy in spherical nuclei, the yrast-traps (an yrast state is a state of lowest excitation energy for a given angular momentum) or pairing isomers. The states which co-exist have the astonishing property of preserving their identity up to relatively high excitation energies, as in the case of the superdeformed states located several MeV above the yrast line. This implies that these states do not mix with the other states around and below them.

Nuclei showing evidence of shape co-existence occur in several mass regions, from the light neutron-rich nuclei around  $N=20$  and  $N=28$  up to  $^{186}\text{Pb}$  where triple shape co-existence (spherical, oblate and prolate) was observed. In this case, the mean field potential clearly shows three local minima corresponding to the co-existence of three  $0^+$  states. Shape co-existence has also been observed in neutron-deficient krypton isotopes, in particular with the beams from SPIRAL. This phenomenon may show novel features in drip-line nuclei, because the co-existing shapes can have different properties with respect to particle emission. Thus it may happen that an unbound co-existing state mixed with a bound state with a different shape can play the role of a doorway state for particle emission. Alternatively, an unbound state may have an extended lifetime if its particle emission would lead to a state of quite different shape in the daughter nucleus. This is uncharted territory in terms of both theory and experiment and will involve a complex interplay between collective excitations and the particle continuum. It opens the door to a promising new field for the new facility.

***Shape coexistence at SPIRAL2: probing the nuclear potential far from stability***

*With SPIRAL2 it will be possible to study shape co-existence in multiple Coulomb excitation measurements. They will be performed at beam energies below the Coulomb barrier so that one can ignore the role of the nuclear interaction. Some of these experiments can be done with beam intensities as low as  $10^3$  atoms/s, on a high-Z target. It will be necessary to use a high-efficiency, high granularity  $\gamma$ -ray detector in coincidence with a charged-particle detector or a spectrometer to correct for the Doppler effect.*

**High-spin states and rotational bands**

When a deformed, stable nucleus rotates, the energy of the intruder states is significantly affected by the rotational frequency. This may give rise to characteristic particle configurations on which many rotational bands are built. The study of rotational band properties may be used to determine these configurations and hence determine the shell energies in nuclei far from stability. Moreover, in the de-excitation of an intruder state along a rotational band by the emission of  $\gamma$ -quanta, the nucleus may at some point become unstable against neutron emission, and one may thus observe the novel phenomenon of a  $\gamma$ -delayed neutron emission. An analogous proton emission has already been seen in proton-rich nuclei. However, on the neutron rich side, the particle emission is fast because it is not hindered by the Coulomb barrier. Such measurements would immediately give information on the position of the intruder state within the sequence of single-particle levels. By studying high-spin states, K-isomers, and rotational bands in exotic nuclei one will also be able to pin down the properties and positions of single-particle levels and hence gain access to the shell properties of these nuclei. Experimentally, the structure of exotic nuclei, such as  $^{78}\text{Ni}$  for example, can be inferred by studying states of high angular momenta populated in deep-inelastic reactions.

***Deep inelastic reactions to populate states of moderately high-spin states in exotic nuclei***

*Rapid N/Z equilibration drives the neutron flow in deep inelastic reactions. In certain cases, using a beam of neutron-rich nuclei on a heavy target with a large N/Z ratio (typically  $^{238}\text{U}$ ) yields ejectiles that are even more neutron-rich than the projectile and are in high-spin states. For instance, the deformation in the N=60 region can be explored with  $^{94}\text{Kr}$  and  $^{98}\text{Sr}$  beams at 5 MeV/nucleon impinging a  $^{238}\text{U}$  target. These studies can be performed either on a thick (15-20 mg/cm<sup>2</sup>) or a thin target (1-2 mg/cm<sup>2</sup>) target. In both cases, high-efficiency germanium detectors of good granularity are needed. In the thin target experiment, the identification of the ejectile is performed using a magnetic spectrometer. The minimum intensity is of the order of 10<sup>6</sup> atoms/s for a one-week experiment.*

*The measurement of the structure of the very neutron-rich  $^{78}\text{Ni}$  nucleus, assumed to be doubly magic, is a key-experiment. It will consist in feeding the high-spin states of  $^{78}\text{Ni}$  using a deep-inelastic reaction induced by a 4.5 MeV/nucleon beam of  $^{81}\text{Ga}$  or other neutron-rich gallium isotopes on a  $^{238}\text{U}$  target.*

*In this context SPIRAL2 will be the unique facility to perform such experiments within the next decade making use of its copious beams of neutron-rich projectiles.*

The search for strongly deformed nuclei at high angular momentum has been one of the most active research fields in nuclear structure in recent years, since it provides a stringent test of shell model predictions at large deformations. Extensive experimental investigations have been carried out in connection with superdeformed nuclei, which occur when quantum shell effects help to stabilize the nucleus in a strongly deformed prolate shape (with a major to minor axis ratio of approximately 2:1). Several regions of nuclei have been found to possess such a second minimum in the nuclear potential landscape, displaying remarkable properties in their population and decay modes. These studies, including for example the investigation of the role played by the giant dipole resonance in the feeding of superdeformed states, will strongly benefit from the availability of high-intensity beams of radioactive ions, which will allow one to produce very high spin states in exotic neutron-rich nuclei. Such nuclei are out of reach with beams of stable nuclei.

Together with the study of superdeformed nuclei, one of the most appealing quests in nuclear structure is the search for a severely elongated, axially symmetric, hyperdeformed shape, with an axis ratio of (3:1). Such states have been predicted to exist at the highest values of spin, typically above 70  $\hbar$ , in a number of nuclei, including some that are neutron rich. The possibility to populate exotic hyperdeformed shapes has so far motivated a number of experiments employing large arrays of germanium detectors, which have mainly focused the attention on the interplay between reaction dynamics, binding energies and fission barriers. This is because hyperdeformed configurations are expected to exist only in a rather narrow spin window (5-6  $\hbar$ , at most), so that one has to minimize the angular momentum removed by the particle emission in the evaporation process. The lower limit of this window is given by the crossing between normal deformed and hyperdeformed states, while its upper limit is defined by the crossing between the neutron binding energy and the energy of the fission barrier.

In addition, calculations of the potential energy surface based on the liquid drop model have shown that nuclei at very high spins ( $I \approx 70-90 \hbar$ ) may go through a stability region where the equilibrium shape changes from a flattened oblate configuration to a triaxial shape

rotating about its shortest axis (Jacobi transition). For even higher angular momenta, this shape becomes even more elongated until the nucleus eventually fissions. Because the Jacobi transition is expected to take place at higher temperatures, where the population of the residual nucleus takes place, such a transition may act as a gateway to lower-lying discrete structures of a strongly deformed nature.

### ***Search for super and hyper-deformation using the neutron-rich beams from SPIRAL2***

*The search for highly deformed nuclear shapes (i.e. hyperdeformation and Jacobi transitions) will strongly benefit from high intensity, neutron-rich beams, which are expected to populate states of very high angular momentum due to the increase in the fission barrier with neutron number. As an example, the hyperdeformed structures predicted to exist in several neutron rich  $N=108$  nuclei, such as  $^{176}\text{Er}$ ,  $^{178}\text{Yb}$  and  $^{180}\text{Hf}$ , will be produced by the use of the reaction  $^{132}\text{Sn}+^{48}\text{Ca}$ , which would allow the high spin region above  $70 \hbar$  to be investigated better.*

*In addition, lighter  $A=130-140$  nuclei, are expected to undergo Jacobi shape transitions at large angular momenta ( $I \approx 70-90 \hbar$ ). For such very high angular momenta, the fission barrier of the  $^{94}\text{Kr}+^{48}\text{Ca}$  ( $^{142}\text{Ba}$ ) system is 30% to 40% larger than that calculated for  $^{86}\text{Kr}+^{48}\text{Ca}$  ( $^{134}\text{Ba}$ ). With a beam of  $^{94}\text{Kr}$  delivered by SPIRAL2, it will thus be possible to search for the Jacobi transition. This type of experiment requires beam intensities of the order of  $10^9$  atoms/s and a  $\gamma$ -ray detector of very high granularity.*

*The beams of neutron-rich nuclei produced by SPIRAL2 will give access to compound nuclei around the  $\beta$ -stability line such as  $^{200}\text{Pb}$  and up to  $^{206}\text{Pb}$ , perhaps even  $^{208}\text{Pb}$ . It will be possible to reach the  $N=118$  area, where a significant shell effect is predicted at large deformation. A key experiment will then involve the search for a second potential well in  $^{208}\text{Pb}$ . Such a measurement could be done using a  $^{142}\text{Xe}$  beam with an intensity of  $10^{10}$  atoms/s. The experimental techniques would combine a high-efficiency  $\gamma$ -ray detector of high granularity in coincidence with a large-acceptance recoil spectrometer. One could also envisage the complementary detection of charged particles and electrons.*

## **2.4 CREATION OF NEW ELEMENTS: THE SUPERHEAVY NUCLEI**

### **2.4.1 The synthesis of superheavy elements**

One fundamental question posed almost from the beginnings of nuclear physics, has been: “Is there a limit, in terms of the number of protons and neutrons, to the existence of nuclei?”

Both physicists and chemists have sought the limit of existence of nuclei as a function of their numbers of nucleons by attempting to produce nuclei heavier than the nucleus of  $^{238}\text{U}$ , the heaviest species we find here on Earth. Beyond the problem of their existence, other fundamental questions arise: How many isotopes of an element can exist? What are their lifetimes? Which properties determine their stability? How can they be synthesised? Were they ever synthesised in stars? What are their chemical properties? How are the electrons

organized in the strong electric field of such a high  $Z$  nucleus? Up to which element is the ordering scheme of Mendeleev's periodic table still valid?

The underlying question is that of the balance of the forces acting at the interior of the nucleus, resulting from the strong interaction which tends to bind the nucleons together, and the Coulomb interaction which tends to push the protons apart. Macroscopic considerations alone (as in the liquid-drop model) prohibit the existence of nuclei having more than 104 protons. The superheavy nuclei ( $Z \geq 104$ ) owe their existence to microscopic nuclear effects that give additional stability. Strong shell effects help to overcome the Coulomb forces and stabilise the nucleus with respect to fission. The magic numbers from 2 to 82 are common to both protons and neutrons, and logically the next closed proton shell should be at  $Z=126$ , analogous to the  $N=126$  neutron shell in  $^{208}\text{Pb}$ . However since the 1960s, macroscopic calculations corrected for shell effects (the approach of Strutinsky) have resulted in  $Z=114$  being regarded as the next proton magic number together with  $N=184$  for the neutrons. More recently, relativistic and non-relativistic microscopic calculations indicate that there may be an island of stable nuclei located in the neighbourhood of ( $Z=120$ ,  $N=172$ ) and ( $Z=126$ ,  $N=184$ ) respectively. The landscape of this area of stability has taken shape throughout the last decades. So a "side valley" of isotopes stabilized by deformation has been found around  $Z=108$  and  $N=162$  with this Hassium isotope being detected in a chemistry experiment at GSI in 2001.

Experimentally, these nuclei can be looked for either in Nature, where many fruitless searches have been made, or by synthesising them artificially in nuclear reactions. Starting in the 1940s and 1950s experiments to synthesise elements beyond uranium involving neutron evaporation with subsequent  $\beta^-$ -decay and fusion reaction with deuterons and helium beams were used to climb up in atomic number to mendelevium ( $Z=101$ ). Thereafter, beginning in the late 1950s scientists in Berkeley, California and in Dubna, Russia started to irradiate actinide targets with light ion beams and were able to reach  $Z=106$  in this way. Another reaction scheme leading to relatively low excitation energies of the compound nucleus and therefore often called "cold" fusion uses targets of lead or bismuth. The elements  $Z=107-112$  produced at GSI up to 1996 have been identified in atomic number ( $Z$ ) and mass ( $A$ ) by their  $\alpha$ -decay chains which end in known elements. Most recently a decay chain assigned to the nucleus  $^{278}113$  produced by the same method has been reported by a group from RIKEN in Japan. This method of unambiguous identification encounters two difficulties:

- the systematic way in which the cross-section falls by a factor of 10 when the atomic number increases by 2. This is primarily due to two effects: the first, quasi-fission, contributes to the reaction by a mechanism which tends to separate the collision partners at the initial stage of fusion. The second, fission, is directly related to the instability of these superheavy nuclei, and occurs after fusion itself.
- the method of identification by  $\alpha$ -decay is only possible for neutron-deficient isotopes which end in known isotopes.

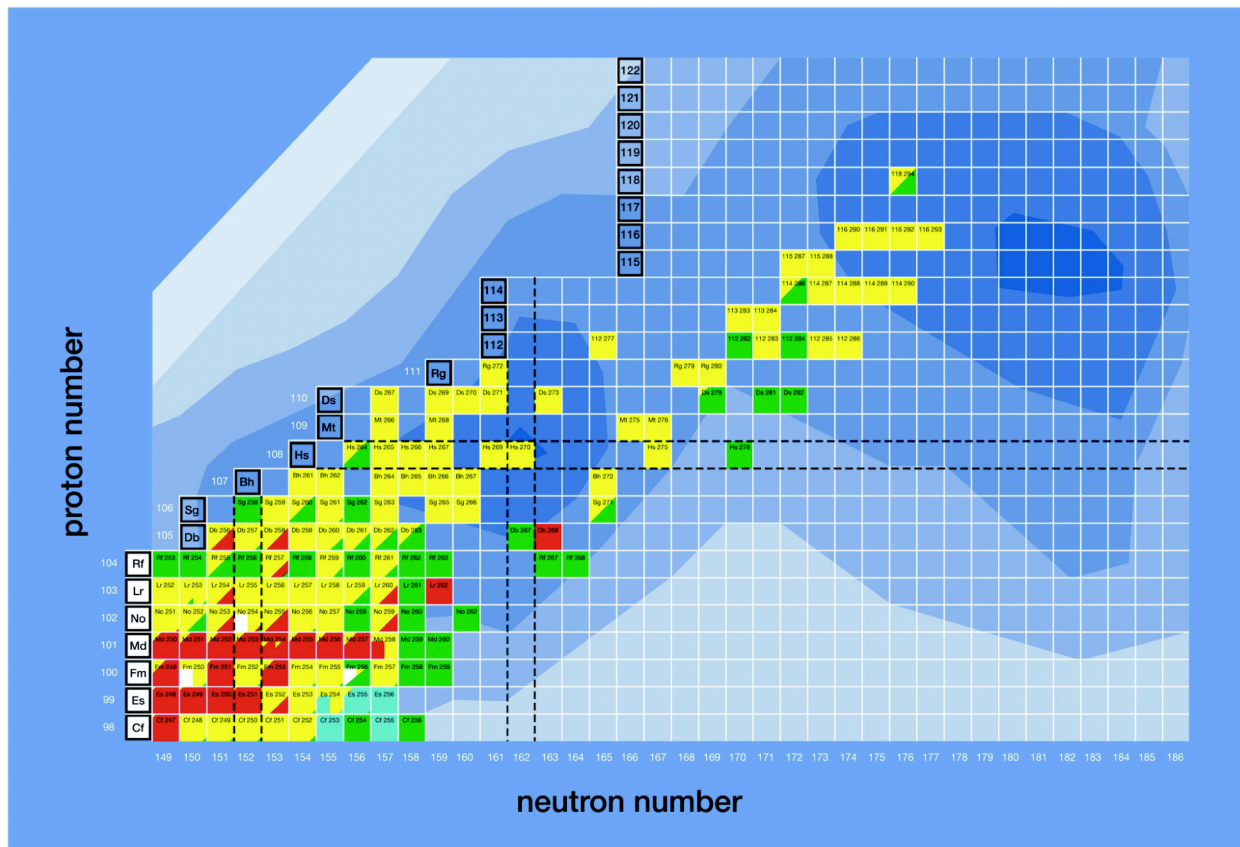


**Figure 2.4.1:** Part of the chart of nuclides in the superheavy element region with the shell correction energy from microscopic-macroscopic model calculations (in blue) showing the regions of stronger binding around  $Z=108$  and  $114$  and  $N=162$  and  $184$ .

In parallel, studies of “hot” fusion using an actinide target, have produced nuclei richer in neutrons. The results obtained in Dubna show cross-sections between 5 pb and 0.1 pb for elements from  $Z=112$  up to  $Z=118$ . On the other hand, their identification remains ambiguous because the decay chains of the nuclei produced end with the fission of unknown nuclei.

In the short term, the results obtained from hot fusion in Dubna must not only be validated in another laboratory but preferably via another method of production and identification. One of the possibilities would be a chemical characterization of one daughter of the element synthesized. For example the great-grand-daughter of element 114 corresponds to the element 108, whose chemistry is well known. Confirmation of the discovery of element 112 in the course of a chemistry experiment on element 108 (hassium), which "entered" the originally

observed  $\alpha$ -decay sequence on the grand-daughter level, is another example. Figure 2.4.1 shows the present situation in terms of a section of the chart of nuclides in the superheavy element region.

Chemistry is also used to investigate the directly produced "parent" species in the case of nuclear species with longer half-lives. Chemical techniques will become more important for the more neutron rich isotopes nearer to the island of stability. A few experiments have been performed to try to study a longer-lived isotope of element 112 produced in the reaction  $^{48}\text{Ca} + ^{238}\text{U} \rightarrow ^{283}112^*$ . Recently, an experiment aimed at the production of element 114 in the reaction  $^{76}\text{Ge} + ^{208}\text{Pb} \rightarrow ^{284}114^*$  was performed at GANIL with the LISE3 separator. This allowed the experimenters to set an upper limit on the cross-section for the synthesis of this element of about 1 pb. Further experiments looking for element 114 are in preparation and further searches for element 113 are under consideration at GSI and at Dubna.

***Stable-isotope beams of high intensity from SPIRAL2: discovery of new isotopes made possible***

*The ultimate goal of the synthesis of the superheavy elements is to reach the long predicted island of stability. To reach the nucleus ( $Z=126$ ,  $N=184$ ), one could envisage complete fusion reactions such as  $^{76}\text{Se} + ^{238}\text{U} \rightarrow ^{314}126_{188}$  or  $^{86}\text{Kr} + ^{232}\text{Th} \rightarrow ^{318}126_{192}$ . With estimated masses, these reactions are energetically possible, even if – despite the relative “stability” of these nuclei – their cross-sections are undoubtedly extremely small. The stable-isotope beams of very high intensity delivered by SPIRAL2 will make it possible to progress towards this goal. In addition to the very intense beams, this experimental programme would require specialised installations dedicated to these measurements: handling highly radioactive components including actinide targets, targets resistant to heat, a spectrometer with a very high acceptance (transmission higher than 60%) and very good beam rejection (higher than  $10^{13}$ ) and fast detection.*

*The intensity of the neutron-rich beams delivered by SPIRAL2 will allow, in a first stage, for the synthesis of new isotopes of the “light superheavy” nuclei. Studies of reaction mechanisms remain to be carried out to show the influence of the neutron number on the production cross-section. Coupled with chemistry, these new isotopes can contribute to the identification of the missing nuclei in the chart of the nuclides.*

*As in the case of hot fusion, the high  $N/Z$  ratio of the island makes the identification of the nuclei via  $\alpha$ -decay chains inadequate: linking between known nuclei and the island of stability cannot be assured. It is necessary to develop new direct methods of identifying the  $Z$  and  $A$  of the nuclei created, in order to remove any ambiguity: ion traps, mass spectrometers or time-of-flight measurements, high-resolution calorimeters, laser spectroscopy and, for nuclei with “long” lifetimes ( $\approx 1$  s), chemical techniques of identification. These methods will have to be tested on the known “light superheavy” nuclei.*

*Symmetric fusion offers some opportunities for the synthesis of certain isotopes. This is also interesting for the study of the role of the mass asymmetry parameter of the system.*

*The use of radioactive neutron-rich actinide targets is another possible/necessary ingredient together with the neutron-rich beams to approach the region of stability.*

## **2.4.2 Structure of heavy and superheavy nuclei**

It is clear that the studies of synthesis must be accompanied by studies of the nuclear structure and reaction mechanisms, in order to understand the physics of superheavy nuclei in a complete and coherent way. Current devices make it possible to study the structure of the

superheavy elements, and to understand how it influences their stability, i.e. to know their shapes and their decay times. The trends of these variables for individual elements can be expected to vary according to the number of neutrons. Various methods ( $\alpha$ -,  $\gamma$ -, and electron spectroscopy, Coulomb excitation, ion trapping) give access to their characteristic properties (spin, parity, first excited states, quadrupole moments, fission barriers (see figure 2.4.2), masses).

The production cross-sections of the transfermium nuclides are sufficiently high to make it possible to carry out detailed studies of their spectroscopy. The objectives are:

- to determine the orbitals responsible for the configurations of such nuclei and their properties
- to study the collectivity of the nuclei, in particular the deformation around the small islands of deformation ( $^{254}\text{No}$  and  $^{270}\text{Hs}$ )
- to study the role of K-isomerism with respect to their lifetimes and  $\alpha$ /sf-ratios and compare this to the ground state
- to determine the masses of the nuclei
- to estimate the fission barriers.

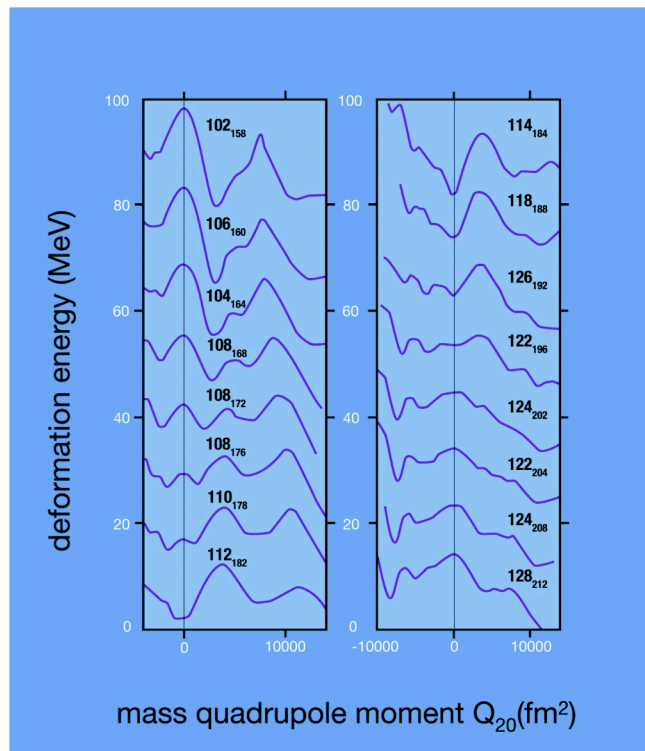


**Figure 2.4.2:** Fission barriers of a representative set of superheavy nuclei obtained from HFB calculations with the Gogny D1S interaction.

The mean-field models of Hartree-Fock-Bogoliubov type or relativistic mean-field models make it possible to calculate these quantities, but there are serious disagreements between them. The experimental studies must thus provide strong constraints, in order to predict better the properties of the superheavy nuclei that would be located around the next magic number in  $Z$ . It is difficult to obtain direct experimental information on the spins and parities of low-lying levels in the heaviest nuclei that are known today. However, there is an emerging consensus on the existence of significant deformed shell gaps for neutrons at  $N=162$  and for protons at  $Z=108$  (see figure 2.4.3). The spectra of odd nuclei around these numbers give

fingerprints of these gaps and deliver thereby the first hints on the position of the spherical single particle levels. Shell effects depend critically on both neutron and proton numbers. However, there are large proton shell gaps at 104 and 108 for similar deformations and the deformation is predicted to vary rather slowly along an isotonic line and more rapidly along isotopic lines. If this prediction is correct, the exploration of the neutron deformed shell gap should be easier than that of the equivalent proton gap.

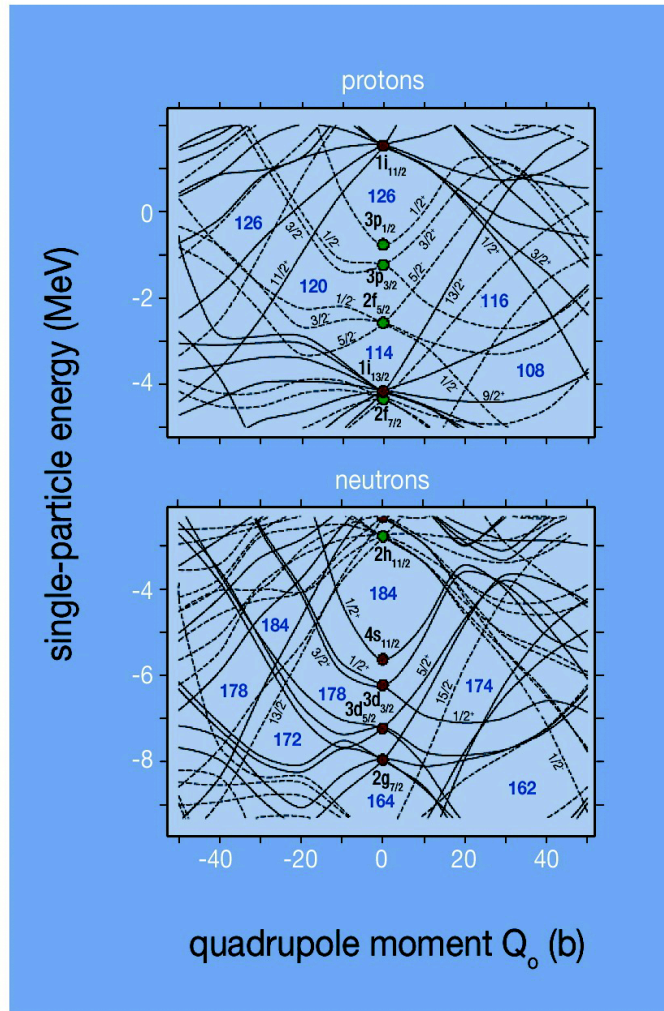


**Figure 2.4.3:** Proton (top) and neutron single particle spectra obtained for  $^{292}_{116}_{176}$  with the Skyrme Hartree-Fock-Bogoliubov method. Large deformed shell gaps can be seen for several values of the number of neutrons and protons.

The large density of single particle states around the Fermi level and the presence of high- $j$  orbitals should also favour the presence of K-isomers which will affect the  $\alpha$ -decay chains. Such an isomeric level has already been detected in  $^{270}_{110}$  and nicely explained by theory. Some others are known in transactinide nuclei and are presently under intensive study. Their presence seems to be a rather general phenomenon but up to now our theoretical and experimental knowledge of them is extremely limited; they would however bring precise information on the quasi-particle spectra in the superheavy region.

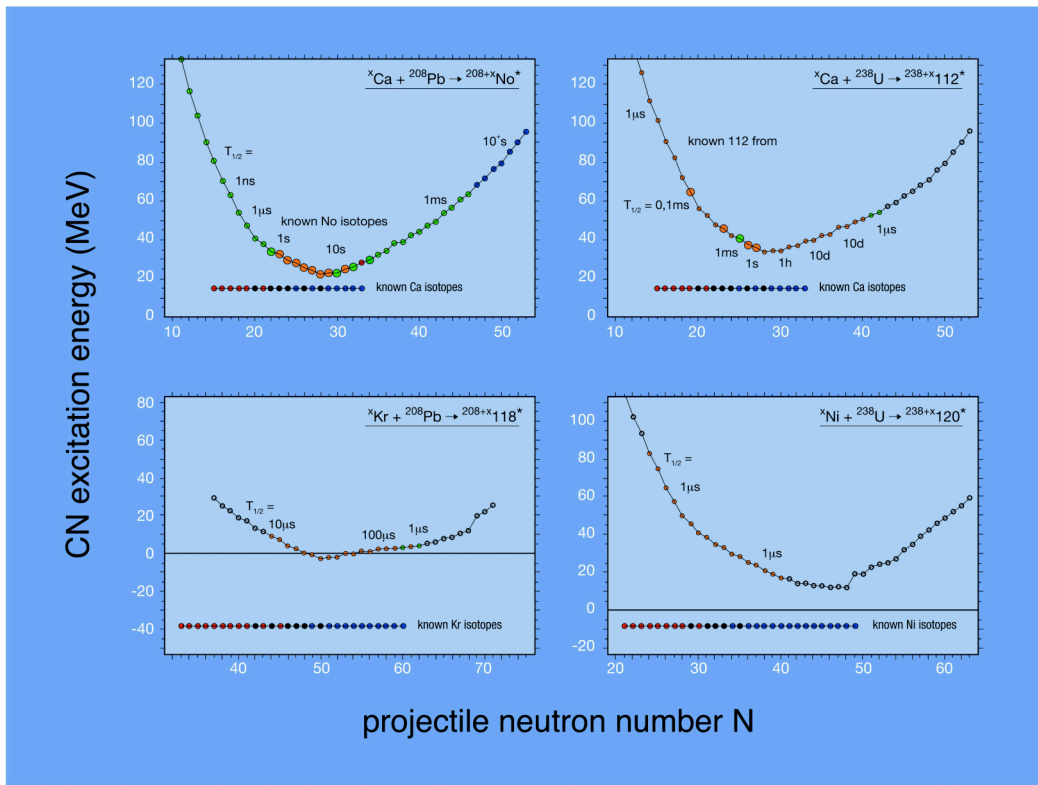


**Figure 2.4.4:** Excitation energies of compound nuclei for the production of nuclei with  $Z=102, 112, 118$  and  $120$  as a function of the isotopes produced with stable and unstable projectiles indicated by black and red/blue dots, respectively. Observed (large circles) and predicted (small circles) decay modes are indicated by the usual colour code as well as the predicted half lives. The x-axis gives the neutron number of the projectile as well as that of the compound nucleus.

The theoretical models of nuclear masses all rely on the parametrisation of experimental masses. Superheavy elements have an unusual ratio of protons over neutrons and thus bring specific constraints to the isospin dependence of the formulae. It has also been seen that the strong correlations between neutrons and protons are not well described by macroscopic models and that models where all the nucleons are treated self-consistently are more realistic for heavy systems. A good knowledge of the masses of several superheavy nuclei would bring constraints to these mass formulae for nuclear asymmetries, which are not reached in another region of the nuclear chart. Such constraints will have an impact on the description of lighter exotic nuclei whose masses are out of reach of experiment.

To study the nuclear structure of heavy and superheavy nuclei, complementary techniques are used: either in flight  $\gamma$ -ray or electron spectroscopy at the target position or decay- and isomer spectroscopy detecting electrons and  $\gamma$ -rays at the focal plane in coincidence with a characteristic  $\alpha$ -decay or an isomeric decay detected after a recoil separator. Some structure information can be obtained also by  $\alpha$ -fine-structure measurements. With current facilities, one has reached isotopes up to  $Z=105$  (dubnium) at GSI. The high-intensity stable-isotope beams delivered by SPIRAL2 will allow us to extend the spectroscopy to a wider range of nuclei in terms of neutron number and higher  $Z$  (see figure 2.4.4). This is necessary to explore and to understand the trends in the single particle levels that ultimately indicate the onset of the long sought shell gap.

### ***Spectroscopy of heavy nuclei at SPIRAL2***

*The production of new neutron-rich isotopes in the transfermium area, particularly between rutherfordium and hassium ( $Z=104-108$ ) is of major interest, and the radioactive ion beams delivered by SPIRAL2 will finally allow us to explore these areas. Reactions such as:  $^{130-132}\text{Sn} + ^{136}\text{Xe}$  are presently seen as a new path to give access to the isotopes  $^{266-268}\text{Rf}$  (with  $N=162-164$ ). New isotopes  $^{267-271}\text{Sg}$  may be reached using reactions like  $^{137-141}\text{Xe} + ^{130}\text{Te}$ . These nuclei, which cannot be formed with stable-isotope beams, are essential for the identification of the new elements synthesised in hot fusion with actinide targets. Indeed, the decay path of the latter crosses this area of the neutron-rich nuclei, which is inaccessible at present.*

*With the high-intensity stable-isotope beams delivered by SPIRAL2, it will also be possible to carry out spin and parity measurements of the ground state and excited states in odd transfermium nuclei, by  $\alpha$ -,  $\gamma$ - and electron spectroscopy. Further examples are measurements of the  $^{254}\text{No}$  nuclear structure properties and of its formation (the production cross-section is of the order of  $2 \mu\text{b}$ ). Of specific interest are the quadrupole moment (measured by Coulomb excitation), the lifetime and the charge state distribution. Laser spectroscopy of this key isotope could also be undertaken. Finally a  $^{254}\text{No}$  mass measurement with traps or efficient and very selective spectrometers would give a new handle on these elements.*

*The use of radioactive or high intensity beams must be accompanied by the development of adequate targets and the use of radioactive targets should also become more general.*

*New techniques must also be explored: Measurements of quadrupole moments after fusion in inverse kinematics or by a lifetime measurement (with the use of a plunger or a charge-state plunger), laser spectroscopy, mass determinations using traps, and fission barrier studies by (d,p) reactions in inverse kinematics.*

*Again, this research requires the setting up of a new spectrometer of very high acceptance (transmission higher than 60%) and of very good beam rejection (higher than  $10^{13}$ ) and the use of a  $\gamma$ -spectrometer of high efficiency and very high granularity (like AGATA), permitting very high counting rates. It will also be necessary to develop experimental devices combining electron and  $\gamma$ -ray spectrometers. In addition, the focal plane after the spectrometer has to be equipped with particle and  $\gamma$ -ray detectors to allow for decay spectroscopy by recoil- $\alpha$ - $\gamma$  correlations.*

### **2.4.3 Reaction mechanisms and dynamics**

The recent successes in the synthesis of the superheavy elements in Dubna, Darmstadt and Tokyo should not make us forget the many gaps and open questions that still exist in this field of research. Many of them were summarised in the previous section. The process leading to the formation and the survival of a superheavy residue is complex and far from being completely understood. Several reaction channels are in strong competition during the process. They are responsible for the extremely low cross-sections observed for the synthesis. One way to view the process of superheavy element synthesis is to make the assumption that it takes place in three steps: capture, fusion and survival of the compound nucleus during its de-excitation.

During the capture, two processes compete: true fission and quasi-fission. In quasi-fission the two partners are in close contact for a given time and form a composite system but they

separate without forming a single compound nucleus. These two mechanisms lead to very similar observables and are thus difficult to disentangle experimentally. For both processes the characteristics of the scission fragments and the angular and energy distributions of the light particles and neutrons are indeed very close. The lifetimes of the composite systems may be different in the two processes and this may allow us to distinguish between them: quasi-fission probably has a much shorter lifetime than fusion-fission because of the different trajectories followed on the potential energy surface.

For this reason, direct measurements of the reaction times have been carried out using the single-crystal blocking technique. The weak point of this method is the necessary assumption that small times correspond to quasi-fission and longer times to fusion-fission; no clear separation between the two processes has been observed.

The backtracing technique that has been developed recently now gives access to the distributions and the correlation of pre- and post-scission neutrons. For several superheavy systems two components in the neutron multiplicity distribution have been observed, which are probably linked to the two competing processes: low multiplicity corresponds to the quasi-fission process and high multiplicity to fusion-fission. The use of this method may reconcile earlier disagreements between results because the analysis was based only on average values for the neutron multiplicities, and the different disintegration processes were not separated. Many puzzles remain to be solved, e.g. the behaviour of the total fusion or capture cross-sections. In a simple picture they are expected to decrease when the mass of the composite system increases but experimental cross-sections measured in  $^{48}\text{Ca}$  and  $^{58}\text{Fe}$  induced reactions show a more constant behaviour. Here other degrees-of-freedom, such as the structure of both the reaction partners and the composite system, and the neutron number of the entrance channel come into play. SPIRAL2 will provide highly intense stable-isotope beams as well as unstable neutron rich projectiles and will thus be an ideal tool to study the isospin dependence of the reaction mechanism.

In terms of theory most of the models agree in predicting or reproducing cross-sections for capture reactions and for the formation of evaporation residues but they diverge by several orders-of-magnitude in their description of the intermediate stages that lead to the synthesis. Overall it is essential to bring strong experimental constraints to these models all of which contain a great number of parameters. The importance of the dynamical aspects of these processes is now well established. Nevertheless, the nature and the amplitude of the dissipation, in the entrance and the exit channels, and its dependence on temperature and deformation still remain a subject of controversy. The dynamical evolution of shell effects also needs to be investigated in detail.

Over the next few years, direct fission time measurements of the superheavy elements will be pursued as a function of their charge, mass and excitation energy by means of the single-crystal blocking technique. These measurements should help us to locate the island of stability via the observation of increasing fission times. The determination of the different parameters characterising the quasi-fission/fusion-fission competition can be improved by the determination of the particle emission sequence obtained by the X-ray fluorescence technique, which is a direct time measurement complementary to single-crystal blocking.

However these measurements have to be put together with precise measurements of the angular distributions and kinematical characteristics (energy, mass, charge, angle...) of the scission fragments and the properties of the pre- and post-scission neutron emission. The

correlations between all these different observables will allow us to obtain, through backtracing, the distributions and the evolution of the parameters that govern the capture mechanism. Such information should put strong constraints on the current models and as a consequence could improve their predictive powers. Up to now information on  $\gamma$ -rays has been little exploited in this field. Investigations of the giant dipole resonance excitation, both the multiplicity and the total energy taken away by the  $\gamma$ -rays, will provide an additional tool to complete the discrimination between the different processes. In particular, this may shed light on the influence of the deformation and the angular momentum of the partners on the reaction mechanism. Experiments aimed at obtaining these different pieces of information simultaneously might be necessary. If so, a powerful  $\gamma$ -ray detection array will be essential.

***Better understanding of reaction mechanisms and dynamics to reach the heaviest elements***

*The optimization of the entrance channel (projectile, target, incident energy,) used to form superheavy elements needs a better understanding of the intermediate processes intervening in the reaction mechanism. The investigation of these processes will help to explain/predict the (low) cross-section for the synthesis of superheavy elements. In particular, the competition between quasi-fission and fusion-fission has to be better understood.*

*Direct measurements of fission lifetimes obtained by the single-crystal blocking method and the X-ray fluorescence techniques have to be associated with precise measurements of the kinematical characteristics (energy, mass, charge, angle) of the scission fragments and the emitted light particles and  $\gamma$ -rays. The correlations between the various observables will then make it possible to obtain, by backtracing, the distributions of the physical parameters describing the evolution of the systems. This ensemble of information will thus provide predictive power for the theoretical models under development.*

*The high-intensity beams delivered by SPIRAL2 will constitute a very powerful tool as they will offer the possibility to pursue the present investigation with stable-isotope beams, and at the same time they will help to extend this investigation to very neutron- rich systems with radioactive ion beams, since the neutron excess of the partners seems to play an important role in the competition between the different processes and their cross-sections.*

With the launching of SPIRAL2, which consists of both an accelerator of stable heavy ions and a system for producing neutron-rich beams, GANIL will be in a particularly favourable position to carry out this research. Indeed, the stable-isotope beams produced will be two orders-of-magnitude higher in intensity than those currently available, while the heavy, exotic beams can be accelerated to energies in the range necessary for the study of these fusion reactions.

#### **2.4.4 Chemistry of superheavy elements**

Chemical elements are the "elementary particles" of chemistry, and superheavy elements are perhaps the most fascinating of them and are certainly the most exotic. Research into their chemistry derives its fascination from the increasingly strong relativistic effects on the inner atomic electrons with larger  $Z$ . These electrons are moving with about 80% of the speed of light. This makes these elements extremely interesting objects in quantum chemistry. Relativistic effects manifest themselves in deviations of chemical properties from the established trends in the periodic table of the elements, see figure 2.4.5. Chemistry experiments - even with only one superheavy element atom produced per hour or per day - can reveal such effects. Moreover, these experiments determine basic chemical properties and

they map out the architecture of the periodic table. Theoretical developments, the results of sophisticated atomic and molecular calculations, have had an important impact on this field. The diversity and complexity of possible chemical studies depends strongly on the half-life of the species under investigation. As a result it is highly desirable to gain access to the longest-lived, i.e. the most neutron-rich, nuclides. Here, the neutron-rich ion beams from SPIRAL2 may open new possibilities.

As already mentioned above, chemistry can play a crucial role in the unambiguous identification of a newly synthesised chemical element. At the time of writing, chemistry experiments have reached sensitivities below the one picobarn level for nuclides with half-lives of at least a few seconds. Besides their potential to identify a superheavy element, this technique also provides samples for nuclear decay and nuclear structure studies, which are sometimes superior to physical techniques. This is, for example, the case for measurements of longer-lived species in a low-background environment. The use of highly radioactive, neutron-rich actinide targets not only in hot-fusion reactions but also in multi-nucleon transfer reactions - combined with an unsurpassed efficiency – enabled the discovery and investigation of the most neutron-rich nuclides amongst the heaviest actinides and some lighter transactinides. Ongoing studies of the N=162 neutron-shell nucleus  $^{270}\text{Hs}$  and its neighbouring isotopes gives just one example. For all these investigations, independently of whether stable or radioactive ion beams will be used, the highest beam intensities - as projected for SPIRAL2 - always play a key role. However, the high sensitivity of chemical methods is also an advantage and can be exploited in all studies where only low beam intensities are available.

**Periodic Table**

**Figure 2.4.5:** Periodic Table of the Elements. Superheavy elements 104 through 112 take the positions of the seventh period transition metals below hafnium in group 4 and mercury in group 12. While chemical studies have justified placing the elements rutherfordium through hassium into the periodic table, the chemically "unknown" heavier elements still need to be investigated. For element 112 – presently under investigation – the range of chemical properties between mercury and radon is indicated. The arrangement of the actinides reflects the fact that the first actinide elements still resemble, but to a decreasing extent, the chemistry of the d-elements: e.g. thorium lies below the group 4 elements zirconium and hafnium.

Nuclear chemistry experiments are also best suited to study "below-target" n-rich products from transfer reactions with medium-heavy projectiles. While the actinide targets are the same as those mentioned above, the best-suited n-rich projectiles are presumably the ones on or beyond a neutron shell. Thus  $^{82-84}\text{Ge}$  may be interesting cases  $^{132-134}\text{Xe}$  would certainly be the ideal choice. These beams, in combination with  $^{238}\text{U}$ ,  $^{244}\text{Pu}$  and  $^{248}\text{Cm}$  targets, will allow access to yet uncharted regions of the n-rich, light actinide (actinium to americium) nuclides approaching the N=152 neutron shell. The known chemical properties of these elements and the expected half-lives of the nuclides of interest clearly make chemical techniques an ideal tool for these studies.

## 2.5 SYMMETRIES

Symmetry is a central concept in physics and plays a key role in our understanding of both the properties of matter and Nature's fundamental forces. Symmetry has been of central importance to nuclear physics from the birth of the discipline, providing continual guidance for developments in this field. One example of a specific nuclear-physics symmetry, to be discussed in more detail in the following section, is isospin symmetry, which is a consequence of the approximate charge independence of nucleon-nucleon forces. Another early example is Wigner's spin-isospin symmetry, based on an extension of isospin invariance, assuming not only the charge independence of nuclear forces but their spin independence as well.

Since the introduction of the isospin and spin-isospin or supermultiplet symmetries, back in the 1930s, many more examples of symmetries have been found and exploited in nuclear physics and, in particular, they have found fruitful application in the context of three known models of atomic nuclei. First of all, it has been demonstrated, notably by Racah and Elliott in the 1940s and 1950s, that the nuclear shell model, either with a pairing interaction or with a quadrupole interaction, admits analytical solutions based on symmetries. These elementary shell-model symmetries—SU(2) for pairing and SU(3) for quadrupole—can be extended to higher symmetries if more complex situations, such as the inclusion of the isospin degree of freedom, are envisaged. Secondly, in the context of the geometric collective model, proposed by Bohr and Mottelson in the 1950s, symmetries have found fruitful application for the description of rotations and vibrations and, more recently, of the associated quantum phase transitions where they have been applied at the critical point of the transition. Finally, in the interacting boson model, proposed by Arima and Iachello in the 1970s, the application of symmetry techniques has reached further refinement with the development of dynamical symmetries, either global or partial, to explain a wide variety of observed nuclear structures ranging from vibrational to rotational, and the introduction of dynamical supersymmetries to

achieve a simultaneous description of bosonic even-even and fermionic odd-mass nuclei with a single effective Hamiltonian.

### 2.5.1 Strong interactions and isospin symmetry

Isospin symmetry is a consequence of the assumption that nuclear forces are independent of charge. The symmetry is characterised by the isotopic spin (“isospin”) quantum number  $T$ . This amounts to regarding the neutron and the proton as two states of the same particle: the nucleon. Even though it is known that this symmetry is broken to a certain extent already by the strong interaction, in a significant way by the weak interaction and, most significantly, by the electromagnetic interaction, the isospin formalism remains an extremely powerful tool to understand the structure of nuclei. The concept of isospin symmetry is expressed most clearly in the nuclei known as “mirror nuclei”, nuclei  ${}_Z X_N$  and  ${}_{Z'} Y_{N'}$  of the same mass  $A=N+Z=N'+Z'$ , for which the number of neutrons in one is equal to the number of protons in the other ( $N=Z'$ ) and *vice versa* ( $Z=N'$ ), resulting in a very similar structure in both. More generally, isobaric nuclei (nuclei with the same mass number,  $A$ ) have corresponding levels, which can be grouped into multiplets of states of common isospin. However, the isospin symmetry breaking terms of the nuclear Hamiltonian should lead to each nuclear state having, in addition to its main component of isospin  $T$ , minor components of differing isospin. The amount of isospin mixing, as derived *e.g.* from experiment, can be taken as a measure of the magnitude of the symmetry violation. The breaking of the isospin symmetry by the Coulomb force increases with  $Z$  and for a given mass it is at a maximum for  $N=Z$  nuclei. The study of the heavier nuclei with  $N \approx Z$  is thus of fundamental interest. Another interesting aspect of heavy mirror nuclei is the possibility to search for exotic matter distributions in the nucleus, *i.e.* to test theoretical predictions for proton skins, by means of Coulomb energy differences of isobaric analogue states since the Coulomb repulsion between the protons in the nucleus is directly related to their spatial distributions.

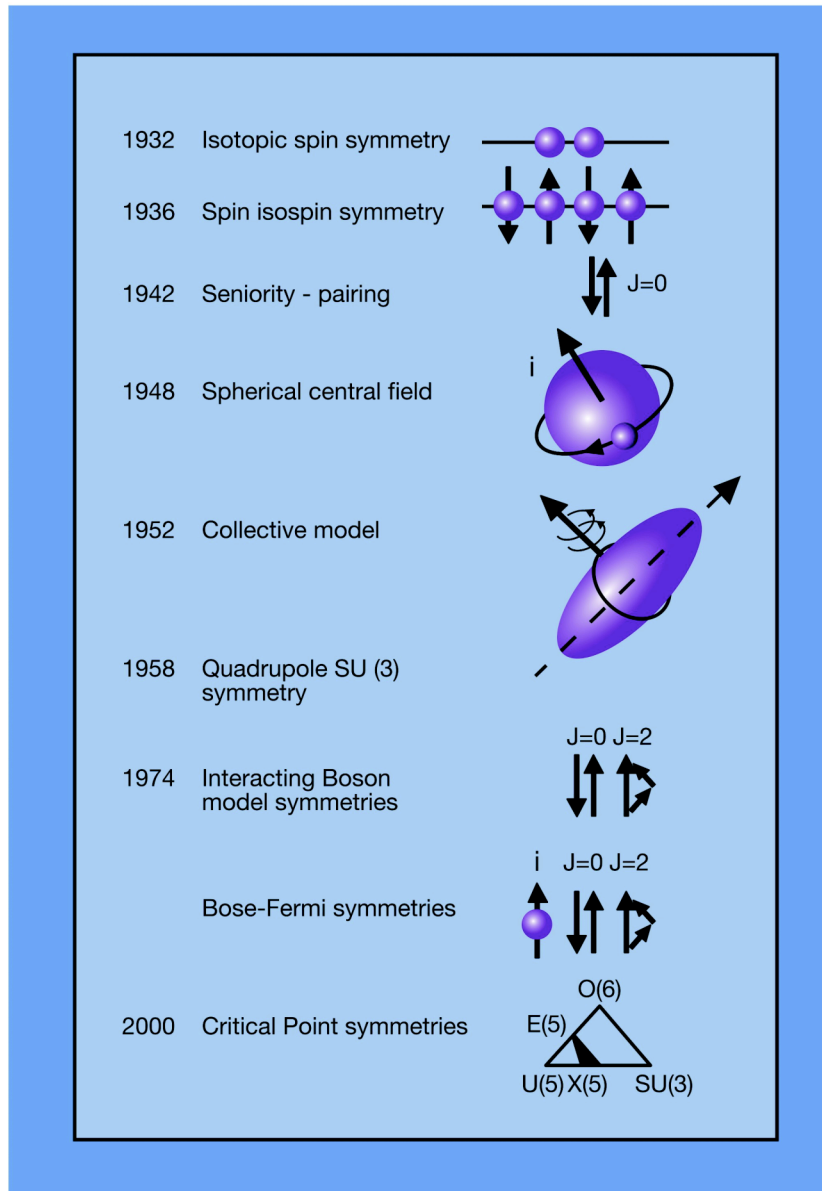


**Figure 2.5.1:** Overview of a number of realisations of symmetries in nuclei, either in the context of the nuclear shell model, the geometric collective model or the interacting boson model.

Progress has been made in the study of mirror nuclei up to  $A=54$ . The levels of the nuclei have been studied up to relatively high spins, following in most cases rotational-like bands. Level differences have been measured as a function of angular momentum in these nuclei and when data for  $T=1$  bands in  $N=Z$  odd-odd nuclei and in the more exotic  $T_2=-1$  members of the multiplets became available, it was realized that the perturbative inclusion of the Coulomb interactions among protons (with charge-invariant model wave functions) was not enough to explain the measured energy differences. In order to reproduce the experimental data, an isospin non-conserving term has been introduced in the shell-model effective interaction. This term has the form of an additional pairing term (monopole and quadrupole) in the energy-difference formulae.

The isospin symmetry breaking can also be studied by looking at the isospin mixing of the nuclear states. In fact, every nuclear state is expected to contain, in addition to the main component of isospin  $T$ , minor components of different isospin. Isospin mixing can be directly accessed by measuring the isospin forbidden ( $\Delta T=0$ )  $E1$  transitions in  $N=Z$  nuclei. An early experiment on  $^{64}\text{Ge}$ , did not confirm the large isospin-violating  $E1$  amplitude which had been claimed for a  $5^- \rightarrow 4^+$  transition in this nucleus. Hartree-Fock calculations in this domain indicate that the isospin mixing probability in  $N=Z$  nuclei increases from roughly 1% at  $Z=28$  to about 4% at  $Z=50$ . For masses heavier than  $^{64}\text{Ge}$  no detailed spectroscopic information could be obtained up to now.

### ***Probing isospin symmetry at SPIRAL2***

*Experimentally several probes can be used to test isospin symmetry. They make use of the following:*

- *$E1$  transitions between states of equal isospin are forbidden in  $N=Z$  nuclei.*
- *$B(E1)$  values between corresponding states in mirror nuclei should be equal.*
- *Mirror  $\gamma$ -ray transitions of any multipolarity with  $\Delta T=1$  should have equal reduced strength.*
- *The reduced matrix elements of  $E2$   $\gamma$ -ray transitions between analogue states of an isobaric multiplet should vary linearly with isospin projection  $N-Z$ , with a slope given by the isovector effective charge.*
- *The  $\beta$  transitions between  $I^\pi=0^+$  states are only allowed between members of the same isobaric multiplet and forbidden between states having different isospin.*

*At SPIRAL2, energy difference (mirror and triplet energy differences) measurements will be extended to heavier  $T=1$  isobaric mass triplets. These measurements require the combination of several efficient arrays including a neutron detection system in coincidence with charged-particle and  $\gamma$ -ray arrays.*

*Information on the isospin-symmetry breaking for  $Z \neq N$  can be obtained by comparing the strengths of analogue  $E1$  transitions in mirror nuclei. If isospin is a good quantum number, these transitions should have the same reduced strength. Experimentally, these investigations can be performed by measuring the lifetimes, branching ratios and multipole-mixing ratios in the decay of analogue states.*

A further subject of interest is the precise measurement of super-allowed Fermi transitions from a few odd-odd,  $Z=N$  nuclei with  $A$  greater than 60. The absolute strengths of these transitions, properly corrected for nuclear structure and radiative effects, provide information on the  $V_{UD}$  element of the Cabibbo-Kobayashi-Maskawa quark-mixing matrix, complementary to those provided by the polarised-neutron decay. In this case, the validity of the isospin symmetry between parent and daughter level is assumed, and the second-order corrections due to symmetry violating effects must be determined from independent experimental or theoretical results. Measurements of the branching ratios are also crucial in order to determine precisely the isospin impurities and to extract the superallowed branching ratio. For the heaviest  $N=Z$  nuclei, the total amount of strength going into the numerous Gamow-Teller transitions might be significant and they need to be measured with great care. More challenging are the measurements of the decay of  $T_z=-1$  nuclei. In these nuclei, the superallowed transition strength is much more diluted in other  $\beta$  transitions, whose intensities have to be measured via  $\beta$ -delayed  $\gamma$ -rays. As detailed in another section, these measurements can be performed at the low energy line of SPIRAL2, which will be the ideal facility for studying some of these interesting nuclei.

### 2.5.2 Wigner energy and spin-isospin symmetry

Nuclei at the  $N \approx Z$  line are unusually tightly bound, requiring an additional so-called Wigner term, which specifically deals with  $N=Z$  nuclei, in nuclear mass formulae. It usually takes the form  $|N-Z|$  or a function thereof. Generally, an increase in the nuclear binding energy may be the consequence of additional correlations. This is well known in the case of a pairing interaction between identical nucleons where it leads to pair correlations in the ground state. Since identical nucleons have the same isospin projection  $T_z$ , the interactions between them necessarily are characterized by  $T=1$ , *i.e.* they are isovector. The interactions between a neutron and a proton can also be scalar in isospin and the spikes in the nuclear binding energy at  $N=Z$  are a consequence of this  $T=0$  part of the nuclear interaction. While pairing correlations between identical nucleons are by now well understood, those due to the combined effect of pairing in the  $T=0$  and  $T=1$  proton-neutron channels are more complex, and it can be shown that, if these are of comparable magnitude, they lead to an  $\alpha$ -type clustering effect, *i.e.* a quartetting rather than a pairing effect, which gives rise to the extra binding energy of  $N=Z$  nuclei. At present, the evolution of the Wigner energy with mass is unknown and it is not clear if some effect will remain at mass numbers approaching  $A=100$  or whether the effect will completely disappear (see figure 2.5.2). An even more exciting possibility is that, in the region of  $N \approx Z$  nuclei beyond those with presently known mass, the Wigner effect will actually be enhanced because of a specific combination of single-particle orbits ( $f_{5/2}$ ,  $p_{3/2}$  and  $p_{1/2}$ ) and their energies in that region.

### 2.5.3 Nuclear superfluidity and neutron-proton pairing

Correlations between pairs of particles have a fundamental importance in all the fields of physics involving  $N$ -body systems. Superconductivity in metals is a well-known and well-understood phenomenon arising from the interaction between pairs of electrons with opposite momenta. The superconducting state that is realized in certain materials can be expressed as a freely moving (non-interacting) collection of such strongly correlated “Cooper pairs” and described with Bardeen-Cooper-Schrieffer (BCS) theory.

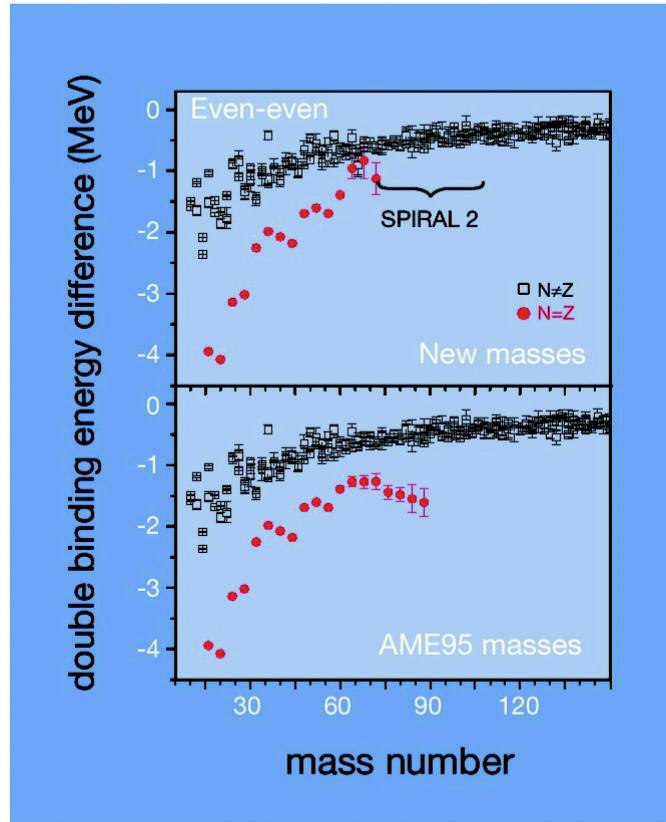


**Figure 2.5.2:** The Wigner effect in  $N=Z$  nuclei can be illustrated with the double binding energy difference, which for even-even nuclei is defined as  $[B(N,Z)-B(N-2,Z)-B(N,Z-2)+B(N-2,Z-2)]/4$  where  $B(N,Z)$  is the binding energy of a nucleus with  $N$  neutrons and  $Z$  protons. The figure illustrates the extra binding energy of  $N=Z$  nuclei for which this quantity lies well below the double binding energy differences of other nuclei. Only mass measurements on heavier  $N=Z$  nuclei can tell us whether the Wigner term will disappear completely. Also shown is the region of nuclei that will become accessible with SPIRAL2.

The pairing effect in condensed-matter, atomic and nuclear physics is well known. In atomic nuclei it results from a coupling of neutrons and protons in pairs and gives rise to nuclear superfluidity. Here also strong correlations involving Cooper pairs arise. In the nuclear domain, the strongest interactions involve nucleon pairs that are close in space, reflecting the fact that the nucleon-nucleon force has a range that is small compared to the size of the nucleus. In addition, a unique feature of nuclei is that they consist of a combination of two fermionic fluids (neutrons and protons) and as a consequence, the nucleons can form four types of Cooper pairs (see figure 2.5.3), each of which can be in a state of relative orbital angular momentum zero and hence well correlated in space. The ground states of the majority of nuclei are very well described in terms of superfluid condensates, in which the pairs of nucleons are formed like the Cooper pairs of electrons in superconductors. This is reflected in nuclear binding energies, *e.g.* by odd-even mass differences.

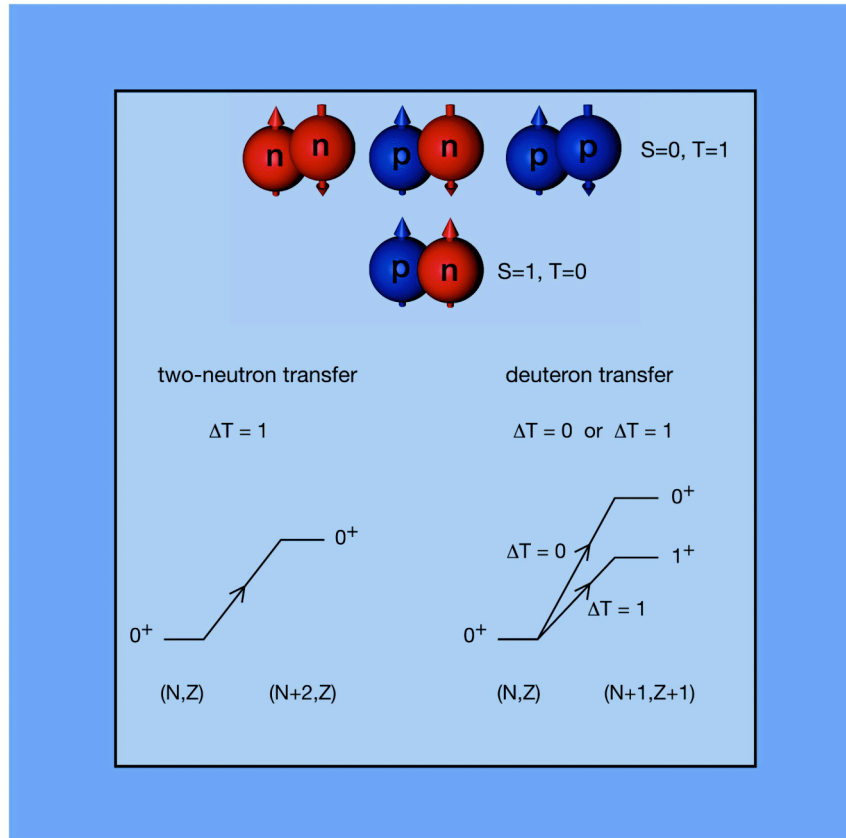


**Figure 2.5.3:** Possible nucleonic isoscalar  $T=0$  and isovector  $T=1$  Cooper pairs. In the isoscalar pair, the spins of the nucleons are parallel while in the isovector pair they are antiparallel. An established way of revealing the existence of isovector pairing correlations between identical nucleons is through the study of two-nucleon transfer ( $2n$  or  $2p$ ) for which such correlations give rise to a collective enhancement. Similarly, the existence of isoscalar pairing correlations in  $N=Z$  nuclei may lead to a collective enhancement of the transfer of a deuteron. Specifically, one should look for  $\Delta T=0$  transfer between the  $0^+$  ground state in even-even  $N=Z$  nuclei and  $1^+$  states in neighbouring odd-odd nuclei.

As a consequence of spin-isospin symmetry, the neutron-neutron, neutron-proton or proton-proton pairs are characterised by the quantum numbers of total spin ( $S$ ) and isospin ( $T$ ). To date, only the nuclear superfluid phases associated with Cooper pairs of like nucleons - protons with protons ( $pp$ ) or neutrons with neutrons ( $nn$ ) - have been observed. Whether there also exists strong deuteron-like isoscalar ( $T=0$ ) correlations, remains a hotly debated open question. The reason is that in order for a nucleon pair to exploit the short-range nuclear force and form a correlated Cooper pair, the constituent nucleons must occupy orbits within the same valence shell. Such “normal” pairing couples the nucleons in pairs with opposite spins and occupying orbits which are symmetric with respect to time inversion. This is called isovector pairing ( $T=1$ ) with zero total angular momentum for each pair of nucleons ( $S=0$ ). The requirement of strong spatial correlation, *i.e.* that the nucleons occupy the same valence shell strongly limits the regimes in which strong  $np$ -pair correlations may exist. For medium-mass to heavy nuclei relatively close to the  $\beta$ -stability line only like nucleons fulfil this criterion. For very exotic nuclei, *i.e.* nuclei with  $N/Z$  ratios that, for a given mass number, differ significantly from those near stability, pair correlations can no longer be treated as a small residual interaction, since, *e.g.*, with respect to the binding energies of the outer nucleons, their effect is of the same order-of-magnitude as the binding energy generated by the remaining part of the nuclear potential. When  $N=Z$ , isoscalar  $np$  pairing ( $S=1$ ,  $T=0$ ), a

pairing mode excluded for identical particles according to the Pauli principle, may become significant. For proton rich nuclei, approaching the double spherical shell closure at  $N=Z=50$  ( $^{100}\text{Sn}$ , the heaviest bound  $N=Z$  nucleus) neutrons and protons occupy very similar orbitals, and there is therefore a large spatial overlap of the wave functions describing them. In addition, there are a sufficient number of valence particles to create a correlated state which, according to theoretical predictions, may give rise to special effects of np pairing which are very different from the normal pairing effects observed closer to stability. In fact, some theoretical calculations actually suggest that np isoscalar pairing in such cases may compete effectively, or perhaps even dominate over, the isovector pairing modes which include not only like-particle but also np-isovector pairing.

Because of experimental breakthroughs, such as the construction of the SPIRAL2 facility, it may soon be possible to probe eventual signals of the superfluid phase of nuclear matter resulting from np Cooper pairs. The search for this new phase of nuclear matter and the study of its manifestations represents one of the most significant challenges in nuclear structure physics for the coming years.

***Searching for signals of superfluid phase in nuclear matter***

*Several manifestations of such an isoscalar superfluid state that could be tested experimentally may be anticipated namely:*

- *Enhanced probability to add or remove a spin-one (deuteron-like) np pair.*
- *The presence of energy gaps in the spectra of odd-odd  $N=Z$  nuclei.*
- *A new np-coupling scheme replacing seniority coupling for near-spherical nuclei.*
- *Significantly different behaviour at medium to high spins of rotational bands built on deformed states due to the quenching of the Coriolis anti-pairing effect.*
- *Enhanced  $\beta$ -decay rates between the ground state of an even-even  $N=Z$  nucleus and the lowest  $I^+$  state of its odd-odd neighbour.*

The most promising region of the nuclear chart to study isospin symmetry and isoscalar np pairing is along the  $N=Z$  line. In particular this is true for the heaviest possible  $N\approx Z$  nuclei, which are also most difficult to access experimentally. The experimental method of choice to study excited states in these nuclei, even up to moderate spin values, is the in-beam spectroscopy of fusion-evaporation reactions induced by a proton-rich radioactive ion beam. The final evaporation residues of interest could be identified by means of efficient charged particle and neutron detectors or by tagging techniques using a recoil separator and focal plane arrays for detecting, e.g. characteristic  $\beta$ -delayed proton decays. Even with intense, stable-isotope beams it is possible to access highly neutron deficient nuclei but such experiments face increasing difficulties due to the large background from the prolific reaction channels leading to nuclei closer to the  $\beta$  stability line. It is commonly accepted that stable-beam experiments are operating currently at their limits of sensitivity, defined not by the event rate but by the selectivity of the detector systems, of the order of  $10^{-5}$  to  $10^{-6}$ . Even though proton-rich radioactive ion beams are available to provide the necessary increase in “signal-to-noise ratio”, for the most exotic proton-rich evaporation residues the intensities of such beams provided by the first- and second-generation radioactive ion beam facilities have been insufficient. The method of production for proton-rich radioactive ion beams is described elsewhere. It relies on fusion-evaporation reactions between a high-intensity stable-isotope beam from SPIRAL2 and a thick target and re-acceleration of the evaporation

residues by the CIME cyclotron. Significantly higher currents for the most neutron-deficient beam species are expected from this combination.

Two-nucleon transfer provides an excellent tool to study correlations in the nuclear wave function. In particular, a powerful experimental probe of possible isoscalar np pairing correlations in the ground states of heavy  $N \approx Z$  nuclei is to study deuteron transfer, as indicated above. This can be measured by means of ( $^3\text{He}, p$ ) reactions. The nuclei of interest are produced from an intense stable primary beam impinging on a thick target and re-accelerated as discussed above. The resulting proton-rich beam is then allowed to impinge on a  $^3\text{He}$  gas cell. Due to the kinematics of the reaction, the protons will be emitted primarily in the backward direction and can be detected *e.g.* by an annular silicon detector. The forward moving final nucleus is identified in a recoil mass separator.

### ***Seeking a new form of pairing with 2 particle transfer***

*As outlined above, studies of proton-neutron pairing can be made using fusion-evaporation or transfer reactions, e.g. ( $^3\text{He}, p$ ) in inverse kinematics, with proton-rich radioactive ion beams. For transfer reactions, beams of typically  $10^4$ - $10^5$  atoms/s will be needed. An interesting example for SPIRAL2 would be to study the reaction  $^{72}\text{Kr} (^3\text{He}, p) ^{74}\text{Rb}$ , in particular the branching ratio for populating the  $T=1$  and  $T=0$  states. The heaviest  $N=Z$  nucleus employed so far in such reactions is  $^{40}\text{Ca}$  while attempts are being made to study deuteron transfer on radioactive  $^{56}\text{Ni}$ . A study of the  $^3\text{He} (^{72}\text{Kr}, p) ^{74}\text{Rb}$  reaction would be a large step forward for our understanding of np correlations in nuclei.*

An alternative approach to probe the nature of pair correlations in proton-rich nuclei is to study the structure of levels in nuclei with  $N=Z$  at moderate to high angular momenta. As indicated above, the Coriolis effect induced on the paired nucleons in a deformed rotating nucleus, which drives them to align their intrinsic angular momenta along the collective rotational axis, is selective with respect to the residual interaction. In the case of normal  $T=1$ ,  $S=0$  pairing the Coriolis effect acts to break the nucleonic pairs, leading to discontinuities (backbending) in the rotational behaviour. On the contrary, in the case of strong  $T=0$ ,  $S=1$  (i.e. deuteron-like) correlations the np pairs are already spin aligned and the Coriolis force is not expected to perturb the system as violently. There should thus be significant differences in rotational behaviour depending on whether a deformed nucleus is dominated by isovector ( $T=1$ ) or isoscalar ( $T=0$ ) pair correlations.

For a near-spherical nucleus strong residual  $T=0$  pair correlations are expected to lead to a new spin-aligned coupling scheme as opposed to the seniority coupling found closer to stability. Dramatically different spectral features are expected. Furthermore, the structure of even-even and odd-odd nuclei at moderate to high angular momentum is expected to show strong similarities if significant  $T=0$  np correlations are present. Such phenomena can be probed experimentally using fusion-evaporation reactions and  $\gamma$ -ray spectroscopy by observing heavy  $N \approx Z$  nuclei in excited states up to moderate spins.

The presence of  $T=0$  pairing may slightly enlarge the pair gap at low spins producing a systematic shift in the rotational g-band – S-band crossing frequency in  $N=Z$  nuclei as compared to neighbouring nuclei. This idea, first suggested for  $^{72}\text{Kr}$ , has been explored in the medium spin region of  $N=Z$  nuclei with  $A=70$ -80. The evidence for the shift of the crossing frequency is, however, not yet conclusive since possible shape changes precluded precise

determinations of the band crossing frequencies. In order to test the predictions of nuclear models, which are also affected by large uncertainties, new experimental data on heavier N=Z systems is badly needed.

***Seeking a new form of pairing with electromagnetic properties in the N=Z region***

*A complete study of yrast states up to moderate angular momentum in the  $^{88}\text{Ru}$ ,  $^{90}\text{Rh}$ ,  $^{92}\text{Pd}$ ,  $^{94}\text{Ag}$ ,  $^{96}\text{Cd}$  and  $^{98}\text{In}$  N=Z nuclei should be a major goal for future radioactive ion beam facilities. As an example, the fusion-evaporation reaction  $^{33}\text{Ar} + ^{58}\text{Ni} \rightarrow ^{91}\text{Pd}^*$  near the Coulomb barrier is a suitable experiment for SPIRAL2. In this reaction one may access the  $T_z = -1/2$  nucleus  $^{89}\text{Rh}$  via evaporation of a proton and a neutron, as well as its mirror nucleus  $^{89}\text{Ru}$  via two-proton evaporation.  $^{89}\text{Rh}$  is a likely ground state proton emitter and recoil decay tagging at the focal plane of a recoil mass separator could be one way to enhance significantly the selectivity. The N=Z nucleus  $^{88}\text{Ru}$  would be populated with relatively high yield in the 2pn channel and one could expect to observe the yrast line up to high angular momentum. A tantalizing possibility is the theoretical prediction of this being a “doubly-magic superdeformed (SD) nucleus” with N=Z=44. The SD states in this nucleus are predicted to become yrast at very low angular momentum as compared to other known SD nuclei in this mass region and might be observable at SPIRAL2. This opens the exciting and unique possibility to search for evidence for T=0 np pair correlations at high angular momentum in a strongly deformed, near-rigid nuclear system for which the experimental signature for such correlations should be rather clean. Furthermore, many of the nuclei populated in this and similar reactions will exhibit  $\beta$ -delayed proton emission that could be used for the tagging of prompt  $\gamma$ -rays by using the spatial and temporal correlations between events at the focal plane and at the target. For such fusion-evaporation reactions a beam intensity of  $10^7$ - $10^8$  beam particles per second will be necessary. The emitted  $\gamma$ -rays need to be detected with a highly efficient germanium detector array. Highly efficient detectors for charged particles, neutrons and/or a magnetic spectrometer for selecting evaporation residues are also required.*

### ***Isospin-symmetry breaking in electromagnetic properties of heavy N=Z nuclei***

*As already stated, electromagnetic properties of corresponding states in mirror nuclei are a powerful tool to test isospin symmetry. One example is provided by the observation of E1 transitions in N=Z nuclei, which are forbidden by isospin conservation. Lifetime measurements of excited states de-exciting through E1 transitions in heavy N=Z nuclei would allow a direct determination of the isospin mixing. Moreover B(E1) values in mirror nuclei should be equal. As an example of a suitable experiment at SPIRAL2 one can consider the fusion-evaporation reaction  $^{30}\text{S}+^{40}\text{Ca} \rightarrow ^{70}\text{Kr}$  near the Coulomb barrier. This reaction allows access to the A=67,  $^{67}\text{Se}$ - $^{67}\text{As}$  mirror pair. These nuclei de-excite through E1 transitions and therefore the experimental determination of the lifetimes of the corresponding states provides a direct test of the isospin symmetry. The availability of intense beams of such unstable isotopes will also allow one to perform Coulomb excitation experiments to determine the electromagnetic transition matrix elements in mirror nuclei. An additional interesting aspect is the sensitivity to exotic matter distributions in the nucleus, such as the theoretically predicted proton skin effect.*

### **2.5.4 N-body systems and dynamical symmetries in nuclei**

In a general way and in spite of their great complexity,  $N$ -body systems are often characterised by astonishingly regular behaviour and particularly simple responses to excitation. This is especially true in atomic nuclei that, despite being composed of several hundred nucleons in strong interaction, manifest behaviour of surprising regularity. These regularities find their origin in the concept of symmetry, and in particular in symmetries associated with the total Hamiltonian including the interactions, which for this reason are called dynamical. Dynamical symmetries have played an increasingly important role in many fields of physics because they are at the heart of the process of unification of phenomena. Famous, early nuclear-physics examples of dynamical symmetries are SU(2) which is the algebra of the pairing interaction and SU(3) which is that of the quadrupole interaction. Dynamical symmetries have also played a key role in more recent developments in the framework of a model of the nucleus in terms of pairs of nucleons (the interacting boson model). Three dynamical symmetries emerge naturally from this model, U(5), SU(3) and SO(6), corresponding to spherical nuclei, ellipsoidally deformed nuclei with axial symmetry and soft triaxial nuclei. Empirical manifestations of these structures have been found throughout the nuclear chart and are now seen to represent the three commonly occurring shapes that the nucleus adopts. These are the symmetries of a one-fluid nuclear model but further theoretical studies have revealed the existence of more complex symmetries associated with two-fluid systems. These have subsequently found experimental confirmation in the form of so-called nuclear scissors states, *i.e.* collective excitations in which neutrons and protons move out of phase. One of the goals of SPIRAL2 is the study of very neutron-rich nuclei, and with increasing neutron excess one may envisage the development of a neutron skin, which constitutes a *third* fluid, distinct from the neutron and proton fluids in the core of the nucleus and giving rise to a rich symmetry structure. It will thus be possible with SPIRAL2 to seek the signs of the possible existence or otherwise of these new three-fluid dynamical symmetries in exotic nuclei.

### 2.5.5 Nuclear phase transitions and symmetries at the critical point

In nuclear physics so-called quantum or structural phase transitions occur in the zero temperature thermodynamic limit as a result of the variation of a control parameter in the Hamiltonian. The experimental observation that states of very different shapes can co-exist in a single nucleus was made a long time ago and it is now generally accepted that shape co-existence is characteristic of many nuclei. Moreover, it can happen that, as the mass number changes in a series of nuclei, the energies of states with different shapes cross and, in particular, the ground state can change its deformation from one nucleus to the next. This can be regarded as a nuclear shape phase transition.

Shape phase transitions occur in a variety of nuclear models. In fact, before any real Hartree-Fock calculation was performed, it was recognized that, in this mean-field approximation, second-order phase transitions can occur associated with the onset of broken rotational and other symmetries. The study of phase transitions in nuclei was further stimulated by the introduction of the interacting boson model, where it was shown that a mean-field approximation of its Hamiltonian maps onto a subspace of the Bohr-Mottelson geometric collective model. It is in the context of the latter model that it was suggested recently that critical points of phase transitions can sometimes be associated with so-called critical-point symmetries and analytically solvable, effective Hamiltonians. For particular choices of the nuclear potential energy as a function of the quadrupole deformation parameters ( $\beta, \gamma$ )—usually involving an infinite square well—exact solutions to the collective (rotor and vibrator) Hamiltonian have been obtained. These are called E(5) and X(5) critical-point symmetries for the different transitions between vibrator, axially symmetric and  $\gamma$ -soft rotor. The isotopes  $^{150}\text{Nd}$  and  $^{152}\text{Sm}$  have been shown to be good candidates for X(5) symmetry. The advent of SPIRAL2 will allow us to study a much more extended region of the nuclear chart, in particular for medium-mass to heavy neutron-rich nuclei, where this intriguing phenomenon could be studied more systematically (see figure 2.5.4).

## 2.6 COLLECTIVE EXCITATIONS IN UNSTABLE AND WEAKLY BOUND NUCLEI

In spite of the fact that work on giant resonances (GR) has involved much effort (both experimental and theoretical) in stable nuclei over several decades, the study of the collective excitations in exotic nuclei is still in its infancy.

*Studying exotic nuclei over the years, has led to the observation that extremely neutron-rich nuclei are very different from the stable nuclei to which one is accustomed. Some of them are abnormally large, their surface is very diffuse, the pairing correlations can be extreme and their shell structure is probably very peculiar. One thus expects drastic changes in the response of exotic nuclei to external stresses and in the associated collective modes such as vibrations or*

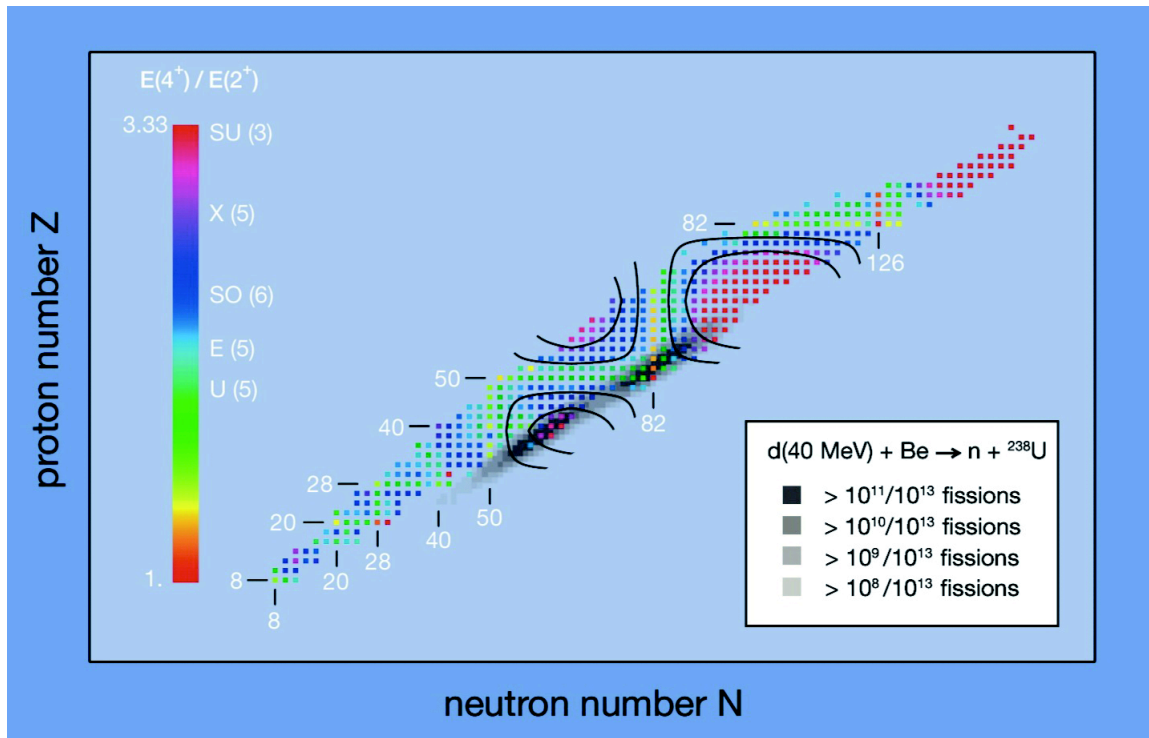


**Figure 2.5.4:** The ratio  $R(4^+/2^+)$  of excitation energies of the first  $4^+$  to the first  $2^+$  state in all even-even nuclei where both energies are known at present. The value of this ratio gives a first indication of the character of the nucleus, that is, whether it can be considered as U(5) vibrational ( $R=2$ ), SU(3) rotational ( $R=3.33$ ) or SO(6)  $\gamma$ -soft ( $R=2.50$ ). Also the geometrical symmetries at the critical points between U(5) and SO(6) [E(5),  $R=2.20$ ] and between SO(6) and SU(3) [X(5),  $R=2.91$ ] are indicated. The ellipse-like curves are an attempt at extrapolation of these symmetries into exotic regions based on the  $P$ -factor (as introduced by Casten) which is defined as the product of valence neutron and proton numbers divided by their sum. The outer (colour-1) curves give the locus of nuclei with possible E(5) symmetry while the inner ones (colour-2) contain those with possible X(5) symmetry. Also shown are the regions of the chart that will become accessible with SPIRAL2.

rotations. These changes may lead to a better understanding of the asymmetric nuclear matter properties, or give access to new features of exotic nuclei. The knowledge of basic quantities like the nuclear incompressibility or, equivalently, the density dependence of the asymmetry energy and the nucleon effective mass in an asymmetric medium, will benefit a lot from measurements of collective monopole and quadrupole responses in isospin-asymmetric systems. Moreover, the collective response also makes it possible to probe under extreme conditions of neutron/proton ratio nuclear properties such as:

- the matter density distributions, and thus the nuclear shapes,
- the modifications of the nucleon-nucleon interaction due to the medium,
- the dynamics of the balance between the various degrees-of-freedom in dissipative collisions.

In this sense, the collective modes must be thought of as tools which are both essential to reveal some properties of the nucleus and also complement perfectly the other ways to study nuclear structure described earlier.

## 2.6.1 Giant resonances and matter properties

Giant resonances (GR) are collective modes of nuclear excitation. Their energies are correctly predicted by models treating the GR as a coherent superposition of particle - hole states, whereas further correlations, like the coupling with many-particle – many-hole states, give a contribution to their width. The theoretical state-of-the-art uses microscopic calculations directly based on the nucleon-nucleon effective interaction. Knowledge of this interaction is a major issue for the nuclear physics community and for several decades it has been mainly constrained by ground state properties such as masses and radii. It is now possible to test these interactions using the predictive power of the microscopic calculations for the energy localization of the collective modes such as the Giant Dipole Resonance (GDR). However the GDR position has been measured only for about 90 stable nuclei all lying on the  $\beta$ -stability line, and it is necessary to extend these measurements to unstable nuclei in order to gain a complete picture. The inelastic excitation studies described below should provide such crucial data.

The giant monopole resonance (GMR), an isotropic compression mode (known also as the “breathing mode”), is of fundamental importance for the determination of the nuclear compression modulus  $K_\infty$ . In fact, it has been shown that it is difficult to determine the nuclear incompressibility using measurements of only a few nuclei, because different contributions (associated not only with the volume, but also with the surface and symmetry compressibility) play a role. In this sense, measurements of the monopole in isospin-asymmetric systems would be of paramount importance for determining the symmetry compressibility, i.e. the density dependence of the asymmetry energy. They would greatly help to determine the compressibility of neutron rich matter, the importance of which also stems from the impact on nuclear astrophysics. Indeed, the properties of the nuclear equation-of-state are crucial for the understanding of dense matter in the Universe, e.g. in supernovae cores and in neutron stars. Hence, measuring the GMR in heavy unstable nuclei could provide crucial information on the asymmetry term of the nuclear incompressibility. Nuclear matter is in fact rather incompressible, and the GMR lies at a relatively high energy.

In order to probe giant resonances directly in unstable nuclei, it would be of great interest to perform inelastic scattering on light particles such as  $\alpha$ -particles. These reactions have been successfully used to study giant resonances in stable nuclei. However, the reaction energies required to reach sizeable cross-sections are several tens of MeV/nucleon. This energy region is beyond SPIRAL2 beam energies. A future extension of the facility towards this higher energy regime should be strongly investigated: it would open a wide field of frontline experiments, such as  $(\alpha, \alpha')$  reactions. For instance, the use of an active target at SPIRAL2 such as MAYA or ACTAR will be perfectly designed to perform GMR measurements with a low detection energy threshold and a  $4\pi$  solid angle coverage at typical energies of 30 MeV/nucleon. This low energy threshold is needed in order to use the inverse kinematics method, where the recoiling  $\alpha$  has a typical energy of 200 keV for a GMR inelastic excitation at 0 degree in the centre-of-mass.

The so-called isovector-GMR should also provide information on the equation-of-state in asymmetric matter since it should show how neutrons and protons could be compressed differently in the nuclear medium. Very few data exist on this mode. These studies could be performed either by inelastic scattering, although the low reaction energy provided by SPIRAL2 is not optimized for these reactions, or by studying the pre-equilibrium phase following fusion reactions.

In the past, heavy-ion inelastic scattering even at moderate energies (around 25 MeV/nucleon) has been shown to be able to excite giant resonances in stable nuclei like  $^{208}\text{Pb}$ . For example, the ISGQR excitation and decay in  $^{208}\text{Pb}$  has been measured using  $^{17}\text{O}$  beams at 22 MeV/nucleon with a cross-section of approximately 50 mb/sr and a rather large peak/background ratio. In this sense, low-energy reactions of unstable nuclei on medium-mass target nuclei such as carbon, oxygen, magnesium and sulfur can be envisaged at SPIRAL2. One of the limitations of these reactions is that the angular distribution, in contrast to the case of light ion scattering, does not have a high sensitivity to the induced transition multipolarity. However, photon decay data can provide the required sensitivity to GR multipolarity. For example, decay back to the ground state following heavy ion scattering is dominated by the lowest multiplicities, E1 and E2, while higher multiplicities are extremely unlikely to contribute to the ground state decay. Gamma-decay to the ground state can also yield data on the electromagnetic strength of resonances. In the same study of  $^{17}\text{O}$  inelastic scattering on  $^{208}\text{Pb}$ , it has already been observed that the measured angular correlations for the ground state decay corresponding to two regions of excitation energies (9-11 MeV and 12-15 MeV) are sensitive to the transition multipolarity.

Photon decay from Giant resonances to low lying excited states is also a potential source of information. Such decays may evidence coupling of giant resonance modes to low frequency collective modes. They may also constrain the isospin character of the resonance through the suppression of E1 transitions between collective states of isoscalar character. In the case of nuclei far away from stability one expects an increasing isospin mixing and therefore the study of  $\gamma$ -decay from giant resonances is a good probe for this phenomenon.

## 2.6.2 Soft modes, neutron skins and haloes

One of the most studied collective modes, because it is also among the most easily accessible, is undoubtedly the isovector giant dipole resonance. It corresponds schematically to oscillations with opposite phases of the whole ensemble of protons versus the whole ensemble of neutrons. When the nucleus studied moves away from stability, the theoretical predictions indicate that the presence of a halo or a skin of neutrons seems to give rise to a new kind of dipole mode, in which the excess of neutrons oscillates with respect to the more strongly bound core. This is called a “pygmy” resonance. This new vibration needs to be studied systematically. In fact, in light nuclei there has been evidence of low-energy dipole modes but in many cases these modes are not collective. In medium-mass nuclei, including nickel and tin isotopes, different models (e.g. non-relativistic and relativistic mean field models, or more sophisticated models which include the coupling between particles and shape oscillations) predict different amounts of collectivity for the low-lying dipole. This is mainly because the models differ in their isospin-dependent sector, which is known to be hard to constrain. In this sense, it can be said that the dipole strength measurements should be highly instrumental in providing us with information on the isospin-dependent part of the effective nucleon-nucleon interaction. For instance the low-lying dipole strength is predicted to increase with the neutron number for the Sn isotopes in HFB+QRPA calculations. Recent experimental data show that the strength of the pygmy resonance in O and Sn isotopes does not always increase with neutron number, presumably because of sub-shell structure. To reproduce the data it appears to be necessary to include the coupling to low-lying vibrations. Moreover, the study of pygmy resonances is also crucial for determining reaction rates and thus the abundance of the elements created by nucleosynthesis in the so-called r-process. It has been shown that the predicted r-process abundances are strongly dependent on the presence of the Pygmy dipole resonance if the temperatures or neutron densities are low

enough that the  $(n,\gamma) - (\gamma,n)$  equilibrium is disturbed( see section 4.4). In a more general way, the asymmetry of isospin affects all of the properties of the dipole mode: the E1  $\gamma$ -decay is more fragmented when the neutron number increases and part of the intensity of the dipole response is shifted down to lower energy.

Theoretical models have also predicted low-lying strength, in the quadrupole, monopole or octupole case. A first remark is that in neutron-rich nuclei the low-lying modes are expected to have a predominantly neutron content, therefore they should not turn out to be either pure isoscalar or pure isovector modes. This opens up the possibility of exciting them in different reactions from those usually employed for stable nuclei. The quadrupole states are known to be very sensitive to the nuclear shape, or to the effective mass: basic quantities whose direct observation cannot always be achieved. Moreover, the question can be asked whether neutron-rich nuclei possessing a skin, or a halo, display monopole or quadrupole states at lower energy than the GMR associated respectively with the compression or the effective mass of low-density nuclear matter. The predicted soft GMR mode, located below 10 MeV for very neutron-rich nuclei, may be observed.

### 2.6.3 Particle- $\gamma$ coincidence and measurement of level densities

Quite recently, an experimental method based on particle- $\gamma$  coincidences was developed which gives access at the same time to the radiative response of the nucleus and the level-densities up to excitation energies of the order of 10 MeV. In the first case, the study of the de-excitation  $\gamma$ -rays in the continuum gives access to the *average* values of electromagnetic properties. This radiative response of the nucleus is constructed by analysis of the spectra around the resonance, or more precisely by the Lorentz extrapolation that describes it. This method thus gives particularly sensitive results to interpret. When the energy decreases this extrapolation is even more doubtful because of the considerable contributions of M1 transitions to the de-excitation.

However, an intriguing question is the dependence of the level densities on isospin (the neutron excess): it is a crucial ingredient in the astrophysical r-process calculations, aimed at nucleosynthesis predictions. Since the r-process involves many unstable nuclei, the SPIRAL2 beams are expected to provide the corresponding measurements: the (N-Z) dependence of the level density could be studied with the experimental method mentioned above.

#### ***Study of new collective excitation modes in weakly bound nuclei***

*The investigation of Pygmy resonances and measurement of their properties, in particular their electromagnetic response, could be carried out by measuring the  $\gamma$ -decay of the nuclei produced in a neutron transfer reaction. The measurement of the de-excitation  $\gamma$ -ray associated with a resonance in the  $(d,p\gamma)$  reaction at approximately 15 MeV/nucleon could be done in inverse kinematics with the beams from SPIRAL2. This requires beam intensities of the order of  $10^7$  atoms/s and a high-efficiency, segmented  $\gamma$ -ray detector in coincidence with a recoil spectrometer to detect the ejectile and to correct for the Doppler effect.*

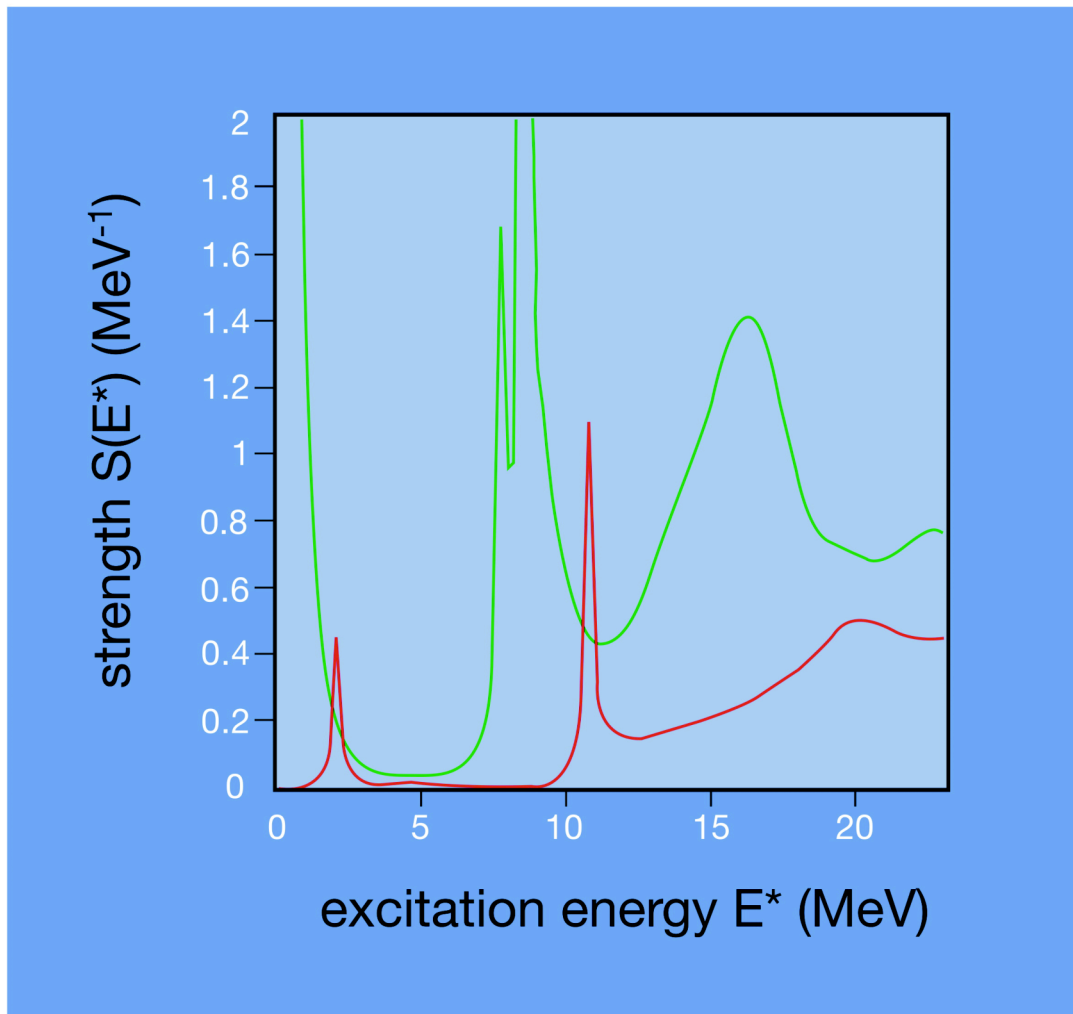


**Figure 2.6.1:** Hartree Fock Bogoliubov (red) and quasi-particle random phase approximation (green) response function for the two-neutron transfer reaction on  $^{22}\text{O}$ . The giant pairing vibration (GPV) is the intense coherent excitation located around 15 MeV.

#### 2.6.4 Pairing vibrations

Pairing vibrations are coherent excitations of a pair of particles on top of a nuclear core. These pairs can behave as a rather independent system, thus adding two neutrons to a nucleus will increase the nuclear energy by a fixed value. The resulting energy spectrum is vibrational. Such a mode gives direct information on pairing phenomenon in nuclei. These vibration modes have been extensively studied with pair transfer reactions around the doubly-magic  $^{208}\text{Pb}$  nucleus. Several predictions show the possibility of exciting the giant pairing vibration (GPV) in neutron rich nuclei. This very collective mode in the two neutron transfer channel is expected to lie typically at energies of 15-20 MeV. For instance, figure 2.6.1 displays such a mode for the unstable  $^{22}\text{O}$  nucleus. It has however never been observed in studies of reactions induced by stable-isotope beams.

*Giant Pairing Vibrations with exotic beams*

*With weakly bound probes, it is expected that the probability of exciting the GPV will be greatly enhanced, due to the good energy matching. For instance, the  $^{116}\text{Sn}(^6\text{He},^4\text{He})$  reaction has a “Q-value” of 14.6 MeV. With the high intensity  $^6\text{He}$  beam available at SPIRAL2, it will be a perfect tool to study such modes using typical reaction energies of 5 MeV/nucleon.*

### **2.6.5 Pairing critical temperature**

One interesting possibility in hot nuclei, is to study the pairing phase transition. Nuclear superfluidity is expected to vanish above a given critical temperature  $T_c$ , due to the thermal excitations. Several calculations predict a critical temperature around (0.5-1) MeV. This value is linked with the pairing interaction acting between the nucleons. For instance the neutron-pairing gap is predicted to collapse at a temperature of 800 keV in  $^{124}\text{Sn}$ , using finite temperature HFB calculations. The addition of fluctuations beyond the HFB mean field, makes the transition much smoother in finite systems such as nuclei. A measurement of the critical temperature in exotic nuclei may therefore give crucial indications of the evolution of pairing effects far from stability.

#### ***Pairing phase transition and the breakdown of superfluidity***

*Such studies could well be undertaken with the SPIRAL2 beams, in order to extend the ( $^3\text{He}, \alpha\gamma$ ) measurements performed on the stable dysprosium and ytterbium nuclei. The SPIRAL2 radioactive ion beams of intermediate mass will be perfectly designed for such studies.*

### **2.6.6 The giant dipole resonance built on excited states**

The giant dipole resonance built on highly excited nuclear states is an important experimental tool to probe the properties of hot rotating nuclei. This is based on the observation of the  $\gamma$ -ray spectrum from the decay of hot nuclei produced in heavy ion fusion reactions. This  $\gamma$ -decay is weak since it is in competition with the particle evaporation which is several hundreds time more probable. Several important regions in the energy-spin plane can be identified. There is a collective regime at low excitations and spins where shell effects are important. In the case of neutron rich nuclei, an important question is whether or not the pygmy part of the giant dipole resonance response survives with temperature.

### ***Pygmy resonance in hot neutron-rich nuclei***

*Possible experiments with SPIRAL2 aimed at answering this point are the fusion reactions  $^{112}\text{Sn} + ^{12}\text{C}$  at 4.9 MeV/nucleon and  $^{132}\text{Sn} + ^{12}\text{C}$  at 5 MeV/nucleon (which gives an  $E^*=54$  MeV and  $T\sim 1.5$  MeV) leading respectively to the  $^{124}\text{Ba}$  and  $^{144}\text{Ba}$  compound nuclei. The  $\gamma$ -ray spectrum associated with  $^{124}\text{Ba}$  should show a bump centered at about 15.2 MeV corresponding to the GDR centroid energy. In the case of the  $\gamma$ -ray spectrum of the  $^{144}\text{Ba}$  one expects to see the GDR bump with a centroid located at about 14.5 MeV and an extra yield located around 10 MeV corresponding to the pygmy resonance. From the comparison of the  $\gamma$ -ray spectra with a statistical code, which includes the  $\gamma$ -decay, one should be able to extract the centroid energy, the width and the strength of this additional resonance. In order to get a more neutron rich barium isotope one could even run  $^{132}\text{Sn}$  on a  $^{14}\text{C}$  target leading to  $^{146}\text{Ba}$ . For beams with  $10^8$  atoms/s and detection efficiency of 50% for  $\gamma$ -rays and 10% for residues these experiments can be carried out with 4-5 days of beam time.*

At higher excitation energies the hot nucleus behaves like a liquid drop. At even higher spins the nucleus may undergo a shape transition to Jacobi shapes and eventually fission. The Jacobi shape transition is known to take place in rotating stars. It has been found that at a certain critical angular momentum the stable equilibrium shape of a self-gravitating system rotating synchronously changes abruptly from a slightly oblate spheroid to a triaxial ellipsoid rotating about its shortest axis. Atomic nuclei idealized as charged incompressible liquid drops endowed with a surface tension should undergo a similar shape transition. This oblate-to-triaxial transition was found also in the more realistic self-consistent, semi-classical nuclear Thomas-Fermi model under the same assumption of synchronous rotation. Recently, the new version of the liquid-drop model, LSD, demonstrated its application to this problem. The experimental signatures of such an abrupt change of the nuclear shape are expected to be found in observables related to the moment-of-inertia. Especially promising for the search for the Jacobi nuclear shape transitions are: i) the  $\gamma$ -decay of the Giant Dipole Resonance (GDR) built on such states; ii) the giant backbend in the E2  $\gamma$ -transition energies.

Experimental indications of the Jacobi phase transitions were observed so far only through the study of the giant dipole resonance for the light nuclei  $^{45}\text{Sc}$  and  $^{46}\text{Ti}$ . Indeed, to be observable the critical angular momentum for the Jacobi transition should be at a spin somewhat lower than that of the fission limit. The spin window between the transition to a Jacobi shape and the fission is expected to be large for neutron rich nuclei. For example in the LSD model, the  $^{72}\text{Zn}$  ( $Z=30$ ,  $N=42$ ) nucleus is predicted to be strongly oblate up to spin  $I<42\hbar$ . Above  $I=42\hbar$ , the nucleus enters the Jacobi shape regime, having very elongated shapes with increasing deformation until  $I>64\hbar$ , where fission starts to dominate. Because of the relatively low mass ( $A=72$ ), the moment of inertia is low, thus the rotational frequencies are rather high. Therefore one would expect the Coriolis effects to play an even more important role than in the  $^{46}\text{Ti}$  case. The figure 2.6.2 shows the predicted GDR strength functions for different spin values (from 0 to 64  $\hbar$ ) of hot  $^{72}\text{Zn}$ . One can see that due to the Jacobi shape transition and the rotational effect a low energy component develops and, as a function of spin, its energy becomes lower and the strength larger.

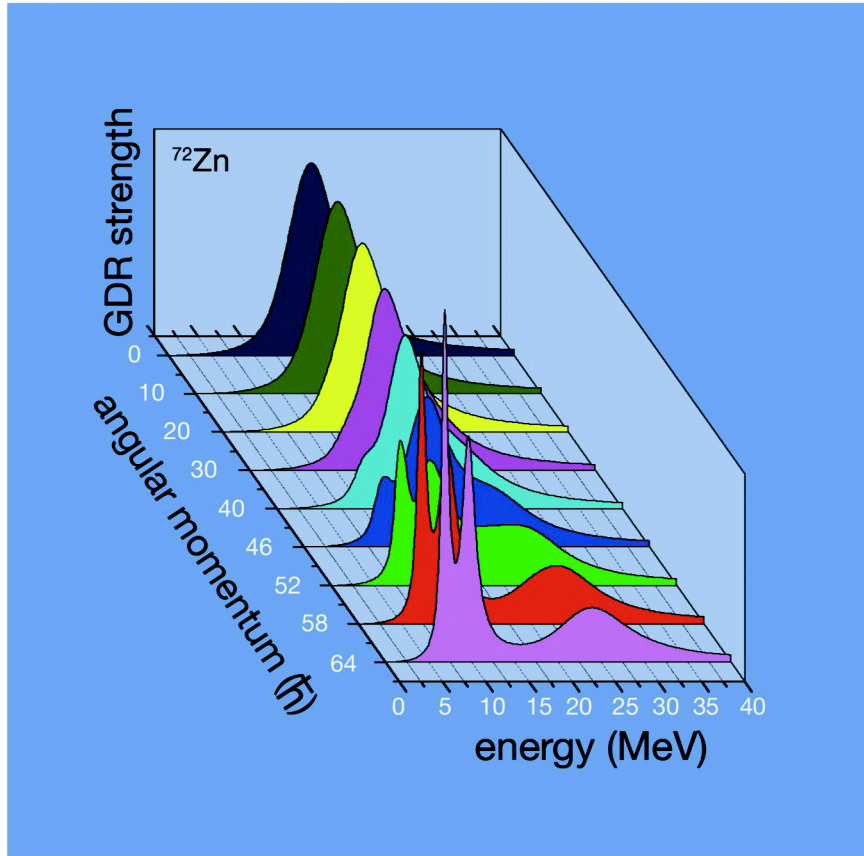


**Figure 2.6.2:** The GDR response as a function of spin (from 0 to 64  $\hbar$ ) in the neutron rich Zn isotopes.

Finally, it should be noted that a shape transition is also expected to occur around a critical temperature  $T_c=1$  MeV. Indeed, above this temperature, the nucleus becomes spherical, due to thermal excitations. Investigations have been performed for instance in the superdeformed  $^{152}\text{Dy}$  nucleus. Again, the evolution of  $T_c$  with respect to isospin could be undertaken at SPIRAL2, in order to probe shell structure for exotic nuclei. Moreover hyperdeformation is suspected to occur in the unstable  $^{176}\text{Er}$ ,  $^{178}\text{Yb}$  and  $^{180}\text{Hf}$  nuclei, which could be produced at the SPIRAL2 facility.

### 2.6.7 Pre-equilibrium phase in fusion reactions: the role of dynamic dipole oscillations

With the energies delivered by SPIRAL2, it will be possible to study the pre-equilibrium phase and collective modes in the fusion reaction. The study of the *dynamic* pre-equilibrium GDR has already been tried in stable systems by comparing different entry channels (more precisely N/Z and excitation energies) resulting in the same compound nucleus (e.g.  $^{40}\text{Ca} + ^{100}\text{Mo}$  and  $^{36}\text{S} + ^{104}\text{Pd}$ ) but the results are not significant mainly because the systems are still too similar. The pre-equilibrium GDR is observed via the measured  $\gamma$ -ray multiplicity and quantified by the excess obtained compared to the *static* GDR.

*The Giant Dipole Resonance and the pre-equilibrium phase in fusion reactions*

Recent calculations predict that with a beam of  $^{108}\text{Mo}$ , the excess of  $\gamma$ -radiation coming from the decay of a pre-equilibrium GDR could be a factor of 3 larger than is measured today using stable-isotope beam. This type of experiment can be carried out with beam intensities of the order of  $10^8$  atoms/s. They need an efficient  $\gamma$ -ray detection system up to high transition energies (i.e.  $\sim 8\text{-}15$  MeV).

### 2.6.8 The collective rotation and the order to chaos transition

The collective rotational motion both in the discrete and in the region of the quasi-continuum has not yet been investigated in neutron rich nuclei and the high intensity exotic beams of SPIRAL2 give the opportunity to carry out experiments to examine them. In fact, due to the increase of the fission barrier in these nuclei one can more easily populate the highest spin states and therefore one should be able to investigate the order to chaos transition in the extreme regime of angular momentum. While low-lying excited states are characterized by good quantum numbers, at higher transition energies the concept of quantum numbers breaks down, owing to the high level density and mixing between the states. The disappearance of quantum numbers is a signature of quantum chaos, for which experimental evidence has been found in the neutron resonance region, at 6-8 MeV of thermal energy. The transition between order and chaos occurs in *warm* nuclei. The warm excitation energy region has been studied in deformed nuclei through the analysis of the features of quasi-continuum spectra with  $\gamma$ -ray transition energies in the interval 0.8-2 MeV.

The measured quasi-continuum spectra were found to originate from  $\gamma$ -ray transitions de-exciting strongly mixed rotational bands. The band mixing mechanism depends on the residual interaction and the increase in level density and the phenomenon is also called *rotational damped motion*. Because of the configuration mixing, the rotational E2  $\gamma$ -decay from an off-yrast compound state at spin I is fragmented over many final states with spin I-2. The width of the associated B(E2) strength function is defined as  $\Gamma_{\text{rot}}$ , that is the rotational damping width.

Several experimental efforts have been made to study the mass, deformation and configuration dependence of the rotational damping. The configuration dependence of rotational damping at a fixed deformation is particularly interesting as it shows the importance of nuclear structure effects in the order-chaos transition region. Mixed band calculations based on the cranked shell model plus residual interaction predict a variation of  $\Gamma_{\text{rot}}$  with neutron number, which is due to the shell structure. This is because  $\Gamma_{\text{rot}}$  is dominated by the dispersion of rotational frequencies arising from particle alignment (depending on particle orbits) along the rotational axis. The shell structure effect of the rotational damping is illustrated in figure 2.6.3 Experiments with neutron rich nuclei such as  $^{176}\text{Yb}$  are therefore very important to probe in detail the rotational damping picture and to obtain a better understanding of the order-chaos transitions.

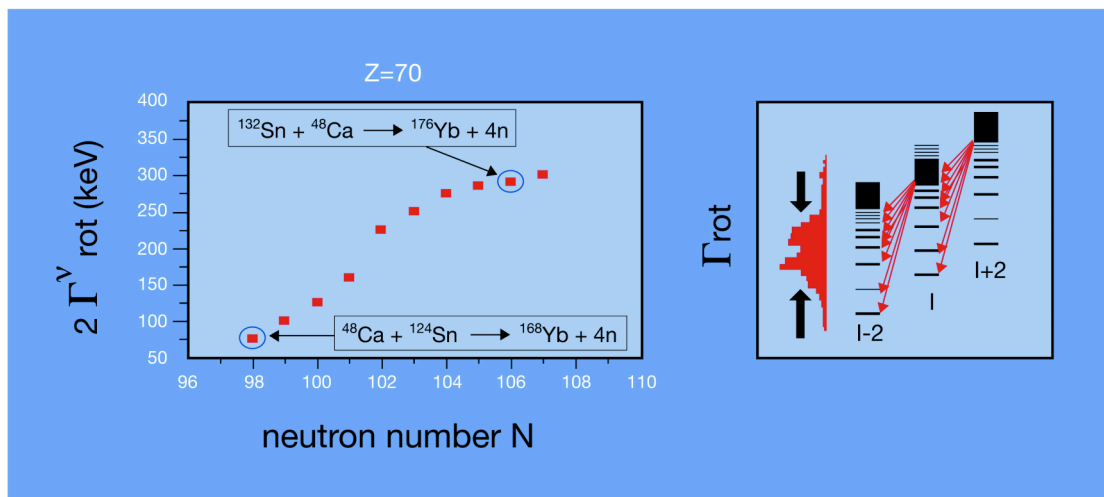


**Figure 2.6.3:** Expected values of the rotational damping width as a function of neutron number for the Yb isotopes.

For the ytterbium ( $Z=70$ ) region the exotic nucleus  $^{176}\text{Yb}$  should be better populated at high spins ( $I \approx 70\hbar$ ), via the reactions  $^{132}\text{Sn} + ^{48}\text{Ca}$ , than  $^{168}\text{Yb}$ , as a consequence of the  $\approx 5$  MeV increase in the fission barrier in moving from  $N=98$  to  $N=106$ .

## 2.7 WHAT FORCES ARE RESPONSIBLE FOR THE BINDING OF NUCLEI?

The properties of composite physical systems generally result from the sum of the interactions between pairs of their components. This does not seem to be true for the atomic nucleus, making it a unique example of complex systems characterised by strong many-body correlations.

### Discovering the nature of the nuclear forces: “realistic” 2- and 3-body interactions

From a certain point of view, the interaction between two nucleons can be regarded as relatively well known. Although not fully understood, the interaction between pairs of nucleons can be modelled on the basis of systematic measurements of the reactions between free nucleons. These are known as “realistic” forces. With significant theoretical effort, it has been possible to carry out exact calculations for nuclei containing up to a dozen nucleons, interacting via realistic forces. It was found that it is necessary to include 3-body forces (i.e. interactions between three nucleons which are not reducible to 2-body interactions) in order to reproduce, for example, the binding energies (the energy necessary to disperse all of the components of a system) of light nuclei. These 3-body forces account for up to half of the binding energy of light systems with  $A \leq 12$ .

Two- and three-body nuclear forces cannot yet be calculated starting from Quantum Chromodynamics the underlying microscopic theory of strong interactions. At present, nuclear forces must be modelled taking account of experimental constraints from measured nuclear properties. Measurement of reactions involving three nucleons cannot answer all the relevant questions and must thus be supplemented by studies of light nuclei whose experimental structure properties can be compared with exact calculations. The restriction to

light nuclei is essential since exact calculations can only be made for a relatively small number of nucleons. However, only 4 stable nuclei contain fewer than 8 nucleons, and it is thus necessary to study exotic nuclei. Moreover, only by studying exotic nuclei is it possible to vary the ratios of protons and neutrons over a wide range, whereas light stable nuclei practically always contain the same proportion of the two species of nucleon. This is why there is an extensive experimental and theoretical research programme underway to understand the structure of these exotic nuclei to try to find evidence for new systems (bound or not) like the very neutron-rich hydrogen isotopes  $^5\text{H}$  and  $^7\text{H}$ , containing 4 and 6 neutrons, respectively, and only one proton, or the quadrineutron  $4n$ , which is even further away from the stability line.

### ***The binding energies of the light nuclei and 3-body forces***

*With the intense beams of exotic nuclei produced by SPIRAL2, and by using reactions involving transfer of nucleons or charge-exchange transformation of protons into neutrons, it will be possible to conduct studies aimed at the clarification of the binding energies of light nuclei. Of particular interest are beams of  $^6\text{He}$  and  $^8\text{He}$ , containing respectively 4 and 6 neutrons, but only 2 protons. SPIRAL2 will deliver an  $^8\text{He}$  beam with an intensity of  $10^9$  atoms/s on target. This will allow one to perform unprecedented reaction studies, to thus gain new insight into the structure of light exotic nuclei and to seek new (unbound) nuclear systems. A significant constraint on the theory of the nuclear forces could come from systems containing neutrons exclusively, like the quadrineutrons or the hexaneutrons, even although they exist only in the form of resonances.*

### **Constraints on the forces used in the effective approximations**

Our knowledge of the forces between nucleons not only makes it possible to calculate in an almost exact way the structure of the light nuclei, but also provides the theoretical underpinning for the approximations necessary to treat heavier nuclei. In contrast to the exact calculations carried out for light nuclei, the models that are used in the description of medium-heavy and heavy nuclei only take into account certain specific aspects of the structure of the nucleus. These models employ “effective” forces, which describe the complex nuclear dynamics in terms of a relatively small number of degrees-of-freedom. As examples we have the forces between nucleons considered as independent particles, the interactions between substructures when the nucleus is described as an assembly of aggregates, or couplings between nucleons in various orbits when the nucleus is modelled by the mixture of several distributions of the nucleons in a limited number of “shells” (configuration mixing).

Although closely related to the approximation used, and only applicable within this restricted framework, these forces have been used with considerable success because they are readily applicable and thus allow direct comparisons with experiment.

### ***Structure of nuclei: indirect constraints of effective forces***

*Most of the phenomena to be studied with SPIRAL2 will have a direct impact on the effective forces employed in theoretical models. In particular, because stable nuclei exhibit only a weak variation of the proton to neutron ratio, the study of the isospin dependence of the effective forces necessitates experimental information on exotic nuclei. SPIRAL2 is designed to access the unexplored region of exotic nuclei and to extract observables that will constrain the effective forces.*

### ***Direct measurements: the case of the spin-orbit interaction***

*Certain theoretical approaches can be directly tested by studying nuclear collisions. This is the case for the optical potentials, which describe the interaction between two nuclei or between a nucleon and a nucleus. Beams of exotic nuclei from SPIRAL2, bombarding various targets, allow the study of such potentials and to thus clarify the role of the proportions of neutrons and protons on the nuclear forces.*

*A significant example is the case of the “spin-orbit” interaction. The nucleons exhibit a preferred direction, called the spin. In a magnetic field, they behave as small compasses which seek to be aligned in the direction of the field. One observes in fact that they present only two states: aligned or opposed to the field. Nucleons in nuclei appear to be more bound when their spin is opposed to their orbital moment, i.e. when the nucleons point in the direction opposite to their axis of rotation in the nucleus. This interaction, known as the spin-orbit interaction, is similar to a magnetic coupling between their intrinsic magnetisation and the magnetic field which they generate by their rotation at high speed. However, in nuclei this additional attraction is created by the strong interaction, which holds the nucleons in the nucleus, and not by the electromagnetic forces. The characteristics of this spin-orbit interaction are still poorly known, particularly its variation with the type of nucleons (dependence on isospin).*

*A way of highlighting this interaction and its properties is to bombard nuclei with nucleons that have been aligned in a precise direction, i.e. polarised nucleons. The variation of the probability of diffusion with the initial orientation is directly related to the force of the “spin-orbit” interaction. In the case of exotic nuclei, the impossibility of forming them into a target forces one to perform the inverse experiment and to use them as a beam on a polarised target. The change in this spin-orbit force with the isotopic composition of the nucleus is one of the significant points to be examined. These studies must be made with sufficient energy so that the nucleon entering into the collision can penetrate into the nucleus and thus feel the nuclear force.*

*As indicated earlier, the spin-orbit force is closely related to the structure of nuclei, and in particular to the extra stability observed for certain “magic” nuclei. The variation of the spin-orbit effects with neutron or proton number in nuclei is one of the challenges in the research to be carried out with SPIRAL2.*

### ***3. DYNAMICS AND THERMODYNAMICS OF CHARGE ASYMMETRIC NUCLEAR MATTER***

A deeper understanding of the behaviour of neutrons and protons in a charge asymmetric nuclear medium is essential to test and to extend our present knowledge of the nuclear interaction. The structure of the nucleon-nucleon effective force, the nucleon effective mass and the competition between mean-field and two-body collisional effects certainly all depend on the charge asymmetry of the systems considered. Hence it is clear that the isospin degree-of-freedom opens a stimulating new field of exploration, allowing us to obtain an insight into new nuclear properties. In this way one can investigate the properties of the nuclear equation-of-state (EOS) and the associated phase diagram, to learn about the static properties of asymmetric matter and access the thermodynamics of exotic nuclei. It will also be interesting to study reaction mechanisms for charge asymmetric systems under different conditions of excitation energy and impact parameter. In fact the reaction dynamics of charge asymmetric heavy ion collisions represents a unique tool to provide information on the density and momentum dependence of the isovector interaction away from normal conditions.

The exploration of some of the topics presented in this chapter will be started thanks to the first beams delivered at the SPIRAL2 facility. However, a better quantitative understanding of the properties of asymmetric nuclear matter requires an extension of the energy range of SPIRAL2 beams towards higher bombarding energy (at least 30 to 50 MeV/nucleon). This extension will be crucial if we are to address many of the interesting and attractive topics outlined in this chapter. SPIRAL2 will establish a strong bridgehead in terms of exploring how exotic beams will transform our understanding of reaction mechanisms and the nuclear EOS in asymmetric nuclear matter. If we are to capitalise on the SPIRAL2 beams in this way a new  $4\pi$  detector with low detection thresholds, based, for example, on the FAZIA concept, will be necessary to collect the maximum amount of information.

A variety of astrophysics issues such as the structure of neutron stars or supernovae explosions are linked to the asymmetry term of the EOS, reinforcing the need for research programmes probing the bulk properties through strong perturbations. This is also of great importance for Nuclear Structure problems (in particular for drip-line nuclei, skins, synthesis of new elements and collective motion) as well as for a more microscopic picture of Nuclear Physics at large.

The reaction dynamics in the SPIRAL2 energy range appears quite complex, in particular looking at the possibility of future beams at energies greater than 15 MeV/nucleon. The role of the isospin degree-of-freedom in several reaction mechanisms, ranging from the formation of compound systems to the sudden break-up of nuclear sources into many pieces, needs to be investigated within the framework of transport theories for fermionic systems. In this way one can study the origin of interesting isospin effects, such as the isotopic content of pre-equilibrium emission, isospin distillation, fragment isotopic distributions, neutron-proton collective flows and directly relate them to the properties of the nuclear interaction. Moreover one can study the thermodynamical properties of the complex sources formed during the collision. The by looking at the configurations obtained in multifragmentation reactions it would be possible to derive the co-existence zone of exotic nuclei by making a connection with the occurrence of liquid-gas phase transitions.

## 3.1 THERMODYNAMICAL ASPECTS

### 3.1.1 Level densities and entropy

The density of nuclear states is strongly connected to the nuclear matter EOS. Like the saturation energy and the nuclear compressibility modulus, the level density probes the bulk properties of nuclear matter at saturation density and puts strong constraints on the interaction. The level density parameter is a crucial quantity for the understanding of the thermal properties of excited nuclei, to localise the opening of decay channels, to study the correlations in nucleonic matter and to describe the competition between the various sequential decay channels. It governs the nuclear caloric curve at low and moderate excitation energies (typically below the multifragmentation threshold of  $\approx 3$  MeV/nucleon).

The nuclear level density not only plays a central role in many phenomena but is also a prototype of the co-existence of both descriptions of the nuclear many-body system since it is simultaneously sensitive to bulk properties and to a few active orbitals located around the Fermi surface. The level density parameter is related to the effective mass, a property of the effective interaction that is sensitive to the nuclear core, to the neutron-proton composition and also depends on the coupling between intrinsic degrees of freedom and surface vibrations. The level density parameter is also related to the shell structure. It is reduced in a magic nucleus (see figure 3.1). With increasing excitation energy of the nucleus, the expected decrease in the effective mass leads to a decrease in the level density parameter, which is strongly dependent on the asymmetry  $N/Z$ .

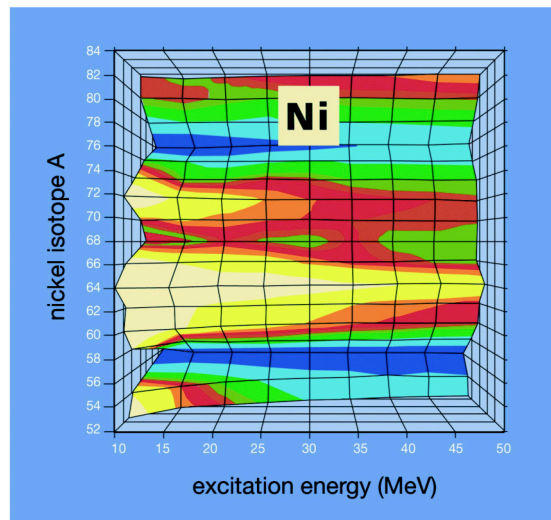


**Figure 3.1:** Evolution of the level density parameter as a function of the excitation energy and of the mass for various isotopes of Ni. The darker regions correspond to a lower density parameter  $a=6$  while the lighter area is associated with  $a=9$ . In magic nuclei the density is lower because of shell effects. Here the neutron magic numbers  $N=28$  and  $50$  ( $A=56$  and  $78$ ) survive up to rather high excitation energy. The sub-shell  $N=40$  appears to be less robust.

The  $\gamma$ -decay in the continuum can give invaluable indications of the level-densities, even if their extraction rests on a certain number of assumptions (Fermi gas model at high energy) and is based on existing data (discrete states at low energy, spacing between neutron resonances). The measurement of the level-densities between the superfluid regime (discrete states with low energy) and the Fermi gas regime is of fundamental interest for the study of the phase transitions of nuclear matter. It is also possible, with a knowledge of the level-densities, to have access to the entropy, the temperature or the heat capacities, thus opening

the door to the study of the thermodynamic properties of complex systems such as atomic nuclei.

### ***Measuring level-densities and accessing the thermodynamics of atomic nuclei***

*Bombarding light targets ( $p, {}^3\text{He}$ ) with SPIRAL2 beams with masses between  $A=150$  and  $A=200$  accelerated to about 15 MeV/nucleon, one can measure level-densities by studying the evolution of the radiative response of the nucleus with angular momentum and excitation energy. For this purpose,  $\gamma$ -rays must be measured in coincidence with particles. By deconvolution of the inclusive  $\gamma$ -ray spectrum (using a decay code, such as CASCADE for instance) one can access the level density in an excitation energy range of a few MeV/nucleon. A  $\gamma$ -ray detector of very high granularity and high resolution is necessary for this type of study.*

*Finite size effects, temperature and  $N/Z$  asymmetry dependence of the level density parameter at higher excitations will be extensively studied by measuring the statistical decay of a large number of isotopes of a compound nucleus formed by fusion with neutron rich and neutron deficient projectiles.  ${}^{114-145}\text{Xe} + {}^{40,48}\text{Ca}$  reactions at energies from the barrier up to the maximum attainable with CIME are good candidates for this type of experiment.*

### **3.1.2 Coulomb instabilities and temperature limits**

The limits in temperature that a nucleus can support help to constrain the nuclear EOS at finite temperature, close to the saturation density. For stable nuclei, the temperature limits are thought to be somewhat higher and, to study this variable, one must control the energy deposited, the degree-of-equilibrium and the reaction mechanism. Close to the proton drip line, it is predicted that Coulomb instabilities lower this limiting temperature significantly.

SPIRAL2 beams will make feasible the investigation of the influence of the isospin degree-of-freedom on the decay modes of a whole isotopic chain of compound nuclei produced in fusion-evaporation reactions - from the neutron-deficient isotopes, right up to the nuclei richest in neutrons - by measuring with precision all emitted particles in coincidence with the evaporation residues. Moreover, these studies will allow us to explore the influence of the Coulomb interaction on the expansion phase of systems in the absence of collisional compression.

A knowledge of statistical decays and limiting temperatures for light nuclei (neon to calcium) is also essential for thermodynamical studies. Indeed, these are key ingredients in characterising the freeze-out stage in fragmentation phenomena, which is constituted of many excited fragments and light particles. In recent experiments, these primary fragments have been reconstructed and one observes a saturation in their excitation energy per nucleon. Is this saturation due to a basic property of a dilute system (in which the temperature of fragments could not exceed a given value), or a limit on the energy deposition imposed by the dynamics of the collision, or an intrinsic limitation in very light nuclei? Answers should be obtained by the studies proposed here.

Finally, since fragments inform us of the isospin content of the dilute system, it is crucial to have information on the decay of these nuclei formed via the fusion of light nuclei. One could typically use C to Ne beams on light targets. Bombarding energies in the range 10 to 20 MeV/nucleon are well suited for these studies.

### ***Studying the limiting temperature and the role of the Coulomb interaction on nuclear dynamics***

*A key-experiment would be the study of a chain of tungsten compound nuclei, formed by  $^{114-145}\text{Xe} + ^{40,48}\text{Ca}$  reactions at energies from 5 MeV/nucleon up to the maximum energy possible with the CIME cyclotron. An alternative is the use of the isotopic chain created with Kr as a projectile on Fe targets. To reach the limiting temperature over the whole chain, it will be necessary to go higher in energy and thus, provided that the initial intensities of the radioactive ion beams produced by SPIRAL2 are sufficient, to consider a further post-acceleration so as to reach 30 MeV/nucleon. The intensities necessary for this type of experiment are approximately  $10^6$  atoms/s on target, coupled with a new highly efficient  $4\pi$ -charged particle array.*

### **3.1.3 Multifragmentation and the liquid-gas phase transition**

Due to the nature of the interaction between the constituents and by analogy with the transformations in a van der Waals fluid, a first order transition of the liquid-gas type is expected to occur in nuclear matter at low densities and finite temperatures. Searching for signatures of such a phenomenon in finite and highly excited systems is one of the challenges of the field since it allows one to define and verify in the laboratory the fundamental concepts of the thermodynamics of small systems, a recent, very active and cross-disciplinary research area. As far as nuclear physics is concerned the dense matter properties and the associated phase diagram are also of paramount importance.

The fragmentation process observed in heavy-ion reactions shows many features compatible with such a phase transition in a finite system. For example, a negative heat capacity has been deduced from the measurement of the fluctuation of the energy balance of the total energy stored in the multifragmenting system. The observation of fossil signals of spinodal decomposition in the charge correlations between fragments suggests that the phase transition is induced by fluctuations of density amplified by mechanical instabilities in the spinodal region.

The same analyses done with exotic nuclei will allow us to study the phase diagram as a function of the isospin degree-of-freedom. This is important since, according to quantal RPA calculations of mean-field instabilities, the liquid-gas co-existence zone is expected to shrink in charge-asymmetric nuclei, see figure 3.2.

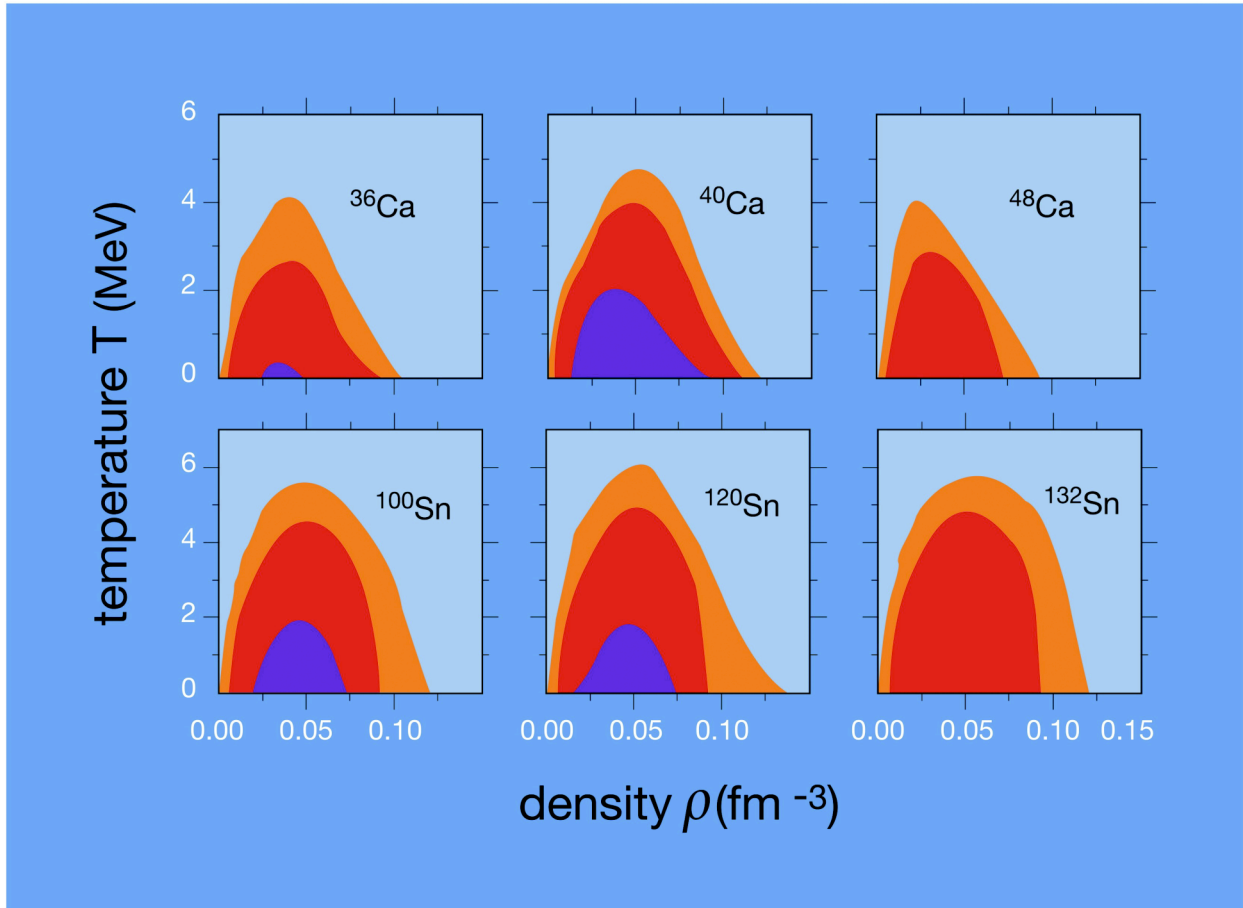


**Figure 3.2:** RPA calculations describing the phase diagrams for exotic nuclei.

Since the Coulomb energy is disruptive and participates in the expansion of the system, the threshold for multifragmentation in central collisions should depend strongly on the neutron-to-proton ratio. This effect could be used to induce a breaking of the nucleus at moderate excitation energy and study the competition between thermal and mechanical instabilities. Phenomena associated with a low density material, clusterisation and condensation, new collective modes, non-standard shapes or dilute surfaces are expected to be likely in the structure of nuclei at the drip lines. All these features are also present in the multifragmentation of nuclei indicating that the study of this process is a useful laboratory to obtain information of value for the understanding of nuclei having large values of  $N/Z$  asymmetry.

***Identification and study of the liquid-gas transition with post-accelerated beams from SPIRAL2***

*Incident energies of the order of 30 MeV/nucleon are needed to reach the multifragmentation threshold in central collisions. As in section 2.2, it will thus be necessary to post-accelerate the beams from SPIRAL2. The phase transition was observed in certain systems like Xe+Sn or Au+Au. It will therefore be particularly interesting to use the same elements while varying the  $N/Z$  ratio, as with  $^{114-145}\text{Xe}+\text{Sn}$  or  $^{176-205}\text{Au}+^{197}\text{Au}$ .*

## 3.2 LARGE AMPLITUDE MOTION

### 3.2.1 Quantum tunnelling in complex systems: the nuclear case

Heavy-ion fusion dynamics at energies near and below the Coulomb barrier has been the object of many experimental and theoretical studies in various laboratories for more than twenty years, using stable-isotope beams and, more recently, radioactive ion beams (RIBs) as well. RIBs from next-generation facilities like SPIRAL2 will provide a unique opportunity for measuring cross-sections and mapping barrier distributions in a wider range of systems where the differences in nuclear structure may lead to significantly different situations. The use of RIBs will certainly help to address various important open questions such as the fusion path for relatively heavy nuclei, namely with a mass number larger than 20-25. For lighter systems very interesting experiments have been performed in recent years, using both stable and exotic beams, showing the influence on fusion dynamics of the presence of weakly bound nucleons, and of unexpected structures like nucleon halos as well. The new perspectives offered by SPIRAL2 in this field are described elsewhere in this Report. Sub-barrier heavy-ion fusion cross-sections are generally dominated by strong couplings to nuclear shape vibrations, deformations and/or nucleon transfer degrees-of-freedom. The method of extracting fusion barrier distributions from the second derivative of the fusion excitation function has been a major breakthrough for the understanding of the kind of couplings involved in the various cases. Hence, an intimate link has been established between nuclear structure and reaction dynamics, and the availability of the new beams from SPIRAL2 will open up much wider possibilities, particularly in connection with studies of fusion between heavy and/or neutron-rich nuclei. Such experiments will be fascinating, as will be made clear below.

An attractive line of measurements with medium-heavy systems may concern cases where very positive Q-values exist for the transfer of neutrons between projectile and target. From the very beginning of experiments on sub-barrier fusion, this process has been indicated as responsible for at least part of the observed enhancements and, more specifically, for the large isotopic effects observed in a number of cases.

There are systems where those Q-values reach incredibly large values, up to 20-25% of the barrier height. They would be very interesting to study, because one might expect very large effects on the sub-barrier fusion cross-sections. Other very attractive measurements involve various so-called "simple" cases, typically systems where the colliding nuclei are magic or nearly magic. It has become clear that such cases are far from being simple, despite our expectations. Among the systems with stable nuclei, one may cite the case of  $^{40,48}\text{Ca} + ^{40,48}\text{Ca}$  where the cross-sections are still awaiting a satisfactory theoretical interpretation, and  $^{16}\text{O} + ^{208}\text{Pb}$  where the observed structures in the barrier distribution seem to indicate the importance of multi-phonon octupole excitations of  $^{208}\text{Pb}$  and, possibly, of projectile excitation.

### ***Measuring fusion cross-sections in medium-heavy systems***

*A couple of examples: the first is the system  $^{52}\text{Ca} + ^{32}\text{S}$  where  $Q(2n)=+11.0$  MeV and is 26% of the Coulomb barrier (43 MeV). A second system would be  $^{26}\text{Si} + ^{142}\text{Ce}$ , where the  $Q$ -value for the pick-up of a neutron pair is as high as +18 MeV.*

*Concerning magic or semi-magic nuclei, one can make use of exotic beams of e.g.  $^{132}\text{Sn}$ ,  $^{56}\text{Ni}$  or  $^{68}\text{Ni}$ . A particularly interesting case would be to measure the fusion of  $^{132}\text{Sn} + ^{48}\text{Ca}$  (both magic and both very neutron-rich). As a by-product, the evaporation residues of  $^{132}\text{Sn} + ^{48}\text{Ca}$  would allow the study of nuclear structure in a poorly known region of the nuclear chart around  $^{180}\text{Yb}$ . Indeed, it has not been possible so far to access very neutron-rich and heavy nuclei with fusion reactions.*

*It is important to notice that such experiments are possible with good quality beams of only  $\sim 10^5$  atoms/s, provided that high-efficiency experimental set-ups and good targets are available.*

### **3.2.2 Heavy-ion fusion near and below the Coulomb barrier: Heavy and very heavy systems**

The longstanding efforts to understand the processes involved in the synthesis of superheavy nuclei have shown that capture inside the Coulomb barrier, with the formation of a di-nucleus, is not a sufficient condition for complete fusion between heavy nuclei. Complex reactions compete with fusion and a considerable part of the total cross-section goes into deep inelastic and quasi-fission channels. Only if the evolution of the di-nucleus towards fusion continues is a fully equilibrated compound nucleus formed, which then decays by particle evaporation or fission. Such a dynamical hindrance to fusion has been known for many years, but recent experimental results have brought renewed interest in this phenomenon, and the perspectives offered by RIBs are appealing.

For heavy symmetric or nearly symmetric systems a considerable hindrance of fusion was observed around the barrier. The macroscopic extra-push model, taking into account the nuclear structure of both the projectile and target, reproduces correctly the extracted fusion probabilities in the critical region roughly above  $Z_1 \times Z_2 = 1600$ . However recent experiments on the production of  $^{202}\text{Pb}$ ,  $^{216}\text{Ra}$  and  $^{220}\text{Th}$  compound nuclei have shown that fusion is increasingly inhibited near the barrier, even for  $Z_1 \times Z_2$  values as low as 700, when the entrance channels have increasing mass-symmetry, due to the competition with quasi-fission. The fusion probability (or hindrance) for heavy systems has also been linked to the structure of the colliding nuclei, i.e. shell closures and/or static deformations.

Now, it was predicted, and it has been observed in some cases, that shell structures, and consequently deformation regions, change when one goes from the stability line towards neutron-rich exotic nuclei. The advantage of using very neutron-rich (and high-intensity) beams for the production of superheavies, is also clear from the point of view of the exit channel, i.e. on the basis of producing a compound nucleus very near to the predicted  $N=184$  closed shell. This is not possible with the present stable-isotope beams, either using cold or hot fusion. In any case, it is felt that a deeper understanding of the fusion dynamics for medium-heavy systems, involving RIBs, is necessary, on the basis of the microscopic and macroscopic properties in the entrance channel, namely surface vibrations, deformation, neutron transfers, shell closures and the mass asymmetry. All this will allow us to focus better the next-generation experiments aimed at producing shell-stabilised, superheavy nuclei in the vicinity of  $Z=114$ ,  $N=184$ .

### ***Measuring fusion cross-sections in heavy systems***

*The systems  $^{132,136}\text{Sn} + ^{96}\text{Zr}$  and  $^{84,88}\text{Se} + ^{138}\text{Ba}$  lead to thorium isotopes and may give a deep insight into dynamical and/or shell effects in the fusion probability; a comparison with the fusion cross-sections of e.g.  $^{20}\text{O} + ^{208}\text{Pb}$  will teach us about the effect of the mass asymmetry for neutron-rich systems.*

*RIBs of heavy zinc and germanium isotopes (e.g.  $^{82-85}\text{Ge}$ ,  $^{78-80}\text{Zn}$ ) may help the approach to the  $N=184$  shell in cold fusion with  $^{208}\text{Pb}$ . Alternatively, hot fusion of neutron-rich calcium or titanium beams on radioactive actinide targets might be used.*

*Using heavier beams like  $^{132-136}\text{Sn}$  on  $^{160}\text{Gd}$  or  $^{164}\text{Dy}$  may lead to superheavy nuclei by fusion of a spherical rigid projectile (the  $^{132}\text{Sn}$  beam) with a neutron-rich deformed target, leading to compound nuclei in the region of  $Z=114-116$ ,  $N=178-182$ .*

*Synthesis of very heavy nuclei could also be tried by hot fusion of nearly symmetric systems where both projectile and/or target are deformed. A possible case would be  $^{144}\text{Xe} + ^{150}\text{Nd}$ , leading to  $Z=114$ ,  $N=180$ .*

### **3.2.3 Fusion dynamics in the presence of a large charge asymmetry in the entrance channel**

Although mass and charge drift between projectile and target in a nuclear collision may be very slow processes, the  $N/Z$  ratio equilibrates very quickly, after a few nucleon exchanges (few  $10^{-22}$  s). It was suggested long ago that the excitation of the GDR (E(GDR)) may be at the origin of this fast equilibration time. Indeed, the oscillation period of the GDR can be roughly estimated as  $2\pi/E(\text{GDR}) \approx 3 \times 10^{-22}$  s, which is comparable to the  $N/Z$  ratio equilibration time. About 10 years ago, it was suggested that this feature could be exploited in deep-inelastic collisions, to produce very exotic nuclear species, which are not otherwise accessible. Moreover the dynamical, prompt dipole radiation may act as a cooling mechanism along the fusion path at energies above the Coulomb barrier to help the formation of super-heavy elements in fusion reactions. The dynamical alignment of the dipole oscillation, in the reaction plane, will result in a strong anisotropy of the photon emission with respect to the beam axis. This radiation could be used as a clear signature of a fusion reaction with radioactive ion beams. The effect has been clearly seen in semi-classical transport simulations that provide quantitative evaluations. Including quantal effects we get the suggestion of possible couplings to other collective modes. From experiment there are several pieces of evidence from fusion and deep-inelastic collisions.

However, to perform this kind of study, there is a need for detailed information concerning mass, charge exchange and  $N/Z$  evolution as a function of the projectile and target combination, the bombarding energy and the emission angles of the ejectiles (in the case of deep-inelastic collisions). Such information is necessary to optimise the production of the desired species.

### ***Measuring pre-equilibrium dipole radiation***

*Evidence of pre-equilibrium dipole radiation has been reported, for instance, in fusion reactions of Ca + Mo and O + Mo, at beam energies corresponding to roughly 100 MeV of total energy available in the centre-of-mass. These investigations will be extended to systems with larger N/Z asymmetry in the entrance channel and to the study of the excitation function of the mechanism in the beam energy range of 3-15 MeV/nucleon. Such experiments are very demanding and require the detection of  $\gamma$ -rays in coincidence with the fragments preferentially identified by their charge and their mass. Exotic beams offer the opportunity to explore the equilibration of the N/Z ratio over a very extended range that is otherwise inaccessible. Such complete experiments should become possible in the near future with the advent of the  $\gamma$ -ray spectrometer AGATA coupled to a  $4\pi$  charged particle detector.*

### **3.2.4 Dissipation in low energy binary collisions and competition with fusion**

Deep-inelastic collisions offer both a unique opportunity to study phenomena occurring in nuclear matter under extreme conditions with respect to shape, intrinsic excitation energy, spin, N/Z ratio (isospin) etc and the possibility of controlling these conditions by choosing appropriate initial and final reaction parameters. Thus, it is possible to probe the simple modes of nuclear excitation produced in damped nuclear collisions, how intrinsic degrees of freedom are converted into collective modes, how these modes decay and how relaxation processes occur within a small quantal system that is initially far from equilibrium. The short lived, rotating dinuclear complex formed in the early stage of the collision separates into projectile-like and target-like fragments which then dissipate their excitation energy by emitting light particles and  $\gamma$ -rays. The fragments share an excitation energy determined by the degree of damping of the initial relative motion. Energy damping and mass exchange increase with the amount of rotation (or lifetime) of the dinuclear complex. The shape of the angular distributions of the reaction products is thus strongly correlated with the energy loss, which in turn is strongly correlated with the net exchange of mass and charge between the reaction partners. Hence the velocity and the angular distribution of the reaction products furnish natural clocks from which it is possible to determine the equilibration times of the various degrees-of-freedom (e.g. N/Z ratio, mass, excitation energy) in an almost model-independent way. These aspects of strongly damped collisions are relatively well explained by classical equations of motion including dissipative terms and a diffusion process based on the Fokker-Planck equation or within the mean field approach using the stochastic nucleon exchange model.

Although most of the gross features of deep-inelastic collisions are relatively well understood, many questions still await unambiguous and conclusive answers. Thus a full understanding of the energy damping and of the energy sharing between the two reaction partners vs. damping remains to be achieved. Nucleon exchange between projectile and target, which is at the origin of mass and charge drift, N/Z equilibration, energy damping and sharing as well as angular momentum transfer, is very sensitive to the mass, charge and shape asymmetry and to the relative kinetic energy in the entrance channel. Correlations, due to the coupling between all those variables introduced by nucleon transfer are not yet well understood. In charge asymmetric systems these dissipation mechanisms are sensitive to the isovector part of the nuclear interaction, the symmetry energy. Thanks to SPIRAL2 beams, investigating how the energy, mass and asymmetry sharing between projectile-like and target-

like fragments depends on the incident asymmetry will furnish essential information on this fundamental (but poorly known) ingredient of the nuclear interaction.

Moreover, the study of the interplay, in the energy range of 5-15 MeV/nucleon, of fusion, including incomplete fusion, vs. deep-inelastic reactions in neutron-rich or neutron-deficient systems also provides valuable information on the density behaviour of the symmetry energy. For instance, according to transport theories, a stiff symmetry term leads to a more repulsive dynamics. Hence, from this kind of study, one can place tight constraints on the symmetry energy dependence around normal density (slope, curvature). This can affect important properties of neutron-rich nuclei, such as compressibility, monopole frequency, saturation density and neutron skin.

#### ***Studying the competition between low energy reaction mechanisms***

*One possibility would be to compare the fusion vs. deep-inelastic cross-sections in two reactions having different charge asymmetry, but equal total mass:  $^{46}\text{Ar}$  ( $N/Z=1.56$ ) +  $^{64}\text{Ni}$  ( $N/Z=1.22$ ) (neutron-rich system),  $^{64}\text{Ge}$  +  $^{46}\text{Ti}$  ( $N \approx Z$ ), to study the effect of the symmetry energy and of the Coulomb interaction on the fusion path.*

*Most information on energy damping and energy sharing has been obtained through inclusive or semi-inclusive experiments making use of charge and mass conservation and relying on the binary character of the reaction process. To benefit from the larger range of SPIRAL2 beams, even with moderate intensities, the use of a new  $4\pi$  charged product detector, with low detection thresholds, would be mandatory.*

### **3.3 REACTION MECHANISMS AT FERMI ENERGIES**

#### **3.3.1 Reaction mechanism and thermodynamical equilibrium**

To extract properties of highly excited nuclei from the details of collisions, the dynamical evolution has to be controlled since the system under study involves many degrees-of-freedom with different relaxation times. The thermal equilibration of a nuclear system can be studied as a function of the energy deposited, analysing the kinematics of the products freed during the collision through the construction of some "ad-hoc" observables. With the advent of radioactive ion beam facilities, such studies will be done with very large variations of bombarding energy and isospin in the entrance channel. This will provide the time hierarchy for the various degrees-of-freedom. By using several projectile/target combinations with different isospin, and by observing the distribution of the  $N/Z$  ratio for the light particles emitted as a function of velocity, one obtains the degree of equilibrium in the nuclear system under study. This technique was used in the experiments done with the detector FOPI at GSI, where the energy supplied is essentially of collective origin. At lower bombarding energies, most of this energy should be available for thermalising the system. Since the degree of equilibration depends on the mass of the system, it is important to study both light and heavy systems at the same time. Similar studies can be performed to investigate the degree of isospin diffusion and isospin equilibration in reactions, such as semi-peripheral collisions, where thermal equilibration is not expected (20-40 MeV/nucleon).

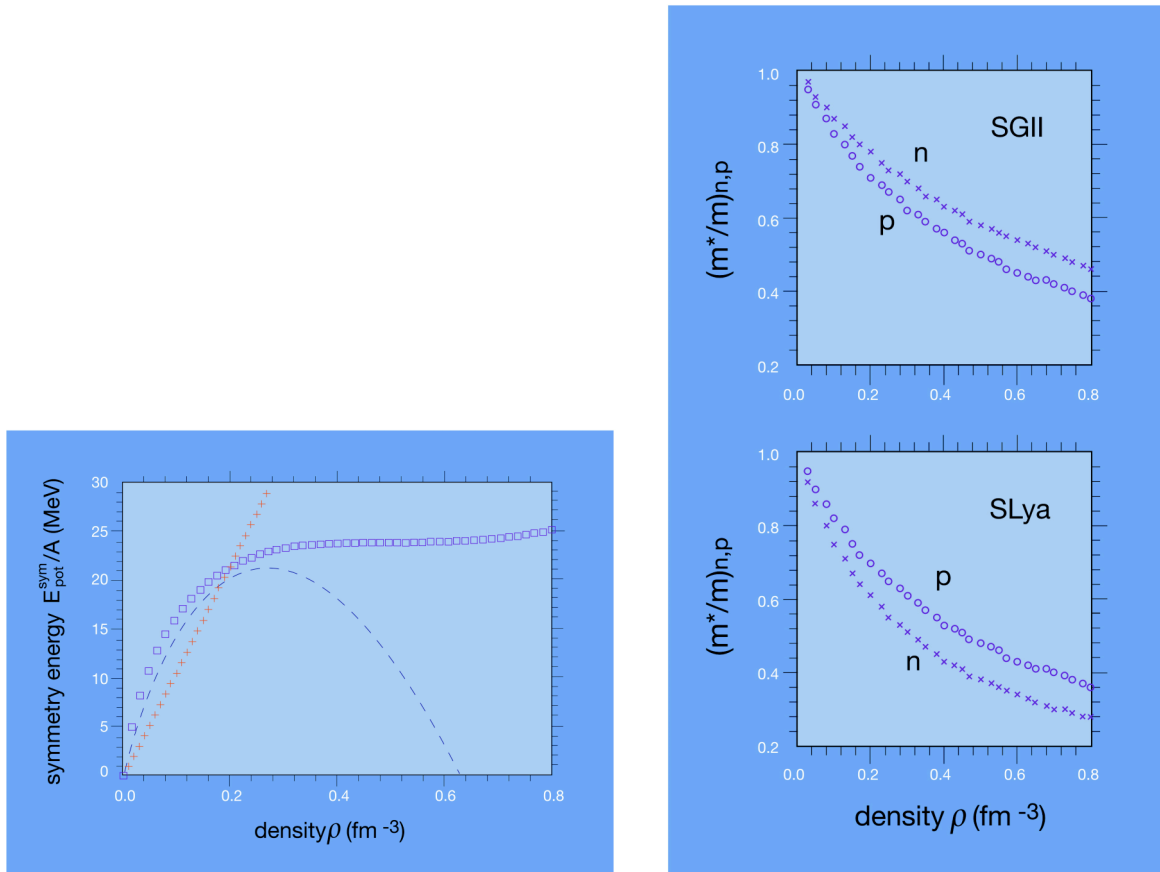


**Figure 3.3:** (a) Left: Symmetry energy as a function of density using various parametrisations of the effective Skyrme interaction. (b) Right: effective masses as a function of the SGII and SLya Skyrme parametrisation..

In this way one can study isospin diffusion in cases where not only the  $N/Z$  gradients, but also density gradients are present, such as in situations where a low-density region (neck region) develops in between the projectile and target. The results are related to the behaviour of the symmetry energy around normal density and to isospin effects in the  $n$ - $n$  cross-section. The typical density behaviour of the symmetry energy as a function of density, for several Skyrme interactions, is depicted in figure 3.3a. One can also learn about fundamental properties of nuclear matter, such as transport coefficients, the principal of which are: viscosity, heat conduction and diffusivity. These coefficients describe the behaviour of matter in situations near but not at equilibrium including irreversible transport of momentum, energy and neutron-proton imbalance across a nuclear system. In reactions, obviously, equilibrium is reached only transiently, so conditions are suitable for determination of the coefficients. The strategy generally needs to include a transport model with adjustable transport properties that can be compared to suitable data. The optimum for viscosity would be comprehensive data on stopping. Of interest, in the context of systems with widely varying neutron-proton ratio, is the diffusivity related to the nuclear symmetry energy and, in the kinetic limit, to in-medium neutron-proton cross-sections. A promising observable for the determination of diffusivity is the transport of the neutron-proton imbalance between the projectile and target in asymmetric systems, as discussed above. The transport coefficients should vary rapidly with system excitation, because of the changing role of the Pauli principle and, thus, their determination invites studies at different beam energies. The importance of dissipative

transport changes with system size and, thus, in testing the conclusions, one should carry out studies of systems of different sizes.

***Using the isospin degree of freedom at SPIRAL2 to study the degree of equilibration and isospin diffusion***

*Good combinations for such studies at SPIRAL2 are  $^{102-118}\text{Ag}$ , or  $^{74-94}\text{Kr}$  on  $^{54,58}\text{Fe}$  targets or  $^{114-145}\text{Xe}$  on  $^{112,124}\text{Sn}$ . To extract the drift coefficients one needs to access the variances of the mass and charge distributions, i.e. it is essential to identify both the mass and the charge of the fragments over a large mass range. New  $4\pi$  charged particle- as well as neutron-detectors should permit the acquisition of reliable data and allow us to determine to what degree proton- and neutron- exchanges are correlated.*

### **3.3.2 Fragmentation in semi-peripheral reactions at the Fermi energies**

The more sophisticated transport models (stochastic theories) predict fluctuations of great amplitude in the density and isospin content in the interaction region of binary collisions at Fermi energies (20-50 MeV/nucleon), with the possibility of direct intermediate mass fragment (IMF) emission from the overlap zone (the neck region).

The estimation of time scales for fragment formation from velocity correlations appears to be a very exciting possibility to investigate the de-excitation mechanisms of such complex systems: one can follow the properties of clusters produced from sources with a "controlled" and variable degree of equilibration. In this way one can work out a continuous transition from fragments produced rapidly via neck instabilities to clusters formed in the dynamical fission of the projectile(target) residues to those evaporated (statistical fission). Along this line it would even be possible to disentangle the effects of volume and shape instabilities in neck fragmentation. The isospin dynamics will look different in the various scenarios and rather dependent on the symmetry term of the EOS. An interesting neutron enrichment of the overlap ("neck") region is expected, due to the neutron migration from higher (spectator regions) to lower (neck) density regions. This effect is also nicely connected to the slope of the symmetry energy. Neutron and/or light isobar measurements in different rapidity regions appear important. Moreover, moving from mid- to "spectator"- rapidities an increasing hierarchy in the mass and (N/Z) of the fragments is expected. An interesting related observable is the corresponding angular correlation, due to the driving force, of the projectile(target)-like partners.

***Investigating fragmentation mechanisms with SPIRAL2***

*To control these reaction mechanisms and the degree of dissipation, it is necessary to detect coincidences between the quasi-projectile and the mid-rapidity intermediate mass fragments, which must be identified in both mass and charge. These studies can be done with beams similar to those mentioned in the preceding paragraph.*

### **3.3.3 Early stage of the reaction dynamics between neutron-rich nuclei**

Energetic particle emission and collective flows appear particularly sensitive even to the momentum-dependent part of the nuclear interaction. Several experiments can be performed, looking at the pre-equilibrium stage of the reaction, to gain some insight into the behaviour of

the symmetry energy at densities larger than normal. Indeed, the pre-equilibrium phase of the reaction is expected to be particularly sensitive, since in this stage larger isospin asymmetries and densities can be reached. From experiments with stable-isotope beams around the Fermi energy it has been possible to obtain detailed information exploiting, as probes for the pre-equilibrium stages, energetic protons and hard photons. In particular, the sensitivity to the momentum dependence of the nuclear interaction has been observed as an increase both in yield and energy (slope) of the emitted protons especially in central collisions, thus providing information on important properties of the nuclear EOS.

In asymmetric matter a splitting of neutron- and proton-effective masses is expected. The sign of the splitting is quite controversial (see figure 3.3b). Hence it appears very important to try to extract information on this fundamental question from nuclear collisions. Moreover, the isospin content of the fast particle emission can largely influence the subsequent reaction dynamics, in particular the isospin transport properties (charge equilibration, isospin diffusion). One can reach the paradox of a detection of isospin dynamics effects in charge symmetric systems.

Studying pre-equilibrium particles, where high momenta are also reached, one may try to select the density of the sources (transverse momentum  $p_t$  selections). Important probes would be:

- i) N/Z of fast nucleon emission as a function of transverse momentum. As anticipated above, at the Fermi energies one also expects to see effects from the n/p splitting of the effective masses.
- ii) Spectra and yields of hard photons ( $E > 30$  MeV) produced via (n,p) bremsstrahlung. The effect of the n-p mass splitting in asymmetric matter is expected to be probed via accurate measurements of the hard photons in neutron-rich and neutron-poor heavy ion reactions at intermediate energies. Different multiplicities and slopes can be expected for different mass splitting ( $m_n^* > m_p^*$  or  $m_n^* < m_p^*$ ) with respect to a reaction almost symmetric in isospin. Both hard photons and energetic nucleons are known to be sensitive probes of the first stage of the reaction reflecting the interplay between the mean field and the nucleon-nucleon collisions. However, while hard photons do not interact with the nuclear matter and leave the interaction zone carrying only information on the momentum distribution of the colliding nucleons, the pre-equilibrium nucleons feel the momentum dependent mean field not only before, but also after the collision when they have to overcome the mean field nuclear potential to be emitted. For these reasons, complementary information could be obtained from the two different probes.
- iii) Neutron/Proton correlation functions. The time-space structure of the fast particle emission and its relation to the baryon density of the source can be investigated using this probe. Again one expects to observe the combined effects of the density and momentum dependence of the symmetry term.
- iv) E-slope of the Lane Potential. A systematic study of the energy dependence of the (n/p) optical potentials in asymmetric nuclei will shed light on the effective mass splitting, at least around normal density.

- v) Neutron-Proton collective Flows and light isobar flows. Through these observables one may again check symmetry transport effects. Measurements for different ranges of  $p_t$  allow us to focus on momentum dependence effects. The analysis of differential neutron-proton transverse flows below the balance energy appears to be a very promising tool.

***Investigating properties of pre-equilibrium emission with SPIRAL2***

*Experiments with  $^{57,65}\text{Ni}$  or  $^{112,124}\text{Sn}$  on nickel targets at energies around 30 MeV/nucleon could be envisaged, in order to compare with existing data obtained with stable-isotope beams.*

### **3.3.4 Isospin Distillation (Fractionation)**

Studying the isospin content of the Intermediate Mass Fragments in central collisions one can test the symmetry term in dilute matter and related instabilities. This subject is important in terms of observing a liquid-gas phase transition in violent heavy ion reactions, where, after the initial collisional shock, low-density regions can be easily reached during the expansion phase. The experimental observation of signals, in the fragment charge correlation analysis, of the partition of the system in nearly equal-sized fragments supports the idea that the phase transition is induced by fluctuations in the density, amplified by mechanical instabilities in the unstable (spinodal) region of the nuclear matter phase diagram.

In neutron-rich systems, important new features, such as the neutron distillation effect are predicted: the heavy fragments are richer in protons, while the lighter fragments are richer in neutrons. Some experimental evidence for this has already appeared, although a more careful analysis is still needed, to disentangle the various possible contributions to the distillation, such as pre-equilibrium effects, and to prove the mechanism driving the fragmentation process. A reconstruction of properties of primary fragments at freeze out (kinetic energy distributions, isospin content) is also important to allow us to assess the degree of equilibration of the source. A new, unambiguous determination of the masses and charges of the fragments is crucial if we are to reach conclusions on this type of research.

## 4. THE ELEMENTS AND THEIR ORIGIN

### 4.1 INTRODUCTION

Nuclear physics and the visible Universe are intimately related as most of the astrophysical processes are driven and governed by nuclear physics. This spans from Big Bang nucleosynthesis, a cornerstone of modern cosmology, via the life and death of stars to the observed abundances of the elements in the Universe. A reliable description of these astrophysical scenarios depends crucially on measurements of nuclear structure and reaction dynamics involving short-lived nuclei located very far away from the valley of  $\beta$ -stability.

The present and future generations of Earth- and space-bound observatories promise a wealth of high-quality data on elemental abundances and explosive stellar events. In particular, observations of freshly synthesised radioisotopes produced during explosive events provide a direct measure of the physical conditions prevailing during the explosion (such as the temperature, the density, the entropy or the neutron excess), allowing the identification of the explosion mechanisms. High-resolution  $\gamma$ -spectroscopy allows one to determine the velocity of the nuclei, providing important information on the explosion dynamics and element mixing. In addition the use of  $\gamma$ -ray observations enables us to trace the ongoing nucleosynthesis throughout the Universe.

Pre-solar grains are literally stardust that condensed from the gas phase in the cooling outflows of stars, before the formation of our solar system. These grains became swept up in the interstellar medium from which the Sun, Earth and planets formed some  $4.6 \times 10^9$  years ago. Most of the pre-existing dust was vaporised as the nascent solar system heated up. However, a small fraction, the pre-solar grains, survived the solar system formation, protected inside asteroids. Occasionally, pieces of these asteroids fall to the Earth, from which it has been possible to extract the pre-solar stardust. Because the atoms in the grains are the original atoms from the parent stars, by studying this dust we can probe processes that occur inside stars and in the interstellar medium and their composition reveals what was directly ejected from a given stellar environment. The recent discovery of highly anomalous compositions with respect to solar abundances in these pre-solar grains constitutes a major breakthrough in the understanding of nucleosynthesis in the Universe. Some of these grains originate from slow neutron capture processes and have probably been synthesised in Asymptotic Giant Branch (AGB) stars. Some others are of novae or supernovae origin.

This progress in astronomical and meteoritic observations has to be supplemented by advances in nuclear physics. SPIRAL2 will allow the measurement of data and reaction rates for key nuclei that cannot be produced in existing facilities. The future facility will contribute prominently to several areas of active research in nuclear astrophysics, such as explosive hydrogen burning, s- and r-process nucleosynthesis. These processes are believed to be linked to astrophysical observations such as novae, X-ray bursts, burning in AGB stars and type II supernovae explosions or neutron star collisions.

Novae or X-ray bursts are triggered by the mass flow from a companion star onto a compact object like a white dwarf or neutron star, respectively. Once the accreted surface layer reaches a critical temperature and density, nuclear reactions ignite a thermonuclear runaway that could eventually end up with the disruption of the entire white dwarf in the case of type Ia supernovae. In novae and X-ray bursts the explosive burning of hydrogen and the

decay of freshly synthesized matter provide the energy for the dramatic brightening of the stars. In this case the reaction flow occurs through proton-rich nuclei.

The elements heavier than iron are produced by nuclear reaction networks involving neutron-captures and  $\beta$ -decays. The slow neutron capture process (s-process) occurs in AGB stars and operates close to the valley of stability. Its contribution to the solar elemental abundances is relatively well understood. For certain unstable s-process nuclei neutron-capture and  $\beta$ -decay rates can compete. Hence the s-process path branches at these nuclei and the relative mass flow at such branching points allows us to determine the stellar conditions (temperature, neutron density) at which the s-process operates. SPIRAL2 will allow the measurement of neutron-capture cross-sections of such branching-point nuclei.

While it is well established that the rapid neutron-capture process (r-process) runs through extremely neutron-rich nuclei the astrophysical site at which the r-process occurs is still not identified. To solve this mystery it is crucial to determine the properties (masses, half-lives, neutron capture rates etc.) of the nuclei along the r-process. SPIRAL2 will offer the possibility to study nuclei on (or close to) the r-process path, significantly reducing the nuclear uncertainties in r-process models.

## 4.2 CLASSICAL NOVAE AND X-RAY BURSTS

Classical novae and X-ray bursts are cataclysmic events, which occur in binary systems. They are triggered by a thermonuclear runaway that takes place on the surface of compact stars onto which matter is accreted from a close companion. In the case of novae, the compact star is a white dwarf whereas in X-ray bursts it is a neutron star. Nova outbursts are characterised by an energy release that is only exceeded by supernovae and  $\gamma$ -ray bursts phenomena. Novae have been known for more than twenty centuries since they emit intense radiation in the optical wavelengths. Typically, about thirty novae of this type are expected to explode in the Milky Way per year, becoming the second, most frequent type of thermonuclear explosion in the Galaxy after X-ray bursts. However, it is difficult to detect novae from space- or ground-based observatories because of interstellar dust absorption. In contrast, X-ray bursts have been discovered more recently by space observations since the major fraction of their energy output is emitted in the form of X-rays, which are absorbed by the Earth's atmosphere. From the recent use of space observatories about 65 Galactic low-mass X-ray binaries that exhibit such bursting behaviour have been found since their first discovery in 1976.

Contrary to type Ia supernovae, for which the white dwarf is fully disrupted by the violence of the explosion, classical novae are expected to recur with periodicities of the order of  $10^4 - 10^5$  y. X-ray bursts recur on timescales of hours to days. Another difference between classical nova and type Ia supernova explosions is the amount of mass ejected (the whole star in a thermonuclear supernova;  $10^{-4} - 10^{-5} M_{\odot}$  in a nova) as well as the mean ejection velocity ( $>10^4$  km s $^{-1}$  in a supernova,  $10^2 - 10^3$  km s $^{-1}$  in a classical nova). It is unlikely that matter is ejected in X-ray bursters owing to the strong gravitational field of the neutron star

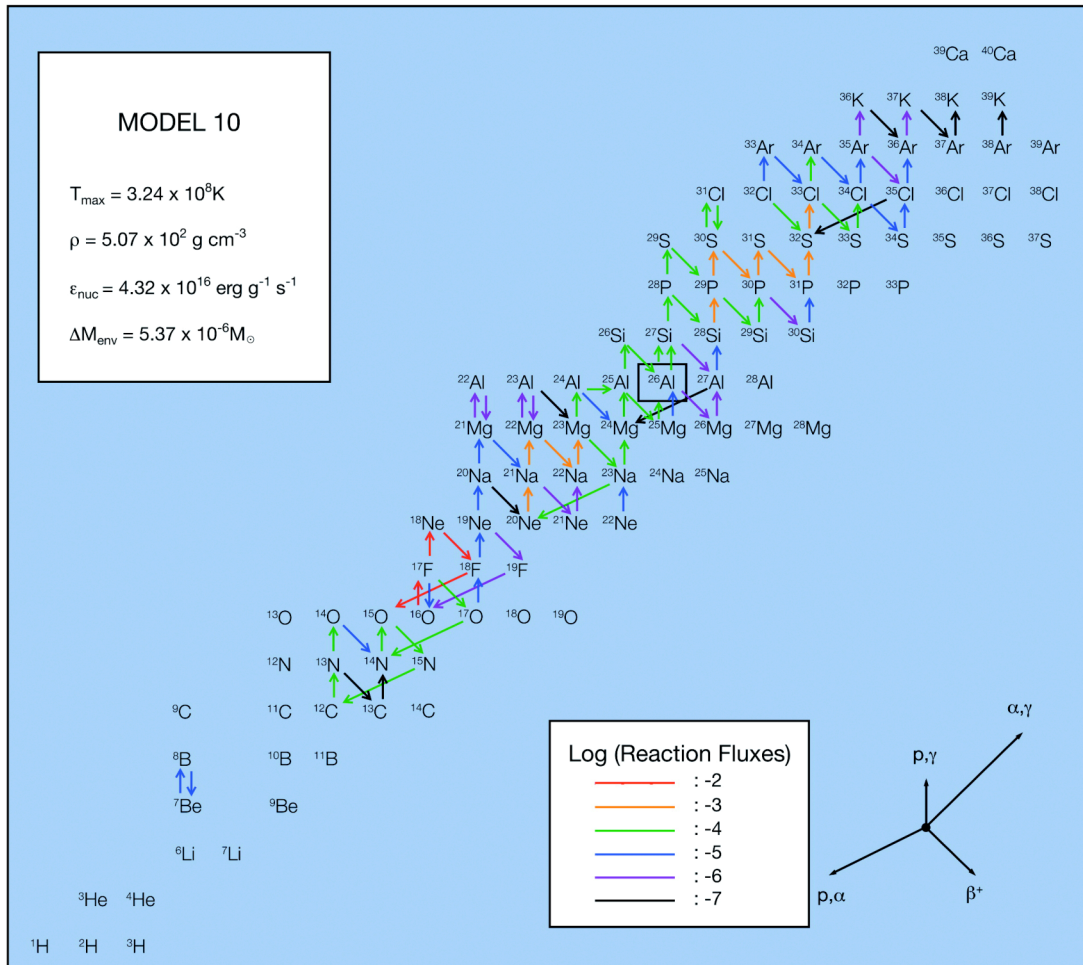


**Figure 4.1:** Main reaction rates occurring at the peak temperature during a nova explosion from a 1.35 solar mass ONe white dwarf.

#### 4.2.1 Classical nova explosions

The prevailing temperatures during nova outbursts,  $T_{\text{peak}} \sim 2$  to  $3 \times 10^8$  K, are high enough to induce extensive nuclear reactions in the envelope, suggesting significant deviations of the intermediate-mass elemental abundances from those obtained in hydrostatic hydrogen burning. Although novae scarcely contribute to the Galaxy's overall enrichment in heavy elements they may inject into the interstellar medium significant amounts of some of their most abundantly produced species, i.e.  $^{13}\text{C}$ ,  $^{15}\text{N}$ ,  $^{17}\text{O}$  and to a minor extent other species such as  $^7\text{Li}$ ,  $^{19}\text{F}$ , or  $^{26}\text{Al}$ . Classical nova outbursts on low-mass CO white dwarfs are characterised by a moderate nuclear reaction flow, which does not extend much beyond oxygen. In contrast, novae exploding on white dwarfs composed of oxygen and neon seed nuclei (ONe) involve a larger nuclear reaction network, spanning up to the silicon (1.15 solar mass ONe) or argon (1.35 solar mass ONe) isotopes (see figure 4.1). This suggests that the observation of large amounts of intermediate-mass nuclei (such as phosphorus, sulphur, chlorine or argon) in a nova explosion reveals the presence of an underlying massive (ONe) white dwarf.

In agreement with the elemental observations of the nova ejecta, the theoretical endpoint in novae nucleosynthesis is limited to  $A < 40$ . The nuclear reactions in the silicon-calcium region are powered by the leakage from the NeNa-MgAl region, where the reaction network is

confined during the early stages of the thermonuclear runaway. The main reaction that drives the nucleosynthesis towards heavier species is  $^{30}\text{P}(p,\gamma)^{31}\text{S}$ . Its rate is currently based on Hauser-Feshbach estimates only and suffers from a large uncertainty in the domain of nova temperatures.

Among the species synthesised during classical nova outbursts, several radioactive nuclei have deserved particular attention as being  $\gamma$ -ray emitters. The production of  $^{13}\text{N}$  and  $^{18}\text{F}$  isotopes may lead to prompt  $\gamma$ -ray emission at and below 511 keV through electron-positron annihilation. The long-lived  $^7\text{Be}$  and  $^{22}\text{Na}$  would be observed later on in the explosion, when the envelope gets optically thinner, through discrete lines at 478 and 1275 keV, respectively.  $^{26}\text{Al}$  is another important radioactive isotope that can be synthesised during nova outbursts, although only its cumulative emission can be observed because of its slow decay. The detection of any of these  $\gamma$ -ray signatures in a classical nova event is a challenge. Recent observations of the  $\gamma$ -radiations in novae with the  $\gamma$ -ray observatories in space gave no indication for  $^{22}\text{Na}$  and  $^{26}\text{Al}$  activity, which makes an order-of-magnitude discrepancy between the predicted and observed intensities of the  $^{22}\text{Na}$   $\gamma$ -rays. Unfortunately, theoretical predictions are currently limited by some nuclear uncertainties associated with key reactions, such as the  $^{18}\text{F}(p,\alpha)$ ,  $^{18}\text{F}(p,\gamma)$ ,  $^{22}\text{Na}(p,\gamma)$ ,  $^{23}\text{Mg}(p,\gamma)$  and  $^{25,26}\text{Al}(p,\gamma)$  reactions that deserve particular attention from the nuclear physics community.

#### 4.2.2 X-ray bursts

In X-ray bursts, the explosion takes place on the surface of a neutron star in a binary system after it has accreted mass from the envelope of its companion. During the burst, temperatures and densities can reach values (few  $10^9$  K,  $\rho \sim 10^6$  g/cm<sup>3</sup>) that are significantly larger than for novae. As a result, detailed nucleosynthesis studies involve hundreds of isotopes (up to the so-called SnSbTe cycle) and thousands of nuclear reactions. Indeed, the main reaction flow moves far away from the valley of stability, and even merges with the proton drip-line beyond  $A=38$ . Very detailed nucleosynthesis calculations, with a complete reaction network up to the SnSbTe mass region, have been carried out using detailed hydrodynamic stellar models in one-dimension. However they suffer from the uncertainties in the rates of the nuclear reactions involved.

In contrast to classical novae, where the main nuclear activity is driven by proton-capture reactions in competition with  $\beta^+$ -decays, X-ray bursts are triggered by a combination of nuclear reactions. They include H-burning through rapid proton captures (rp-process) and He-burning. The latter starts with the triple  $\alpha$ -reaction and is followed both by the breakout of the CNO cycle via  $^{14,15}\text{O}+\alpha$ , plus a competition between proton captures and  $(\alpha,p)$  reactions (the so-called  $\alpha$ p-process). It is of special interest that H-burning continues after the main peak of the explosion through the rp-process. This extends the main path much beyond  $^{56}\text{Ni}$ , up to the SnSbTe region and leads to a time-dependent luminosity profile which depends on a set of nuclei with rather long half-lives (waiting points) present in the reaction flow. When the process reaches nuclei close to the dripline, proton capture (for example on  $^{64}\text{Ge}$  or  $^{68}\text{Se}$ ) proceeds to unbound nuclei, which quickly decay by re-emitting the unbound proton. Therefore the rp-process is blocked until  $\beta$ -decay occurs. This holds true unless two-proton captures via an intermediate resonant state are fast enough to bridge the unbound nucleus. This process strongly depends on the properties of the intermediate unbound nucleus on which the first proton-capture is made (proton separation energy, spin of the resonance, width). Other important points to consider in the reaction rates are the role of proton captures

from thermally excited states and the occurrence of isomeric states. They could significantly enhance the reaction rates, depending on their quantum numbers.

A major drawback in the modelling of X-ray bursts comes from the lack of observational constraints on nucleosynthesis. This arises because it is difficult for the freshly synthesised matter at the surface of the neutron star to be ejected into the interstellar medium. A recent attempt to overcome this limitation has been provided by high-resolution spectra obtained with XMM-Newton. This provides some insight into the chemical species (carbon, nitrogen, oxygen, neon and iron) that are present in the envelope at different epochs.

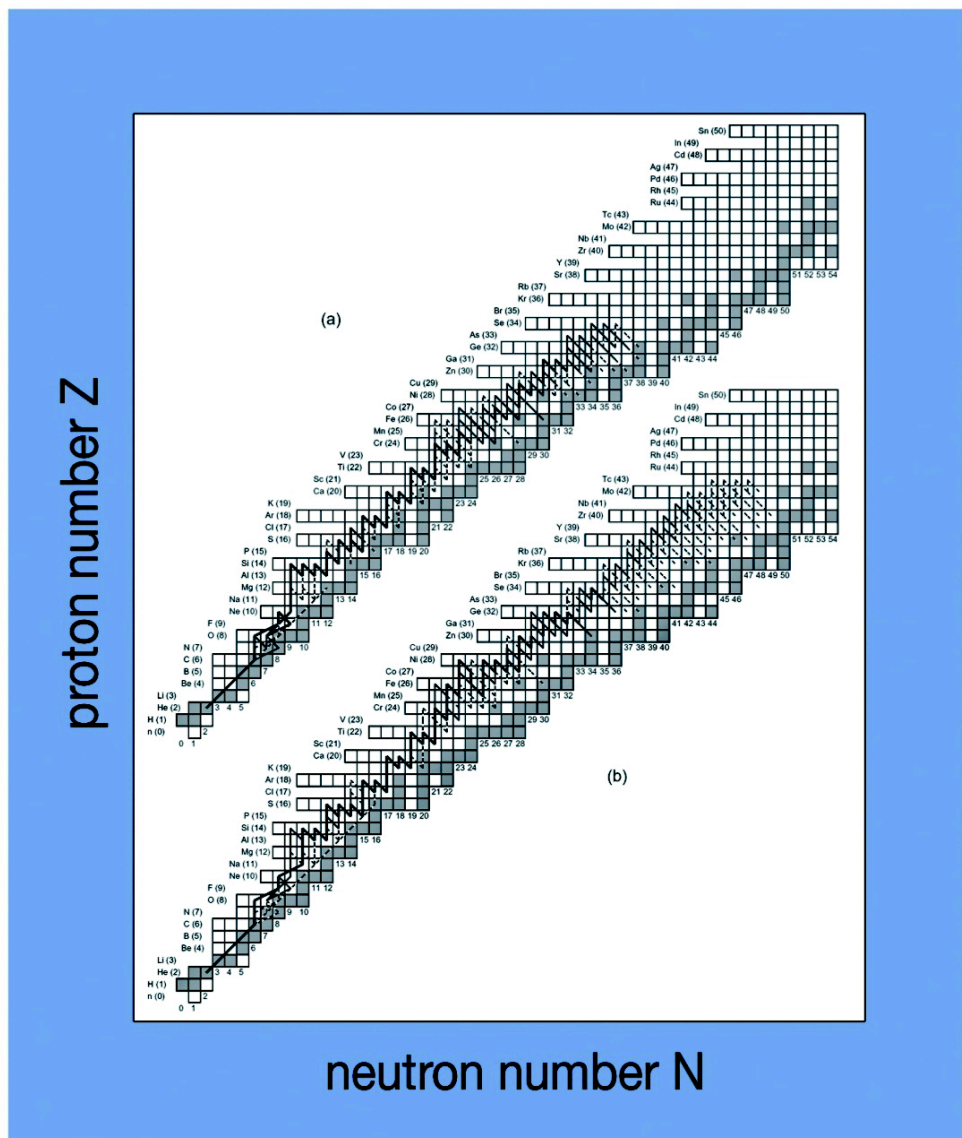


**Figure 4.2:** Time-integrated reaction flow over a complete X-ray burst from a one-zone model simulation. The strength of the reaction flow is indicated by the thickness of the lines: more than 50% flow (thick solid line), 10%-50% flow (thin solid line), and 1%-10% flow (dashed line).

### 4.2.3 Nuclear physics requirements for novae and X-ray bursts

A significant amount of experimental information relevant to the study of nova outbursts is already available. One may be confident that, in the near future, novae will become the first explosive stellar site for which all relevant nuclear physics input will be primarily based on

experimental information. The remaining uncertainties are focused on only a handful of nuclear reaction rates, ( $^{18}\text{F}(p,\alpha)$ ,  $^{25}\text{Al}(p,\gamma)$  and  $^{30}\text{P}(p,\gamma)$ ), which still have to be measured.

In contrast, the situation is much more complex in X-ray bursts: requirements include mass measurements along the rp-process path and a much better knowledge of key reactions at the *waiting points* (for example the  $^{30}\text{S}(\alpha,p)$  and  $^{34}\text{Ar}(\alpha,p)$  reaction rates). Recent hydrodynamic calculations suggested that, apart from the waiting point nuclei which should be studied, individual nuclear reaction rates on other nuclei are not as crucial as they are in novae outburst models. The reason is that during high temperature X-ray bursts many nuclear reaction flows take place and individual nuclei can be by-passed by alternative flows.

### **Direct measurements**

*High intensity radioactive ion beams will permit the direct measurement of some key reaction rates, in particular for charged particle reactions occurring in explosive stellar burning like classical novae and X-ray bursts. The direct method allows us to overcome the insoluble problems related to indirect measurements, like the determination of interference effects between several resonances.*

*The direct measurements will be performed at SPIRAL2 using the maximum yield method. This requires dedicated spectrometers, like DRAGON at TRIUMF or ARES at Louvain-la-Neuve, a high efficiency  $\gamma$ -ray spectrometer like EXOGAM and/or a charged particle telescope like MUST2. Some of the important reactions in classical novae are:  $^{18}\text{F}(p,\alpha)$ ,  $^{18}\text{F}(p,\gamma)$ ,  $^{25,26}\text{Al}(p,\gamma)$  and  $^{22}\text{Na}(p,\gamma)$ . They will be measured at about 0.2 MeV/nucleon. These radioactive ion beams will be produced through (d,n) and (d,t) reactions on stable targets at a few MeV/nucleon.*

*The break-out reaction from the hot CNO cycle,  $^{15}\text{O}(\alpha,\gamma)^{19}\text{Ne}$ , is very important since it could trigger the onset of the rp-process. So far, only an upper limit for this reaction rate is known, which is not sufficient. The direct measurement of this reaction rate for explosive scenarios is a key experiment for SPIRAL2 thanks to the high intensity of the  $^{15}\text{O}$  that is foreseen at SPIRAL2 ( $10^{11}$  atoms/s). The  $^{15}\text{O}(\alpha,\gamma)^{19}\text{Ne}$  reaction should be studied at about 0.7 MeV/nucleon.*

*Proton and  $\alpha$ -capture rates for nuclei close to the proton drip line are needed if we are to understand better how nucleosynthesis proceeds in X-ray bursts. The 2p capture process is expected to compete with the long-lived  $\beta$ -decay for nuclei close to the drip line (e.g.  $^{64}\text{Ge}$ ,  $^{68}\text{Se}$ ...). In such cases, the determination of hitherto unknown resonances (energies and widths) in the unbound systems would place better constraints on the existence of these 2p captures.*

*The study of low energy excited states is important to estimate the number of proton captures which occur from thermally excited states. It is therefore important to know the spectroscopy of the low-lying states in the nuclei involved, particularly in the case of odd nuclei.*

### **Indirect measurements**

*The resonant elastic scattering technique has been shown to be an efficient means of studying bound or unbound excited states using relatively low-intensity radioactive ion beams on a gas filled or solid target. This method allows one to determine the energies of states, their spins and particle decay-widths for proton and/or  $\alpha$  captures depending on the choice of the gas target. Elastic scattering cross-sections are relatively large. However, resonance widths of astrophysical interest may be too narrow for the resonance to be seen in experiments involving low beam intensities. In such cases, the high intensity of several radioactive ion beams from SPIRAL2, the fact that their energies are well suited and the availability of a high resolution spectrometer like VAMOS will ensure access to most of the resonances of astrophysical interest.*

*Inelastic scattering is an interesting way to study resonances above the particle emission threshold for astrophysical purposes. In this case, a RIB impinges on a light target and is excited via the inelastic scattering process. If the excited state is particle unbound it decays via several channels that may be studied. Excited states, spin values, decay-widths and branching ratios that are necessary to determine the capture cross-section in the stellar energy range, will be determined using a combination of highly segmented silicon detectors, an efficient  $\gamma$ -ray array and a recoil spectrometer.*

*Transfer reactions ( ${}^3\text{He},d$ ) will give access to spectroscopic factors, which are important parameters to calculate  $(p,\gamma)$  cross-sections which can not be measured directly. Other transfer reactions will feed levels of astrophysical interest, which decay by particle emission.*

#### ***Summary of the requirements for novae and X-ray bursts studies***

*The energy range for studies related to novae and X-ray bursts such as the above-mentioned reaction rates will be explored. Typical energies for direct reactions are below 2 MeV/nucleon, whereas energies up to 10 MeV/nucleon are needed for the inelastic scattering method. Therefore, the use of a small linear accelerator is of paramount importance to set the energy range from 0.1 MeV/nucleon to about 2 MeV/nucleon. The higher energy part will be covered by the CIME cyclotron. Ancillary detectors such as highly segmented charged particle detectors and high efficiency  $\gamma$ -arrays will be used in combination with a magnetic spectrometer. In the case of direct reaction experiments, this spectrometer must have an excellent beam-rejection factor.*

### **4.3 THE S-PROCESS NUCLEOSYNTHESIS**

The solar abundance distribution represents the average enrichment of the Galaxy  $4.6 \times 10^9$  years ago when the solar system was formed. Chemical evolution prior to this point has become an intense field of investigation. With modern ground and satellite based telescopes spectral analyses from the ultra-violet to the far infrared provide almost complete element patterns even for extremely faint and/or metal poor stars. Likewise, chemically peculiar stars, which witness ongoing s-process nucleosynthesis in their deep interiors, or the expanding supernova ejecta can be accessed in great detail as well. Spectroscopic studies of stellar atmospheres have been complemented by analyses of circumstellar dust grains from AGB stars or supernovae, which survived the homogenisation in the proto-solar cloud and are preserved as minute inclusions in meteorites. The isotopic composition of these pre-solar grains clearly exhibits enrichments, which can be attributed to particular nucleosynthesis scenarios.

The abundances of the elements beyond iron are essentially shaped by neutron capture nucleosynthesis, either by the slow (s) or rapid (r) processes associated with stellar He burning and explosive scenarios, respectively. The s- and r-processes each account for approximately 50% of the abundances in the mass region  $A > 60$ . The rare proton-rich nuclei cannot be produced by neutron capture reactions. This minor part of the abundance distribution is ascribed to the p-process that is assumed to occur in explosive Ne/O burning in supernovae. Among these processes, the s-process is most accessible to laboratory experiments and stellar models and also the one on which we can most readily make astronomical observations.

The s-process is characterised by relatively low neutron densities, resulting in neutron capture times much longer than typical  $\beta$ -decay half-lives. Accordingly, the s-process reaction path follows the stability valley, and the s-process abundances are determined by the respective  $(n, \gamma)$  cross-sections averaged over the stellar neutron spectrum. While isotopes with small cross-sections are built up to large abundances, the yields of isotopes with large cross-sections are limited because they are more easily consumed. This behaviour is most evident for nuclei with closed neutron shells. Their small cross-sections give rise to sharp s-process maxima in the abundance distribution at  $A = 88, 140, \text{ and } 208$ , an elegant illustration of the intimate correlation between the relevant nuclear properties and the resulting abundances. On the other hand, the cross-sections of isotopes between closed shells are large enough that flow equilibrium is reached, leading to an almost constant value of the product cross-section times abundance,  $\sigma N_s$ , as a function of mass number. A third important phenomenon is displayed by the s-process branching points, which occur whenever the reaction path encounters an unstable isotope with a sufficiently long half life that neutron capture can compete with  $\beta$ -decay. Such branching points give rise to local abundance patterns that can be used for probing the physical conditions at the stellar s-process site, e.g. the neutron density, temperature, pressure, or even the convective mixing that transports freshly produced s-process material to the stellar atmosphere. So far most branching analyses are based on solar isotope patterns, but important information on the s-process neutron density in particular stars can be derived directly from spectroscopic data.

The status of  $(n, \gamma)$  data for the s-process indicates that experimental techniques have reached a stage, where the 1% accuracy level required for meaningful analyses of particular abundance patterns can be met. However, this has been achieved so far only for a minority of the relevant isotopes. Apart from the remaining key nuclei, a large number of cross-sections with uncertainties in excess of 10% await improvement, in particular in the mass region below  $A = 120$ . In contrast to the stable isotopes, for which the existing techniques and facilities allow reliable measurements, the situation for the unstable isotopes, which act as branching points in the s-process, is far from being adequate. Apart from a few activation measurements, the only case, which has been studied in full detail, is  $^{151}\text{Sm}$ . More experiments on unstable targets are clearly needed for quantitative branching analyses.

### ***S-process studies at SPIRAL2***

*SPIRAL2 will be very well suited to produce the samples of unstable isotopes required for studying s-process branching points. These samples could be subsequently irradiated by intense neutron fluxes in order to determine their  $(n,\gamma)$  cross-sections. A dedicated neutron time-of-flight beam-line can be envisaged at the SPIRAL2 facility.*

*For some selected cases when the final reaction product is radioactive  $(2n,\gamma)$  cross-section studies are feasible via the neutron activation technique. Nevertheless, the neutron-energy spectrum has to be scaled from 14MeV down to about 100keV to mimic the neutron energy in stellar conditions. The determination of neutron-capture cross-sections on the radioactive nuclei  $^{85}\text{Kr}$  and  $^{60}\text{Fe}$  could be considered as the first key experiments for the SPIRAL2 facility. An alternative means of studying  $(n,\gamma)$  cross-sections would be to use indirect methods such as the  $(d,p)$  reaction. This technique is described in detail in the next chapter.*

## **4.4 THE R-PROCESS NUCLEOSYNTHESIS**

Approximately half of the elements beyond iron are produced via neutron-captures on very short time scales in neutron-rich environments, i.e. the so-called r-process. Several observables account for the existence of such a process. Despite its importance, the exact site(s) where the r-process(es) occur(s) still remain(s) a great mystery. The most frequently suggested astrophysical environments are high-entropy ejecta from type II supernovae (SN) and neutron-star mergers. The shock-heated helium or carbon outer layer of type II SN could provide a moderate neutron flux (a weak r-process) through  $^{13}\text{C}(\alpha,n)$  reactions which could account for several isotopic anomalies found in pre-solar grains. The key for understanding the r-process(es) resides in a close interaction between astronomy, cosmochemistry, the astrophysical modelling of explosive scenarios and nuclear physics.

The credibility of any nucleosynthesis model must be checked against observations. The Sun was long considered a suitable choice for this purpose, being the only sample for which one can determine a well defined isotopic composition throughout the periodic table of the elements. However, several stellar-processes mixed up during the formation of the proto-solar nebula and built up the solar elemental abundance. There is therefore an active search for weakly mixed abundances among which two are depicted below.

With the combined use of the Hubble space telescope, of ground-based high resolution spectrographs and the increasing quality of the modelling of stellar opacities, detailed elemental abundances in very old, ultra-metal-poor giant halo stars have been obtained for elements ranging from  $Z \sim 32$  to the heaviest thorium, uranium and plutonium. In some cases like europium and barium, even the isotopic abundances have been obtained in these objects. In these stars, one avoids unravelling the complicated chemical evolution problem since the observed abundances result from the ashes of one or a few stellar events. A certain class of ultra-metal-poor stars exhibits a very similar solar-like abundance pattern for heavy-mass nuclei beyond  $A=130$ , even if stemming from very different regions of the galactic halo. Therefore, a robust r-abundance pattern above  $A=130$  may be a signature of a unique early “main” r-process of primary nature that could be governed by the nuclear physics properties of very unstable nuclei. Below  $A=130$ , one observes “under-abundances” as compared to solar, with a strong odd-even- $Z$  staggering, also not observed in solar r-material. The missing part to the solar pattern reflects the need for another “weak” r-process of secondary nature.

The abundance patterns of certain refractory inclusions in meteorites reflect the stellar events in which they were formed. The use of new ionic nano-probes, which reveal the composition of sub-micrometer size pre-solar grains, is also modifying our view of the r-process. Large isotopic anomalies, with respect to solar, are found in some silicon carbide (SiC) pre-solar grains. There is compelling evidence that some of these grains (type X) have a supernova origin since they contain traces of extinct  $^{44}\text{Ti}$  and  $^{26}\text{Al}$  radioactivity. These grains also exhibit molybdenum and zirconium isotopic abundances that are intermediate between the s- and r-process nucleosynthesis, with an enriched composition in  $^{96}\text{Zr}$  and the odd-mass isotopes  $^{95,97}\text{Mo}$ .

These pieces of information point to the existence of various r-processes which could be understood and correlated with a plausible explosive site only with a better knowledge of the neutron-rich progenitors of the observed r-elements.

In very hot and neutron-dense environments, the r-process develops through neutron-captures on very short timescales until reaching nuclei with sufficiently small binding energy ( $S_{1n} \sim 2-3$  MeV). There, the rate of captures is balanced by that of photo-disintegration induced by the ambient photon bath. The process is stalled at these waiting point nuclei (with charge  $Z$ ) until  $\beta$ -decays occur, depleting the mass flow to the  $Z+1$  isotopic chain where subsequently neutron capture could occur. These waiting point nuclei are likely to be found at closed-shells. After successive  $\beta$ -decays and neutron captures at a closed shell, the process is progressively driven closer to stability where  $\beta$ -decay lifetimes become longer. Consequently, a leakage from the closed shell can occur through neutron-captures, which can proceed further to the next upper shell. At the end of the r-process, radioactive progenitors decay back to stability via  $\beta$ - or  $\beta$ -delayed neutron-decay towards the valley of stability. The accumulation of r-elements which form the so-called r-peaks at masses  $A \sim 80, 130$  and  $195$  on the abundance curve of the elements is a direct imprint of the existence of waiting point progenitors far from stability.

The location, height and shape of these peaks could be traced back from the neutron separation energies, the half-lives, the neutron delayed emission probability ( $P_n$ ) and the neutron-capture cross-section around the nuclei where the leakage occurs.

In a weak r-process scenario, neutron densities and temperature are lower. Consequently,  $\beta$ -decay can dominate over the longer neutron-capture rates before reaching an equilibrium between photo-disintegration and neutron capture as mentioned above. The location of the branching points in each isotopic chain is found where the  $\beta$ -decay time is shorter than neutron-capture time. Therefore both the neutron-capture cross-sections and the  $\beta$ -decay lifetimes should be determined. They could in turn place important constraints on the astrophysical environment in which a weak r-process can occur.

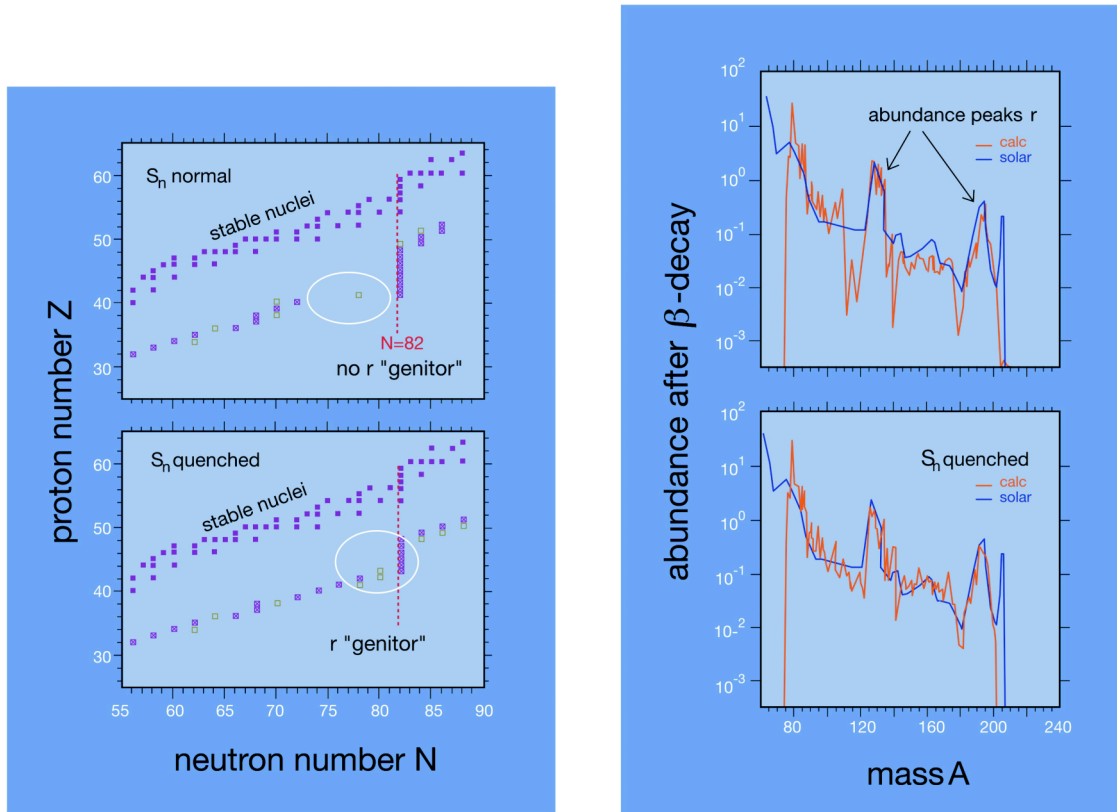


**Figure 4.3:** The r-process waiting points (w.p.) for the FRDM mass models are shown in the vicinity of the neutron shell closure  $N=70, 82$  for a neutron density  $d_n=9.5 \times 10^{20} \text{ cm}^{-3}$  and a temperature of  $1.2 \times 10^9 \text{ K}$ . Nuclei with more than 10% of the population of an isotopic chain are represented by an open square. Open squares with a cross indicate w.p. nuclei with the maximum abundance in an isotopic chain. The nuclei in the valley of stability are displayed as full squares. The bottom part shows the expected w.p. using the masses close to  $N=70, 82$  from HFB calculations with the SkP force. It is shown that the region within the circle at  $Z \sim 40, A \sim 78$  contains more progenitors. The right part shows a comparison between calculated (calc) and solar r-abundances using the two different mass models.

Nuclear binding energies (obtained from mass differences between adjacent nuclei) reflect the extent to which a nuclear edifice could “survive” under extreme temperature and density conditions. It is expected that nuclei with high  $S_n$  values, located at the major shell or sub-shell closures, would be the main waiting-point nuclei. Beyond closed shells, nuclei quickly photo-disintegrate. Mass values far from stability are poorly known and the r-process progenitors are in most cases far from being attainable experimentally. Therefore, the modeling of this process is based on a combination of measured mass values near stability and theoretical extrapolations far off stability. Nevertheless, many uncertainties have to be solved to reach a precision of about 50 keV in the binding energy, which is required to model the r-process. The behaviour of the binding energy surface around the shell closures is essential. Using masses from an “unquenched” model (FRDM or ETFSI-1), one obtains a local increase in the  $S_n$  values around neutron number  $N=70$  and a very abrupt drop at  $N=82$ . They originate from a predicted strong quadrupole deformation around  $^{110}\text{Zr}$  and a strong shell closure at  $N=82$ , respectively. As a result neutron-captures are stalled for a while around  $A \sim 110, N \sim 70$  and subsequently directly reach the closed shell  $N=82$ . This leaves few waiting point progenitors in between these two regions, leading to a significant trough in the fit of the abundance curve of the elements at  $A \sim 120$  as shown in figure 4.3. The “quenched” mass

models (such as ETFSI-Q or HFB/SkP) bring back r-progenitors before reaching the N=82 shell closure, filling the trough at A~120 in closer agreement with the solar r-abundance curve. This closer agreement does not imply a shell weakening at N=82. In particular, some recent models rather predict a doubly magic character for  $^{110}\text{Zr}$ , which would also have important consequences for the abundances of the A~120 nuclei. This emphasises that a better knowledge of the behaviour of the major shell closures far from stability is of the utmost importance to help determine which explosive process(es) account(s) for the observations. The study of shell-closure evolution is a common quest between nuclear structure and astrophysics. Very fundamental and competing aspects of nuclear forces come into play to modify the strength of a shell closure, among them the neutron-proton interactions and the diffuseness of the surfaces of neutron-rich nuclei.

***Mass measurements of astrophysical interest at SPIRAL2***

*The masses of key nuclei that are corner stones in modeling the r-process path will be measured at SPIRAL2. In fact, a detailed knowledge of the structure as well as the binding energy for key nuclei located around shell closures is necessary to establish the waiting-point progenitors far from stability, that are responsible for the three r-peaks located at masses A~80, 130 and 195 on the abundance curve of the elements. These selected key nuclei for the r-process, and for which mass measurements should be performed with a precision better than ~50keV are:  $^{76-80}\text{Ni}$ ,  $^{80-84}\text{Zn}$ ,  $^{78-82}\text{Cu}$ ,  $^{85}\text{Ga}$ ,  $^{96-100}\text{Kr}$ ,  $^{108-112}\text{Zr}$ ,  $^{122-130}\text{Pd}$ ,  $^{128-131}\text{Ag}$ ,  $^{131-134}\text{Cd}$  and  $^{146-150}\text{Xe}$ .*

The  $\beta$ -decay studies far off stability are important for at least two reasons: first to infer the abundance of the stable nuclei from the time elapsed at the neutron-rich waiting point nuclei, secondly to constrain the global duration of the r-process by summing the lifetimes of all isotopic chains to build the heaviest elements in Nature like thorium, uranium and plutonium. Determinations of half-lives and  $P_n$  values are especially important at closed shells. The neutron delayed emission probability smooths the r-abundance curve, as compared to the even-odd staggering observed in the s-abundance curve. One can intuitively infer that short lifetimes would make the building of r-process peaks difficult, but the synthesis of heavier masses easier. At the opposite extreme, long lifetimes would block the process at a given shell closure as the neutron fuel would be exhausted and it could not proceed further. Again, these nuclear structure parameters need to be measured in order to determine whether one r-process could produce the overall mass range of elements or if the abundance curve results from a superposition of several processes. If occurring in the high entropy bubble of a supernova explosion, the r-process should develop with a short dynamical timescale in order to avoid its suppression by the high neutrino flux of the neutrino-driven wind. Hence, a better knowledge of the  $\beta$ -decay rates at the closed-shells (and especially the importance of first forbidden transitions) and extent to which shells are quenched, will allow one to deduce if the r-process could occur in such environments. In the case of odd nuclei, low-lying excited states could be thermally excited. This could drastically change the lifetime and/or neutron-capture rates of the nuclei involved in the r-process. Therefore energy and spin assignments of low-lying states should also be determined. So far detailed spectroscopic studies of only two neutron-magic r-progenitors have been performed, i.e.  $^{80}\text{Zn}$  and  $^{130}\text{Cd}$ .

The present experimental limits for studying masses and  $\beta$ -decays around the N=82 shell closure is shown in figure 4.4. It is clear that the main hindrance to studying the r-process

resides in the extraction of the refractory fission fragments (below  $Z=47$ ) from the conventional target ion source systems.

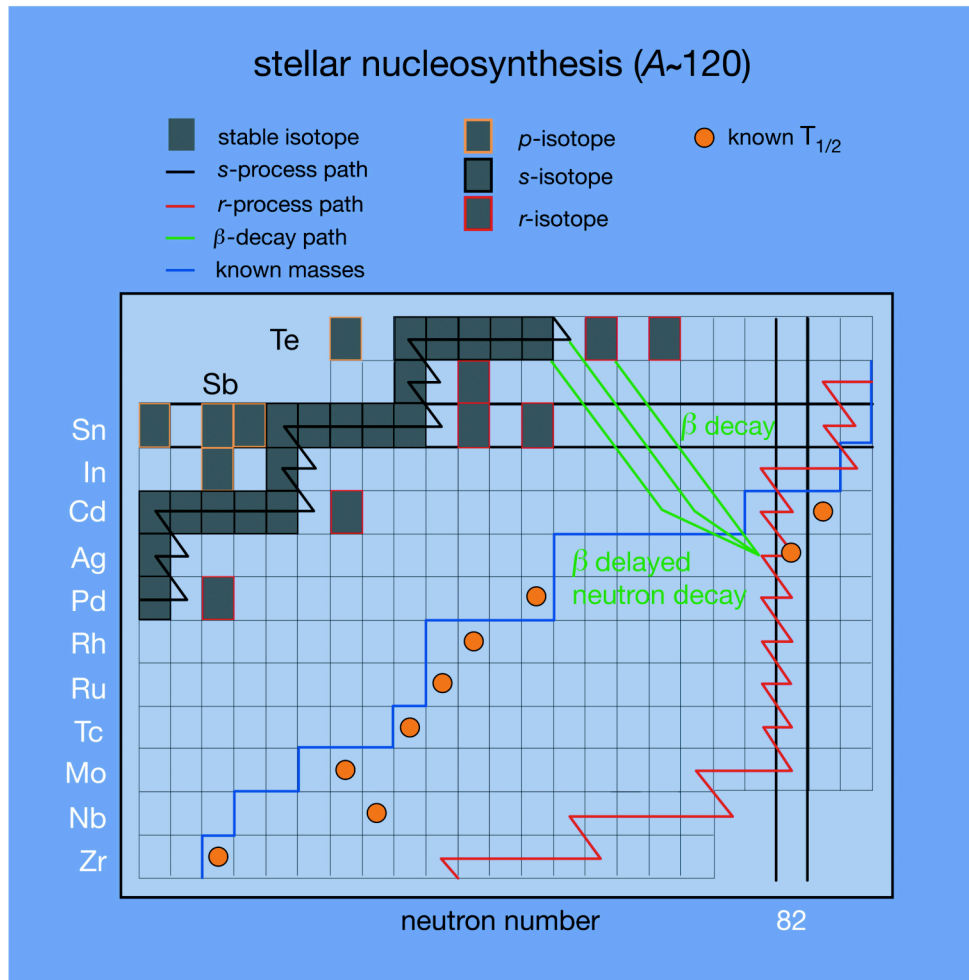


**Figure 4.4:** Limits of the present  $\beta$ -decay and mass studies of the  $r$ -process at the  $N=82$  shell-closure.

### ***$\beta$ -decay studies and the $r$ -process at SPIRAL2***

*$\beta$ -decay studies are requested to infer the abundance of the stable nuclei and to constrain the  $r$ -process duration. Both half-lives and  $P_n$  values will be measured at SPIRAL2 for several selected nuclei located around the closed shells that are important in this context. The nuclear structure of the waiting-point nuclei needs to be studied in order to constrain better the stellar  $r$ -process conditions, which is an important ingredient for determining in which astrophysical sites  $r$ -process(es) develop in the Universe. These key nuclei are:  $^{76-80}\text{Ni}$ ,  $^{80-84}\text{Zn}$ ,  $^{78-82}\text{Cu}$ ,  $^{85}\text{Ga}$ ,  $^{96-100}\text{Kr}$ ,  $^{108-112}\text{Zr}$ ,  $^{122-130}\text{Pd}$ ,  $^{128-131}\text{Ag}$ ,  $^{131-134}\text{Cd}$  and  $^{146-150}\text{Xe}$ .*

When the  $r$ -process path comes closer to stability, after successive neutron-captures and  $\beta$ -decays at major shell closures, the half-lives of the nuclei involved become longer. If the

neutron flux that prevails in the star is large enough, neutron captures could eventually compete with  $\beta$ -decays. The determination of neutron-capture cross-sections ( $\sigma_n$ ) brings access to the rate of leakage of the r-process towards the next shell closure for a given neutron density value. The  $\sigma_n$  values are also important parameters in the case of weak r-process scenarios, where  $\beta$ -decays could compete with neutron captures. Such a process could account for the observed isotopic anomalies in some pre-solar grains and for the production of masses up to  $A \sim 130$  in the ultra-metal-poor stars. Since the direct measurement of neutron-capture cross-sections on very unstable nuclei is technically not feasible, their determination should be provided by models or by indirect methods. For nuclei far from stability and at closed shells, the use of statistical models is very hazardous, since the neutron-separation energy is small and consequently the level density very low. In such cases, the main contribution is obtained from direct captures on a few bound states, mainly of s- or p-waves, and/or by resonances above the neutron-energy threshold. Neutron-capture through the soft Pygmy Resonance could also play an important role if the energy of the soft Pygmy vibration mode is peaked around the neutron emission threshold.

### ***Neutron-capture reaction studies with beams from SPIRAL2***

*$\beta$ -delayed neutron spectroscopy could be a means of studying resonances above the neutron-emission threshold in order to simulate the  $(n,\gamma)$  reaction. For instance the study of the  $^{132}\text{Cd}(\beta n)$  decay may lead to the feeding of neutron-unbound states that are important for determining the  $^{131}\text{In}(n,\gamma)$  cross-section, i.e. up to 1 MeV above the  $S_{1n}$  value. A dedicated high efficiency neutron detector has to be used to study the low-energy neutrons emitted after  $\beta$ -decay.*

*High resolution  $(d,p)$  reactions are thought to be the best tool to study the neutron capture properties of rare isotopes at all RIB facilities. These transfer reactions will be performed for selected neutron-rich beams from SPIRAL2 like  $^{80,82}\text{Zn}$ ,  $^{82,84}\text{Ge}$ ,  $^{98}\text{Kr}$ ,  $^{95}\text{Y}$ ,  $^{97}\text{Nb}$ ,  $^{130,136}\text{Sn}$ ,  $^{128-130}\text{Cd}$  and  $^{146}\text{Xe}$  with a  $\text{CD}_2$  target. This simulates the neutron-capture and gives access to both the bound and unbound states provided that the energy of the RIB is large enough. This technique will provide the energies, spectroscopic factors and angular momenta of the levels which will be used subsequently to determine the (entrance channel of) neutron-capture cross-section  $(n,\gamma)$  at stellar temperatures better. In the most favourable cases, the full  $(d,p\gamma)$  reaction will be studied using a total-energy  $\gamma$ -ray spectrometer, revealing the  $\gamma$ -widths (exit channel) of the levels of astrophysical interest. This experiment requires a highly segmented array of silicon detectors (such as the MUST2 or TIARA array), beam-tracking detectors, and a large acceptance spectrometer like VAMOS.*

## ***5. FUNDAMENTAL INTERACTIONS: SEARCHING FOR PHYSICS BEYOND THE STANDARD MODEL***

To a large extent, the study of fundamental interactions in nuclei is dedicated to the structure of the charged current weak interaction and tests of the underlying fundamental symmetries. The major motivation for this research direction is the search for possible types of new physics, beyond the Standard Model of the electroweak interactions, using the atomic nucleus as a laboratory.

The Standard Model of particle physics provides the theoretical framework in which electromagnetism, the weak interaction and many aspects of the strong interaction can be described with a remarkably good precision, within a single coherent framework. Gravity has yet to be fitted into this framework. Amongst the major challenges and central goals of current physics research are to find a unified quantum field theory for all four fundamental interactions, to investigate the limits of the Standard Model and to search for physics beyond this model. This is vigorously addressed in several subfields of physics. Nuclear physics has always played a major role in contributing to the last two of the above challenges. Several foundations of the Standard Model such as the assumption of maximal parity violation and the vector axial-vector character of the weak interaction have their origins in a detailed analysis of nuclear  $\beta$ -decay processes. Precision low energy experiments, searching for deviations from the Standard Model assumptions as possible indicators for new physics, continue to yield information of this type that is complementary to results from particle physics experiments.

Although the measurements in this field of physics are highly specialised and the experimental equipment is usually designed for only one type of measurement and aimed at an extreme precision, it is nevertheless possible to indicate a certain number of experimental pre-requisites necessary to carry out this type of experiments well. As the phenomenon studied is  $\beta$ -decay, the nucleus does not need to be accelerated, but rather maintained at rest or at very low energy. Such experiments are therefore best done at a low-energy beam line. To test certain symmetries, it will in addition be necessary to have the means to polarise nuclei. In all cases, the beam must be intense and very pure in order to minimize errors due to poor statistics and systematic effects arising from contaminants. SPIRAL2 will produce many such beams and an active programme of such measurements can be pursued in the low energy cave.

The Standard Model has two families of fundamental fermions (i.e. leptons and quarks), each consisting of three generations. The forces are mediated by bosons, i.e. the photon,  $W^\pm$  and  $Z^0$  bosons and the gluons. The protons and the neutrons constituting the nucleus are composed of quarks and gluons and are affected by all fundamental interactions. The leptons, governed by the weak interaction, are not sensitive to the strong interaction. In the Standard Model, the baryon number as well as the total lepton number and the lepton family number are conserved. In addition, weak interactions mix the quark flavours, such that the observed mass eigenstates of the quarks are not identical to the weak interaction eigenstates. This mixing is described by the Cabibbo-Kobayashi-Maskawa (CKM) matrix. Recent experiments indicate that for the leptons a similar mixing exists in the neutrino sector. This is strongly related to neutrino oscillation experiments and the search for a finite mass of the electron neutrino in tritium decay. Investigations of the nature of neutrino oscillations and the

behaviour of neutrinos rank among the most urgent questions in physics. Neutrino masses will have a significant impact on e.g. cosmology, but turn out to be so small that they do not affect the nuclear  $\beta$ -decay observables at the present levels of precision.

The electroweak part of the Standard Model is at present the best understood and therefore most suited to probe its potential extensions to physics beyond the Standard Model. For this one can either try to isolate the weak force, or else make use of the interference between the electromagnetic, weak and strong interactions in specific nuclei so as to optimise the sensitivity to weak interaction properties while simultaneously suppressing the effects of the other two interactions. This is possible because of the large number of different nuclear states available in Nature. Any deviation from the Standard Model expectation then represents a possible hint of new physics and provides criteria for the proposed Standard Model extensions.

The speculative models beyond the current Standard Model involve e.g. left-right symmetry, fundamental fermion compositeness, new particles, leptoquarks, supergravity, supersymmetry, etc. Precision measurements in nuclear  $\beta$ -decay can contribute to the evaluation and further development of such models. In particular experiments in nuclear  $\beta$ -decay contribute to the precise testing of the unitarity of the CKM matrix, test fundamental symmetries of the weak interaction such as e.g. parity (P) and time reversal (T) and investigate the structure of the weak interaction. The first case requires precision measurements of the characteristic quantities (i.e. Q-value, half-life and branching ratio) of superallowed  $\beta$  transitions, while the other two topics are addressed by precision measurements of several different correlations between the spins and momenta of the particles involved in nuclear  $\beta$ -decay.

## 5.1 NUCLEAR STRUCTURE FOR EXAMINING THE STANDARD MODEL: PROPERTIES OF SUPERALLOWED $\beta$ -DECAY

It is well established that quarks participate in the weak interactions with a mixture of their mass eigenstates, as described by the CKM matrix. The Standard Model implies CKM unitarity. This unitary condition of the CKM matrix implies that  $V_{ud}^2 + V_{us}^2 + V_{ub}^2 = 1$ . A violation of unitarity could be due to, for example, couplings to exotic fermions, the existence of right-handed currents or of an additional Z boson, or to supersymmetry. The leading element,  $V_{ud}$ , depends only on the quarks in the first generation and is determined from the ratio  $V_{ud} = G_V / G_F$ , with  $G_V$  the coupling constant of the vector interaction in semileptonic decays and  $G_F$  the coupling constant in  $\mu$ -decay. The matrix element  $V_{us}$  is obtained from K-meson decays. The third matrix element,  $V_{ub}$ , is obtained from B meson decays and is so small that it does not play a role at the present level of precision.

The value of  $V_{ud}$  can be extracted from the superallowed nuclear  $\beta$ -decays, from neutron decay and from pion  $\beta$ -decay.  $\beta$ -decay has two components according to the angular momentum of the emitted particles: Gamow-Teller and Fermi. For pure Fermi transitions the initial and final states have the same angular momentum and in the special case where there is no change of isospin, it is called a “superallowed” transition. This particular type of decay occurs along the  $N=Z$  line and is particularly interesting since the Fermi matrix element,  $M_F$ , becomes accessible and the vector coupling constant  $G_V$  (and thus  $V_{ud} = G_V / G_F$ ) is extracted

starting from the comparative half-life,  $ft$ , where  $f$  is the statistical rate function and  $t$  is the half-life of the transition, corrected for the branching ratio and for electron capture:

$$ft=K / [ G_V^2 \langle M_F \rangle^2 + G_A^2 \langle M_{GT} \rangle^2 ],$$

$$\text{with } \langle M_F \rangle^2 = T(T+1) - T_Z T_{Zf}$$

For superallowed Fermi transitions  $M_F^2=2$  and  $M_{GT}=0$ . The factor  $K$  is a combination of several fundamental constants. However, since the transformation of an “up” quark into a “down” quark takes place inside the nuclear volume, certain corrections must be applied that are appropriate for superallowed Fermi transitions

$$\mathfrak{F}t = ft (1 + \delta'_R) (1 + \delta_{NS} - \delta_c) = \frac{K}{2 G_F^2 V_{ud}^2 (1 + \Delta_R)}$$

The nucleus-independent radiative correction  $\Delta_R=0.0240(8)$ . The nucleus-dependent radiative correction  $\delta_R=\delta'_R + \delta_{NS}$ , where  $\delta'_R$  is independent of nuclear structure and the second term ( $\delta_{NS}$ ) does depend on the details of nuclear structure. The correction  $\delta'_R$  is currently evaluated up to order  $Z^2\alpha^3$  and is about 1.5% for all relevant superallowed transitions. The correction  $\delta_{NS}$  is calculated in the nuclear shell model with effective interactions and is well below 0.5% in all cases. Finally,  $\delta_c$  is the isospin symmetry-breaking correction. Theoretically calculated values for this agree reasonably well, yielding 0.2% to 0.6% depending on the particular transition. Nevertheless, the (small) scattering between the calculations of different authors has for a long time been considered as the possible cause for the apparent breakdown of unitarity that followed from the data (see below).

In order to evaluate  $\mathfrak{F}t$ , three experimental quantities are necessary: the lifetime  $t_{1/2}$  of the transition, the branching ratio BR (which is sometimes extremely weak) and the energy balance ( $Q_{EC}$ -value). To reach the required high precision of about  $10^{-3}$  or better, advanced spectroscopic methods are required. Since  $\beta$ -spectroscopy cannot determine the value of  $Q_{EC}$  with the precision necessary, direct measurements (using Penning traps) of the masses of the parent and daughter nuclei are essential. It is important to note in particular that  $f$  depends on  $Q_{EC}^5$ . From a set of several hundred independent measurements the average  $\mathfrak{F}t$  value for the set of twelve best known transitions is obtained as  $\mathfrak{F}t=3072.7(8)$  s (figure 5.1), corresponding to  $|V_{ud}|=0.9738(4)$ . Three of these have been determined only very recently. Combining this result for  $|V_{ud}|$  with the values  $|V_{us}|=0.2200(26)$  and  $|V_{ub}|=0.0037(5)$  recommended by the Particle Data Group yields for the unitarity test  $\Sigma V_{ij}^2=0.9967(14)$ , which deviates  $2.4 \sigma$  from the Standard Model.

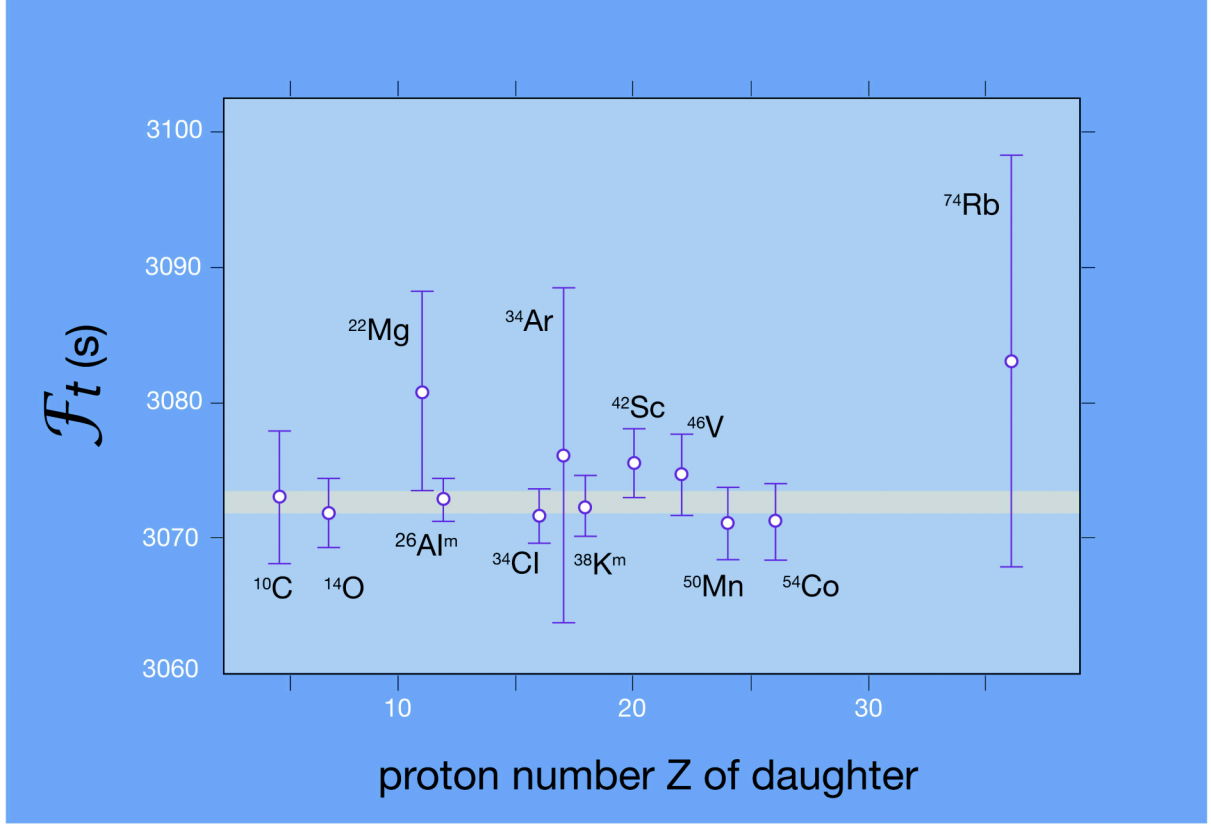


**Figure 5.1:**  $Ft$ -values for the twelve best known superallowed Fermi transitions. The band indicates the one standard deviation region.

The  $V_{ud}$  matrix element can also be determined from neutron and pion  $\beta$ -decay. For these, the radiative correction  $\Delta_R$  is the same as for the Fermi transitions but the nuclear structure dependent corrections  $\delta_c$  and  $\delta_{NS}$  are absent. But since neutron decay is a mixture of Gamow-Teller and Fermi transitions, an additional experiment is required to determine the two contributions. Usually the  $\beta$ -asymmetry parameter,  $A$ , in the decay of polarised neutrons is used for this. In the case of the pion, which decays by a pure Fermi transition, one avoids this particular problem but the branching ratio for the  $\beta$ -decay of the pion is only about  $10^{-8}$ ! For neutron decay one has:

$$f_n \tau_n (1 + \delta_R) = \frac{K / \ln 2}{G_F^2 V_{ud}^2 (1 + \Delta_R) (1 + 3\lambda^2)}$$

with  $\tau_n$  the neutron lifetime and  $\lambda$  the ratio of the Fermi and Gamow-Teller parts in the decay. Using the world average values recommended by the Particle Data Group (i.e.  $\tau_n = 885.7(8)$  s and  $\lambda = -1.2695(29)$ ) yields  $|V_{ud}| = 0.9741(19)$ . This value is in good agreement with the one obtained from the superallowed Fermi transitions, but is a factor of four less precise. The unitarity test with this result from neutron decay yields  $\Sigma V_{ui}^2 = 0.9973(39)$ .

Recently, significant progress has been made in terms of pion  $\beta$ -decay, viz. the decay  $\pi^+ \rightarrow \pi^0 e^+ \nu_e$ . The branching ratio for this process has been determined to be  $1.036(6) \times 10^{-8}$  in an experiment at the Paul Scherrer Institute, corresponding to an improvement by a factor of about five and leading to  $|V_{ud}| = 0.9728(30)$ . Although still less precise, this value is in good

agreement with the result from the superallowed Fermi transitions. With this result the unitarity test becomes  $\Sigma V_{ui}^2=0.9948(59)$ .

type of $\beta$ -decay	$ V_{ud} $
nuclear $0^+ \rightarrow 0^+$	0.9738(4)
neutron	0.9741(19)
pion	0.9728(30)

**Table 5.1:** Comparison of values for  $|V_{ud}|$  obtained from nuclear decays, from neutron decay and from pion  $\beta$ -decay.

In the past few years, important new information has become available from two experiments involving the decay of the  $K^+$  meson. The new values obtained from  $K \rightarrow \pi e \nu$  and  $K \rightarrow \pi \mu \nu$  decays, viz.  $|V_{us}|=0.2272(30)$ , respectively  $|V_{us}|=0.2252(22)$ , are significantly different from the previously adopted value. Combining the weighted average of these two values, viz.  $|V_{us}|=0.2259(18)$ , with the value  $|V_{ud}|=0.9738(4)$  from the superallowed Fermi decays yields  $\Sigma V_{ui}^2=0.9993(11)$  which is in excellent agreement with unitarity. It is thus of utmost importance that efforts be made to further verify and confirm this new value for  $|V_{us}|$ . Additional measurements to determine  $|V_{us}|$  from K decays are ongoing and others are planned. These are the first experiments to determine  $|V_{us}|$  in over 20 years. It is fair to say that the result from nuclear physics is at least partially responsible for spurring the particle physics community to improve their measurements.

If it turned out that the unitarity condition for the first row of the CKM matrix is indeed satisfied, this will provide more precise limits for several types of physics beyond the Standard Model other than those that could be obtained up to now from this unitarity test. These comprise e.g. limits on the mixing angle for left- and right-handed currents as well as on scalar contributions to the weak interaction. In addition, continued efforts to improve the precision of the average  $\mathfrak{A}$ -value for these superallowed transitions will further increase the sensitivity of the unitarity relation to non-Standard Model physics and should therefore be pursued vigorously. It is important to note in this respect that for the superallowed Fermi transitions, the error bar on  $|V_{ud}|$  is at present mainly determined by theoretical quantities, i.e. the radiative correction  $\Delta_R$  (which is also present in neutron and pion  $\beta$ -decay) and the nuclear structure dependent corrections  $\delta_c$  and  $\delta_{NS}$ ).

In order to further constrain physics beyond the Standard Model, efforts should therefore be made

- on the **theoretical side** to improve the precision for the radiative correction  $\Delta_R$ , and the nuclear structure dependent corrections  $\delta_c$  and  $\delta_{NS}$  and
- on the **experimental side** to
  - improve the precision of the input values for the  $\mathfrak{A}$ t-values of the set of well-studied cases, whenever possible, and
  - extend the present set of high precision results with  $\mathfrak{A}$ t-values of similar precision ( $\cong 10^{-3}$ ) for the superallowed transitions of  $T_z=-1$  isotopes (i.e.  $^{18}\text{Ne}$ ,  $^{22}\text{Mg}$ ,  $^{26}\text{Si}$ ,  $^{30}\text{S}$ ,  $^{34}\text{Ar}$ ,  $^{38}\text{Ca}$  and  $^{42}\text{Ti}$ ).

An improvement of the precision for the half-life, branching ratio and Q-value for  $^{10}\text{C}$  and for the Q-value of  $^{14}\text{O}$  to the  $2\text{-}3 \times 10^{-4}$  level, would further reduce the scalar-current limit obtained from the superallowed Fermi transitions significantly.

To cross check the calculations of the isospin correction  $\delta_c$  the  $\mathfrak{S}t$ -value should be determined for cases with large calculated  $\delta_c$  corrections, i.e.  $^{18}\text{Ne}$ ,  $^{30}\text{S}$ ,  $^{38}\text{Ca}$  and  $^{42}\text{Ti}$  among the light nuclei (for which  $\delta_c \cong 1\%$  is calculated), and  $^{62}\text{Ga}$ ,  $^{66}\text{As}$ ,  $^{70}\text{Br}$ ,  $^{74}\text{Rb}$  and to a lesser extent  $^{78}\text{Y}$ ,  $^{82}\text{Nb}$ ,  $^{86}\text{Tc}$ ,  $^{90}\text{Rh}$ ,  $^{94}\text{Ag}$  and  $^{98}\text{In}$  among the heavier nuclei (for which  $\delta_c \cong 1.5\%$  is calculated). This will provide a more detailed and improved understanding of isospin near the  $N=Z$  line and, if the  $\mathfrak{S}t$ -values for these transitions are consistent with the others, at the same time verify the calculations' reliability for the existing cases. Data leading to the  $\mathfrak{S}t$ -value are already available for several isotopes of the just mentioned  $T_z=0$  and  $T_z=-1$  series. A first experimental result of  $\delta_c$  was already obtained for  $^{74}\text{Rb}$ , confirming the reliability of the calculations at the present level of precision. These efforts should be continued for as many isotopes as possible. Key isotopes in this respect are  $^{30}\text{S}$  and  $^{62}\text{Ga}$ .

### ***Measurements of superallowed $\beta$ -decays and test of the Standard Model at SPIRAL2***

*As all the above-mentioned nuclei lie on the  $N=Z$  line they should be produced by fusion–evaporation reactions, which are envisaged within the framework of SPIRAL2. For the nuclei with  $38 < Z < 50$ , many of which are close to the proton drip line, the highest possible production rates are required in order to reach the required precision. In addition, as the  $\beta$ -decay strength becomes very dispersed above  $Z \cong 31$ , advanced detection set-ups with very high efficiency will be required to determine the half-lives and the branching ratios of the superallowed decays of interest. The determination of the  $Q_{EC}$  values requires Penning trap based mass measurements in order to reach the required precision.*

In parallel efforts will be undertaken at other facilities to improve the precision for the values of  $|V_{ud}|$  from neutron and pion  $\beta$ -decay as well.

## **5.2 KINEMATICS OF $\beta$ -DECAY: CORRELATION PARAMETERS AND THE QUEST FOR NEW PHYSICS**

The general description of the weak interaction at low energy implies various types of Lorentz invariant corresponding to interactions of the vector (V), scalar (S), axial-vector (A) and tensor (T) type. In addition, all these possible interaction types can have different properties with regard to transformations of space and time. After it was established in nuclear  $\beta$ -decay experiments in the 1960s that the weak interaction is predominantly of V-A character (i.e. maximally parity violating within experimental error bars) and no evidence for time reversal violation other than the CP-violation in the 2<sup>nd</sup> and 3<sup>rd</sup> generation of quarks was found, the weak interaction was incorporated in the Standard Model as a pure V-A interaction with the observed small CP-violation but no other type of time reversal violation.

The presence of non-Standard Model V-A interactions as well as of other more exotic interactions such as S and T interactions can be probed by observing various types of correlation between the spins and the momenta of the particles involved in the  $\beta$ -decay

process. Pure Fermi  $\beta$ -transitions are sensitive to V and S interactions, while pure Gamow-Teller  $\beta$ -transitions are sensitive to A and T interactions. The coefficients that characterise these correlations do not depend on the structure of the interaction alone but, in addition, also probe the properties of the different possible interaction types with regard to transformations of space and time. Comparison of very precise correlation measurements with forecasts made within the framework of the Standard Model can give an indication of the existence of new physics “beyond the Standard Model” as well as of the masses and couplings of the corresponding bosons that are related to new non-Standard Model interactions. No evidence for either right-handed V, A interactions nor for S or T interactions has been found as yet.

The study of the mechanisms inducing the seemingly maximal violation of parity (or equivalently of new time reversal invariant V and A interactions) requires precision measurements of pseudoscalar quantities like e.g. the  $\beta$ -asymmetry parameter  $A$ , the longitudinal  $\beta$ -polarisation  $P_L$ , or a combination of both.

Searches for new sources of time reversal violation, different from that observed in the decay of K and B mesons (which is incorporated in the Standard Model via the CP violating phase in the CKM matrix), can be carried out by measuring triple-correlation terms appearing in the  $\beta$ -decay rate. Until now, only such terms dominated by the parameters  $D$  and  $R$  have been measured. The  $D$  coefficient probes time reversal violating V and A interactions, while the  $R$  parameter is sensitive to the existence of time reversal violating exotic S and T interactions.

All correlation coefficients are sensitive to the possible presence of scalar and/or tensor type contributions, the exact sensitivity depending on the particular correlation that is observed. One coefficient, the  $\beta$ -neutrino angular correlation coefficient  $a$ , is sensitive to all possible interaction types, whatever the transformations of parity and inversion of time. This coefficient has been measured in the past for several transitions. The results of these measurements have provided the experimental basis establishing the V-A nature of the weak interaction. In the past decade, the advent of atom and ion traps has triggered a revival of such measurements as it is believed that with the very pure as well as backing free and scattering free samples that can be prepared in traps, a significant gain in precision can be reached.

### ***$\beta$ -decay kinematics and the search for time reversal violation with beams from SPIRAL2***

*Especially important for weak interaction studies are the nuclei near the  $N=Z$  line, i.e. with nearly equal numbers of protons and neutrons, for which nuclear structure effects are rather well under control. If fast transitions (i.e. with  $\log ft < 5.5$ ) are used, recoil effects are also small or can be taken into account. For correlation measurements in nuclear  $\beta$ -decays, radiative corrections are only important at the  $10^{-4}$  level and below, which is well below the precision level of 0.1% to 1% that measurements in nuclear  $\beta$ -decay can aim for in the coming decade. The well-studied superallowed pure Fermi transitions are very well suited to the search for scalar currents. The superallowed transitions between the  $T=1/2$  mirror nuclei are of interest to study the presence of scalar currents, of non-Standard Model  $V$ ,  $A$  type interactions (viz. parity violation) and of time reversal violation. Finally, the mirror decay of  $^{19}\text{Ne}$  as well as fast pure Gamow-Teller transitions, are of interest to search for tensor currents and test time reversal invariance in nuclear  $\beta$ -decay.*

In the following paragraphs the different types of correlation measurements of interest to search for physics beyond the Standard Model will be discussed in more detail.

#### **5.2.1 New time reversal invariant Vector and Axial-Vector interactions.**

Precision measurements of observables sensitive to the helicity structure of the Weak interaction provide powerful means to probe specific scenarios of new physics beyond the Standard Model in which the maximal violation of parity is restored at some level due to the exchange of non-standard new bosons. In nuclear  $\beta$ -decay the most interesting observables in this respect are the  $\beta$ -particle emission asymmetry relative to the spin of the decaying nucleus and the longitudinal polarisation of the emitted  $\beta$ -particles. Note that both these observables are in addition also sensitive to S or T type interactions.

Relative measurements comparing the longitudinal polarisation of positrons in  $^{12}\text{N}$  and  $^{107}\text{In}$  decays emitted along two opposite directions with respect to the nuclear spin (the so-called polarisation asymmetry correlation), provide the most stringent tests of parity violation in nuclear  $\beta$ -decay so far.

In such relative measurements the uncertainties associated either with the degree of polarisation of the decaying system or with the analysing power of the polarimeter are strongly reduced. The measured quantities have reached a level of precision of a few parts in  $10^{-3}$ . All measurements so far are consistent with the Standard Model predictions.

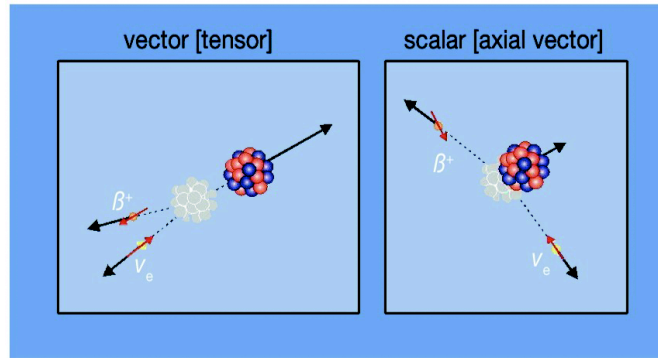


**Figure 5.2:** Kinematics for the different possible types of  $\beta$ -decay. Fermi  $\beta$ -transitions can proceed through vector (V) and scalar (S) interactions. Gamow-Teller transitions through axial-vector (A) and tensor (T) interactions (for axial-vector and tensor interactions the spin of the positrons has to be reversed). Only vector and axial-vector type interactions have been observed to date.

An example of a scenario to interpret helicity observables beyond the Standard Model is provided by Left-Right symmetric models, involving only vector and axial vector couplings but allowing the presence of right-handed gauge bosons. In the most simple extension, assuming no mixing between bosons, the above mentioned experiments in nuclear  $\beta$ -decay provide limits on the mass of a hypothetical right-handed gauge boson at the level of about  $320 \text{ GeV}/c^2$  (90% C.L.). Within the same scenario, the limits obtained by precision measurements in  $\mu$ -decay are at the level of  $400 \text{ GeV}/c^2$ . Despite great efforts, the limits from  $\beta$ -decay and  $\mu$ -decay turn out not to be competitive with those obtained from direct searches for new heavy charged bosons performed at colliders, which are about  $700 \text{ GeV}/c^2$ . However, within generalized left-right symmetric extensions to the Standard Model, results from purely leptonic, semi-leptonic and purely hadronic weak interactions cannot be compared on the same basis due to the different sensitivities to combinations of the coupling parameters. Moreover, parity restoration mechanisms that involve quark-lepton interactions cannot directly be probed in the pure leptonic  $\mu$ -decay. In such a context any new effort at low energies to search for new bosons in the mass range between  $500 \text{ GeV}/c^2$  and  $1 \text{ GeV}/c^2$ , is therefore highly valuable.

In order that polarisation asymmetry correlation experiments become sensitive to the mass range above  $500 \text{ GeV}/c^2$  one has either to get a better understanding of the spin rotation of positrons during scattering in a metal host foil, such that further progress can be made using the low temperature nuclear orientation method for this type of experiment, or new polarisation techniques have to be used.

An alternative method is to perform high-precision measurements of the  $\beta$ -emission asymmetry parameter in the decay of polarised nuclei. Best suited in this case are fast pure Gamow-Teller  $\beta$ -transitions or the mixed superallowed transitions between the  $T=1/2$  mirror nuclei. In both cases a precision of the order of 0.2 % is required, however. Several projects of this type have been started recently. The first is at the Los Alamos National Laboratory. There the proof of principle to measure the electron decay asymmetry in the decay of polarized  $^{82}\text{Rb}$  in a magneto-optical trap has recently been demonstrated at LANL. Presently the method to determine the nuclear polarisation is being optimised. The second project, at Leuven and ISOLDE-CERN, uses the low temperature nuclear orientation method to polarise

the nuclei. A first result, although still with limited precision, has been obtained already with  $^{114}\text{In}$ .

### ***Precision measurements of asymmetry in $\beta$ -decay of polarised nuclei at SPIRAL2***

*Much of the progress in the last decade has been due to the development of new techniques to polarise nuclei or to the efficient use of existing methods. Significant further progress can be expected from efforts towards the production of highly polarised, high intensity and high purity samples combined with advanced  $\beta$ -particle detection techniques. Although measurements of the  $\beta$ -asymmetry parameter and longitudinal polarisation are challenging as to the required precision (per mil level) and control of systematic effects, ongoing and planned developments at several places might eventually allow us to meet these goals.*

*Finally it is worth noting that in order to reach a precision of the order of 0.2 % for the  $\beta$ -asymmetry parameter in  $T=1/2$  mirror  $\beta$  transitions, new and precise measurements of the observables leading to the  $ft$ -values of these transitions are required. In order that this is not the limiting factor, the precision of these  $ft$ -values, which is now typically about 2%, has to be improved by a factor of five or more.*

## **5.2.2 New time reversal invariant Scalar and Tensor interactions**

A recent analysis of all experiments in nuclear and neutron  $\beta$ -decay sensitive to scalar and tensor components in the weak interaction yielded lower limits of  $|C_S^{(+)}/C_V| < 0.08$  and  $|C_T^{(+)}/C_A| < 0.08$  (90% C.L.) for scalar and tensor type coupling constants (figure 5.3), with the vector coupling constant  $C_V=1$  and  $C_A/C_V= -1.27$ . To improve further on these limits for scalar and tensor couplings it is best to determine the  $\beta$ - $\nu$  correlation coefficient  $a$  (sensitive to S- and T-interactions) or the  $\beta$ -emission asymmetry parameter  $A$  (mainly sensitive to a T-interaction). The  $\beta$ - $\nu$  correlation coefficient  $a$  is measured with unpolarised nuclei. To determine the  $\beta$ -asymmetry parameter  $A$  the nuclei should be polarised. For both  $a$  and  $A$  a precision in the range from 0.5% to 1% or better is required to improve on the above limits for scalar and tensor coupling constants.

The ongoing efforts with respect to the determination of  $A$  were discussed in the previous section. As for the  $\beta$ - $\nu$  correlation coefficient  $a$  a very precise measurement was carried out with  $^{32}\text{Ar}$  at ISOLDE. The result was in agreement with the Standard Model within the 0.6% error bar. A significant gain in precision as well as improved reliability can be expected from the recent development of atom and ion traps for weak interaction studies.

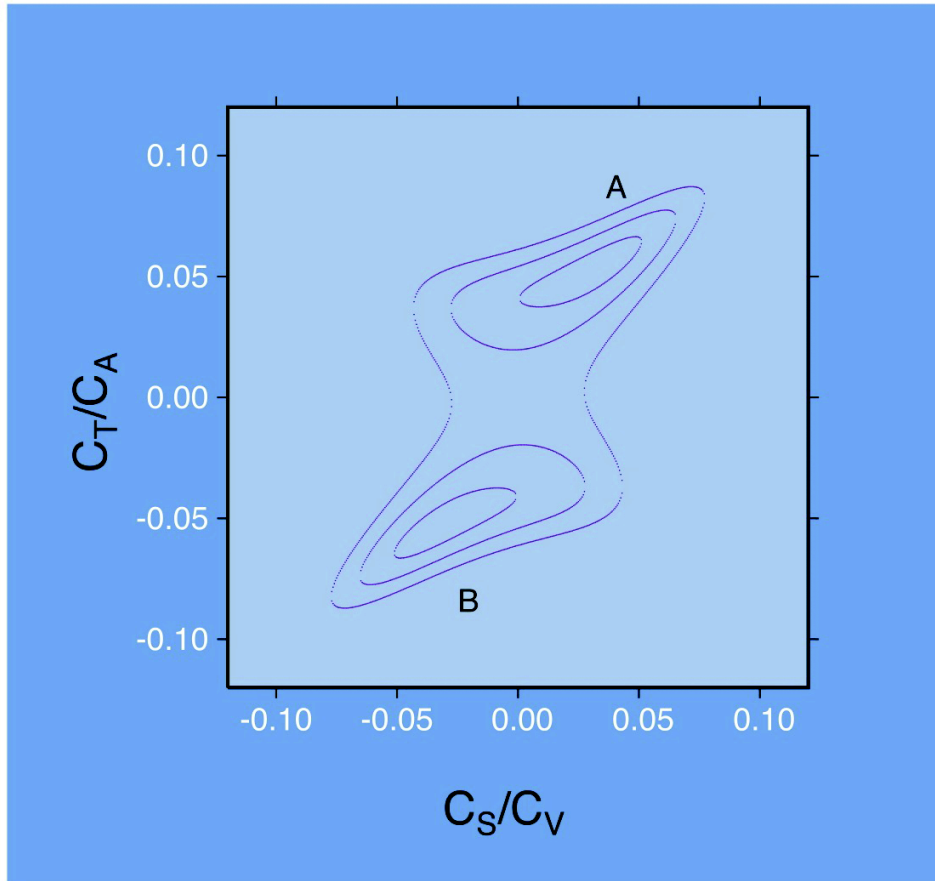


**Figure 5.3:** Contours of constant  $\chi^2$  for the parameters  $C_S/C_V$  and  $C_T/C_A$  obtained in a fit assuming right-handed scalar and tensor currents with the value for  $C_A/C_V$  fixed to the value at the minimum.

The use of traps will provide very thin sources in vacuum, thus avoiding the need for a material host, which will significantly reduce the effects of scattering and allow one to detect the recoil ions after  $\beta$ -decay without the disturbing effects of energy loss in the host material. Laser driven magneto-optical traps (MOT) are well suited for alkaline and alkaline-earth elements and have the advantage that the nuclei in addition can be laser polarised. Paul and Penning traps permit the trapping of any element but their combination with techniques to polarise nuclei is not straightforward. A first precision result using MOT-trapped nuclei is already available and agrees with the Standard Model within the 0.5 % error bar. Another atom trap for  $\beta$ - $\nu$  correlation measurements will be set up at KVI-Groningen as part of the Triup project. Systems using Penning traps and Paul traps are currently being set up as well, the first type at ISOLDE-CERN (WITCH experiment), the second type at GANIL (LPC Trap). The first goal with the LPC-trap that was recently installed at the LIRAT low energy beam line at GANIL is to measure the  $\beta$ - $\nu$  correlation in the decay of  ${}^6\text{He}$  with sub-percent precision.

### ***$\beta$ - $\nu$ correlations and $\beta$ -asymmetry parameter measurements to search for scalar and tensor type weak interactions at SPIRAL2***

*Searches for scalar type interactions require that the  $\beta$ - $\nu$  correlation is determined for pure Fermi superallowed  $\beta$  transitions or for the superallowed  $\beta$ -decays between the  $T=1/2$  mirror nuclei. In all these cases radiative corrections and recoil corrections are negligible or well under control. However, as was mentioned before, the precision of the  $ft$ -values for these mirror transitions (now typically  $\cong 2\%$ ) should be improved by a factor of 5 to 10 in order to reach the highest sensitivity for non-Standard Model physics.*

*For tensor interactions the  $\beta$ - $\nu$  correlation or  $\beta$ -asymmetry parameter have to be determined for fast, pure Gamow-Teller transitions. A key experiment is the measurement of the  $\beta$ - $\nu$  correlation in the decay of  ${}^6\text{He}$  with the Paul trap at the LIRAT low-energy beam line.*

*The nuclei of interest in searches for scalar and tensor type weak interactions (i.e.  $T=1/2$  mirror nuclei and relatively light ( $A < 70$ ) nuclei with pure Fermi or pure Gamow-Teller transitions) should be readily produced at SPIRAL2.*

### **5.2.3 Testing time reversal invariance in nuclear $\beta$ -decay**

The CP-violation that is observed in the decay of K- and B-mesons, incorporated in the Standard Model via the quark mixing mechanism, is too weak to explain the excess of baryons over antibaryons that is observed in the Universe. This excess therefore provides a hint of the existence of an unknown source of T-violation that is not included in the Standard Model. As these Standard Model contributions to time reversal violating observables in  $\beta$ -decay are 7 to 10 orders-of-magnitude lower than the experimental accuracies presently available, any sign of the presence of time reversal violation in these would be a signature of a non-Standard Model source of time reversal violation. New time reversal violating phenomena may be generated by several mechanisms like the exchange of multiplets of Higgs bosons, leptoquarks, right-handed bosons, etc. These exotic particles may generate scalar or tensor variants of the weak interaction or a phase different from 0 or  $\pi$  between the vector and axial-vector coupling constants. It is a general assumption that time reversal violation may originate from a tiny admixture of such new exotic interaction terms. Weak decays provide a favourable testing ground in a search for such feeble new forces.

Direct searches for time reversal violation via correlation experiments in  $\beta$ -decay require the measurement of terms including an odd number of spin and/or momentum vectors. The  $D$  triple correlation probes time reversal violation in the vector and axial-vector weak interaction components. To determine this correlation, the momenta of  $\beta$ -particles and neutrinos (the last one from the recoil ions) emitted in mutually perpendicular directions in a plane perpendicular to the nuclear spin axis is to be determined. It also requires the use of mixed Fermi/Gamow-Teller transitions.

The other important correlation with respect to searches for time reversal violation in  $\beta$ -decay is the  $R$  triple correlation, which probes the existence of both parity and time reversal violating scalar and tensor weak interactions. To determine this the transverse polarisation of  $\beta$ -particles emitted in a plane perpendicular to the polarised nuclear spin is to be determined. Final state effects for the  $D$  and  $R$  correlations in nuclear decays are typically of the order of  $10^{-4}$ . For leptoquark models time reversal violating effects in the experimental range  $>10^{-4}$  are not excluded by measurements of other observables, like electric dipole moments.

In  $\beta$ -decay the  $D$  correlation was only measured up to now in the decays of the neutron and  $^{19}\text{Ne}$ . For  $^{19}\text{Ne}$  these measurements have already reached the limit imposed by final state effects, which is at the  $10^{-4}$  level. All results are in agreement with the Standard Model and show no sign of time reversal violation in the V-A weak interaction at this level of precision. The  $R$  correlation was only measured up to now in the decay of  $^8\text{Li}$  and  $^{19}\text{Ne}$ . The experiment with  $^8\text{Li}$  yielded  $R=0.0009(22)$ . The result for  $^8\text{Li}$  has been corrected for the effect of the final state interaction which was calculated to be  $R_{FSI}=0.0007(1)$ . As  $^8\text{Li}$  decays via a pure Gamow-Teller transition this experiment was sensitive to a time reversal violating tensor type interaction. The corresponding bounds for time reversal violating tensor couplings,  $-0.008 < \text{Im}(C_T+C'_T) / C_A < 0.014$  (90% C.L.), are the best limits to date. To search for a time reversal violating scalar component in the Weak interaction a mixed Fermi/Gamow-Teller transition should be studied. As the precision obtained with  $^{19}\text{Ne}$  was rather limited, leading to weak limits for a scalar interaction, the  $R$  correlation is now being investigated in the decay of the free neutron at the spallation neutron source SINQ at the Paul Scherrer Institute. This experiment aims at a precision of about 0.5% by determining the transverse polarisation of electrons emitted in polarised neutron decay using large angle Mott scattering.

***Time reversal violation by correlation measurements in nuclear  $\beta$ -decay***

*New measurements in decays that are selected such that the final state interaction effects are smaller than in the case of  $^{19}\text{Ne}$ ,  $^8\text{Li}$  and the neutron would be highly valuable, as they would provide more sensitive tests of non-Standard Model time reversal violating interactions. In the case of the  $D$  correlation a  $T=1/2$  mirror nucleus should be selected. As for the  $R$  correlation a nucleus with a fast, pure Gamow-Teller transition is required to improve the limits on a time reversal violating tensor interaction. To improve also the sensitivity for a time reversal violating scalar interaction a measurement with a  $T=1/2$  mirror nucleus is again required. There should be no difficulty in producing such nuclei at SPIRAL2. In order to improve on existing results a precision of better than  $10^{-3}$  is needed for both correlation experiments.*

Finally, it is to be noted that several other correlations in neutron and nuclear  $\beta$ -decay are also sensitive to time reversal violating couplings, either through final-state interaction effects (e.g. the  $\beta$ -asymmetry parameter  $A$ ) or through a quadratic dependence on the norm of the coupling constants (e.g. the  $\beta$ - $\nu$  correlation coefficient  $a$ ). The sensitivity of these is, however, usually smaller than in measurements of the  $D$  and  $R$  triple correlations.

### 5.3 FIRST-FORBIDDEN $\beta$ -DECAY

Many isotopes that are produced in nuclear fission decay via first-forbidden  $\beta$  transitions, both non-unique ( $\Delta I=0, 1; \pi_i \pi_f = -$ ) and unique ( $\Delta I=2; \pi_i \pi_f = -$ ) transitions. For several isotopes the first forbidden  $\beta$ -decay is sufficiently pure (i.e. only one branch or a few branches that do not overlap too much) that the spectrum shape factor or correlations in the  $\beta$ -decay can be measured. However, due to the complexity of forbidden  $\beta$  transitions (up to six nuclear matrix elements can play a role) these are usually only suited to study nuclear structure instead of investigating fundamental Weak interaction properties. Only when the nuclear matrix elements involved are sufficiently well known can Weak interaction information be extracted. However, it is not clear at present what precision on the matrix elements is required for this.

In some very specific cases, accidental near cancellation of terms connected with the different nuclear matrix elements can lead to an enhancement of the sensitivity to a possible non-Standard Model admixture by several orders-of-magnitude compared to the case of allowed transitions. This was e.g. shown for the sensitivity of the longitudinal polarisation and the spectrum shape factor of the  $\beta^-$ -decay of  $^{210}\text{Bi}$  to a possible V+A admixture, S- and T-admixtures and time reversal violation. It should be stressed though that in such cases there is still a strong dependence on the nuclear structure, which weakens this sensitivity somewhat. Detailed calculations of nuclear wave functions are thus required in such cases.

## 5.4 ATOMIC PARITY NON-CONSERVATION

Atomic parity non-conservation (APNC) experiments are a fundamental tool in testing our understanding of the electroweak interaction. The observation of parity non-conservation in atoms (and then in deep inelastic electron-deuteron scattering) led to the discovery of the weak electron-nucleon interaction due to the neutral currents. Recent APNC experiments have reached a level of precision to provide a quantitative test of the Standard Model. Moreover, the precision of modern APNC experiments has made them an important tool for studying nuclear structure and P-odd nuclear interactions.

Parity violation in atomic systems arises from the interference between the parity conserving electromagnetic interaction and the parity violating weak interaction. Although most of the binding energy of the atomic electrons comes from their attractive Coulomb interaction with the  $Z$  protons in the nucleus, the weak electron-nucleus interaction mediated by the exchange of neutral gauge bosons  $Z^0$  induces a small correction to the binding energy and parity of the electronic wave functions. This correction results in an electric dipole amplitude between two electronic states that in the absence of parity violating effects would have the same parity, i.e. forbidden transitions.

The dominant (and nuclear spin-independent) part of the PNC Hamiltonian depends on the “weak charge”  $Q_w$ , which contains the Standard Model coupling constants. The “weak charge” is extracted from the experimental data combined with accurate calculations of the electronic wave functions.

The observation of deviations between the values measured in the laboratory and the predictions of the Standard Model in high precision APNC experiments can lead to the discovery of new physics beyond the Standard Model. At low momentum transfer, as is the case in APNC experiments, new particles predicted for instance in supersymmetric models at high mass scales or in Technicolour models generate additional electron-quark PNC interactions.  $Q_w$  can be sensitive to new corrections, weak isospin-conserving and isospin-breaking, usually described by the parameters  $S$  and  $T$ , respectively.

On the experimental side, one has to consider that the effects are very small and the analysis of APNC experiments is complicated by the uncertainties in both atomic and nuclear-structure theory. Wood et al. measured the amplitude of the parity non-conserving transition between the 6S and 7S states of  $^{133}\text{Cs}$ , the only naturally occurring Cesium isotope. The value of weak charge was found to be  $Q_w^{\text{exp}} = -72.06(28)_{\text{exp}}(34)_{\text{th}}$ . This result was different by  $2.5\sigma$  from the Standard Model prediction,  $Q_w^{\text{th}} = -73.20 \pm 0.13$ . Recent papers demonstrate that the deviation between the experimental results and the Standard Model prediction is very

much attenuated by taking into account self-energy and vertex QED radiative corrections: the newly reported value of the weak charge for  $^{133}\text{Cs}$  is  $Q_w^{\text{exp}} = -72.90(28)_{\text{exp}}(35)_{\text{th}}$ .

As already said, the analysis of APNC experiments is complicated by the uncertainties in both atomic and nuclear-structure theory. Fortunately, uncertainties in atomic structure may be reduced considerably by studying parity violation along a chain of isotopes. In this way the dependence on the atomic theory contribution of the parity violating amplitude measured in a APNC experiment will cancel out in the ratio of two measurements performed on two different isotopes of the same element, provided that the atomic contribution does not change appreciably along that isotopic chain.

Based on their long chains of several naturally occurring isotopes, cesium, barium, dysprosium, and ytterbium appear as ideal candidates. In particular, it would be very valuable to extend the measurements that have proved successful for natural Cesium,  $^{133}\text{Cs}$ , to some of its numerous radioactive isotopes. Cesium is often considered to be one of the most interesting candidates for forthcoming experiments because, being an alkaline element, the necessary atomic and nuclear calculations can be done much more precisely than is the case for other elements. Neutron rich Cs isotopes are abundantly produced in nuclear fission. Of these, the isotopes  $^{138}\text{Cs}$  to  $^{141}\text{Cs}$  (with half lives between 25 s and 32 m and with expected yields at SPIRAL2 of about  $10^{10}/\text{s}$ ) are of interest for APNC experiments.

Techniques to produce and trap radioactive ions with high efficiency are very important: in order to perform APNC measurements the first prerequisite is to avoid the loss of the ions. Only the radiative cooling and trapping techniques, possibly combined with Light Induced Atomic Desorption (LIAD), can succeed in this kind of operation. The first successful results have been obtained recently, in particular trapping of radioactive alkalines (i.e., Na, K, Rb, Cs, Fr) has been demonstrated.

Another field of investigation is the measurement of the nuclear anapole moment. Up to now, the nuclear anapole moment has been detected only for  $^{133}\text{Cs}$  (an even neutron-number isotope), and it would be very important to measure it for another isotope (in particular one with an odd neutron-number).

*In order to exploit the beams from SPIRAL2 as fully as possible in these types of weak interaction experiments, it is crucial to provide a **low-energy area**. This will have to be equipped with a **high resolution mass spectrometer** ( $M/\Delta M \approx 10.000$ ) in order to remove isobaric contamination. **High performance nuclear spectroscopy set-ups and precise mass measurements** will be crucial too. For correlation measurements in nuclear  $\beta$ -decay, **traps for ions and/or atoms** must be installed in order to cool them until they are almost at rest and to create experimental conditions where the scattering of the  $\beta$  particles is minimal or even absent and the recoil ions from  $\beta$ -decay can be observed as well if required. Lastly, several options exist to **polarise the nuclei**, such as e.g. polarisation induced by a laser, or by extracting the nuclei at an optimum angle with respect to an incident beam of deuterons. Once polarised the nuclei can then be implanted into a material preserving the polarisation.*

**Superallowed Fermi transitions** can be studied in several complementary directions:  
(1) Improvement of the precision of the half-lives, branching ratios and decay energies of the already well studied superallowed Fermi transitions of the series of nuclei between  $^{10}\text{C}$

and  $^{54}\text{Co}$  in order to further increase the sensitivity of their average  $Ft$ -value to different types of physics beyond the Standard Model. Key isotopes in this respect are  $^{10}\text{C}$  and  $^{14}\text{O}$ . This will require high performance nuclear spectroscopy set-ups and precise mass measurements.

(2) Improvement of the precision of the half-lives, branchings and decay energies of the superallowed Fermi transitions in nuclei on or near the  $N = Z$  line, i.e.  $^{18}\text{Ne}$ ,  $^{22}\text{Mg}$ ,  $^{26}\text{Si}$ ,  $^{30}\text{S}$ ,  $^{34}\text{Ar}$ ,  $^{38}\text{Ca}$ ,  $^{42}\text{Ti}$  and  $^{62}\text{Ga}$ ,  $^{66}\text{As}$ ,  $^{70}\text{Br}$ ,  $^{74}\text{Rb}$ . Key isotopes are  $^{30}\text{S}$  and  $^{62}\text{Ga}$ . This will require experimental development and rests on the exploitation of beams of high optical quality such as those provided by the ISOL method. As these nuclei are close to the  $N=Z$  line, their production will be via fusion-evaporation, already envisaged within the framework of SPIRAL2.

(3) Obtaining first measurements of these quantities for  $Z > 38$  nuclei so as to cross-check calculations for the isospin correction  $\delta_c$ . For this production rates will be even more crucial.

The study of possible **exotic scalar and tensor contributions to the weak interaction**, as well as of **parity violation** and **time reversal violation** by correlation measurements in nuclear  $\beta$ -decay requires high intensity and pure beams of  $T=1/2$  mirror nuclei (e.g.  $^{19}\text{Ne}$ ,  $^{21}\text{Na}$ ,  $^{23}\text{Mg}$ ,  $^{29}\text{P}$ ,  $^{31}\text{S}$ ,  $^{33}\text{Cl}$ ,  $^{35}\text{Ar}$ ,  $^{37}\text{K}$ ,  $^{39}\text{Ca}$ ,  $^{41}\text{Sc}$ ,  $^{43}\text{Ti}$ , ...) as well as of nuclei decaying via a fast and pure Gamow-Teller transition (e.g.  $^6\text{He}$ ,  $^8\text{He}$ , ...). In the first case it is essential that the present precision of the  $ft$ -value for the  $T=1/2$  mirror  $\beta$  transitions be improved by at least a factor of five, i.e. to the level of a few  $10^{-3}$ . This requires high performance nuclear spectroscopy set-ups and precise mass measurements. Further, among the isotopes that will be produced at SPIRAL2 many decay via fast and pure Gamow-Teller transitions. A key experiment is the measurement of the  $\beta$ - $v$  correlation in the decay of  $^6\text{He}$  with the Paul trap at GANIL.

Many isotopes produced in nuclear fission decay via **first-forbidden  $\beta$  transitions**. Due to the complexity of first-forbidden  $\beta$ -decay (up to six nuclear matrix elements have to be taken into account) these are usually only interesting for nuclear structure studies and cannot be used to provide detailed information on fundamental weak interaction properties. Accidentally a near cancellation of terms connected with the different matrix elements leads to an enhancement of the sensitivity to a possible non-Standard Model admixture by several orders-of-magnitude compared to the case of allowed transitions. It should be stressed though that in such cases there is still a strong dependence on the nuclear structure, which weakens the sensitivity somewhat. Detailed calculations of nuclear wave functions are thus required in such cases.

Finally, at SPIRAL2 parity violation can also be studied by performing **atomic parity non-conservation (APNC)** experiments. It would be very valuable to extend the measurements that have proved successful for natural cesium,  $^{133}\text{Cs}$ , to some of its numerous radioactive isotopes. Cesium is one of the most interesting candidates for forthcoming experiments because the necessary atomic and nuclear calculations can be done with high precision. Neutron rich Cs isotopes are abundantly produced in nuclear fission. Key isotopes are  $^{138-141}\text{Cs}$ , which will be abundantly produced at SPIRAL2.

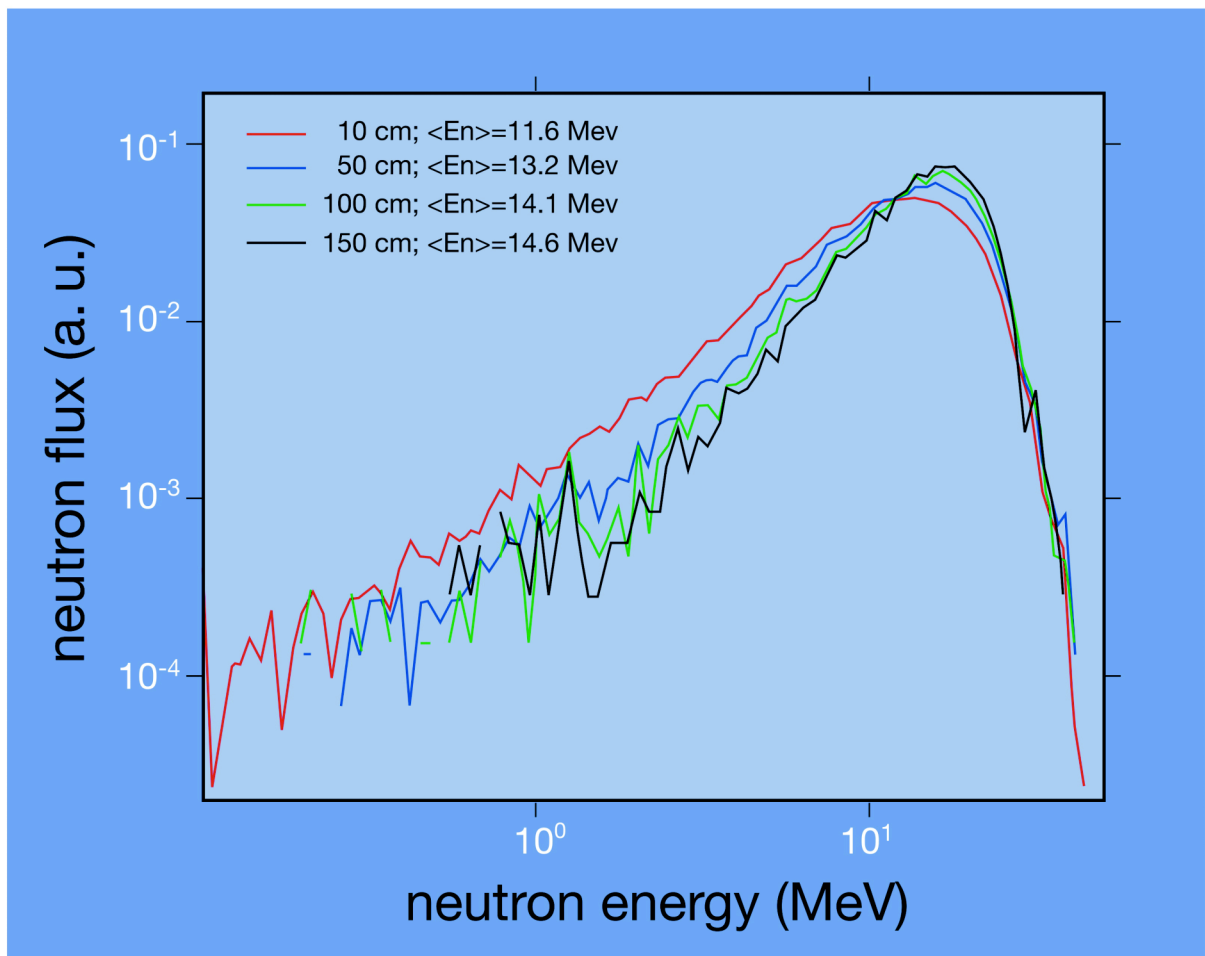
## 6. NEUTRONS FOR SCIENCE (NFS) AT SPIRAL2

### 6.1 INTRODUCTION

The new superconducting linear accelerator, which will act as the driver accelerator of SPIRAL2, will provide a 40 MeV deuteron beam at an intensity up to 5 mA (200 kW). With this primary beam a huge number of neutrons ( $\sim 10^{15}$  n/s) will be produced on a rotating carbon converter in the energy range between 1 keV and 40 MeV. The main goal of this chapter is to examine the possibility of using a linear deuteron accelerator in combination with the target-converter for other purposes than production of RIBs, namely,

- a) **neutron time-of-flight (nToF) measurements with pulsed neutron beams, and**
- b) **material activation-irradiation with high-energy, high-intensity neutron fluxes.**

In this context, figure 6.1 presents the neutron energy spectra (on the left) and neutron beam intensities (on the right) at different distances from the production targets as expected in the case of SPIRAL2. Use of these neutrons is briefly discussed in what follows.



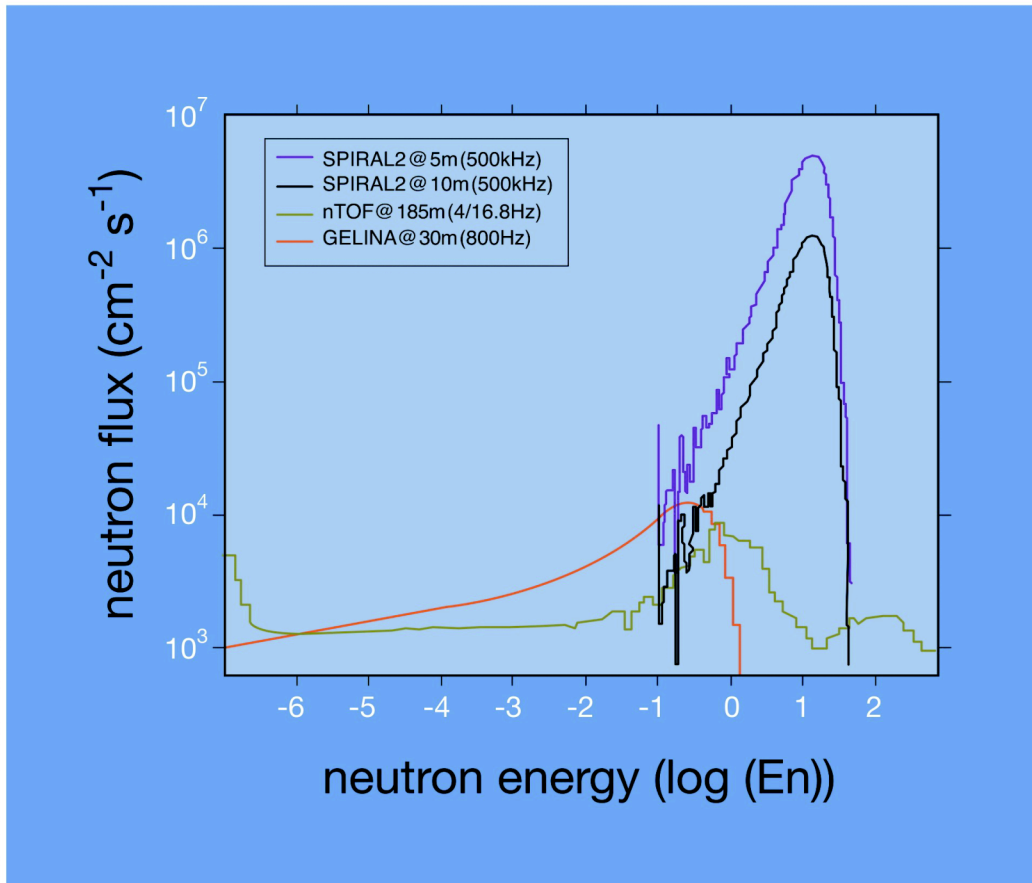


**Figure 6.1:** Neutron energy spectrum expected at SPIRAL2 as a function of distance from the production target (upper panel); Neutron beam intensities expected at SPIRAL2 and compared with existing major nToF facilities in Europe (lower panel).

Materials testing via irradiation in high energy and high neutron fluxes is of great interest for a very extended community working on nuclear waste transmutation (use of Accelerator Driven System –ADS– in particular), intensive neutron sources (SNS, ESS, ...), RIB production with neutrons (EURISOL, RIA, ...), future controlled fusion experiments and reactors (ITER, DEMO, ...), space applications (resistance of electronics, shielding, ...), etc.

High fluxes of neutrons with high energy are very attractive for integral measurements of the transmutation-incineration of nuclear waste and minor actinides in particular. This type of high energy neutron flux has the advantage of increasing the fission over capture ratio (the capture becoming negligible compared to fission), and thus the direct incineration of the element without the production of heavier elements. For this purpose on-line fission rate measurements could be performed with fission ionization chambers with neptunium, americium and curium deposits.

Only very limited data exist for neutron induced reactions above 14 MeV. For many cases both fission and (n,xn) reaction cross-sections are unknown. The neutron energy range between 1 and 40 MeV concerns the nuclear waste transmutation in the case of ADS, future fusion applications, etc., where designers need new and good quality data and relevant codes in order to build evaluated data libraries and also to improve theoretical models. The above energy range corresponds also to the opening of new reaction channels like (n,p), (n,α),

allowing the pre-equilibrium model studies, i.e. the transition between low (evaporation) and high energy models (intra-nuclear cascade).

The high neutron fluxes would allow measurements of small cross-sections and/or the use of very small targets, which might be rare, expensive, and in some cases radioactive. More fundamental studies can also be achieved, e. g. precise measurements of the neutron-neutron interaction length  $a_{nn}$  in terms of the  $t(n,2n)d$  reaction are crucial in few-body physics in order to define without ambiguities the nucleon-nucleon interaction.

High energy neutrons (above  $\sim 1$  MeV) would also allow the production of radioactive elements or isomeric nuclei via  $(n,xn)$ ,  $(n,p)$  or  $(n,\alpha)$  reactions. Therefore, having very high neutron fluxes one will be able to prepare a number of radioactive or isomeric targets for fundamental physics studies to be performed afterwards with stable or radioactive ion beams, both available at GANIL. Below a number of case studies on the physics with SPIRAL2 neutrons are presented in more detail.

## 6.2 NEUTRON TIME-OF-FLIGHT (TOF) MEASUREMENTS

### 6.2.1 Proposed conditions and potential improvements

The SPIRAL2 initiative proposes a neutron time-of-flight beam line at zero degrees for which the neutrons are produced by a 40 MeV deuterium beam incident on a thick graphite target. The beam will be pulsed at 500 kHz leaving 2  $\mu$ s between bursts. The burst width is a few hundred picoseconds. Two flight paths of 5 and 10 m are proposed. Flux estimates were made with MCNPX and amount to  $8.8(2.2)\times 10^6$  n/(cm<sup>2</sup> s) for 5(10) m. About  $6\times 10^{12}$  neutrons are produced per second and at this pulse rate the deuteron average current is  $\sim 28$   $\mu$ A.

It seems possible that from the side of the accelerator and neutron source a gain of maximum  $\sim 50$  % may be expected by bunching the beam prior to entry into the Radio Frequency Quadrupole (RFQ) and another  $\sim 50$  % by using lithium or beryllium instead of graphite as a target-converter. It will be argued below that any gain in intensity enhances the potential for the time-of-flight measurements. For the time being such potential enhancements will be ignored. Arguments will be given for the establishment of additional 2.5 and 20 m flight paths.

### 6.2.2 General comments

At  $6\times 10^{12}$  n/s the intensity of SPIRAL2 for time-of-flight measurements is less than that for the Gelina facility ( $3\times 10^{13}$  n/s). This first of all precludes competitive moderated spectrum time-of-flight measurements at SPIRAL2. This conclusion is further underlined by the fact that for moderated spectrum measurements a maximum frequency of about 10 kHz would be required, lowering the intensity another factor of 50 compared to the above estimate.

For the fast spectrum the situation is altered by the strong forward emission of the neutrons as a consequence of the breakup component of the spectrum. In fact, for  $E_d=33$  MeV it was measured that the yield at zero degrees is 18 times larger than the forward emission for isotropic emission. As a consequence, at the same distance from the source, the SPIRAL2 fast flux at this angle is about twice to three times that of Gelina, where the spectrum is essentially

isotropic. An important difference is the hardness of the spectrum. For SPIRAL2 the spectrum peaks at 14 MeV, whereas for Gelina this is 1-2 MeV. In the neutron energy range 5-35 MeV SPIRAL2 competes favourably in terms of intensity with the wide energy time-of-flight source at WNR (LANL), offering similar time resolution and flight path lengths. Another important difference for SPIRAL2 is the expected absence of a strong accompanying  $\gamma$ -flash in the beam. This feature is essential for the effective utilisation of short flight paths for the measurements discussed below. Such short flight paths are prohibited at an electron-accelerator based source like Gelina due to the  $\gamma$ -flash induced pile-up and detector disturbance.

In brief, the range from 0.3 to 35 MeV for cross-section measurements is an energy range that is of particular importance for energy applications, notably ADS and Generation-IV(GenIV) fast reactors, as well as for fusion related devices.

### 6.2.3 $\gamma$ -ray production cross-sections for inelastic scattering and (n,xn)

Inelastic neutron scattering and (n,xn) cross-sections on major construction materials, fuel and inert fuel components, moderators and coolants are among the most needed in nuclear technology applications. This includes ADS, GenIV reactors, fusion devices and security installations. The primary importance of these reactions lies in their impact on the energy distribution of the fast spectrum, thereby significantly altering most reaction rates through the so-called indirect effect. Significant uncertainties in estimated  $k_{\text{eff}}$  values for fast systems result as a consequence of the large uncertainties associated with these cross-sections. Even precision estimates of  $k_{\text{eff}}$  in light water reactors are affected. Other issues where inelastic scattering and (n,xn) reactions play an important role concern radiation shielding and, as a consequence, damage to containment structures, as well as radiation heating. In the latter case the  $\gamma$ -production cross-sections themselves are of major importance. Naturally, (n,xn) reactions additionally play an important role in neutron multiplication, e.g. for ADS and for fusion.

It should be noted that measurements of inelastic and certainly of (n,xn) cross-sections in the energy range of importance - threshold to 20 (30) MeV - are considerably more sparse than total, fission and capture cross-section measurements. At the origin of this sparseness and the often considerable scattering of the available data lie technical difficulties associated with direct measurements on the basis of neutron detection and the availability of neutron sources with suitable conditions. For reactions on actinides, the databases rely mostly on models. A typical example is the  $^{233}\text{U}(n,2n)$  reaction competing with the fission of  $^{233}\text{U}$  in the thorium based fuel cycle with fast neutron flux. As illustrated in figure 6.2 (on the left) the three main databases disagree strongly in this particular case. Equally, the (n,2n) reaction cross-sections are poorly known for  $^{241}\text{Am}$  (see figure 6.2 on the right), being one of the most important minor actinides to be incinerated.

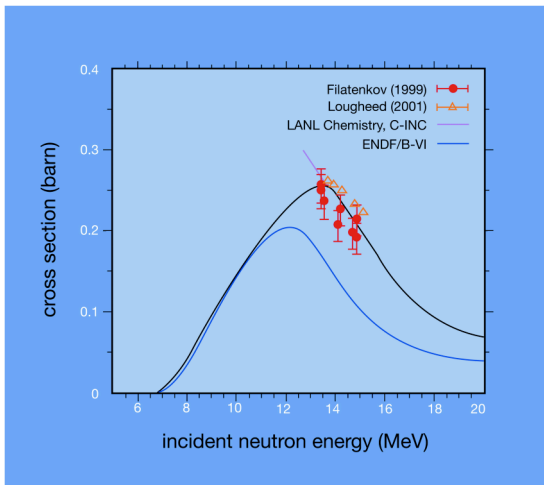
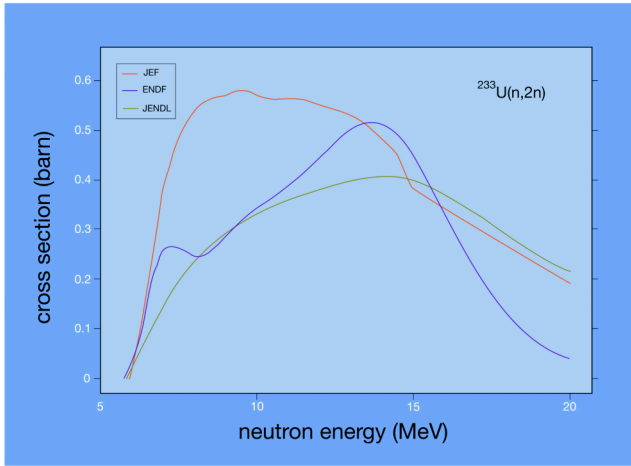


**Figure 6.2:** The present data status of the  $^{233}\text{U}(n,2n)$  (on the left) and  $\text{Am}(n,2n)$  (on the right) reaction cross-sections and different evaluations.

Other examples are the  $(n,n')$  and  $(n,2n)$  reactions on  $^{208}\text{Pb}$  as presented in figure 6.3. It has been estimated that the errors on the  $(n,n')$  cross-sections on lead, being the essential material in the design of ADS, would imply an uncertainty of  $\sim 2\%$  on the criticality calculations of such a system.

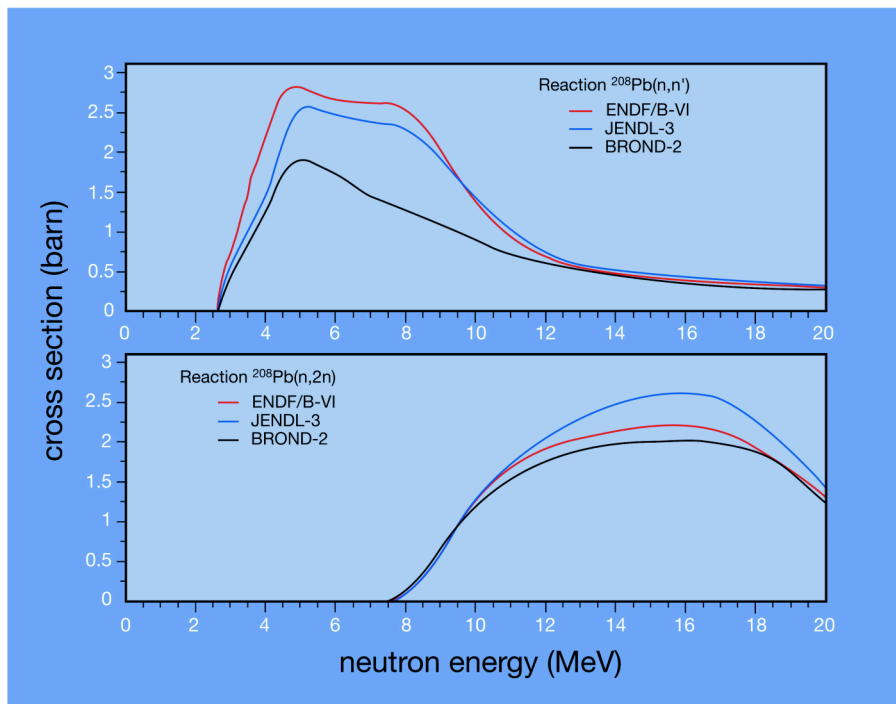


**Figure 6.3:** The  $^{208}\text{Pb}(n,n')$  (upper part) and  $^{208}\text{Pb}(n,2n)$  (lower part) cross-sections as compiled in different data files.

It was shown recently that  $\gamma$ -ray production cross-sections for photons associated with inelastic scattering and  $(n,xn)$  reactions can be reliably measured with good resolution over a wide energy range at time-of-flight facilities. These cross-sections can be used to construct estimates of the inelastic and level inelastic cross-sections and the  $(n,xn)$  cross-sections. More importantly these cross-sections are of importance to benchmark nuclear model calculations that in turn will provide the best estimates for the desired cross-sections and the neutron emission spectra. These  $\gamma$ -ray production cross-sections can serve to address issues in level density modelling,  $\gamma$ -strength functions, neutron optical models and pre-equilibrium treatments.

Recently, at the Gelina ToF facility a setup for high-resolution measurements with two large volume HPGe detectors using the fast spectrum at 200 m flight path length was developed. It was applied to  $^{52}\text{Cr}$ ,  $^{58}\text{Ni}$ ,  $^{209}\text{Bi}$ ,  $^{207}\text{Pb}$  and will shortly be employed for  $^{206}\text{Pb}$  and  $^{208}\text{Pb}$ . An example of the good energy resolution that was achieved is presented in figure 6.4 on the left and the full range of the measurements is shown in figure 6.4 on the right. It was also shown for  $^{207}\text{Pb}$  that  $(n,2n\gamma)$  measurements can be performed with this setup as well. A significant drawback of this arrangement is the very long measurement time (up to 1000 h) as a result of the low count rate (10 cps), prohibiting a rapid survey over the mass table. Required sample masses are large making studies of enriched isotopes expensive, whereas these are essential for clean spectra, disentanglement of inelastic and  $(n,xn)$  channels and studies of isotopic chains.

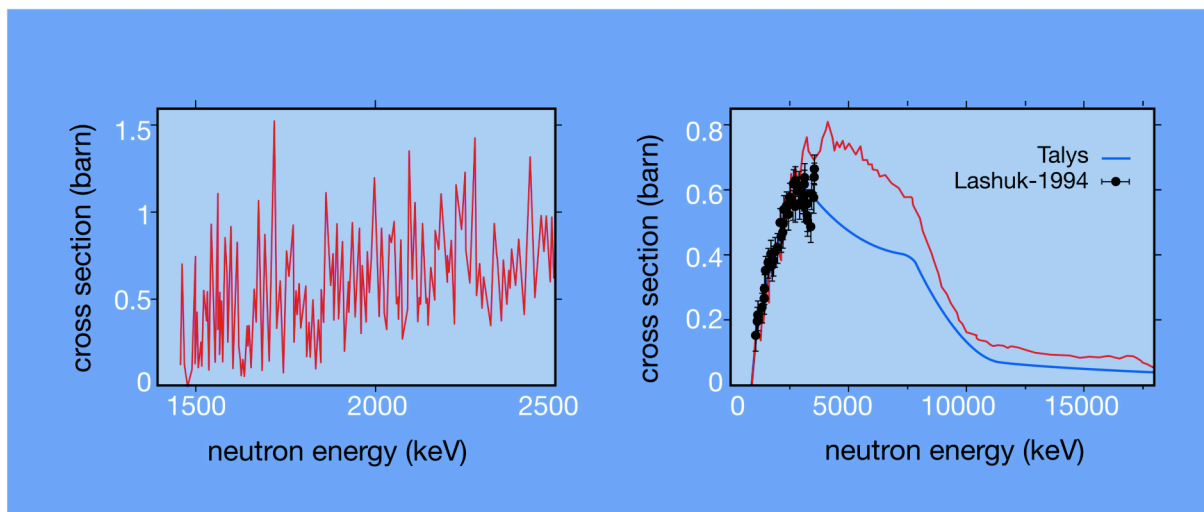


**Figure 6.4:** Detail of the excitation function for the  $2^+_1$  to ground state transition for  $^{52}\text{Cr}$  (on the left); full excitation curve for the 896 keV transition of  $^{209}\text{Bi}$  (on the right). Both measured at Gelina.

It is clear that in many cases the need for very good energy resolution is limited to the first 1 or 2 MeV above the inelastic threshold. At higher energies the instrumental resolution is broadening rapidly and the level density becomes progressively higher. On top of this, resonance widths increase and eventually become larger than the level spacing leading to a rapid washing out of the residual structure with increasing energy. In this range, an energy resolution of several percent would be adequate.

Obviously, a flight path shorter than 200 m would be sufficient. At Gelina this is prohibited by the very strong  $\gamma$ -flash. Even at 200 m with a 2 cm  $^{\text{nat}}\text{U}$  filter in the beam from one in five to one in two bursts results in a prompt  $\gamma$ -ray scattered by the sample and deposited in the detector. With conventional electronics this implies a dead time of 25  $\mu\text{s}$ , so that for such a burst no neutron-induced event is observed. In this context, an innovative method of prompt  $\gamma$ -spectroscopy, developed by IReS Strasbourg, would be used to measure such reactions. It has already been employed at Gelina, with a flight path of 200 m. It was also shown during these experiments that the effective dead-time can be reduced to 2.5  $\mu\text{s}$  using a fast digitiser (65 Mega Samples Per Second, MSPS) and on board data processing with an FPGA, thus leaving an effective range at 200 m of 20 MeV. Nevertheless, a shorter flight path would severely compromise this range of interest, since there would be a prompt  $\gamma$ -ray for each burst and the time range would be reduced to exclude measurements above 10 MeV. What is really needed is a neutron source for which a short flight path results in a number of observed prompt  $\gamma$ -rays per burst and detector of not more than  $\sim 10\%$ .

### ***SPIRAL2 & other facilities***

Prompt  $\gamma$ -ray spectroscopy has also been used at FZK (Karlsruhe), ORELA (ORNL) and WNR (LANL), where in the last case the beam has a frequency of 600 kHz with the flight path of 20 m. Table 6.1 summarises some of the potential installations where (n,X) measurements are performed.

In general, different neutron beam characteristics at various installations are suited to study the (n,X) reactions. However, none of them are ideal to measure (n,X) reactions on most of the actinides, except the nTOF facility thanks to its high intensities. On the other hand, the strong  $\gamma$ -flash present there can only be removed with beam extraction at the angle of some tens of degrees, the construction of which is not yet decided.

At SPIRAL2, the beam intensity expected is of the same order as at nTOF, but with a much higher frequency. A flight path of 20 m would allow coverage of the energy range of interest for the (n,X) reactions. At this distance the beam intensity would be large enough to allow targets of only a few hundreds of mg and still reasonable energy resolution (below 10 %). Equally, segmented detectors might be helpful in this respect. Indeed, in this case only segments are blocked where a  $\gamma$ -ray from the flash has been detected. However, one must be aware that the activity of the target cannot be separated from the reactions, so that in any case the final cross-section has to be obtained by subtraction of the long background runs.

Table 6.1: Major characteristics of (n,X) cross-section measurements at different facilities.

Beam Distance Period	$\Delta t$ between Flash and a neutron of 20 MeV	Time resolution for a 1 MeV energy resolution at 20 MeV	$\Delta t$ between two bursts with wrap- around at 0.5 MeV	Typical mass (a.u.)
200 m n_TOF 2-14 s Gelina 1.25 ms	2.565 $\mu$ s made possible with digital electronics	84 ns	19.8 ms	~90 g at Gelina ~ 2 g at n_TOF
20 m Los Alamos 20.34 m 1.8 ms	0.257 $\mu$ s Flash is weak, distributed over more than 100 bursts	8 ns	1.98 $\mu$ s the activity cannot be separated from the reaction	2.25
3 m Louvain 3.25 m 50-60 ns	0.038 $\mu$ s Flash cannot be separated from physics	1 ns TOF is impossible, beam must be mono-energetic	0.3 ms beam must be mono-energetic	0.023 high statistics, but $\gamma$ flash and activity not separated from the reaction

### ***SPIRAL2 vs Gelina***

To bring out the potential advantages of SPIRAL2 for this type of measurements reaction rate estimates were performed for  $^{56}\text{Fe}(n,n')$ ,  $^{56}\text{Fe}(n,2n)$ ,  $^{56}\text{Fe}(n,p)$  and  $^{56}\text{Fe}(n,\alpha)$ . These estimates are based on the  $E_d=33$  MeV measurements for the C(d,n) flux by Shin et al. and Fe cross-sections from the JEFF-3.0 library, judiciously extended above 20 MeV. The present estimates are for a 10 m flight path. One assumed further that a single detector with an absolute peak efficiency of  $2 \times 10^{-3}$  corresponding to a 95 % HPGe at about 12 cm from the sample. The sample diameter was 5 cm and the thickness was given by the criterion of 10 % neutron attenuation for a total cross-section of 2.5 b (77 g of Fe). Table 6.2 shows the counts per second that would result in the case when a single  $\gamma$ -ray is emitted. In reality the number of emitted  $\gamma$ -rays will be larger, the average increasing with energy. Conservatively an average of two will be assumed leading to roughly  $5 \times 10^4$  cps. For comparison, at Gelina the count rate would be about 10 cps. Evidently, the improvement comprises nearly four orders-of-magnitude.

Table 6.2: Expected count rates at 10 m for 77 g of Fe, one 95% HPGe detector at 12 cm and one  $\gamma$ -ray emitted per reaction ( $E_d=33$  MeV,  $I_d=28$   $\mu$ A on graphite target).

Reaction	Count rate, cps
$^{56}\text{Fe}(n,n')$	18000
$^{56}\text{Fe}(n,2n)$	5800
$^{56}\text{Fe}(n,p)$	1300
$^{56}\text{Fe}(n,\alpha)$	475

To understand how these four orders-of-magnitude can be used effectively one first needs to take a look at three experimental constraints: energy resolution, dead time and the rate of prompt events.

### Energy resolution

Figure 6.5 shows the relative energy resolution for several conditions. For large volume HPGe detectors, a time resolution of 8 ns fwhm is routinely achieved at Gelina using conventional electronics and was demonstrated to be accessible with a 400 MSPS 12-bit digitiser, as well. Even, under these favourable conditions the energy resolution at 10 m is worse than 10% above 20 MeV, whereas it stays below 7.5 % for the entire energy range at 20 m. Thus, for a physically meaningful measurement a 20 m flight path would be required.

For a Ge detector, the 8 ns fwhm is achievable with conventional electronics at the expense of a great number of lost events, especially below  $E_\gamma=500$  keV, as a result of the use of the slow rise time rejection scheme. Using a 400 MSPS 12 bit digitiser similar timing can be achieved without this set back. This is not the case for the lower sampling rate of 65 MSPS, mentioned above.

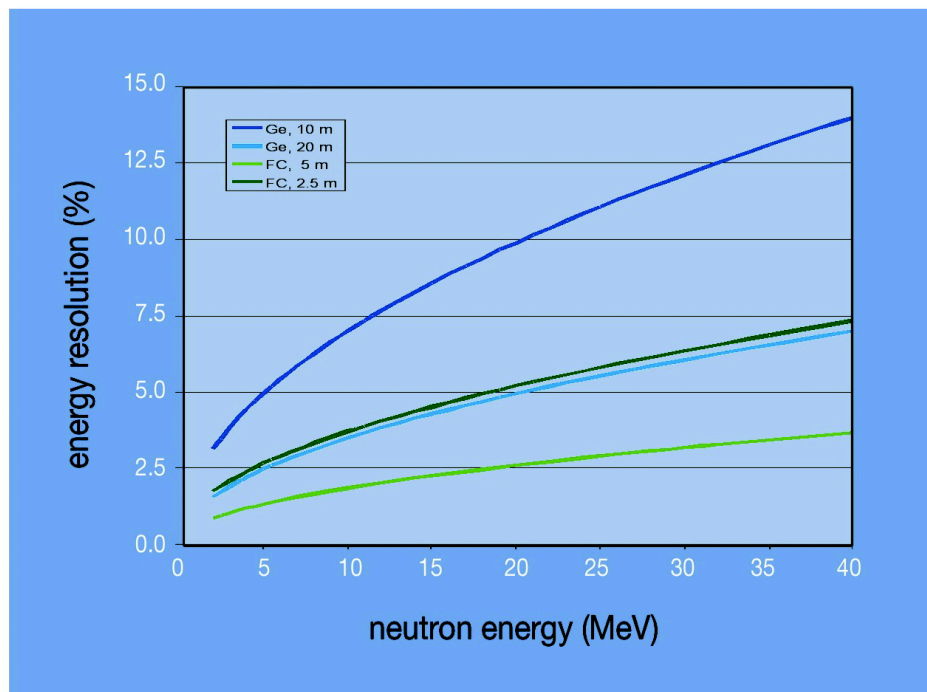


**Figure 6.5:** Relative energy resolution (fwhm) for different flight path lengths and detectors. An accelerator burst width of 0.3 ns was assumed. The flight path uncertainty was determined by the source (0.6 cm) and the sample (0.6 cm). The time resolution for Ge was taken as 8 ns, whereas 1 ns was assumed for the fission chamber.

### Dead time

For precise cross-section measurements dead time corrections should be of the order of a few percent. As argued above the dead time for conventional electronics is long (about 25  $\mu$ s), whereas for fast digitisers it can be as short as 2.5  $\mu$ s, provided the data transfer rate is negligible. The latter was demonstrated with on-board processing by means of an FPGA for the 65 MSPS digitiser of IReS Strasbourg and is expected to be available in the future for the 400 MSPS digitiser under test at Gelina, as well. Thus a  $\sim 2.5$   $\mu$ s dead time and a 2 % dead time correction would imply a count rate for a single detector of maximum 8000 cps. This is

still a factor of 800 higher than the rate at Gelina, so that the statistics obtained in 1000 h there would be attained in slightly more than one hour at SPIRAL2.

### ***Rate of prompt events***

Shin et al., measured a prompt photon yield at zero degrees for  $\gamma$ -rays above 1.5 MeV of  $4.2 \times 10^{-3}$   $\gamma$ /sr/d. At 28  $\mu$ A and 5 cm sample diameter this implies that  $1.5 \times 10^7$  of such  $\gamma$ -rays are incident on the target. Assuming all are scattered isotropically and taking a 1 % total efficiency this implies  $1.5 \times 10^5$   $\gamma$ /s detected. Thus, for one in three bursts the detector sees a scattered photon (10 m flight path). This seems far from the desired few percent, however, it is no problem to come to the wanted value by going to 20 m and reducing the sample size by a factor of 200. The present estimate at 10 m merely highlights the reduction of the prompt background compared to that at Gelina, where the same value was attained only at 200 m and with the help of a thick uranium filter.

### ***Summary***

SPIRAL2 offers favourable conditions for the measurement of cross-sections for  $\gamma$ -rays emitted in inelastic and (n,xn) reactions. Adequate energy resolution over the entire accessible range requires a 20 m flight path. At 20 m, a 100 h run on a 200 times smaller sample mass, would result in similar statistics to those attained in Gelina in a 1000 h run. Thus, systematic studies on isotope chains are readily accessible, since enriched samples on the order of 0.4 g would suffice. Under these conditions the prompt  $\gamma$ -rays will not disturb the measurements. The small samples have the added advantage of negligible sample size and  $\gamma$ -attenuation corrections.

A measurement facility of this type can readily be deployed to provide a coherent study of several isotope chains (Si, Fe/Ni, Zr/Mo, W, Pb, Th/U) throughout the mass table to assist nuclear model development and can be focussed on key materials of interest to applications (Si, Cr, Fe, Ge, Pd, ...). The potential for the use of advanced HPGe detectors/arrays in these measurements is evidently large. Any increase in efficiency (detector number) allows one to reduce the sample masses further, thus enabling the study of more exotic samples. Any decrease in the Compton background would potentially enable the technique for the study of weaker cross-sections, such as those associated with (n,xp) and (n,x $\alpha$ ) reactions. Increased detector numbers and segmentation open the route to measurements on more highly radioactive targets than the 'stable' actinides. It may be noted that in connection with radiation damage the study of (n,xp) and (n,x $\alpha$ ) reactions is of particular importance to support radiation damage studies. A well-known problem area for which measurements are particularly scarce is the range from 5 to 35 MeV, which is exactly the range covered by SPIRAL2.

Important experimental constraints not mentioned above are a well-collimated beam and a measurement room with negligible background count rate. The latter would require effective shielding between the measurement room and the source, a defining collimator sufficiently upstream to allow the detectors to be shielded from this collimator and a beam dump sufficiently downstream to allow effective shielding towards the detectors. Evacuated flight paths would be needed.

## 6.2.4 Fission cross-section measurements

For the energy range provided by SPIRAL2 fission cross-sections for minor actinides are of key importance for studies related to waste management in nuclear reactors. The main isotopes of interest are those of americium and curium, but contemporary studies include those of uranium, thorium and protactinium that are of interest to the Th/U fuel cycle. In addition, such cross-section measurements, and in particular an accurate study of their shape, would greatly help nuclear model development (fission barrier systematics, level densities, transition states and fission modes, etc.).

To enable such measurements use can be made of Frisch-gridded ionisation chambers using current amplifiers read out with digitisers. Energy resolution would be excellent even at 5 m (see figure 6.5) and events can be separated up to rates of  $\sim 10^6$  cps. Using the same data as above and a 5 m flight path about 10  $\mu\text{g}$  of material would be needed to provide  $3 \times 10^5$  counts in a run of 100 h, or about 3 % statistical error in 0.1 MeV bins (estimated for  $^{243}\text{Am}$ ). As the  $\alpha$ -activity would have to be limited to 1 MBq this implies that measurements are feasible for  $^{230,232}\text{Th}$ ,  $^{231}\text{Pa}$ ,  $^{233,234,235,236,238}\text{U}$ ,  $^{236,237}\text{Np}$ ,  $^{239,240,241,242,244}\text{Pu}$ ,  $^{243}\text{Am}$  and  $^{245,246,247,248}\text{Cm}$  in addition to the  $\beta$ -emitters  $^{233}\text{Pa}$  and  $^{241}\text{Pu}$ . This excludes several important nuclides that are currently poorly studied:  $^{232}\text{U}$ ,  $^{238}\text{Pu}$ ,  $^{241,242}\text{Am}$  and  $^{243,244}\text{Cm}$ . For these the conditions at SPIRAL2 are marginal and another factor of  $\sim 10$  in flux would be desirable. This may be achieved by a shorter flight path (e.g. 2.5 m) and any gain in neutron source intensity, such as suggested above (carbon target versus beryllium or lithium target and primary beam bunching).

The main advantages of SPIRAL2 over the quasi mono-energetic sources, currently employed to study these reactions, are the continuous energy measurement of the excitation curve with good resolution and a better handle on low energy contaminant neutrons. In fact, the low energy neutron problem at a time-of-flight facility is dominated by room scatter and overlap neutrons. The first is minimised by proper collimation, low sample mass and detector arrangements. The second by avoiding, as much as possible, any components near the neutron source that may scatter neutrons into the flight path or that are efficient moderators. Such considerations are generally of no interest for nuclides with a threshold for fission, but are of key importance for nuclei with large thermal fission cross-sections. The latter are often unwanted contaminants in samples consisting predominantly of the former type of fissile nuclei.

## 6.2.5 Double differential (n,chp) cross-section measurements

In view of the conditions at SPIRAL2 being more favourable than those at WNR (LANL) in the energy range from 5 to 35 MeV, it is evident that a measurement programme of double differential charged particle cross-sections, with a setup similar to that pioneered at WNR, would also be feasible at SPIRAL2. The use of such measurements was argued above in terms of applications (radiation damage). In terms of nuclear physics it is important to note that nuclear modelling of this type of reaction at low energy is considerably more complicated than it is at higher energies. The part of the optical model probed by light-charged particle scattering is different from that probed by the light-charged particle that is emitted in a neutron induced reaction (in particular for the  $\alpha$ -particle). The dispersive contribution to the optical model is of key importance and the theory of the imaginary part of the potential is not advanced to the point that it is readily used for cross-section predictions. Moreover the study of complex particle (d,t, $^3\text{He}$ ) emission in equilibrium and pre-equilibrium reactions would

greatly benefit from a systematic set of new results. It would be of interest to encourage experimental activity in this area.

### 6.3 QUASI MONO-ENERGETIC NEUTRONS

It was briefly discussed that DC deuterons in the 0.75 to 4(7) MeV range could be used to produce quasi mono-energetic neutrons with the (d,D) and (d,T) reactions making full use of the 5 mA current available from the source. For comparison, this would provide an intensity gain of 100 to 1000 over most available van de Graaff facilities where such reactions are currently employed. The main point that was not addressed so far and which is worth considering is the requirements on target cooling and stability.

Should a target be feasible, then one has for the first time a neutron source in the range below 14 MeV (4-10 MeV) and above 14 MeV (16-20 MeV) comparable in intensity to neutron generators. Thus, sample masses conventionally employed for instance for fission, capture and activation studies could be reduced 100 to 1000 times, or activation studies would result in 100-1000 times larger activities. The range of achievable measurements is then very large. For instance (n,2n) cross-sections below and above 14 MeV with the activation technique would be greatly facilitated for important target nuclei such as  $^{239}\text{Pu}$ ,  $^{232}\text{Th}$  and  $^{241}\text{Am}$ . All the above mentioned fission cross-sections would be easily accessible. It would be worthwhile to learn about the feasibility of such a neutron source and the state-of-the-art of high power D and T targets.

### 6.4 ASTROPHYSICS WITH NEUTRONS AT SPIRAL2

The very high neutron flux at SPIRAL2 offers two unique options for astrophysical applications:

#### Preparation of radioactive samples

The neutron capture cross-sections of radioactive isotopes are crucial for the interpretation of s-process branching ratios and are of increasing interest for the development of quantitative models of explosive nucleosynthesis in the r- and p-processes. Presently, it is difficult to produce the samples for such measurements in the required amounts and purities. The high flux of neutrons with energies in the MeV range would allow one to obtain suitable samples via (n,p), (n, $\alpha$ ), and (n,2n) reactions by irradiating selected materials either in parasitic mode or in dedicated runs of about a few weeks. The proper choice of the reaction type will help to separate the product nuclei by physical and chemical methods. A promising example is the production of  $^{85}\text{Kr}$  via the  $^{85}\text{Rb}(n,p)$  or  $^{88}\text{Sr}(n,\alpha)$  reactions. Other interesting reactions are  $^{13}\text{C}(n,\alpha)^{10}\text{Be}$  and  $^{66}\text{Zr}(n,\alpha)^{63}\text{Ni}$ . Typically 10 days irradiation would result in more than  $\sim 10^{17}$  atoms created with 10 g samples.

#### Activation

The unstable isotope  $^{60}\text{Fe}$ , which was discovered in deep-sea sediments, has a half-life of  $\sim 1.5$  Million years. Therefore, the proto-solar nebula must have been contaminated by substantial amounts of that isotope. Whether it was produced by a nearby supernova or Red Giant star is still an open issue. A reliable answer can be given only if the s-process production can be determined on the basis of experimental (n, $\gamma$ ) cross-sections of  $^{59}\text{Fe}$  and  $^{60}\text{Fe}$ . Likewise, this important information can be obtained by irradiation of a pure  $^{58}\text{Fe}$  sample and the subsequent detection of the  $^{60}\text{Fe}$  produced. Such double neutron capture

studies could be possible in the high flux of SPIRAL2, provided that the fairly long irradiations can be carried out in parasitic mode in combination with material studies, which are planned anyway.

## 6.5 MATERIAL IRRADIATION STUDIES

The development of new fusion and fission reactor systems depends critically on the development and testing of materials that can retain their strength, ductility, and shape, among other characteristics, under intense radiation. Because of its high flux, particular energy spectrum and versatility, SPIRAL2 has a huge potential to conduct these materials tests. Detector testing and irradiation of electronic components also could be performed within a reasonable irradiation time, thanks to the high neutron fluxes and variable thermal conditions available. Compared to presently available fast neutron generators, the two orders-of-magnitude superior intensity of the SPIRAL2 neutron beam would offer the unique possibility to reach the precisely calibrated spectral flux at the position of irradiated samples by combining various model calculations and data from spectral measurements performed by both the multi-foil activation and proton-recoil telescope methods.

### 6.5.1 Fusion related research

As summarised in Table 6.3 the SPIRAL2 facility would be able to provide comparable neutron flux density and irradiation temperature conditions to those at ITER (controlled fusion demonstration reactor) but for rather limited sample volumes. Typical numbers for SPIRAL2 are as follows: with the neutron flux higher than  $\sim 5 \times 10^{13} \text{ n s}^{-1} \text{ cm}^{-2}$  and material damage rates greater than  $\sim 3$  displacement per atom/full power year (dpa/fpy) one obtains  $\sim 10 \text{ cm}^3$  of a useful irradiation volume. Taking into account realistic beam availability constraints one could expect more than 1 dpa per year in  $\sim 10 \text{ cm}^3$ , i.e. 4 month irradiation per year at full power. It is important to emphasize that a variable temperature environment (between  $20^\circ\text{C}$  and  $1000^\circ\text{C}$  or higher) for irradiations would be possible at SPIRAL2.

One notes that, although the neutron energy distribution of SPIRAL2 (average neutron energy  $\sim 13\text{-}14 \text{ MeV}$ , i.e. being nearly identical to “IFMIF – green line” as presented in figure 6.6) is quite different from the fluxes predicted for the first wall of “ITER – blue line”, the ratio of gas production over dpa rates is rather comparable. In the case of SPIRAL2 one obtains  $\text{He/dpa}=13$ ,  $\text{H/dpa}=51$ , while for ITER one finds  $\text{He/dpa}=11$ ,  $\text{H/dpa}=45$ .

Table 6.3: Maximal (on the target back-plate over the beam spot dimensions) neutron flux, displacement rate, gas production and nuclear heating SPIRAL2. The fpy stands for full power year, dpa – displacement per atom, appm – atom parts per million. All values are for  $^{56}\text{Fe}$ .

	Neutron flux, (n/(s cm <sup>2</sup> ))	Damage rate, (dpa/fpy)	Gas prod. (He), (appm/fpy)	Gas prod. (H), (appm/fpy)	Nuclear heating in <sup>56</sup> Fe, (W/cm <sup>3</sup> )
SPIRAL2	$1.1 \times 10^{14}$	7	95	378	3
ITER*	$4.0 \times 10^{14}$	12	140	540	12

\*These are the maximal expected values.

It seems that SPIRAL2 with the major characteristics summarised above would be able to contribute significantly in testing and qualifying materials under fusion-specific irradiation conditions. In particular, irradiations of miniaturised samples to test their limitations and development qualification of dedicated modelling tools seem to be very attractive. SPIRAL2 could also be considered as an intermediate step towards new generation dedicated irradiation facilities such as IFMIF (d(40 MeV) + Li;  $I_d=200$  mA ) expected only beyond ~2015.

## 6.5.2 Fission related research

As in the case of fusion related research, SPIRAL2 could also be used for fission applications, in particular in the case of advanced material development, calibration and validation of data for commercial fission reactors and particle accelerators. In some particular cases, innovative nuclear fuel is  $\mu$ -structured (in the form of micro-particles), and contains very thin layers of various materials (see figure 6.7). Therefore, even the  $\sim 10$  cm<sup>3</sup> irradiation volumes available at SPIRAL2 are sufficient to test different materials of such fuel and structure components in terms of burn-up, integrity of structure and barriers and resistance to high energy neutron irradiations at variable temperatures.

Thanks to the advances in the numerical simulations and new measurement tools, even a few dpa in a few mm<sup>3</sup> become of great interest, if the results are available in a short time for interpretation and progress in model development. It seems that present numerical simulations have a huge potential to bridge the gap between “small scale” experiments towards “real scale” tests in terms of validation, transposition and extrapolation, in this way building a shorter path from basic science to application oriented design tools.

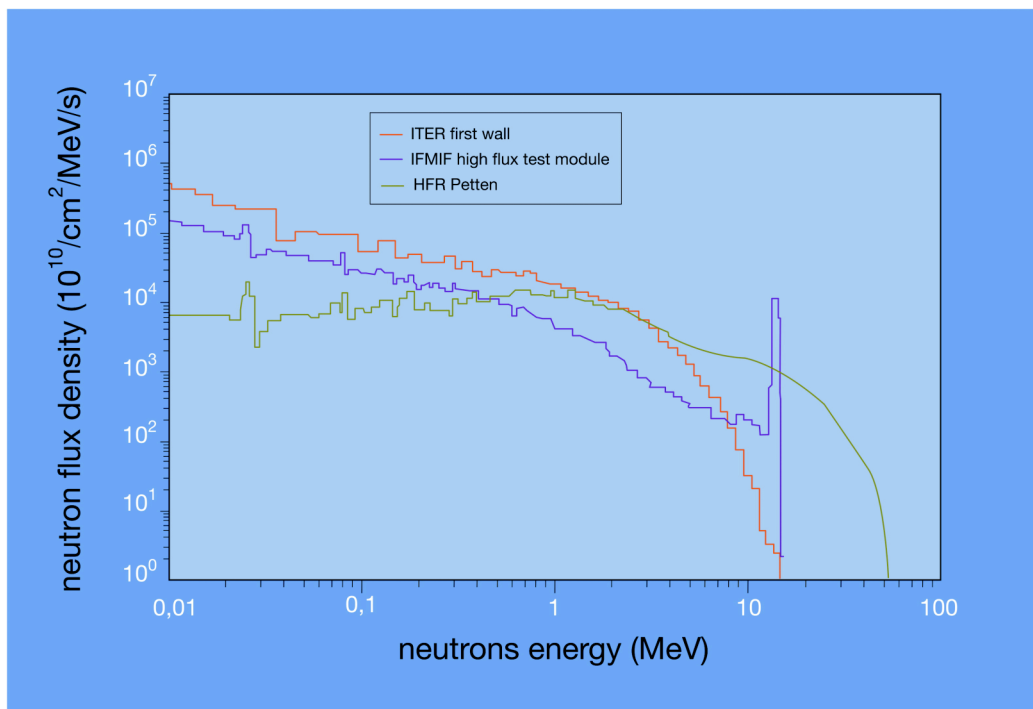


**Figure 6.6:** Comparison of typical energy spectra of neutrons in the case of nuclear reactor “HFR Petten”, “IFMIF” or “SPIRAL2” and “ITER first wall”.

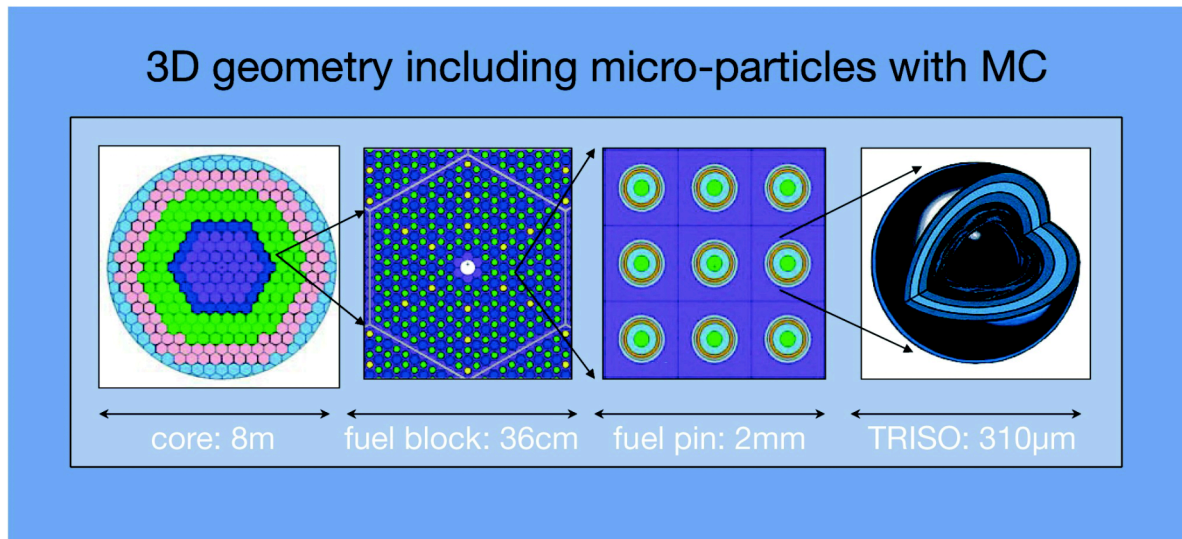


**Figure 6.7:** Simplified picture of different structure elements of the innovative high temperature reactor GT-MHR: from reactor core (~8 m) to microscopic fuel particles (~300  $\mu\text{m}$ ).

Finally, it is important to note that one could also profit from access to the heavy ions of the present GANIL accelerators. Some irradiations could be done with ions and later on with neutrons at the same installation.

### 6.5.3 Testing of neutron detectors

The use of intense fluxes of high-energy neutrons from SPIRAL2 would be ideal for characterisation of so called CVD Diamond Detectors, calibration of which is urgently needed in the neutron energy range from 14 MeV to 20 MeV. In this context, the contributions of competing inelastic reactions such as  $(n,\alpha)$ ,  $(n,p)$ ,  $(n,d)$ , etc. should be known with much better precision than today. In particular, a compilation of data on the reaction  $^{12}\text{C}(n,\alpha)^9\text{Be}$  (see figure 6.8) and also neutron induced reactions on  $^{13}\text{C}$  is urgently needed.

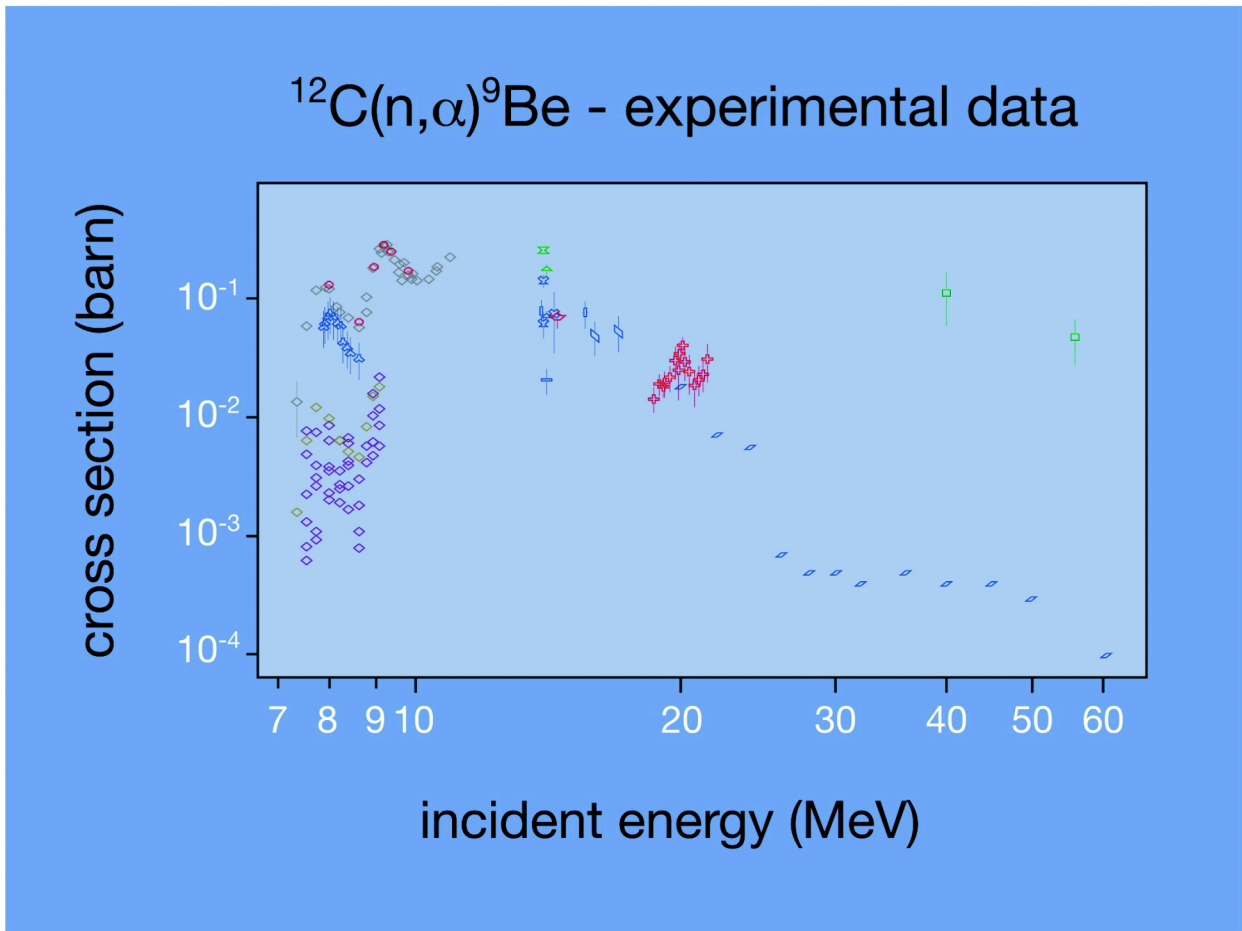


**Figure 6.8:** Status of the available data on the  $^{12}\text{C}(n,\alpha)^9\text{Be}$  reaction channel (note the log-log scale)

Irradiations of such detectors with SPIRAL2 neutrons (desired fluence rates could be obtained in less than 1 hour at full beam power) would permit one to explore radiation damage mechanisms, define sensitivity and the life-time of such and other detectors, optimise their geometry, materials, signal-to-noise ratios, etc. in “hard” irradiation conditions with high energy neutrons.

## **7. *INTERDISCIPLINARY RESEARCH: PERSPECTIVES OFFERED BY SPIRAL 2***

Nuclear Physics has been a prolific source of applications both in other branches of Science and in everyday life. These applications have been based on both the phenomena uncovered by our fundamental studies of the atomic nucleus and the experimental methods and techniques we have invented in order to study nuclei. Nuclear physics has given birth to whole areas of scientific activity: Particle physics, synchrotron radiation studies, reactor- and spallation-based neutron sources and controlled materials modification by ion implantation are amongst the many applications of nuclear physics to other areas of science. Our knowledge of nuclear reactions and decays has allowed us to answer questions about the Age of the Earth, the heating of its interior, how the chemical elements were and are created in stars and how the energy is generated to make the stars shine and fuel the spectacular events such as supernovae, novae, X-ray bursters and the like we see with our telescopes. Our everyday life has also been altered inter alia by nuclear power generation, radiation therapy and non-invasive medical imaging.

From its inception the GANIL facility has played its part in this story by providing excellent facilities for interdisciplinary research. The process of exploiting these facilities has been greatly aided a) by the presence of a laboratory (CIRIL) dedicated to welcoming experimenters working in the interstices between scientific disciplines and developing techniques and facilities to aid them and b) by the availability of a wide range of ion beams (from eV to GeV) of high quality. The interdisciplinary research at GANIL covers the entire domain from ion-atom collisions to the relaxation of materials under irradiation whatever their nature and, of course, the applications of the induced effects and the testing of materials and components. Several important results for the understanding of matter under excitation come directly from experiments performed with the ions from the GANIL accelerators. The unified descriptions of the structural modifications induced by intense electronic excitation, the discovery of phase transitions driven by the ionisation processes and the demonstration of the role of multi-ionisation in the radiolysis of water are all examples. None of these results would have been obtained without dedicated apparatus such as the irradiation chambers and the scanning magnets that ensure that the irradiation fluence provided by the GANIL beams is homogeneous.

SPIRAL2 will provide not only a new range of radioactive beams (RIB) of high quality but also stable beams with extremely high intensities (HISB). Both opportunities open new doors for those who apply the GANIL beams to interdisciplinary problems and this community has a marked interest in exploiting them. In this chapter we outline six areas of particular importance in the field of interdisciplinary research where the SPIRAL2/GANIL beams will make a significant impact. The principal goals for each of these areas are the following:

### **Atomic physics**

The HISB will open up the possibility of performing experiments involving collisions between fast and slow ions. Such measurements are essential if we are to gain an understanding of collision processes in the so-called “intermediate velocity regime”, which is where the maxima of most of the interaction cross-sections occur.

The study of hyperfine quenching in highly charged ions is one route to testing QED (Quantum Electro Dynamics). The application of HISB will improve the precision of these measurements. Similar measurements on radioactive species are also planned in order to obtain information on their nuclear magnetic moments.

#### Condensed matter- RIB

Radioactive ions are extremely useful probes of solids on the atomic scale. This is a field which has been developed and exploited particularly well at ISOLDE-CERN. Given the availability of intense beams of mass-separated ions at SPIRAL2 it could readily become a complementary facility to ISOLDE in this field.

Slow, mono-energetic positrons are interesting and useful probes of surface states and of defects near surfaces in solids. The RIBs from SPIRAL2 could be used as a source of high emissivity, high intensity slow positron beams thus opening up many opportunities for studies of surfaces, materials and atomic physics.

#### Condensed matter - HISB

Radiation damage in materials is one of the crucial issues for the success of Generation III and IV fission reactors and future fusion reactors. The simulation of the long term neutron irradiation of these reactors by bombardment with ions offers significant benefits. Despite the limited thicknesses of the samples that can be modified using the light ions from LINAG, the high rate of damage induced by these beams makes them an interesting tool for radiation damage studies.

## 7.1 FAST ION – SLOW ION COLLISIONS

One of the long-standing desires of atomic collision physicists. is to perform ion-ion collision experiments in the intermediate velocity regime, where the cross-sections peak. Although ion-ion collision experiments are routinely performed by high energy physicists, in atomic physics they have so far been performed only with slow ions, in the context of magnetically confined plasmas. The availability of intense stable beams from LINAG will offer new opportunities to perform such experiments.

There is not just a fundamental interest in understanding the mechanisms involved in ion-atom collisions; such studies are also motivated by the importance of various aspects of the energy deposition of fast ions in matter to an understanding of materials modification and biological effects. The largest effects are observed at the maximum of the stopping power, corresponding to ion velocities close to the mean orbital velocities of the target electrons. This velocity domain is called the “intermediate velocity regime” (see figure 7.1).

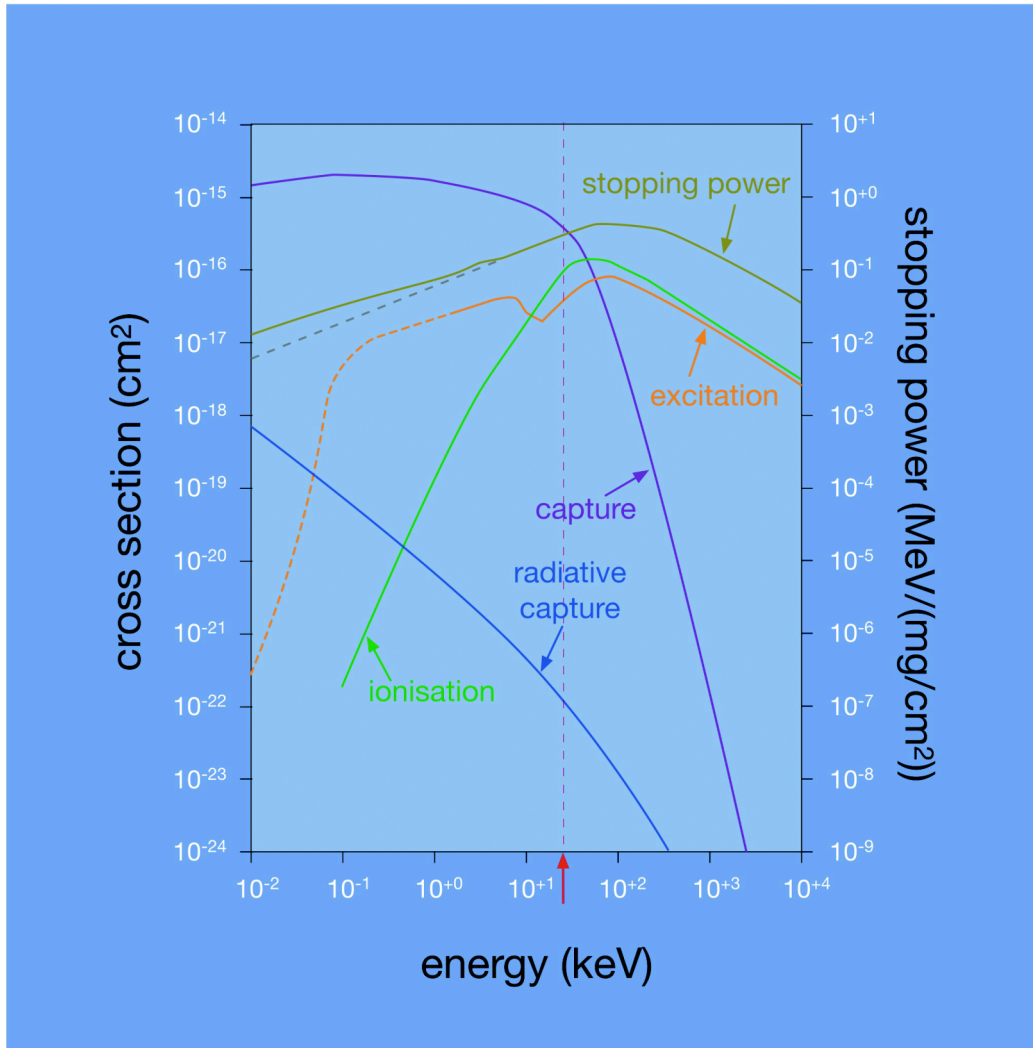


**Figure 7.1:** Cross-sections of elementary atomic collision processes for the system  $p \rightarrow H$ . The dotted line and the vertical arrow indicate the proton energy where it has a velocity equal to the hydrogen electron velocity. Also shown is the stopping power for protons in aluminium.

In this regime the cross-sections for electron capture, loss and excitation are all at a maximum and of the same order-of-magnitude, leading to “interference effects” that must be taken into account in any theoretical treatment. This circumstance leads to the paradoxical situation where, for this velocity regime, cross-sections are very hard to predict while at the same time a knowledge of these cross-sections is most important. It is a fact that, beyond the pure three body case (a bare ion and a hydrogen-like target), none of the most sophisticated available theories is able to treat these three processes together on the same footing. When electrons are bound to the target and/or to the projectile nuclei, many complicated effects have to be considered: capture channels, which are open for bare projectiles may be closed and multi-electron processes often become as large as single-step processes. Moreover, the presence of these electrons can lead directly to an increase (“antiscreening effects”) or decrease (screening) in the collision probabilities. In any case, a significant test of the available theories can only be carried out by beginning with studies of the simplest ion-ion collisions and then moving on to more complex situations where numerous electrons are present.

In the same context, studies of the interaction of heavy ions in hydrogen or deuterium plasmas have been driven by the fact that they are important in the physics of inertial confinement plasma fusion. It has been shown that the ionisation of the medium leads to strongly reduced capture cross-sections, an increase in the projectile charge state and a corresponding increase in stopping power. Present studies and future projects (at FAIR for instance), are extending such studies to plasmas of higher atomic number. However, it becomes, for obvious reasons, harder and harder to produce fully ionised media, and starting with low  $Z$  ions many charge states are present at the same time. Moreover, the ionic charge states are changing very quickly as a function of time, and their dynamics are strongly sensitive to impurities. The resulting observed effects correspond to the average and involve several simultaneous processes. It becomes very hard to extract direct information on the modifications of the elementary processes when the mean charge state of the plasma is changing. Once again, direct studies of ion-ion collision processes are needed.

The availability of intense, stable beams of high optical quality from LINAG offers new opportunities to perform such experiments. A “high” energy beam (typically argon ions at 10 MeV per nucleon delivered by LINAG) will cross a low energy beam (typically argon ions of a few keV per unit charge delivered by an ECR source). The cross-sections to be measured are in the range of  $10^{-16} - 10^{-20} \text{ cm}^2$ , quite large compared to nuclear physics cross-sections. However, beam intensities for highly stripped ions are much lower than for proton (or electron) beams. Thus for 1  $\mu\text{Ae}$  fully stripped argon ion beams of both energies with a 2 mm mean height, a typical acceleration voltage of 10 kV for the low energy ions and a  $10^{-20} \text{ cm}^2$  cross-section, the counting rate would be just  $6 \cdot 10^{-5}$  events per second! However, with 100  $\mu\text{Ae}$  beams becoming available for high energy ions with the LINAG, and pulsed beams (both should be pulsed) of 3/100 duty cycle for instance, one would get 20 events/s. This would open the possibility of performing systematic studies on a large range of projectiles in different charge states and with different velocities.

## 7.2 PROBING NUCLEAR PROPERTIES WITH ATOMIC MEASUREMENTS ON ION BEAMS

For many years, hyperfine quenching (the acceleration of the decay of metastable states by coupling them with short-lived states through the hyperfine interaction) has been studied as a means of measuring fine structure splitting (between, e.g., the  $1s2p \ ^3P_1$  and  $1s2p \ ^3P_0$  levels) in highly charged ions. These experiments are carried out using the beam-foil technique, where a thin foil is used as a target, and one measures the decay length of the excited states created in the foil: a slit with a width of the order of the decay length is moved behind the foil, and the X-ray intensity is recorded as a function of the slit position. Very often the experimental accuracy is limited by the cascades, by statistics and by the alignment of the beam. Typically these experiments were carried out with intensities of the order of one to a few hundred enA of ions in the required charge state (i.e., stripped in a stripper foil before the target and charge analysed to select a charge state of  $q + 1$ , where  $q$  is the charge state one wants to study). The initial state is then populated by electron capture in the target.

Most of the work has been carried out using He-like ions, as a test of QED (Quantum Electro Dynamics) in two-body systems with  $28 \leq Z \leq 79$ . There are several reasons to make accurate measurements of the fine structure of doubly-charged ions over a wide range of  $Z$ . One important reason is connected to the fact that the theoretical and experimental fine-structure values in He disagree by more than 6 standard deviations, with three concurring independent experiments. Consequently, this is a strong incentive to perform such studies

with high-intensity stable beams at SPIRAL2. The second incentive is that QED calculations for bound states with quasi-degenerate states such as  $1s2p\ ^3P_1$  and  $1s2p\ ^1P_1$  are still in their infancy and require more accurate experimental tests.

There are other motives for developing a new generation of hyperfine quenching experiments including those involving radioactive ions. The lifetime of the quenched state is inversely proportional to the square of the nuclear magnetic moment. The measurement of the lifetime will thus lead to a determination of the nuclear magnetic moment. An advantage of this method is that it does not require an a priori knowledge of the magnetic moment to be measured.

#### Stable beams from the LINAG

The LINAG offers high-intensity beams of moderate energy, compared to the GANIL cyclotrons or other facilities such as GSI. For stable ions ranging from vanadium to krypton it is likely that the high-intensities available could more than compensate for the lower energy (a measurement on Ag was performed in barely adequate conditions at GSI at 18MeV/A, and then redone at GANIL with much higher accuracy —1% versus 10%—thanks to the higher energy). One could also improve the experimental procedure by replacing the movable slit by a multi-slit system in front of a multi-strip or segmented detectors. Such an option would be very expensive, and requires that the detector spatial resolution is at most of the same order as the decay length. In that case, one could use the high intensity available at the LINAG to cut into the beam emittance using narrow slits, improving the alignment, improving the statistics, and getting rid of the cascade by looking much further downstream than in previous experiments.

With the energies available at the LINAG, the window of real opportunity is for elements from Ar to Kr or a bit higher. For Kr, the stripping of a  $\sim 20+$  beam with a rather thick C foil ( $\sim 500\mu\text{g}/\text{cm}^2$ ) yields  $\sim 10\%$  hydrogen-like Kr. This is  $\sim 2.5$  times less than at 35 MeV, which would be the ideal energy and could be further improved by using a Be foil. A C target of  $\sim 200\mu\text{g}/\text{cm}^2$  would give  $\approx 60\%$  of helium-like ions. One could then expect a factor of 10 improvement in the counting rate. The decay length at 14.5 MeV/u would be 1mm for  $^{83}\text{Kr}$  (magnetic moment  $0.97\mu_N$  and spin  $9/2$ ). Since these conditions would degrade considerably when going to higher  $Z$ , one could also look at heavier ions with more than two electrons, with detectors designed for UV or visible light. It should be noted that with very high intensities at relatively low energies the stripper would be damaged very quickly. Damage to the target would be even more of an issue as shape changes in the target have some effect on the apparent decay length.

For such experiments one needs a good quality, small diameter, parallel beam (i.e., low emittance). Then the detector can be very close to the beam to improve the counting rate without creating an excessive background. To improve the accuracy another very important parameter is the background, which should be minimised. One factor in doing this is the quality of the vacuum. Another means of dramatically reducing the background is to be able to measure coincidences between the X-rays and magnetically separated ions. One can then ensure that one takes only X-rays from the right charge state, which reduces both the background and contributions from metastable states in ions with different charges. In these conditions one can hope to reach accuracies of  $\sim 0.1\%$ , some ten times better than anything done so far.

### 7.2.1 Radioactive beams after CIME

At SPIRAL2 the intensities of radioactive beams at the exit of CIME are higher than presently available and there is then a hope of being able to design experiments to measure hyperfine quenching in radioactive isotopes, There could be an interest in measuring to 10% the hyperfine quenching of short-lived radioactive isotopes, to get a measurement of their nuclear magnetic moment to 5%. That will require the multi-slit/position sensitive detector combination. If such a system allows for a factor of ten improvement in efficiency compared to the one slit experiments, which have been typically performed with  $5 \times 10^{10}$  particle/s, one could do measurements with the most intense radioactive beams available for Kr and below for helium-like ions or for Xe ions with more electrons (Be-like, Mg-like and Zn-like ions are possible candidates if suitable detectors can be found).

### 7.3 THE NUCLEAR RADIOACTIVE PROBE FOR SOLID STATE PHYSICS

Nuclear Physics techniques have been widely used in materials science for a long time. A prime example is the use of ion beams to modify the properties of materials on the one hand, and to analyse the location and chemical nature of their constituents on the other. Beams of radioactive nuclei greatly expand the scope of such applications and the last decade or so has seen rapid growth and development in the use of low energy ( $< 400$  keV) beams of radioactive isotopes to study the properties of solid state materials. Radioactive ion beams are used to explore where implanted ions end up and to investigate the environment there. In semiconductor materials for instance, it is important to know the nature of the sites on which implanted ions end up; to obtain information on their local environment. Thus at the most basic level an impurity atom may act as an acceptor on a substitutional site but as a donor if it is an interstitial. CERN-ISOLDE, in particular, has been the scene of major advances in this area. Although there is some emphasis to date on semiconductors they have also been used to study metals, insulators, magnetic materials, superconductors, surfaces and interfaces.

The properties of materials are not the result of their crystallographic structure alone but are also determined by any embedded defects or impurities. As an example, silicon acquires its electrical conductivity or photoluminescence properties from the addition of specific impurities, called dopants. Moreover its initial crystallographic structure should be free of defects because they could destroy the efficiency of the doping. This is the same for all semiconductors and insulators. To study in detail the specific effect of impurities and defects, radioactive probes are ideal tools. For that, we must have at our disposal a radioactive isotope that corresponds to, or is the parent of, the chemical element under study. As the rate of data acquisition is determined by the number of radioactive decays ( $\sim 1/\tau$  where  $\tau$  is the radioactive lifetime), the examination of the material can be performed with a small amount of the radioactive species ( $10^8$  to  $10^{12}$  atoms per  $\text{cm}^2$ ) if one uses radioactive nuclei with short lifetimes. This small quantity of atoms (from  $10^{15}$  to  $10^{18}$  atom / $\text{cm}^3$ ) allows the study of bulk materials without major disturbance of the initial structure of the material and also allows the analysis of surfaces.

In many applications the radioactive species act as spies reporting on their local environment in the host material. The implanted atom probes the vicinity of a crystal lattice site. It interacts with its neighbour atoms and information concerning this interaction is then communicated to the outside world by changes in the pattern of its radioactive decay. An

array of techniques including perturbed angular correlations (PAC), Mossbauer spectroscopy and the emission channelling of conversion electrons, allows us to do this. Just as an example, if we wish to know whether a dopant is on an interstitial or substitutional site, channelling using alpha beams is a classical method. Channelling of conversion electrons leads to a decrease in the threshold of dopant impurities by two to three orders-of-magnitude.

For the foreseeable future, silicon will remain the most important semiconductor material. With the steady reduction in the sizes of all features in integrated devices it will be necessary to control impurities and defects at very low concentrations ( $< 10^{10} \text{ cm}^{-3}$ ). Due to the sensitivity one can achieve, this will be an “ideal” field for the application of nuclear solid state physics using radioactive probe atoms. Increasingly, wide band gap semiconductors, such as GaN and ZnO will be of importance for a number of applications. Radioactive probes will be the ideal tool to explore their properties.

Silicon based optoelectronic circuits and devices are of considerable interest because they could provide optical communications functions using integrated circuits produced by almost conventional processing. Silicon has an indirect band gap and hence a low probability of emitting light. One route to silicon based optical emitters is doping with a high non-equilibrium concentration of erbium in the group IV matrix. The special interest in Er is because its atomic transition at  $1.54 \mu\text{m}$  matches the absorption minimum of  $\text{SiO}_2$ . In a typical example, the total Er dose implanted into Si was nineteen times higher than that of Er implanted into SiGe but the intensities of the emissions at  $1.54\mu\text{m}$  are comparable. Thus a combination of SiGe alloy and Si shows potential as a waveguide. For an understanding of the processes involved it is important to know the lattice location of Er in Si. This has been done using emission channelling of conversion electrons. Following the implantation of  $^{167}\text{Tm}$  ions into the Si lattice the angular distribution of conversion electrons emitted in the decay  $^{167}\text{Tm} \rightarrow ^{167\text{m}}\text{Er}$  (2.27s) was monitored following room temperature implantation and annealing up to  $950^\circ\text{C}$ . Directly after implantation 20-25% of the Er atoms are localised near tetrahedral interstitial sites. Following annealing this reaches 90% at  $600^\circ\text{C}$ . The results show clearly and directly that Er is stable on tetrahedral interstitial sites in float-zone Si.

Hydrogen represents one of the most important impurities in semiconductors. It is easily incorporated during manufacture and it interacts very efficiently with other impurities or defects. The free migration of well defined H configurations in III-V semiconductors such as InP can be studied on an atomic scale using PAC with the probe atom  $^{117}\text{Cd} \rightarrow ^{117}\text{In}$ , which is populated in  $^{117}\text{Ag}$  decay. One starts by irradiating the sample with a clean  $^{117}\text{Ag}$  beam. After annealing, the sample is loaded with  $\text{H}^+$ . The Coulomb interaction between ionised acceptors ( $\text{Cd}^-$ ) and donors ( $\text{H}^+$ ) induces the formation of Cd-H pairs. After the decay of  $^{117}\text{Cd}$  into  $^{117}\text{In}$  the pair is transferred to In-H, and since the  $\text{H}^+$  donor no longer feels the attractive Coulomb force it is able to migrate. The onset of the migration process can be observed by PAC.

In the last decade a range of conventional semiconductor physics methods such as deep level transient spectroscopy (DLTS), capacitance voltage (CV), Hall effect (HE), photoluminescence spectroscopy (PL) or electron paramagnetic resonance (EPR) has been combined with the use of radioactive isotopes. The chemical transmutation of the dopant in radioactive decay provides a clear chemical fingerprint. The intensity of the observed electrical or optical signals changes with the characteristic time constant of the radioactive decay and allows one to assign electrical or optical properties to a particular chemical element unambiguously. In a typical experiment, Si samples were implanted with  $10^{12}$ - $10^{13}$   $^{195}\text{Hg}$  ions  $\text{cm}^{-2}$ . The relevant decay chain is  $^{195}\text{Hg} \rightarrow (10\text{h}) ^{195}\text{Au} \rightarrow (183\text{d}) ^{195}\text{Pt}$ . The samples were

furnace annealed at ~1100K for 0.5-1.5 hours. From the DLTS measurements taken shortly after the diffusion and two half-lives of  $^{195}\text{Au}$  later, we see clearly that the relative intensities of the signals change with time following the  $^{195}\text{Au}$  transformation. Since the radioactive decay of  $^{195}\text{Au}$  involves very low recoil energy (0.3eV), the  $^{195}\text{Pt}$  daughter atom stays on site. Besides, it is known that Pt is on substitutional lattice sites. As a result, it is now clear that the Au acceptor level observed is caused by substitutional Au impurities.

Transmutation doping can also be highly effective in some cases in improving the doping efficiency of (II-VI) semiconductors such as ZnSe. This class of semiconductor is characterised by a direct band gap covering a broad range of energies; they are used in optoelectronics. Even simple devices need sufficiently highly doped p- and n-type materials but doping has to be possible. Thus Ag acts as an acceptor in CdTe when on a lattice site. The doping of CdTe with Ag by thermal diffusion results in a high resistivity material with less than 1% of the Ag atoms acting as acceptors. However, if  $^{107}\text{Cd}$  ions are implanted in CdTe at 60 keV and the sample is annealed, the  $^{107}\text{Cd}$  will be located in the Cd sub-lattice. The beta decay recoil energy is small so, following the radioactive decay, the daughter  $^{107}\text{Ag}$  stays on the Cd site. Capacitance voltage measurements reveal that the implantation profile has broadened with diffusion and that the number of acceptors grows with the 6.5 day half-life of  $^{107}\text{Cd}$ . Eventually, essentially all of the  $^{107}\text{Cd}$  has been transmuted into substitutional  $^{107}\text{Ag}$  acceptors indicating a doping efficiency of nearly 100%.

Such techniques are not limited to semiconductors where they were pioneered. They can be applied to studies of the structure and defects of technologically relevant oxides and especially to magnetic layered systems, magnetic semiconductors and systems showing gigantic magnetic resistance (GMR) or colossal magnetic resistance (CMR). Ion beam materials modification is also being progressively extended to photonics. Waveguides and quantum wells are being produced by the implantation of photo-active impurities in different substrate materials such as  $\text{LiNbO}_3$  and  $\text{Al}_2\text{O}_3$ . Understanding the stability of such dopants is a considerable challenge, at both the technological and fundamental levels, and is another field which can be tackled with nuclear solid state techniques.

Besides the impurities-dopant fields, there are two other approaches where radioactive ions can be used. The first is the Mossbauer effect and the second diffusion studies.

The use of the Mossbauer effect has been limited because it relies on the existence of pairs of nuclei such as  $^{57}\text{Fe}/^{57}\text{Co}$  where a low energy Mossbauer state in a stable isotope is fed in the decay of a long-lived parent which can be conveniently produced, purified and incorporated in a suitable matrix. The technique provides detailed chemical and structural information on the environment at the Mossbauer nucleus. If the radioactive parent can be implanted, the requirement for a long half-life is removed and one can identify a large number of Mossbauer system candidates: some 75 cases distributed over 40 elements. Examples, chosen at random, would include  $^{67}\text{Zn}/^{67}\text{Ga}$ ,  $^{161}\text{Dy}/^{161}\text{Ho}$  and  $^{197}\text{Au}/^{197}\text{Pt}$ . The parent nuclei would be produced as radioactive beams which would allow convenient implantation into the sample of interest. A large number of cases one can identify would be readily available at SPIRAL 2.

Self diffusion or hetero-diffusion studies are classically performed using stable atoms (with an isotopic labelling for self-diffusion) or radioactive species. Using stable atoms is nowadays generally associated with a sensitive SIMS profiling but nevertheless radioactive atoms clearly offer a better sensitivity. One of the most challenging fields is radiation

enhanced diffusion. Among others, the retention under radiation of the nuclear fuel fission fragment atoms is an important issue in nuclear safety. For such studies, most teams use implantation of stable atoms (for instance iodine) but this procedure induces extra radiation defects making the analysis intricate. Using radioactive ions allows one to reduce the implantation fluence needed and is consequently very promising.

SPIRAL 2 will provide a great diversity of radioactive probe atoms for materials studies with a wide range of half-lives, long decay chains and even new types of radiation. This means that almost all combinations of host material and probe atoms will be available to us since pure beams of radioactive isotopes can be created and implanted within a fraction of a second. The higher beam energies will also allow implantation at much increased depth in solids, thus opening up studies of multi-layer devices and bulk properties, not just those of the material near the surface. In many applications this should eliminate the need for diffusion following implantation near the surface. The GANIL complex has the ideal characteristics to exploit this fertile interface between nuclear and solid state physics. Experiments in solid state physics are characterised by many, repetitive measurements on a specific material, where one looks systematically at the influence of parameters such as the temperature, pressure or concentration of impurities or defects. In terms of time, the implantation of the radioactive ions will often be a minor part of the experiment. At SPIRAL 2 it will be possible to carry out such measurements with beams of low energy in parallel with experiments using beams accelerated to the Coulomb barrier by CIME.

The GANIL accelerator site is situated on the scientific campus where nuclear and solid state physicists, inorganic and organic chemists, biological and medical researchers work cheek-by-jowl and in certain cases are already working together exploiting the heavy ions delivered by the GANIL accelerators. The specific physical and chemical characterisations necessary to develop the techniques described above are available on campus at the laboratories of the ENSICAEN, University of Basse Normandie and GANIL. As an example the available photoluminescence setup at the SIFCOM laboratory allows one to determine the defects that emit light; the type of measurement necessary to develop optoelectronic devices. Magnetism on the nanometre scale is the future of memory storage and Mössbauer spectrometry, where one quantifies magnetism at the atomic level is available at the CRISMAT laboratory. This will allow the development of new materials with specific radioactive probes that are not accessible on the market. The channeling goniometer available at the CIRIL laboratory associated with specific 2-dimensional detectors developed by nuclear physicists from the LPC laboratory or GANIL Laboratory would allow one to specify the interstitial or substitutional site of specific elements in oxide materials presenting a giant magneto-resistance effect and in which there is a direct link between the injected electrical current and the magnetic properties. This could be combined with magnetic force microscopy developed in the GREYC and SIFCOM laboratories. Turning to nanometre materials or materials under specific confinement, electron paramagnetic resonance [EPR] and nuclear magnetic resonance [NMR (LCS laboratory)], can be powerful tools to characterise optical thin films (CIRIL and SIFCOM laboratories) for surfaces and interfaces for catalysis (LCS laboratory). In the near future an ultra high vacuum chamber on a beam line will be available to study surfaces. Deep level transient spectroscopy [DLTS (SIFCOM laboratory)] is a very powerful technique for developing semi-conductors (LAMIP laboratory)

## 7.4 A HIGH INTENSITY LOW-ENERGY POSITRON BEAM FOR MATERIALS SCIENCE

The use of positrons for characterising solids and their defects is a well-established technique. In this context we can distinguish between the common positron annihilation technique and the use of positron beams.

In the first case, long lived, positron emitting sources are used,  $^{22}\text{Na}$  being the most common. The source is deposited on a thin film placed in between two similar samples that have to be analysed. The emitted positrons are thermalised in the bulk of the sample and annihilate with the electrons of the solid or eventually form positronium. The positron is not a weakly interacting probe and significantly increases the density of electrons in its vicinity. However experiment and theory have shown that positron studies yield valuable information about electron wave functions and the Fermi surfaces of metals and alloys. The positron lifetime, the Doppler broadening and the Angular Correlation of the two-photon Annihilation Radiation (ACAR) are the observables that carry this information. Moreover, these annihilation characteristics are sensitive to the presence of open-volume defects, such as vacancies, vacancy agglomerates, dislocations, free volume as well as to negatively charged point defects. The investigation of crystal defects has become the dominant focus of positron annihilation studies. The positron lifetime and the Doppler broadening spectroscopies require low activity sources ( $\approx 0.8$  MBq), ACAR measurements are much more demanding in terms of activity.

The use of monoenergetic positron beams, particularly of low energy, has opened up the important field of the study of defects in thin films and at interfaces. SPIRAL2 will supply copious beams of positron emitters of suitable end-point energy, which then allow one to produce positron beams based on moderation in the material in which they are implanted. Monoenergetic positrons are obtained at surfaces exhibiting a negative positron work function, e.g. tungsten. The emitted positrons are guided as a beam to the sample. The variation of the incident positron energy in an accelerator stage enables the measurement of near-surface defect profiles. The focusing of the positron beam allows the three-dimensional probing of defect structures, i.e. the development of a positron microprobe. The use of such a microprobe has recently allowed us to visualise, for the first time, the presence of large vacancy clusters in the vicinity of fatigue cracks. These cracks are responsible for the catastrophic failure of materials submitted to cyclic stress and strain (see figure 7.2).

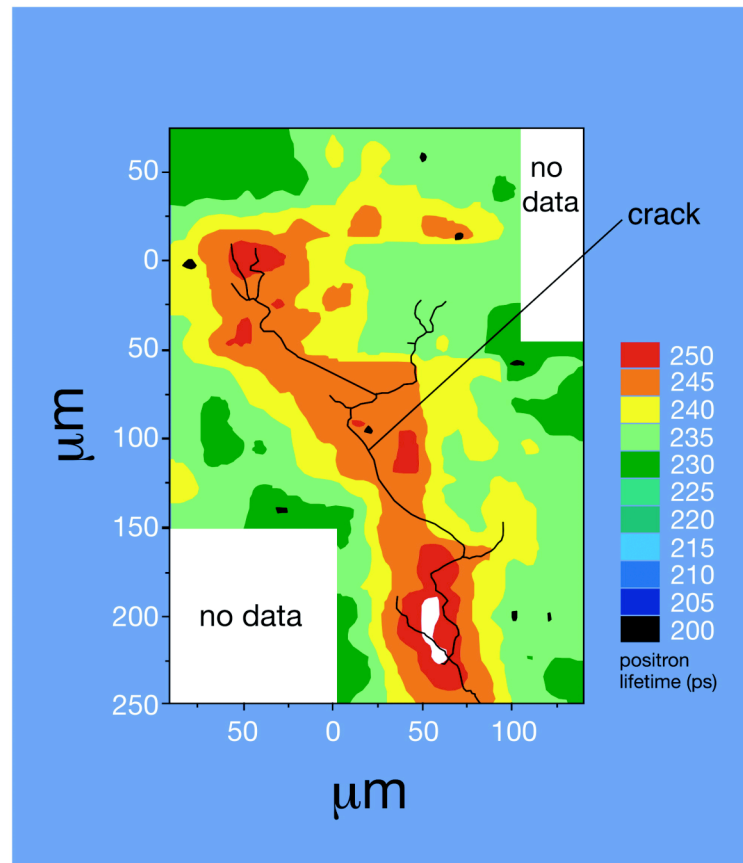


**Figure 7.2:** Fatigue crack in copper and map of mean positron lifetime (ps) at 5 keV positron implantation energy.

The use of low energy positron beams is not restricted to the study of defects on the surface or near-surface of solids. Several spectroscopic techniques using positrons ( instead of electrons) or based on positronium formation and annihilation on surfaces are of outstanding interest for surface physics studies. Differences between electrons and positrons in the inelastic mean free path, in  $e^-e^-$  and  $e^+e^-$  correlations, in relativistic effects and in phase shifts mean that Low-Energy Positron Diffraction (LEPD) has a greater surface sensitivity and is easier to connect to theory than the usual Low-Energy Electron Diffraction (LEED). Positron annihilation induced Auger Electron Spectroscopy (PAES) has been shown to have unique advantages over conventional Auger techniques, including the ability to eliminate the secondary electron background under low energy Auger peaks and the ability to probe selectively the top-most atomic layer. Positronium emission spectroscopy provides a faithful measurement of the surface electronic density of states. There are also prospects of using positrons instead of electrons for transmission electron microscopy.

The development of positron beam techniques is in fact limited by the availability of intense and brilliant sources of positrons and consequently by the intensity of the beams. The majority of the slow positron beams are presently based on sources utilising long lived radioactive isotopes such as  $^{22}\text{Na}$  from commercial sources with maximum activities of  $\approx 3.5$  GBq which restricts monoenergetic beam intensities to  $10^5$ - $10^6$   $e^+/s$ . The price of these sources (2.6 year of period) is around 15 k€/GBq. The use of shorter lifetimes is an alternative that gives more activity but requires an adjacent production site. The preferred isotopes are

$^{64}\text{Cu}$  ( $\tau=12.7$  h) or  $^{18}\text{F}$  ( $\tau=109.7$  min). The isotope  $^{64}\text{Cu}$  was first used at Brookhaven National Laboratory with the sources being produced in their high flux reactor (HFBR). Presently sources of 100 GBq of beta activity are used at Texas University, Arlington. Proton beams are commonly used to produce  $^{18}\text{F}$  in the  $^{18}\text{O}(p,n)^{18}\text{F}$  reaction. This isotope, as a source for positron beams, has also been tested at RIKEN.

On-line production of short lived positron sources by accelerators is an interesting prospective. Washington State University proposes to use the reaction  $^{12}\text{C}(d,n)^{13}\text{N}$  with a 1 kW, 3 MeV deuteron beam. The expected intensity of the positron beam is around  $10^7$   $e^+$ /s. Another possible scheme using a proton beam involves the reaction  $^{27}\text{Al}(p,n)^{27}\text{Si}$ . A number of other reactions involving 37 MeV alpha beams have also been proposed.

To produce monoenergetic positron beams of high intensity ( $>10^8$   $e^+$ /s) several large scale projects are under development. The FRM II-MEPOMUC project uses the high flux of the Munich reactor ( $10^{14}$  n/cm<sup>2</sup>/s) to induce gamma production in Cd ( $^{113}\text{Cd}(n,\gamma)^{114}\text{Cd}$ ); positrons are then produced by pair production in Pt. Intense electron beams produced by LINACs in the energy range of 25-150MeV are the source for, at least, two other projects: EPOS-ELBE at the Halle University and the KEK slow positron facility in Tsukuba, Japan.

SPIRAL2 will provide high intensity beams of short lived isotopes such as  $^{15}\text{O}$  ( $\tau=112$  s),  $^{13}\text{N}$  ( $\tau=9.96$  min),  $^{19}\text{Ne}$  ( $\tau=17.2$  s) etc. For instance, the  $^{15}\text{O}$  ion beam intensity is expected to exceed  $10^{10}$  ions/s. These radioactive beams will have energies of a few tens of keV in the LIRAT facility. They can be focussed on a thin film in contact with a moderator in order to obtain a high brightness source of positrons with activities larger than 10 GBq. Based on this principle, a high intensity monoenergetic positron beam could then be created. This radioactive ion beam option could present several advantages. Compared to the use of very high intensity sources ( $^{64}\text{Cu}$  or  $^{18}\text{F}$ ), the radioactive beam option avoids the handling of very large activities. Due to the short half lives of the isotopes, the residual activity in the positron accelerator will be negligible shortly after operation. On-line production of positron beams with ion or electron beams needs to manage very high thermal loads near the positron moderator. As a result, the positron sources necessarily have large sizes. The radioactive ion beam avoids this problem because of the decoupling of the isotope production and the positron beam device.

Considering the scientific background, the international context and the intensities of the potential SPIRAL2 positron beams, it appears that the radioactive ion beam option might be competitive with respect to the electron LINAC and reactor-based techniques. Before drawing any firm conclusions a careful analysis of costs, advantages and drawbacks must be carried out and this has still to be done.

## 7.5 RADIATION DAMAGE AND RADIATION CHEMISTRY

The main driver for interdisciplinary research with the stable ion beams delivered by SPIRAL2 are the very high fluxes and the short duration of the intense ion pulses. The experiments that need higher fluxes than those presently delivered by the GANIL cyclotrons are focussed partly on collisions and partly on the production of highly damaged samples. For the research on collisions; high fluxes are needed to study the phenomena occurring during the collisions with low-density gas targets and/or to measure differential cross-sections for rare events. A high flux is also necessary to produce a high damage level in materials in a reasonable time for parametric studies. Research on the materials to be used in nuclear

installations, in addition to taking advantage of the neutron beams produced by SPIRAL2, will also benefit from the use of stable ion beams. Direct beams from the LINAG will create homogeneously with a great efficiency a large number of dpa (approximately 0.6 dpa/day for deuterons and 1.1 dpa/day for alphas) on material of thicknesses of the order of one millimetre (300  $\mu\text{m}$  for alpha) thickness. This damage production is limited by the heating of the target. With efficient cooling it could be increased to more than 2 dpa/day (6 kW absorbed by the target). This creation of defects will be accompanied with a very high production of gas that, even if the rate of production is stronger than in the case of the neutrons, will allow the study of the effects on the mechanical properties of the nucleation and the growth of bubbles in the material. For studies of the evolution under irradiation of the mechanical properties, the dose should at least reach the value of 10 dpa. They will need approximately two weeks of irradiation, generally at high temperature.

Research on such materials will also benefit from the improvement in the understanding of the damage mechanisms, which can be obtained from the basic research involving time-resolved experiments. In this domain, the interest of the stable ion beams delivered by SPIRAL2 lies in the duration and the intensity of the ion pulses, which will allow experiments on the first stages of the relaxation of materials after intense electronic excitation with a temporal sub-nanosecond resolution. This resolution is still not sufficient for most of the materials of interest but gives access to the processes involving metastable states (defect production via excitonic processes for example) or to the chemical reactions induced by the electronic excitation. These time-resolved experiments have only been done so far in the field of the weak electronic excitations (pulsed electrons or laser excitations). With the characteristics of the SPIRAL2 beams (200ps and 1mA), the advantage compared to the current high-energy beams concerns the maximum dose per pulse (a gain of a factor 100) and the pulse duration (from 1 ns to 200 ps), see figure 7.3. Thus, phenomena with lower radiolytic yields should be studied with a time resolution improved by a factor 5.

Researchers studying the radiolysis of liquids are particularly interested in this improvement: the radical chemistry which is activated by the ionisation processes have time constants in the ps- $\mu\text{s}$  range (for example for water radiolysis experiments, the number of solvated electrons created by an ion pulse decreases from 4.5 to 3.5  $10^{-7}$  mole/J between 100 ps and 1 ns). Thus, the radiolysis experiments performed with SPIRAL2, which can be directly compared to simulations, will be fruitful for the comprehension of the effects of the ionisation density on the chemistry and thus will give access to information on the radical reactions in the ionisation clusters

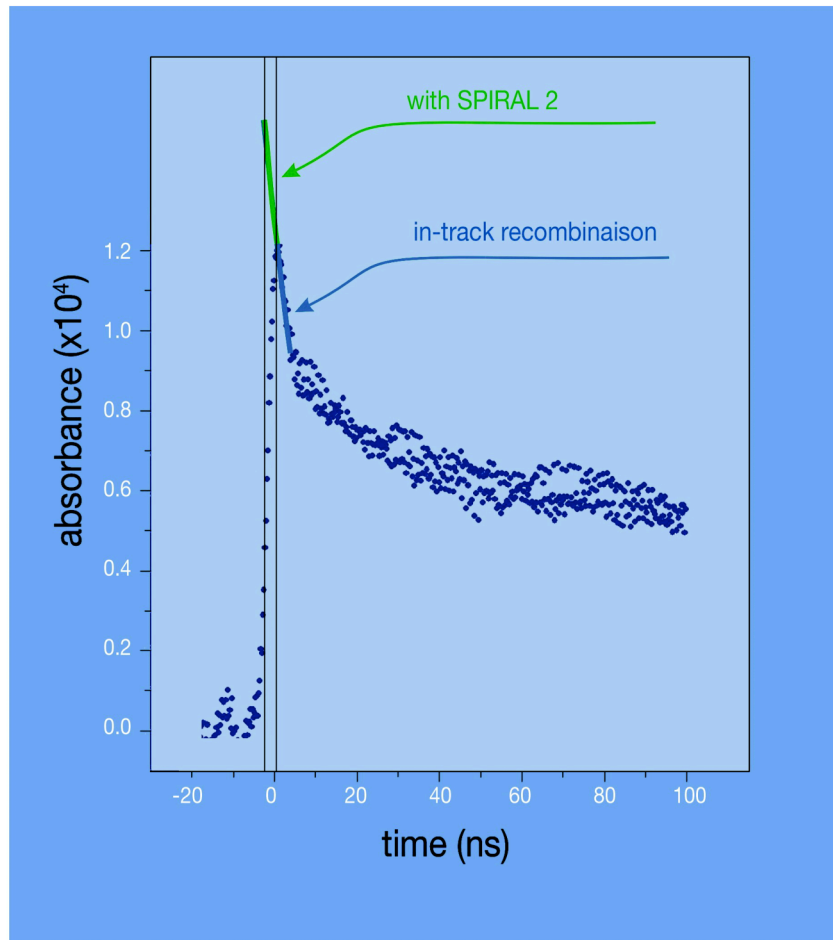


**Figure 7.3:** Absorption kinetics for hydrated electrons in pure de-aerated water after a 1 ns pulse of carbon ions. With SPIRAL2, the precision in the measurement of the in-track recombination will be enhanced by a factor of 2.

. Furthermore, the increase in the dose per pulse will enable the study of the kinetics of the creation and destruction of minority species. For the materials, the same approaches could be developed: the transitory state might then be characterised by luminescence and optical absorption experiments. All these experiments need a particular time structure for the beam: typically one pulse on and  $10^3$  to  $10^7$  pulses off. These studies are upstream of the research on the ageing of the materials for nuclear installations and of the production of nano-structure by ion beams.

What do we need for this kind of research? Firstly a point in the beam line where apparatus including an irradiation chamber and scanning dipoles could be placed. The development of irradiation experiments that require scheduling several times each year can be realistic only if a permanent implantation point could be arranged. For the time resolved experiments, the presence of a pulse suppressor is essential. The pulse suppressor should deliver one unique pulse with a recurrence in the range  $1 \mu\text{s} - 100 \text{ms}$ .

## 7.6 RADIOBIOLOGY

### 7.6.1 Hadrontherapy

The main reasons for the increasing interest in the use of heavier charged particles in radiotherapy are their favourable characteristics such as accurate dose localisation in the Bragg peak as well as high biological effectiveness in that region. These advantages of heavy ions over conventional radiations are of importance in targeting cancerous tissue while minimising damage to surrounding healthy tissue. Up to now, radiotherapy with heavy ions has achieved unprecedented success against several kinds of tumour.

Historically, the pioneers of therapy with light ions were the teams of Berkeley (UCLBL) and San Francisco (UCSF). Between 1954 and 1993 more than 2000 patients were treated with He, Ne, C, Ar and Si ions. At present, only three neutron-therapy centres and four proton-therapy centres are in service in the USA. Only three centres in the world are now using carbon ions for hadron therapy: the NIRS (National Institute of Radiological Science) in Chiba (Japan), the GSI (Gesellschaft für Schwerionenforschung) in Darmstadt (Germany) and the more recent medical centre HARIMAC in Hyogo (Japan). The pioneering facility at GSI has led to the building of a dedicated clinical facility at Heidelberg. In France two centres are in prospect, namely ETOIL in Lyon and ASCLEPIOS in Caen, (the last supported by the Basse-Normandie Region). Protons are more widely used for therapy with more than 20 facilities, that have treated in excess of 30000 patients. Two centres are located in France, at Orsay and Nice.

In  $^{12}\text{C}$  heavy ion therapy, some  $^{12}\text{C}$  ions transform themselves to  $^{11}\text{C}$  through fragmentation reactions with target material. This phenomenon is referred to as autoactivation of the projectiles. Likewise some target nuclei also become radioactive via fragmentation reactions with the target nuclei, which is referred to as target fragmentation.  $^{11}\text{C}$  autoactivity is useful for checking heavy ion treatment, since  $^{11}\text{C}$  is a positron emitter and its distribution in a tumour can be measured by positron emission tomography (PET). This technique is applied to patients in clinical trials at GSI and NIRS.

It has been suggested that  $\beta$ -delayed particle decay beams such as  $^9\text{C}$  or  $^8\text{B}$  could be used in cancer therapy (Li et al., 2003, 2004). These radioactive ion beams emit low energy particles such as alpha particles and protons following their beta decay. This would result in dual irradiation of a tumour, firstly from the external ion beam and secondly from the hadrons emitted in the subsequent radioactive decay. In principle, the dual irradiation to the tumour could lead to an increase in cell mortality. Because of the low energy of the delayed alpha particles (2.9 MeV) and of the delayed protons (3.5-12.3 MeV), the emitted particles have a high biological relative effectiveness when they interact with tissue. Therefore by using  $^9\text{C}$  or  $^8\text{B}$  beams, together with a localisation of the tumour by PET, an enhancement of curative efficacy can be expected if the internal irradiation resulting from the emitted particles is confined to the tumour region. On the other hand, one can decrease the amount of dose released by the incident beam to the target volume and to upstream healthy tissue. A mathematical model designed to evaluate the additional contributions to the cell-killing effect due to emitted particles from  $^9\text{C}$  ions showed an increase of cell inactivation by 10% with a final accuracy in the range of 2.1% as compared to  $^{12}\text{C}$ . In contrast the calculations demonstrated no significant reduction in cell survival for  $^8\text{B}$  beams. The low intensity of the radioactive ion beams is commonly regarded as the big barrier to applying this strategy to cancer therapy. However, with the advance in charged particle accelerator techniques, more

and more intense beams are available. It seems necessary to explore the possible benefit from such kinds of radioactive beams. The optimisation of transport parameters to produce  $^{12}\text{C}$  beams with a higher production rate and purity in the secondary beam line at HIMAC has been carried out and relevant cell radiobiological experiments are actively planned and being performed at NIRS. The SPIRAL2 heavy ion accelerator offers intensities high enough to produce  $^{12}\text{C}$  beams with rates and purity well adapted to such studies. However, due to the maximum energy of the ion beam (less than 20 MeV/u) the range of the particles will not be sufficient to irradiate tumours, even in small animals. Only radiobiological upstream studies can be considered.

## 7.6.2 Radiobiology

Radiobiology experiments are now an important part of the research carried out with the GANIL ion beam lines. The LARIA (Laboratoire d'Accueil en Radiobiologie avec les Ions Accélérés) laboratory allows the researchers to prepare and analyse their biological samples during an experiment. Various biological samples can be exposed in D1 or G4 experimental areas: isolated molecules (nucleic acids, proteins), cultured cells (human, mouse and hamster), and animal models (mouse, rat). The purposes of the experiments range from fundamental interactions in biological matter to application of the ions in hadrontherapy including:

- Understanding the initial physical and chemical events causing biological damage after ion exposure
- Development of microdosimetric models that describe the biological efficiency of different radiations.
- Identifying some specific biological lesions due to ions and understanding the molecular mechanisms involved in their genesis and their repair (comparison with the effects of photons)
- To assess long-term induced cellular damage after exposure to high-LET heavy ions
- Upstream studies to compare the biological efficiency of ions to photons for radiotherapeutic treatments of cancer (assessment of the LET effect)
- Improving fundamental knowledge for the radioprotection of the populations exposed to high-LET particles (areas with radon, astronauts, workers in the nuclear industry, aircrew...)

Thus the facilities to be made available at GANIL allow us to envisage radiobiological experiments with SPIRAL radioactive ion beams, in particular with  $\beta^+$  emitters. Based on the calculations of Li et al., it would be interesting to check the enhancement of cell death induced by  $^{12}\text{C}$  irradiation. However, such experiments will be limited again by the ion range through the container and the cells. Technical developments will be needed in order to expose biological samples, to spread out the Bragg peak and to implant the ions accurately within the cells. In more exploratory research particular attention should be paid to the biological advantages of isotopes that simultaneously emit  $\beta^+$  and Auger electrons since the latter have been shown to be highly potent in inducing cell death.

## 7.7 PRODUCTION OF RADIOACTIVE ISOTOPES FOR BIOLOGY, MEDICAL IMAGING AND NUCLEAR MEDICINE

### 7.7.1 Biology

Commercial preparations of various labelled biomolecules such as nucleotides, nucleosides, amino acids, peptides, proteins (hormones, receptors, cytokines, transduction factors,...) in addition to chemical molecules of metabolic interest are available on the market. The main applications of these molecules for biological research are the detection and the quantification of biomolecules (DNA, proteins,...) and the measurement of a specific metabolic activity (enzymatic, synthesis, degradation, binding,...). Tritium ( $^3\text{H}$ ),  $^{14}\text{C}$ ,  $^{32}\text{P}$ ,  $^{33}\text{P}$ ,  $^{35}\text{S}$ , and  $^{125}\text{I}$  are the radionuclides most commonly used for the labelling of these molecules. Since biological molecules are mainly composed of C, H, O, N (plus P for nucleotides and S for some amino acids), except for radioisotopes of nitrogen ( $^{13}\text{N}$ ), for which the half-life is too short to be commercialised, new isotopes should not have a great interest for these kinds of application. A number of other radioisotopes are also commercially available:  $^{22}\text{Na}$ ,  $^{45}\text{Ca}$ ,  $^{51}\text{Cr}$ ,  $^{57}\text{Co}$ ,  $^{59}\text{Fe}$ ,  $^{63}\text{Ni}$ ,  $^{86}\text{Rb}$ ,  $^{109}\text{Cd}$ .

### 7.7.2 Medical imaging

A more realistic biological application of the radioactive isotopes that could be produced with SPIRAL2 would be medical imaging and nuclear medicine. For the last ten years, there has been an accelerated development of radionuclide-based methods for functional imaging and tumour diagnosis. The commercial radioisotopes are mainly produced using physico-chemical methods and only a few are generated via basic nuclear reactions at reactors or accelerators (cyclotrons). The radioactive decay property that allows the use of radionuclides for imaging is the emission of photons with sufficient energy to be detected in a device external to the body. Radionuclides that are useful for SPECT imaging (Single Photon Emission Computerised Tomography) emit photons in high abundance and with high enough energy ( $> 100$  keV) to readily escape the body and be detected. This is the most common nuclear medical functional imaging technology nowadays. In PET imaging (Positron Emission Tomography), positrons emitted by the radionuclide interact with a negatron (electron) in an annihilation process to produce two coincident 511 keV photons, which are detected simultaneously in a detector ring. For this more recent technology, short-lived positron-emitting nuclides ( $^{18}\text{F}$ ,  $^{11}\text{C}$ ,  $^{15}\text{O}$ ,  $^{13}\text{N}$ ) produced with beams from commercial cyclotrons are currently used. Many other isotopes are available for PET (Table 1) but Fluorine-18 is probably the single most important radioisotope used. It is injected as [ $^{18}\text{F}$ ]fluorodeoxyglucose ([ $^{18}\text{F}$ ]FDG) which gives information about the glucose metabolic rate. Thus it is a very sensitive tracer for the detection of tumours that generally metabolise more glucose, and for cardiac tissue viability since only viable muscle tissue can metabolise glucose. Several isotopes of iodine are also currently used for SPECT or PET, as well as for therapy, because they allow us to localise specifically to thyroid and thyroid-originating cancers. Now, it seems that the main need for the development of new isotopes for biology should be for endoradiotherapy purposes.

Isotopes	Radiation from decay	Use	Indication
$^{11}\text{C}$	$\beta^+$	PET imaging	Functional, metabolic and physiologic tracers

$^{13}\text{N}$	$\beta^+$	PET imaging	Metabolic tracer
$^{15}\text{O}$	$\beta^+$	PET imaging	Metabolic and physiologic tracers
$^{18}\text{F}$	$\beta^+$	PET imaging	Functional, metabolic and physiologic tracers
$^{32}\text{P}$	$\beta^-$	Therapy	Tumours: prostate, ovarian, peritoneal, pleural, malignant effusion, polycythemia vera, thrombocythemia, leukemias, bone mets
$^{64}\text{Cu}$	Auger $e^-/\beta^+$	Therapy / PET	
$^{67}\text{Cu}$	$\beta^-$	Therapy	Non-Hodgkin's lymphoma
$^{67}\text{Ga}$	Auger $e^-$	Therapy/SPECT	Tumour localisation
$^{68}\text{Ga}$	$\beta^+$	PET imaging	
$^{76}\text{Br}$	$\beta^+$	PET imaging	
$^{89}\text{Sr}$	$\beta^-$	Therapy	Bone metastases
$^{90}\text{Y}$	$\beta^+$	Therapy / PET	Bone metastases, hepatoma, pleural/peritoneal effusions, synoviorthesis
$^{94\text{m}}\text{Tc}$	$\beta^+$	PET imaging	
$^{99\text{m}}\text{Tc}$	$\gamma$	SPECT Imaging	
$^{103}\text{Pd}$	Auger $e^-$	Therapy	
$^{111}\text{In}/^{90}\text{Y}$	Auger $e^-/\beta^+$	PET/Therapy	Prostate cancer, non-Hodgkin's lymphoma
$^{123}\text{I}$	$\gamma$	SPECT imaging	
$^{124}\text{I}$	$\beta^+$	PET imaging	
$^{125}\text{I}$	Auger $e^-$	Therapy	
$^{131}\text{I}$	$\beta^-$	Therapy	Thyroid carcinoma, thyrotoxis, lymphoma, goiter, paraganglioma, neuroblastoma, pheochromocytoma
$^{153}\text{Sm}$	$\beta^-$	Therapy	Bone metastases
$^{166}\text{Ho}$	$\beta^-$	Therapy	Myeloma
$^{177}\text{Lu}$	$\beta^+$	Therapy	
$^{186}\text{Re}/^{188}\text{Re}$	$\gamma, \beta^-$	SPECT/Therapy	Synoviorthesis, bone metastases
$^{201}\text{Th}$	$\gamma$	SPECT imaging	Heart
$^{211}\text{At}$	$\alpha/\gamma$	SPECT/Therapy (trial)	Gliomas, various tumours
$^{213}\text{Bi}$	$\alpha/\beta^-$	Therapy (trial)	Myelogenous leukemia

Table 7.1: list of radionuclides used, or in trial, for medical imaging or endoradiotherapy.

Some of these isotopes can be produced in significant quantities at SPIRAL2. No cost-benefit analysis of such isotope production at SPIRAL2 has been carried out to date.

### 7.7.3 Radionuclide therapy

Cytotoxic radionuclides may be divided into 3 groups of radiochemicals: halogens (iodine,  $^{211}\text{At}$ ), metals ( $^{90}\text{Y}$ ,  $^{67}\text{Cu}$ ,  $^{213}\text{Bi}$ ,  $^{212}\text{Bi}$ ) and transitional elements ( $^{186}\text{Re}$ ). Radionuclides can further be categorised into 4 types of cytotoxic agents: pure beta-emitters ( $^{67}\text{Cu}$ ,  $^{90}\text{Y}$ ),  $\alpha$ -emitters ( $^{213}\text{Bi}$ ,  $^{211}\text{At}$ ),  $\beta$ -emitters that emit  $\gamma$ -radiation ( $^{177}\text{Lu}$ ,  $^{186}\text{Re}$ ,  $^{131}\text{I}$ ), and Auger emitters and radionuclides that decay by internal conversion, including  $^{125}\text{I}$  and  $^{67}\text{Ga}$ . In addition to iodine, only a few other elements naturally gravitate to specific organs or cells. Among them,  $^{90}\text{Y}$ ,  $^{89}\text{Sr}$  and  $^{153}\text{Sm}$  have a high affinity for bone. There is only a limited use of therapeutic radionuclides in simple ionic forms (I, Sr), most applications need the isotope to be incorporated into a metal-ligand complex, particle or colloids, or labelled biomolecules. This last technology can be applied to monoclonal antibodies specific to a particular kind of tumour or cancer cell in targeted radionuclide therapy (TRT). Another way to target specific cells (most often neuroendocrine tumours) is to label a receptor-binding protein such as somatostatin, bombesin, annexin or even steroid hormones.

A more recent and experimental approach is radio-targeted gene therapy that consists in transfection of cancer cells with a gene of interest whose expression could improve endoradiotherapy. This could be a gene coding for the receptor for a labelled binding-protein (increased level of this receptor) or a gene coding for a transporter channel such as the sodium iodide symporter (NIS) gene (increased intracellular transport of iodine). An amplification of the toxic effect of the radionuclide should even be expected with the co-delivery of a second therapeutic gene such as herpes virus thymidine kinase (TK) or cytosine deaminase (CD) which results, in the target cells, in the expression of an enzyme that converts a nontoxic prodrug into a toxic drug. Pre-targeting techniques can also be applied. These methods are designed to minimise the radiation to normal tissues due to prolonged residence in the body. One approach uses the interaction between avidin and biotin: targeting antibody biotinylated plus avidin plus radiolabeled biotin.

The choice of appropriate radionuclides for TRT is determined by physical, chemical, biological, and economic factors, such as the character of the emitted radiation, physical half-life, labelling chemistry, chemical stability of the label, intracellular retention time, and the fate of radiocatabolites and availability of the radionuclide. Indeed, an optimal treatment should be based on the combination of therapeutic radionuclides with different particle emission (ex.  $^{111}\text{In}/^{90}\text{Y}$ ,  $^{67}\text{Ga}/^{90}\text{Y}$ ) or using a generator system where the mother and daughter nuclides have different decay schemes (e.g.  $^{114\text{m}}\text{In}/^{114}\text{In}$ ,  $^{134}\text{Ce}/^{134}\text{La}$ ). Many other nuclides could be investigated to see if they are of interest in terms of nuclear decay/biological efficiency (Table 2) or for specific biological purposes such as  $^{52}\text{Fe}$  for iron metabolism studies with PET and  $^{191}\text{Pt}$  for labelling of cyto-toxic drugs used in chemotherapy.

Endoradiotherapy is a fast developing field and has great potential. However there is actually limited availability of suitable radionuclides at present. Most of them are produced chemically with significant levels of impurity and low yields. The production of new isotopes requires a new generation of cyclotrons that can be used to produce beta- and Auger emitters of therapeutic interest. Furthermore, emerging satellite PET scanners will in the near future demand long-lived positron emitters for diagnostics with macromolecular radiopharmaceuticals, and these can also be designed at such centres. SPIRAL 2 could be a valuable tool for upstream research in these fields. Thanks to its high intensity and simpler separation methods (compound-nucleus reactions, well-defined energy dependent channel, little or no chemistry) it would allow the production and the optimisation of new isotopes with dedicated  $\alpha$ - or  $\beta$ -decay parameters). However, SPIRAL 2 should not become a commercial supplier of isotopes because one could not guarantee the availability of products on a

commercial scale and production costs would not be competitive with those of commercially available products. SPIRAL 2 would allow access to a vastly expanded array of isotopes and thus excel as a research tool for new production techniques and the improvement of isotopic yields.

Isotopes	Radiation from decay	Use	Indication
<sup>34m</sup> Cl	$\beta^+$	PET	Functional imaging tracers
<sup>45</sup> Ti	$\beta^+$	PET	Imaging
<sup>60</sup> Cu	$\beta^+$	PET	Imaging cancer
<sup>61</sup> Cu	$\beta^+$	PET	Imaging
<sup>52</sup> Fe	$\beta^+$	Therapy / PET	Bone marrow diseases and scanning
<sup>62</sup> Zn	$\beta^+$	PET	Heart/brain imaging
<sup>72</sup> As	$\beta^+$	PET	Imaging
<sup>75</sup> Br	$\beta^+$	PET	Functional imaging tracers
<sup>81m</sup> Kr	$\gamma$	SPECT	Lung
<sup>82</sup> Sr	$\beta^+$	PET	Heart imaging
<sup>82</sup> Rb	Auger $e^-$	Therapy / PET	
<sup>83</sup> Rb	Auger $e^-$	Therapy	
<sup>86</sup> Y	$\beta^+$	Therapy	Bone metastases, hepatoma, pleural/peritoneal effusions, synoviorthesis
<sup>93</sup> Rb	$\beta^-$	Therapy	
<sup>99</sup> Mo	$\beta^-$	Therapy	
<sup>114</sup> In	$\beta^+/\beta^-$	Therapy	
<sup>117m</sup> Sn	Auger $e^-$	Therapy	
<sup>191</sup> Pt	Auger $e^-$	Therapy	Combination endoradiotherapy/chemotherapy
<sup>127</sup> Xe	Auger $e^-$	SPECT / Therapy	Lung ventilation, brain perfusion
<sup>149</sup> Tb	$\alpha/\beta^+$	Therapy	Targeted alpha therapy
<sup>169</sup> Er	$\beta^-$	Therapy	
<sup>195m</sup> Pt	Auger $e^-$	Therapy	
<sup>192</sup> Ir	$\beta^-$	Therapy	
<sup>201</sup> Tl	Auger $e^-$	SPECT / Therapy	
<sup>212</sup> Bi	$\alpha/\beta^-$	Therapy	Targeted alpha therapy
<sup>212</sup> Pb	$\alpha/\beta^-$	Therapy	Targeted alpha therapy
<sup>223</sup> Ra	$\alpha/\beta^-$	Therapy	Targeted alpha therapy
<sup>224</sup> Ra	$\alpha/\beta^-$	Therapy	Targeted alpha therapy
<sup>225</sup> Ac	$\alpha/\beta^-$	Therapy	Targeted alpha therapy
<sup>255</sup> Fm	$\alpha$	Therapy	Non-Hodgkin's lymphoma

Table 2: list of radionuclides of potential interest for medical imaging and/or endoradiotherapy

## 8. THE SPIRAL 2 FACILITY

### 8.1 INTRODUCTION

The importance of the availability of Rare Isotope Beams (RIB) for a “broad programme of research in fundamental nuclear physics and astrophysics, as well as in applications of nuclear science” was underlined recently by the NuPECC (Nuclear Physics European Collaboration Committee - an expert committee of the European Science Foundation) Roadmap for the Construction of Nuclear Physics Research Infrastructures in Europe (see [www.nupecc.org/pub/NuPECC\\_Roadmap.pdf](http://www.nupecc.org/pub/NuPECC_Roadmap.pdf) and references therein). In this document, the Committee recommended the construction of two next-generation RIB facilities of complementary type in Europe.

One of the two facilities would be based on the in-flight fragmentation (IFF) and the other on the isotope-separation on-line (ISOL) method. The IFF method will be extensively employed at the FAIR facility, which it is proposed to build at GSI (Darmstadt, Germany). In the ISOL method, a thick target is bombarded with a primary, light or heavy-ion beam or with a secondary neutron beam in the case of a fissioning target. The radioactive nuclei produced are extracted from the target and re-accelerated to the energies, from keV to tens of MeV, needed for experiments. The ISOL method provides high-intensity beams of high optical quality, comparable to stable beams. The EURISOL facility is intended to be the ultimate RIB ISOL facility. However, a full engineering design study and R&D programme are required before it can be built and the beginning of operation is not expected until around 2020. Because of the time-line for EURISOL, NuPECC recommends the construction of intermediate-generation facilities that will benefit the EURISOL project in terms of R&D and that will give the community opportunities to perform research with RIB and apply them in other areas of science. Among the intermediate facilities that have been proposed, SPIRAL2 meets all the criteria of European dimensions in terms of physics potential, site and the total investment ( with a total cost estimate of around 130 M€).

In March 2005, the ESFRI (European Strategy Forum on Research Infrastructures) published the “List of Opportunities”, which includes 23 Research Infrastructure projects corresponding to major future needs of the European scientific community. FAIR and SPIRAL 2 are among the selected projects and were recommended as being among the Research Infrastructures necessary to maintain Europe’s position at the cutting-edge of World research.

SPIRAL 2 will reinforce European leadership in the field of exotic nuclei and will serve a community of about 600 scientists. In this very competitive domain, Japan has invested more than 500M€ in its RIKEN-RIBF facility and the US is proposing to build a “Rare Isotope Facility “(RIA, cost about 1 billion €). It is of the outmost importance that the EU maintains its present leadership and secures its future in the field with SPIRAL2 at GANIL for the low energy domain (few keV - 20 MeV/nucl.) and FAIR at GSI for the high energy complementary branch (100-1000 MeV/nucl.).

SPIRAL2 also has a considerable potential for neutron-based research both for fundamental physics and various applications. In particular, in the neutron energy range from a few MeV to about 35 MeV this research would occupy a leading position for the next 10-15 years if compared to other neutron facilities in operation or under construction worldwide.

The French Ministry of Research took the decision to build SPIRAL 2 at the end of May 2005. Its construction cost, estimated to be 130 M€ (including personnel and contingency), will be shared by the French funding agencies CNRS/IN2P3 and CEA/DSM, the authorities

of the Region of Basse Normandie and European partners. The construction will last about five years and operation of the facility will cost about 8.5 M€ per year.

## 8.2 THE GENESIS OF THE SPIRAL 2 PROJECT

From the very beginning of the SPIRAL project, an upgrade – SPIRAL 2 – was envisaged to increase both the range and the masses of exotic nuclei produced by SPIRAL.

The initial idea was to use a deuteron beam produced by GANIL to induce fission in a uranium target. This was the basis for the “SPIRAL Phase II” European research and development contract, coordinated by M.G. Saint-Laurent from 1998 to 2001 (see Report “SPIRAL Phase II, European RTT”, September 2001, GANIL R 01 03).

However, mainly for reasons of safety, the idea of using GANIL for production of the primary beam was soon abandoned in favour of a made-to-measure “driver”.

In the year 2000, photo-fission of a uranium target, as a means of producing the desired fission fragments, began to look like a possibility. This idea – an “electron driver” - compared to a room-temperature or superconducting cyclotron for production of a deuteron beam was examined in a Preliminary Design Study coordinated by D. Guillemaud-Mueller (see report “SPIRAL II: Preliminary Design Study”, November 2001, GANIL R 01 04).

At around the same time, an intermediate energy, superconducting linear accelerator for very high intensity light and medium-heavy ion beams – LINAG – was proposed by G. Auger, W. Mittig, M.-H. Moscatello and A. Villari (see “High Intensity beams at GANIL and future opportunities : LINAG” Report, September 2001, GANIL R 01 02). In its first phase (LINAG I) the acceleration of deuterons by this “driver” would achieve the specifications fixed for SPIRAL 2 , namely  $10^{13}$  fissions per second. The LINAG phase I study was coordinated by W. Mittig (“LINAG Phase I” Report, June 2002, GANIL). In parallel, the Electron Option Preliminary Design study was coordinated by F. Loyer (report "SPIRAL II Electron Option Preliminary Design Study", September 2002, GANIL R 02 03).

The choice between the “electron driver” option and LINAG I was discussed on numerous occasions within the scientific community (GANIL Colloquium, Belgodère, September 2001; Discussion meeting in Paris, October 2001; ...) and by the Scientific Council of GANIL (December 2001 and June 2002).

At the end of 2001 two preliminary Design Study groups set to work to study in detail both options. The two resulting reports were examined by an International Committee of Experts, then by the Scientific Council of June 2002.

LINAG was the solution chosen for the SPIRAL 2 driver, as it offers better technical options, as well as allowing for a future coordination of GANIL's long-term future in the context of EURISOL. Moreover, the possibility of accelerating both light and heavy-ions in the linear accelerator gave a unique and attractive aspect to LINAG allowing for alternative options related to a further extension of the linear accelerator up to intermediate energies,.

The detailed design study (APD) of the SPIRAL2 project was coordinated by A. Mosnier (APD Project leader) and R. Anne (APD Deputy Project Leader) from November 2002 to January 2005.

The White Book of the project based on the APD Intermediate Report (Livre Blanc SPIRAL 2, GANIL, Juin 2004) was submitted to the French Ministry of Research in July 2004. This document included a preliminary version of the SPIRAL 2 Physics Case.

The final SPIRAL 2 technical design study report defining the reference project, variety of options and further extensions was published in January 2005 (The SPIRAL 2 Project APD Report, GANIL, January 2005).

All of the studies and reports mentioned above were put together in close collaboration with a large number of physicists and engineers from various laboratories in France and abroad.

On the basis of referee reports of international experts and Committees (NuPECC and ESFR), the positive evaluations by IN2P3/CNRS and DSM/CEA, and the support of the region of Basse-Normandie the French Minister of Research took the decision to construct SPIRAL 2 in May 2005.

Since the 1st of July 2005, the construction phase of SPIRAL2 has been coordinated by M. Jacquemet (Project Leader) and M. Lewitowicz (Scientific Coordinator) within a consortium formed by CNRS, CEA and the region of Basse-Normandie in collaboration with French, European and international institutions.

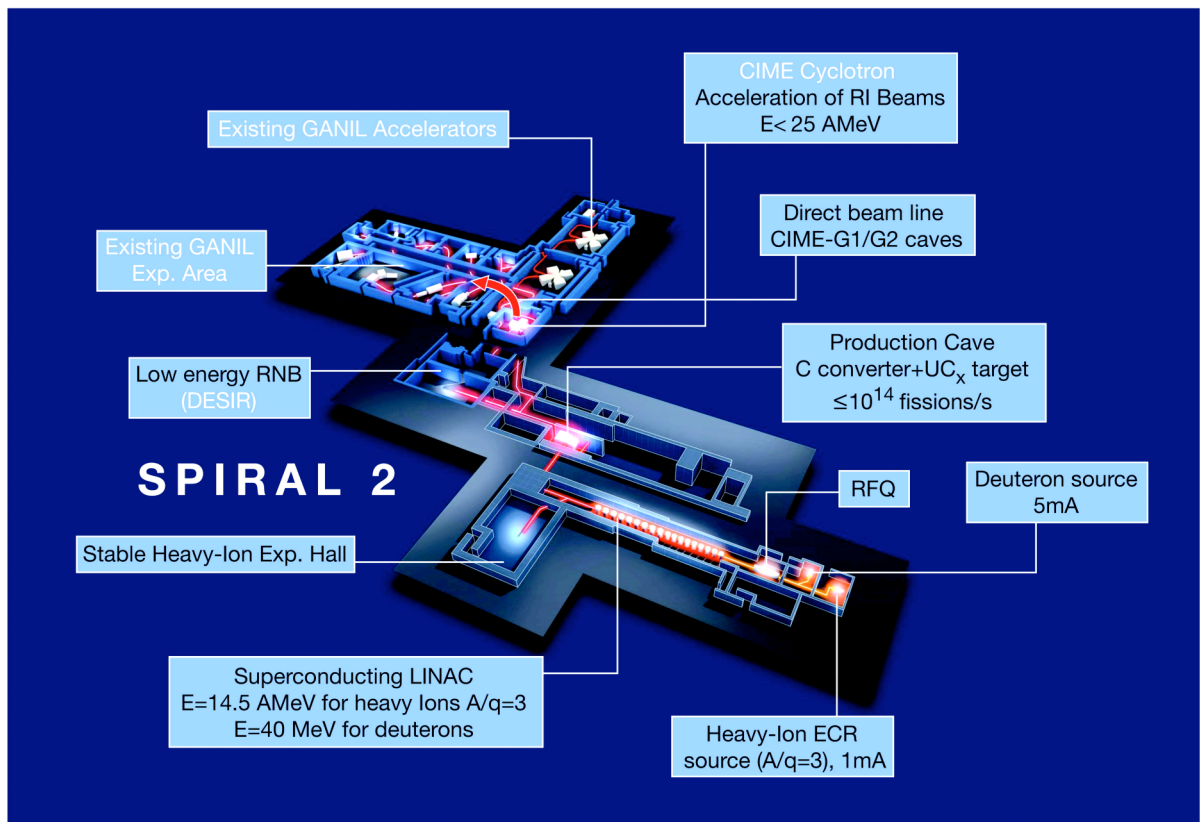


**Figure 8.1** : Schematic layout of the SPIRAL 2 facility at GANIL.

### 8.3 THE FACILITY

The SPIRAL 2 facility (figure 8.1) is based on a high power, superconducting driver LINAC, which will deliver a high intensity, 40 MeV deuteron beam as well as a variety of heavy-ion beams with mass over charge ratio equal to 3 and energy up to 14.5 MeV/nucl.. Using a carbon converter, fast neutrons from the breakup of the 5 mA of deuterons impinging on a uranium carbide target will induce a rate of up to  $10^{14}$  fissions/s. The RIB intensities in

the mass range from  $A=60$  to  $A=140$  will be of the order of  $10^6$  to  $10^{11}$  part./s surpassing by one or two orders-of-magnitude any existing facilities in the World. A direct irradiation of the  $UC_2$  target with beams of deuterons,  $^3He$ ,  $^6,7Li$ , or  $^{12}C$  may also be used if higher excitation energy leads to a higher production rate for a nucleus of interest.

The beams of neutron-rich fission products will be complemented by beams of nuclei near the proton drip line created in fusion-evaporation or transfer reactions. Similarly, the intense, heavy- and light-ion beams from LINAG on different production targets can be used to produce high-intensity beams of light radioactive species with the ISOL technique.

The extracted RIB will subsequently be accelerated to energies of up to 20 MeV/nucl. (typically 6-7 MeV/nucl. for fission fragments) by the existing CIME cyclotron.

As described in what follows, SPIRAL 2 would allow us to perform experiments on a wide range of neutron- and proton-rich nuclei far from the line of stability (figure 8.2) using different production mechanisms and techniques to create the beams.

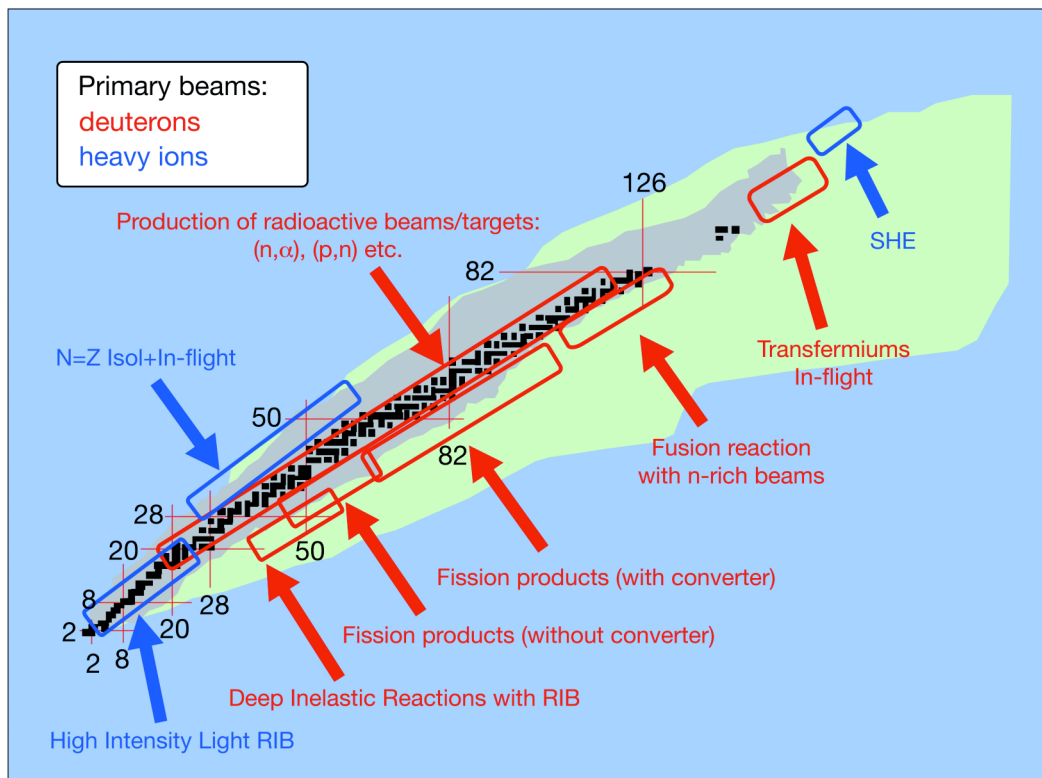


**Figure 8.2** : Regions of the chart of nuclei accessible for research on nuclei far from stability at SPIRAL2.

One of the most important features of the future GANIL/SPIRAL/SPIRAL 2 accelerator complex will be the capability of delivering up to five stable or radioactive beams simultaneously in the energy range from keV to several tens of MeV/nucl..

In the following, the main characteristics of the primary and secondary (neutrons, ions of rare isotopes) beams expected from SPIRAL 2 are presented as well as the future operational modes of the whole GANIL+SPIRAL and SPIRAL 2 facility.

## 8.4 STABLE BEAMS FROM LINAG

### 8.4.1 Light and heavy-ion ( $A/q=3$ ) beams

The driver (LINAG) accelerator for SPIRAL will deliver deuterons up to an energy of 40 MeV with a beam current up to 5 mA and heavy ions with beam currents up to 1 mA. The beams produced will be optimised in energy for ions of mass-to-charge ratio  $A/q=3$ , resulting in an output maximum energy 14.5 MeV/u. The beam energy will be adjustable between the maximum energy and the lowest possible output energy from the RFQ (about 1 MeV/u).

The heavy-ion primary beam intensities of the driver depend on the performance of the dedicated ECR source. For example, among the more promising sources for production of high current ion beams at present are the 28 GHz PHOENIX ion source from LPSC Grenoble and the GTS source from CEA/SBT Grenoble. In order to estimate the currents of  $A/q=3$  beams achievable at SPIRAL 2, table 8.1 summarises the best performances worldwide of ECR sources (2004 data).

**Table 8.1 :** Best currents published by MSU, USA(Artemis) / GANIL, France (ECR4M) / Berkeley, USA(AECR-U , VENUS) / LNS-Catania, Italy, (SERSE) / RIKEN, Japan (RIKEN SOURCES) / SSI-ISN, France (PHOENIX) / CEN Grenoble, France (GTS , CAPRICE)

ION	Q/A	Ionisation potential	Best intensity	Source	Type / Frequency
18O 6+	0,333	122 eV	1500 $\mu$ A (at 25 kV)	GTS	18 GHz
			1200 $\mu$ A	VENUS	28 GHz
			1000 $\mu$ A (at 60 kV)	PHOENIX	28 GHz
			1000 $\mu$ A (at 25 kV)	ECR4M	14 GHz
			1100 $\mu$ A (at 25 kV)	CAPRICE	14 GHz
			1000 $\mu$ A	RIKEN	18 GHz
			1000 $\mu$ A	AECR-U	14 + 10 GHz
			1000 $\mu$ A	ARTEMIS	14 GHz
20Ne 6+	0,3	164	360 $\mu$ A	ECR4M	14 GHz
22Ne 7+	0,318	222	270 $\mu$ A	AECR-U	14 +10 GHz
36Ar 12+	0,333	614 eV	380 $\mu$ A (at 25 kV)	GTS	18 GHz
			200 $\mu$ A	SERSE	14 + 18 GHz
			200 $\mu$ A	AECRU	10+ 14 GHZ
			200 $\mu$ A	RIKEN	18 GHz
40Ar 13+	0,325	689 eV	277 $\mu$ A (at 25 kV)	GTS	18 GHz
			120 $\mu$ A	SERSE	14 + 18 GHz
			120 $\mu$ A	AECR-U	10+ 14 GHZ
			120 $\mu$ A	RIKEN	18 GHz
86Kr 27+	0,314	2728	8 $\mu$ A	SERSE	28 GHz
			8 $\mu$ A	AECR-U	14 + 10 GHz
86Kr 28+	0,325	2900	2 $\mu$ A	SERSE	18 GHz
			2 $\mu$ A	AECR-U	14 + 10 GHz
129Xe 38+	0,29	2630	0,9 $\mu$ A	SERSE	18 GHz
129Xe 20+	0,155	642 eV	320 $\mu$ A (at 25 kV)	VENUS	28 GHz
			310 $\mu$ A (at 25 kV)	GTS	18 GHz
			225 $\mu$ A (at 25 kV)	SERSE	28 GHz
			610 $\mu$ A * (at 60 kV)	PHOENIX	28 GHz
			500 $\mu$ A * (at 25 kV)	SERSE	28 GHz

\* Obtained in pulsed mode with afterglow

State-of-the-art ECR sources allow us to reach the goal of 1 mA beam intensity with  $q/A=1/3$  for the light ions like  $^{18}\text{O}^{6+}$ . For heavier masses up to argon, this goal is probably within reach with some further developments (A-PHOENIX source), including the use of higher frequencies (28 GHz or more). For krypton or xenon, the charge states achieved are respectively 28 + and 44+. Taking into account present developments of the ion sources, a current of the order of 1 mA does not seem to be attainable in the next 10 years. However some tenths of a mA are probably possible. In addition to the ions shown in table 1 the beams of  $\text{H}_2^{1+}$  (up to 5mA at 40MeV),  $^3,^4\text{He}$ ,  $^6,^7\text{Li}$ , C, S, Fe and Ni (from  $\text{CO}_2$  or organic compounds) should be available in the first years of operation of SPIRAL 2. The available maximum

energy will vary from 14.5 MeV/u for  $A/q=3$  to 20 MeV/u for  $A/q=2$ . The production of these and other high-current (especially metallic) beams will require a further R&D programme.

#### 8.4.2 Extension to the $A/q=6$ heavy-ion beams and to higher energies

The LINAG accelerator is designed so that it might serve also for the acceleration of ions with mass-to-charge ratio  $A/q=6$ . It requires the construction of an additional injector, including ion source and RFQ structure (estimated additional cost 3 MEuros). Table 8.2 shows examples of the heavy-ion beams which might be available with this extension. The numbers in table 2 correspond to the beams currently available at the exit of the ECR sources of the GANIL facility. The intensities and maximum energies might increase significantly if a new generation ECR source is used.

**Table 8.2** : Examples of beams which might be available with the  $A/q=6$  extension of the SPIRAL 2 driver.

Element	Mass (A)	Charge State (q)	A/q	Intensity $\mu\text{A}$	Max. Energy MeV/u
C	13	3	4.3	200	11
N	14	3	4.7	200	10.5
N	15	3	5.0	200	10
O	16	3	5.3	200	9.5
O	17	3	5.7	100	9
O	18	4	4.5	200	10.5
Ne	20	5	4.0	200	11.8
Ne	22	5	4.4	200	10.5
Mg	24	7	3.4	10	13.5
S	32	9	3.6	26	13
S	36	8	4.5	40	10.5
Ar	36	10	3.6	160	13
Ar	40	9	4.4	150	10.5
Ca	40	9	4.4	10	10.5
Ca	48	8	6.0	40	8.4
Cr	50	11	4.5	4	10.5
Cr	52	10	5.2	5	9.7
Ni	58	11	5.3	50	9.7
Ni	64	11	5.8	20	8.7
Cu	65	13	5.0	3	10
Zn	70	15	4.7	3	10.5
Ge	76	14	5.4	3	9.4
Kr	78	16	4.9	40	10
Kr	84	14	6.0	50	8.4
Kr	86	16	5.4	45	9.4
Mo	92	16	5.75	3	8.7
Nb	93	16	5.81	1	8.7
Cd	106	21	5.05	5	10
Ag	107	19	5.63	4	9
Sn	112	22	5.09	3	10

## 8.5 RADIOACTIVE BEAMS

### 8.5.1 Beams of fission fragments

Fission fragments will be produced at SPIRAL 2 by the irradiation of a uranium carbide target with the high flux of neutrons produced by the deuteron beam impinging on the carbon converter (up to  $10^{14}$  fissions/s) or by the direct irradiation of the  $UC_x$  target with light ions ( $H_2$ ,  $d$ ,  $^3,^4He$ ). In the latter case a broader mass distribution of outgoing fragments might be obtained but with a lower maximum power (about 6kW) for the primary beam dissipated in the production target. Examples of the anticipated intensities for accelerated beams of fission fragments are shown in figure 8.3.

The production rates for fission fragments have been calculated with the LAHET+MCNP+CINDER code for the  $\sim 5$  mA, 40 MeV deuteron beam striking 7 mm of C converter followed by 56 slices of  $UC_2$ , each 1 mm thick, spaced apart by 0.5 mm. It was assumed that the density of the target  $\rho(UC_2)$  is  $11 \text{ g/cm}^3$  and the beam size is 10 mm diameter. Two different approaches [Rapport SPIRAL PHASE-II GANIL R 01 03] have been considered for the evaluation of final beam intensities: The first, used for Kr, Xe, I and Cd ions, is based on a comparison of the predicted in-target production yields (using the Figner code and the known cross-sections) and those measured after diffusion-effusion and ionisation in the PARRNe2 experiment. These measurements and the comparison, made by the Orsay group, [ref.PARRNe2] give a good indication of the diffusion efficiency for different elements in a uranium carbide target and an ion transfer pipe of small diameter. The second approach, used for Zn, Kr, Sr, Sn, Sb and Xe, based on a theoretical simulation of the diffusion-effusion process, provides some idea of the influence of the target-source geometry. However, since the diffusion-effusion parameters for uranium carbide are not known, diffusion-effusion parameters for a C or Ta-matrix are used instead. The expected radioactive beam intensities (after diffusion, effusion, ionisation and acceleration) shown in figure 3 were obtained for some elements, viz. Kr, Xe, I and Cd, using the first method, and for Zn, Kr, Sr, Sn, Sb and Xe using the second. The assumed

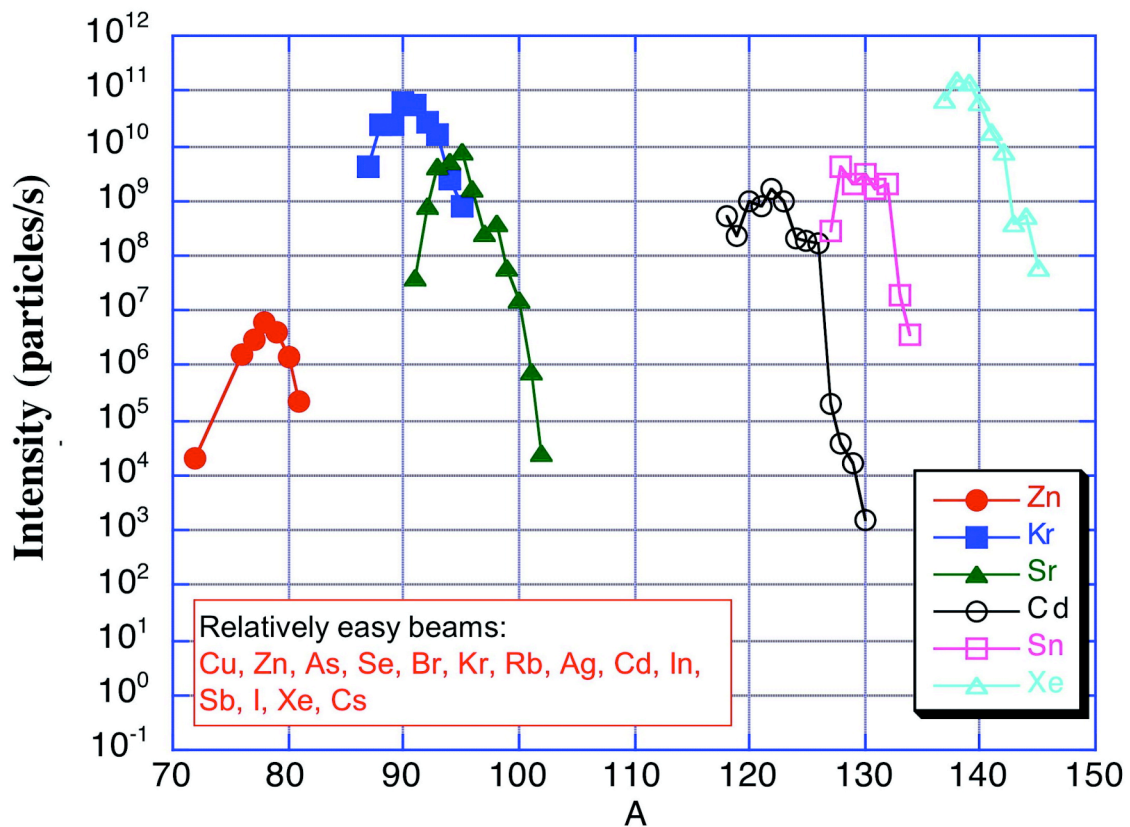


Figure 8.3 : Examples of intensities of fission-fragments beams at SPIRAL2 after acceleration.

1+ and 1+/n+ ionisation efficiencies are 90% (1+) and 12% (1+/n+) respectively for Kr and Xe, but only 30% (1+) and 4% (1+/n+) respectively for Zn, Sr, Sn, I and Cd. The transmissions through the CIME cyclotron and transfer lines were assumed to be 50% and 100%, respectively. Detailed tables with the SPIRAL 2 production rates for fission fragments are to be found in the LINAG Phase I report.

The range of energy of the fission-fragments available from the CIME cyclotron and their purity are discussed in chapter 8.6.

### 8.5.2 Proton-rich beams

The high-intensity heavy-ion beams accelerated by LINAG may be used to produce fusion evaporation residues, either in thin or thick targets (figure 8.4).

In the case of thin-target production, the residues will be studied in-flight after recoiling from the target, either at the target position or at the focal plane of a spectrometer located in the new medium-energy experimental area. As an example one can mention here the production of  $^{80}\text{Zr}$  in the reaction of a  $^{24}\text{Mg}$  beam on a  $^{58}\text{Ni}$  target. The cross section for this reaction has been measured to be  $10 \mu\text{b}$  at 3.3 MeV/u. Taking a rotating target wheel such as developed for the search of super-heavy elements at GANIL, one can estimate that a  $^{24}\text{Mg}^{8+}$  beam of  $200 \mu\text{A}$  might be used without melting the Ni target. This will lead to some  $8 \times 10^4$  ions of  $^{80}\text{Zr}$  per second produced in the target. With a recoil spectrometer having a transmission of 30%, about  $2 \times 10^4$  ions could be delivered to an experimental device.

In the case of thick-target production methods, the ions will be extracted, ionised and re-accelerated by CIME. The thick target would replace the carbon converter and/or UC<sub>x</sub> production target. Various technical solutions have to be studied to decide how best to optimise production taking into account the thermal constraints and effusion efficiencies imposed by the high power of the primary beam, which is deposited in the ISOL or thin production target.

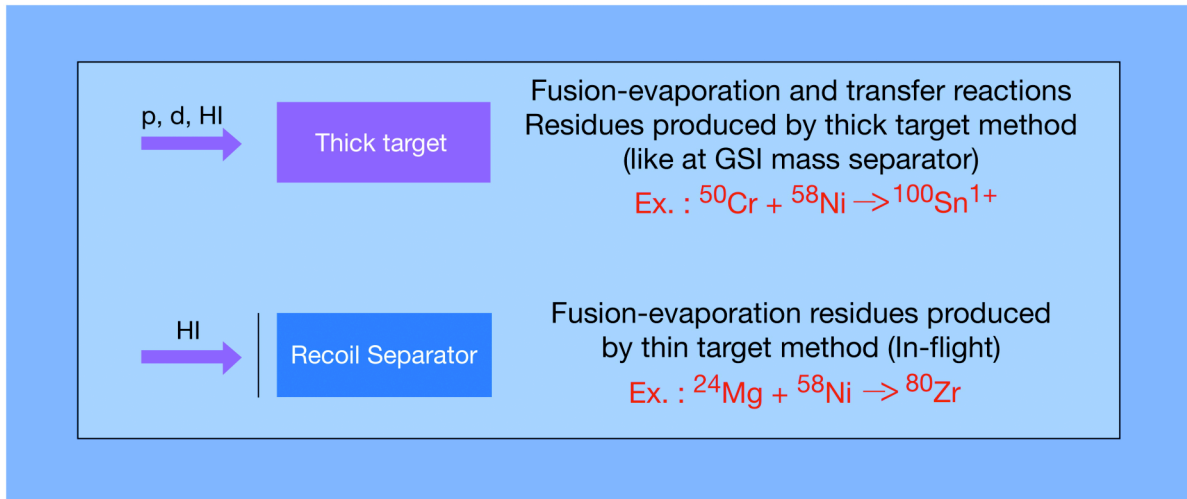


**Figure 8.4 :** Thick and thin target production schemes for proton-rich nuclei at SPIRAL 2.

For some elements, which cannot be extracted from the target, one might consider ion-guide (IGISOL) techniques in the future. In this case, additional space will be needed after the production target. This technique has the advantage that no selection is required before injection into CIME. The IGISOL technique could also be considered for ISOL production with secondary beams.

### 8.5.3 Light RNB

SPIRAL 2 can be used for the production of light radioactive ions via the ISOL method using high-intensity primary beams from LINAG.

Possible radioactive ions which could be produced with high intensity are listed below in tables 8.3 and 8.4:

**Table 8.3 :** Examples of light neutron-rich isotopes that could be produced with SPIRAL2.

Isotope	A/Z	T <sub>1/2</sub> , s	Production reaction
<sup>6</sup> He	3.0	0.81	<sup>9</sup> Be(n,α) <sup>6</sup> He
<sup>8</sup> He	4.0	0.12	<sup>9</sup> Be( <sup>13</sup> C, <sup>14</sup> O) <sup>8</sup> He
<sup>8</sup> Li	2.7	0.84	<sup>11</sup> B(n,α) <sup>8</sup> Li or <sup>9</sup> Be(d, <sup>3</sup> He) <sup>8</sup> Li
<sup>9</sup> Li	3.0	0.18	<sup>11</sup> B(n, <sup>3</sup> He) <sup>9</sup> Li or <sup>9</sup> Be( <sup>7</sup> Li, <sup>7</sup> Be) <sup>9</sup> Li
<sup>11</sup> Be	2.8	13.8	<sup>11</sup> B(n,p) <sup>11</sup> Be
<sup>15</sup> C	2.5	2.45	<sup>9</sup> Be( <sup>7</sup> Li,p) <sup>15</sup> C
<sup>16</sup> N	2.3	7.13	<sup>16</sup> O(n,p) <sup>16</sup> N or <sup>10</sup> B( <sup>7</sup> Li,p) <sup>16</sup> N
<sup>18</sup> N	2.6	0.62	<sup>18</sup> O(n,p) <sup>18</sup> N
<sup>19</sup> O	2.4	26.9	<sup>19</sup> F(n,p) <sup>19</sup> O
<sup>20</sup> O	2.5	13.5	<sup>19</sup> F(n,γ) <sup>20</sup> O or <sup>19</sup> F(d,n) <sup>20</sup> O
<sup>23</sup> Ne	2.3	37.2	<sup>19</sup> F( <sup>6</sup> Li,2p) <sup>23</sup> Ne or <sup>24</sup> Mg(n,2p) <sup>23</sup> Ne
<sup>25</sup> Ne	2.5	0.60	<sup>26</sup> Mg( <sup>13</sup> C, <sup>14</sup> O) <sup>25</sup> Ne or <sup>26</sup> Mg(n,2p) <sup>25</sup> Ne
<sup>25</sup> Na	2.3	59.1	<sup>25</sup> Mg( <sup>12</sup> C, <sup>12</sup> N) <sup>25</sup> Na or <sup>25</sup> Mg(n,p) <sup>25</sup> Na
<sup>26</sup> Na	2.4	1.08	<sup>26</sup> Mg(d, <sup>2</sup> He) <sup>26</sup> Na or <sup>26</sup> Mg(n,p) <sup>26</sup> Na

**Table 8.4 :** Examples of light proton-rich isotopes that could be produced with SPIRAL2.

Isotope	A/Z	T <sub>1/2</sub> , s	Production reaction
<sup>8</sup> B	1.6	0.77	<sup>12</sup> C(p,αn) <sup>8</sup> B
<sup>10</sup> C	1.7	19.3	<sup>11</sup> B(p,2n) <sup>10</sup> C
<sup>11</sup> C	1.8	1224	<sup>11</sup> B(p,n) <sup>11</sup> C or <sup>14</sup> N(p,α) <sup>11</sup> C
<sup>13</sup> N	1.9	598	<sup>12</sup> C(d,n) <sup>13</sup> N or <sup>13</sup> C(p,n) <sup>13</sup> N
<sup>14</sup> O	1.8	70.6	<sup>14</sup> N(d,2n) <sup>14</sup> O or <sup>14</sup> N(p,n) <sup>14</sup> O
<sup>15</sup> O	1.9	122	<sup>14</sup> N(d,n) <sup>15</sup> O or <sup>15</sup> N(p,n) <sup>15</sup> O
<sup>17</sup> F	1.9	64.5	<sup>16</sup> O(d,n) <sup>17</sup> F or <sup>14</sup> N(α,n) <sup>17</sup> F
<sup>18</sup> Ne	1.8	1.67	<sup>19</sup> F(p,2n) <sup>18</sup> Ne
<sup>19</sup> Ne	1.9	17.3	<sup>19</sup> F(p,n) <sup>19</sup> Ne
<sup>21</sup> Na	1.9	22.4	<sup>19</sup> F( <sup>3</sup> He,n) <sup>21</sup> Na
<sup>27</sup> Si	1.9	4.16	<sup>27</sup> Al(d,2n) <sup>27</sup> Si
<sup>35</sup> Ar	1.9	1.77	<sup>35</sup> Cl(p,n) <sup>35</sup> Ar

In order to produce the beams listed above one might use the experience gained in target development at the Louvain-la-Neuve and Oak Ridge laboratories. However, for some of these reactions, a specific R&D programme for the target/ion-source system will be necessary. As an example, a Be-target to be used with different beams of power up to 40 kW should be designed and tested.

To give an impression of potentially achievable rates for these light beams it was estimated that, for example, the in-target production of <sup>6</sup>He and <sup>15</sup>O, assuming a 1-litre target volume, would be 0.2·10<sup>13</sup> atoms/s and 1.0·10<sup>12</sup> atoms /s respectively.

## 8.6 THE PERFORMANCE OF THE CIME CYCLOTRON

The energies and intensities of the SPIRAL 2 beams depend essentially on both the performance of the charge breeder and characteristics of the CIME cyclotron. The energy per nucleon in a cyclotron is proportional to  $(q/A)^2$ , where  $q$  is the charge state and  $A$  is the mass number of the accelerated ion. The available energy range is shown on the CIME working diagram (figure 8.5).

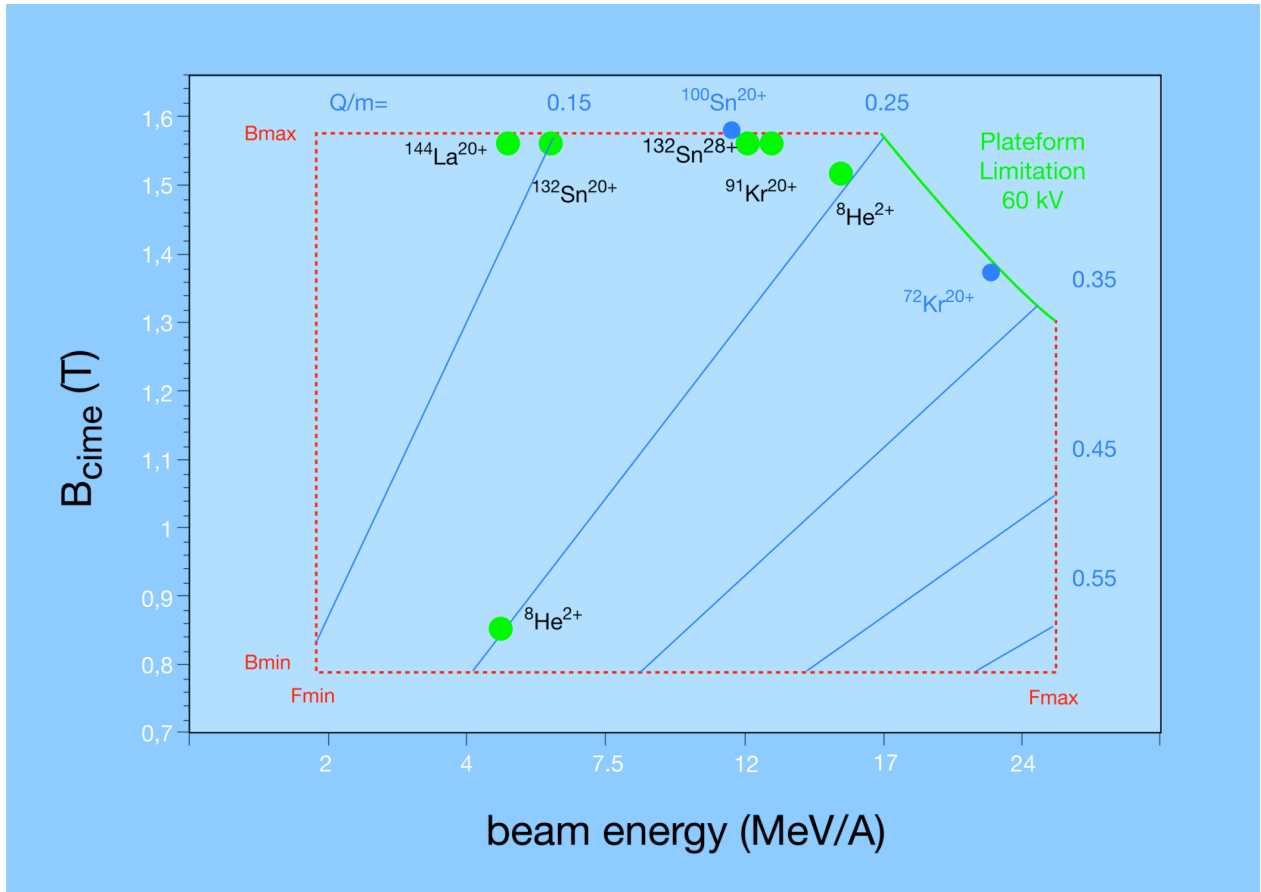
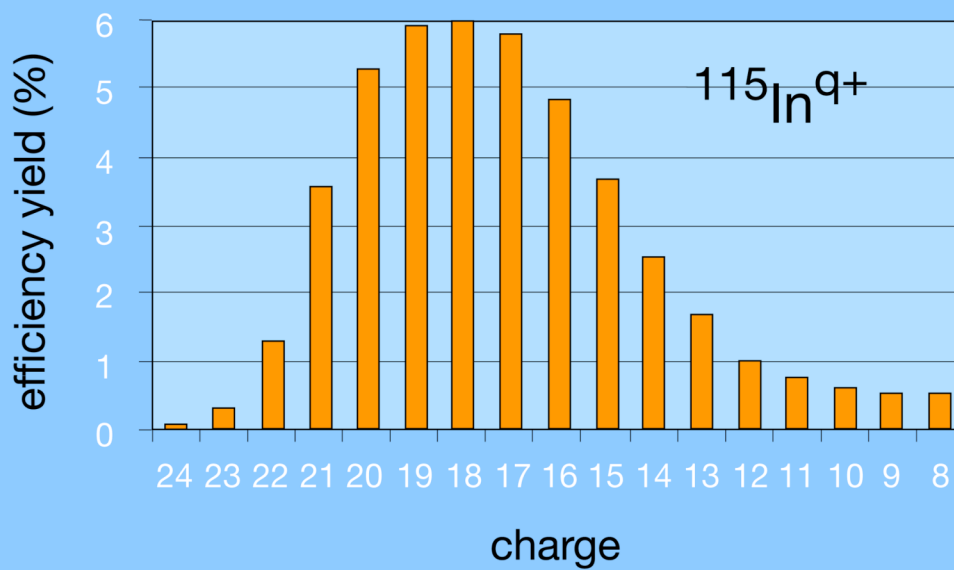


Figure 8.5 : CIME working diagram.

In order to estimate how the intensity of the radioactive beams depends on the performance of charge breeding one can use the results of tests performed at LPSC/SSI with the MicroPHOENIX 10 GHz  $1+$  source and the PHOENIX 14 GHz  $n+$  source shown in figure 8.6. The yields presented in the table correspond to the  $1+/n+$  charge breeding efficiencies. The charge-state distribution measured for Indium ( $Z=49$ ) indicates that the efficiency of the charge breeding decreases by a factor of about 5 going from the  $18+$  to  $22+$  charge state and by factor of 20 from  $18+$  to  $23+$ .

Element	1+ Intensity (nA)	n+ Charge	Yield (%)
$^{20}\text{Ne}$	1000	4	7.5
$^{23}\text{Na}$	660	6	1.3
$^{39}\text{K}$	280	6	6.5
$^{64}\text{Zn}$	42	10	2.8
$^{69}\text{Ga}$	460	11	2
$^{85}\text{Rb}$	90	13	5
$^{88}\text{Sr}$	470	14	3.7
$^{90}\text{Y}$	178	14	3.3
$^{109}\text{Ag}$	175	17	3
$^{115}\text{In}$	130	18	3.3
$^{120}\text{Sn}$	167	19	4.1
$^{208}\text{Pb}$	700 (2+)	25	6.8



**Figure 8.6** : Present performance of the 1+/n+ charge breeding system measured at LPSC/SSI Grenoble (adopted from P. Sortais et al.).

Thus taking an example of the  $^{132}\text{Sn}$  beam at SPIRAL 2 one might estimate the following intensities and maximum energies for different charge states:

**Table 8.5 :** Expected energies and intensities of  $^{132}\text{Sn}$  beams as a function of the charge state.

Isotope	Maximum Energy (MeV/u)	Intensity of the accelerated beam (pps)
$^{132}\text{Sn}^{20+}$	6.0	$2 \times 10^9$
$^{132}\text{Sn}^{21+}$	6.7	$2 \times 10^9$
$^{132}\text{Sn}^{22+}$	7.3	$1.7 \times 10^9$
$^{132}\text{Sn}^{23+}$	8.0	$1.2 \times 10^9$
$^{132}\text{Sn}^{24+}$	8.7	$4 \times 10^8$
$^{132}\text{Sn}^{25+}$	9.4	$1 \times 10^8$

In table 8.6 the maximum energies of several fission-fragment beams for the most probable charge state are shown in comparison to the Coulomb barrier on carbon and lead. In all cases the available energies exceed the Coulomb barrier for a given projectile-target combination.

**Table 8.6 :** Expected energies and intensities of some SPIRAL 2 neutron-rich beams compared to the Coulomb barrier on carbon and lead targets (adopted from SPIRAL PHASE II European RTT, Final Report, Sept.2001).

Isotope	Maximum Energy (MeV/u)	$B_c$ on C (MeV/u)	$B_c$ on Pb (MeV/u)
$^{68}\text{Ni}^{15+}$	12.8	2.9	5.0
$^{78}\text{Ni}^{15+}$	9.7	2.7	4.4
$^{90}\text{Kr}^{17+}$	9.3	3.3	5.0
$^{94}\text{Kr}^{17+}$	8.6	3.3	4.8
$^{128}\text{Sn}^{20+}$	6.4	4.1	5.2
$^{140}\text{Xe}^{22+}$	6.5	4.4	5.3
$^{140}\text{Xe}^{22+}$	6.0	4.3	5.2

## 8.7 MASS PURIFICATION

The use of low energy (keV) RIBs requires in most cases a beam containing essentially a single isotope. This condition might be achieved for many isotopes by combining a chemically selective source (e.g. laser source, surface ionisation source, ECR source with cold transfer tube) with a planned high-resolution mass separator with a mass resolution  $M/\Delta M > 5000$ .

The purity of the high energy RIB will also depend on the chemical selectivity of the ion source as well as on the mass separation capabilities of the CIME cyclotron.

The cyclotron itself, although a good natural mass separator, will not be able to separate high-mass isobars. It has been demonstrated experimentally that the mass resolution of CIME can reach  $R = 1.6 \cdot 10^4$ . One can increase the resolution of the accelerator either by increasing the number of turns made by the beam in the cyclotron by modifying the isochronisms law or by deflecting the parasitic ions by means of an additional RF system.

The use of a non-chemically-selective source, such as a high temperature source (FEBIAD, ECR), results in the production, extraction and transport of a larger variety of ion species. Therefore, the isobaric contamination of the beam becomes a matter of major concern.

**Table 8.7 :** Mass spread around an arbitrary isobar (red)

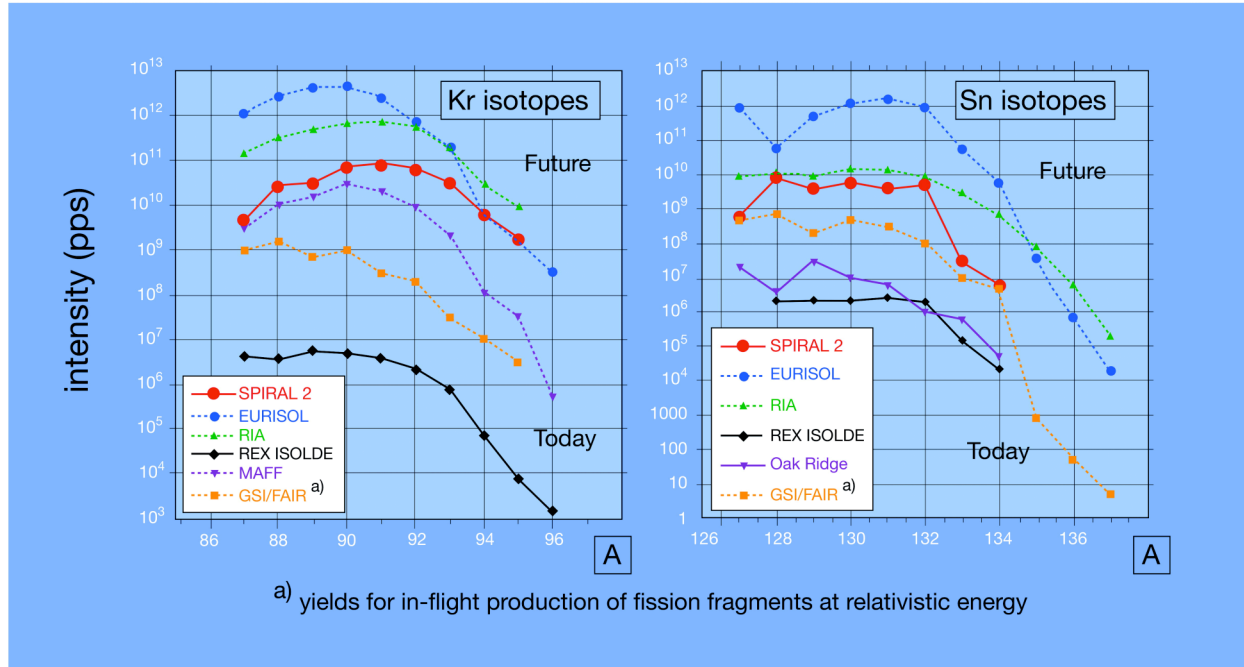
Elements	A	Q	dQ/m		Element	A	Q	DQ/m		Element	A	Q	DQ/m
Kr	91	20	0.00		Cs	132	20	$8.58 \cdot 10^{-5}$		Ba	144	20	$-2.33 \cdot 10^{-5}$
Mo	91	20	$1.28 \cdot 10^{-4}$		I	132	20	$7.39 \cdot 10^{-5}$		Ce	144	20	$4.13 \cdot 10^{-5}$
Nb	91	20	$1.81 \cdot 10^{-4}$		In	132	20	$-1.11 \cdot 10^{-4}$		Cs	144	20	$-8.64 \cdot 10^{-5}$
Rb	91	20	$7.60 \cdot 10^{-5}$		Sb	132	20	$2.69 \cdot 10^{-5}$		Eu	144	20	$5.57 \cdot 10^{-6}$
Ru	91	20	$-3.27 \cdot 10^{-5}$		Sn	132	20	0.00		La	144	20	0.00
Sr	91	20	$1.45 \cdot 10^{-4}$		Te	132	20	$6.99 \cdot 10^{-5}$		Nd	144	20	$6.61 \cdot 10^{-5}$
Tc	91	20	$5.47 \cdot 10^{-5}$		Xe	132	20	$1.03 \cdot 10^{-4}$		Pm	144	20	$4.87 \cdot 10^{-5}$
Y	91	20	$1.77 \cdot 10^{-4}$							Sm	144	20	$5.28 \cdot 10^{-5}$

Table 8.7 shows the mass differences between isobaric species for three representative masses produced. They range from a few times  $10^{-4}$  down to  $10^{-5}$ . The presence in the beam of intense contaminants may lead to significant safety and operational problems.

## 8.8 COMPARISON WITH OTHER RNB FACILITIES

The comparison between the SPIRAL 2 facility and other projects in terms of intensities of accelerated beams is quite complicated because they have different production methods, energies of primary and radioactive beams and other parameters. It also depends directly on the technique used in a particular physics experiment. In the following the comparison will be limited to only two isotopic chains (krypton and tin). In figure 8.7, the accelerated RNB intensities expected from SPIRAL 2 are compared to the performance of other existing (REX ISOLDE, HRIBF Oak Ridge) or planned (FAIR at GSI, EURISOL and RIA) facilities. It should also be noted that at the GSI/FAIR facility the radioactive beams are produced in-flight in the fragmentation of a 1 GeV/u uranium beam. Thus the resulting RNBs have energies about two orders-of-magnitude higher than those at SPIRAL 2 and allow the use of an expanded range of experimental techniques complementary to those used at ISOL facilities. The other facilities indicated in figure 8.7, use the ISOL production method with subsequent post-acceleration of the RNBs to energies ranging from a few MeV/u up to 100 MeV/u.

In particular, the expected SPIRAL 2 intensities for neutron-rich Krypton isotopes are 3 to 4 orders-of-magnitude higher than intensities available today. They will stay highly competitive with respect to the most advanced long-term projects (EURISOL, RIA) for very neutron-rich isotopes due to the expected faster release time from the relatively small volume  $UC_x$  target used at SPIRAL 2.



**Figure 8.7** : Intensities of accelerated beams of Kr and Sn isotopes at present (REX ISOLDE and Oak Ridge) and planned RIB facilities.

## 8.9 ACCESSIBLE REGIONS OF THE CHART OF NUCLEI

In summary, the SPIRAL 2 facility will offer a wide range of intense stable and radioactive beams. Both neutron-induced fission and charged-particle-induced fission will be used to produce high-intensity beams of fission fragments. Fusion-evaporation and transfer reactions with high-intensity, stable light- and heavy-ion beams will allow the delivery of neutron-deficient and light radioactive ions. The same reactions may also serve for the production of radioactive samples (targets) of interest for astrophysics or radiobiology. The intense RIBs can be used in turn to study nuclei even further away from the stability line via secondary fusion-evaporation or deep-inelastic reactions. Altogether, the regions of the Chart of the Nuclides that can be reached with the SPIRAL 2 facility, presented in figure 8.2, cover a large part of the chart of nuclei.

## 8.10 HIGH-INTENSITY NEUTRON BEAMS

The high flux of high-energy neutrons (in the range from 1 to 40 MeV) produced in the carbon converter via  $C(d,xn)$  reactions opens the door to a range of nuclear physics and related applications. Generally, two different methods of using the neutrons have been investigated: materials irradiation very close to the target-converter and a time-of-flight facility with a pulsed neutron beam. One should note that if these opportunities are to be exploited it requires additional investment that is not included in the reference project.

### **8.10.1 Materials irradiation**

Materials testing via irradiation in high fluxes of high-energy neutrons is of great interest for the very extended community working on nuclear waste transmutation (i.e. the use of ADS in particular), intense neutron sources (SNS, ESS, etc.), RNB production with neutrons (EURISOL, RIA, etc.), controlled fusion experiments and reactors (ITER, DEMO, etc.) and space applications (radiation-resistance of electronics, shielding, etc.).

### **8.10.2 Pulsed neutron beam facility**

The use of a neutron beam depends on its specific characteristics in terms of the available neutron flux, energy resolution and usable energy range. These characteristics impose strong technical constraints on the accelerator and experimental hall. The neutrons produced by the  $d + C$  reactions present a continuous spectrum up to  $\sim 55$  MeV. They are peaked at forward angles and at an energy of approximately 12 MeV.

An integrated neutron flux 100 to 1000 times greater than present n-TOF fluxes, in the energy range from 5 to 40 MeV, and with an energy resolution of  $\sim 1\%$  can be reached if the following conditions are met :

- $\Rightarrow$  The deuteron beam has a time structure with a 500 kHz repetition rate corresponding to one pulse out of every 200. We note that this will reduce by a factor 200 the power deposited in the carbon converter. It is suggested that a fast beam-switcher could then deliver the unused portion of the primary beam to other users.
- $\Rightarrow$  A flight path between the converter (i.e. the neutron source) and the physics target of at least 5 to 10 m, with an appropriate experimental area, is constructed.

The use of the intense neutron flux available at SPIRAL 2 is described in detail in chapter 6 of this physics case.

## **8.11 OPERATION OF THE GANIL/SPIRAL/SPIRAL 2 FACILITY**

### **8.11.1 Parallel beams & mode of operation**

The construction of SPIRAL 2 at GANIL will open completely new possibilities for parallel beam operation of the whole facility. The whole GANIL/SPIRAL/SPIRAL2 accelerator complex will allow for the simultaneous use of up to 5 different radioactive and stable beams. Figure 8.8 illustrates one from several possible combinations of different beams delivered in parallel for experiments at low (keV/u), medium (few MeV/u) and high (up to 100 MeV/u) energies.

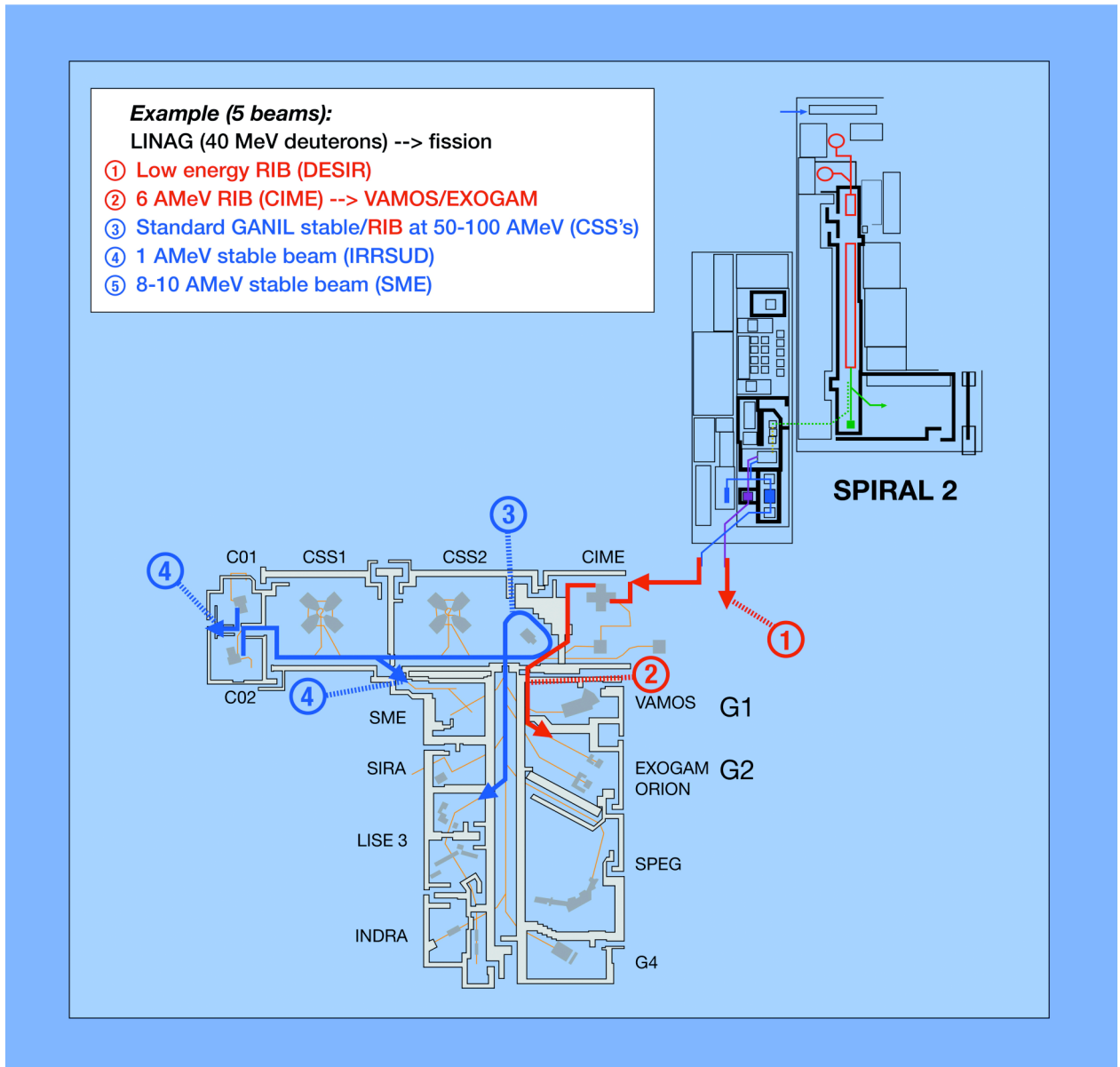


**Figure 8.8** : An example of simultaneous beams from the GANIL/SPIRAL/SPIRAL 2 facility.

Presently the GANIL/SPIRAL facility delivers about 60 weeks per year of stable and radioactive beams (up to 3 simultaneous beams). Thanks to SPIRAL 2 and the construction of a new beam line connecting the CIME cyclotron and the G1 and G2 experimental rooms the available beam time for experiments may be extended up to about 120 (up to 5 simultaneous beams) weeks per year.

## 9. LIST OF CONTRIBUTORS

D. Ackermann  
L. Adoui  
G. de Angelis  
G. Auger  
T. Aumann  
F. Azaiez,  
E. Balanzat  
G. Baldacchino  
M.F. Barthe  
E. Bauge  
P. Bem  
M. Bender  
K. Bennaceur  
J.-F. Berger  
B. Blank  
J. Blomqvist  
Y. Blumenfeld  
S. Boucard  
S. Bouffard  
A. Bracco  
R. Calabrese  
B. Cederwall  
R. Cee  
Ph. Chomaz  
G. Colo  
M. Colonna  
D. Curien  
P. Danielewicz  
R. Dayras  
F. de Oliveira  
M. di Toro  
E. Diegele  
J. Dobaczewski  
T. Ethvignot  
U. Fischer  
G. de France (coordinator)  
M. Freer  
U. Garg  
W. Gelletly  
A. Gillibert  
M. Girod  
S. Goriely  
H. Goutte  
J.P. Grandin  
F. Gunsing  
P.H. Heenen  
M. Heil  
K. Heyde  
S. Hilaire  
S. Hofmann  
P. Indelicato  
Z. Janas  
A. Jokinen  
J. Jose  
F. Kaeppler  
E. Khan  
J. Knodlseder  
A. Krasznahorkay  
K.L. Kratz  
E. Lamour  
K. Langanke  
V. Lapoux  
E.O. Le Bigot  
F. Le Blanc  
X. Ledoux  
M. Leino  
S. Lenzi  
S. Leoni  
M. Lewitowicz  
D. Lunney  
E. Maglione  
A. Maj  
P. Mantica  
J. Marques  
M. Matsuo  
V. Méot  
W. Mittig  
E.C. Morse  
O. Naviliat-Cuncic  
W. Nazarewicz  
G. Neyens  
Y. Novikov  
S. Oberstedt  
T. Otsuka  
F. Parente  
S. Péru  
N. Pillet  
A. Plompen  
C. Prigent  
R. Reifarth  
D. Ridikas  
M.F. Rivet  
E. Roeckl  
M. Rousseau  
P. Roussel-Chomaz  
J.P. Rozet  
G. Rudolf  
K. Rykaczewski  
M.G. Saint-Laurent  
D. Santonocito  
J.-P. Santos  
P. Sapienza  
H. Savajols  
M. Schädel  
H. Schatz  
N. Severijns  
J.L. Sida  
F. Sobrio  
O. Sorlin  
A.M. Stefanini  
C. Stodel  
L. Stuttge  
I. Testard  
Ch. Theisen  
J.C. Thomas  
J.B. Thomas  
I. Thompson  
M. Toulemonde  
P. Van Isacker  
D. Verney  
D. Vernhet  
D. Vieira  
A.C.C. Villari  
C. Volpe  
D. Vretenar  
D. Warner  
J.P. Wieleczko  
J.H. Wörtche  
R. Wyss